

**Functional analysis of CDKF;1: a plant specific
CAK-activating kinase**

**Inaugural-Dissertation
zur
Erlangung des Doktorgrades
der Mathematisch-Naturwissenschaftlichen Fakultät
der Universität zu Köln**

vorgelegt von

Mohsen Hajheidari

aus Karaj (Iran)

KÖLN 2010

Berichterstatter:

*Prof. Dr. George Coupland
Prof. Dr. Martin Hülskamp
Prof. Dr. Ulf-Ingo Flügge*

Tag der mündlichen Prüfung: February 01, 2010.

CONTENTS

1.	INTRODUCTION	1
1.1.	<i>Cell cycle control</i>	1
1.1.1.	Plant cyclin-dependent protein kinases (CDKs).....	2
1.2.	<i>The CTD code</i>	3
1.3.	<i>Small RNA biogenesis pathways</i>	5
1.4.	<i>Small RNAs and flowering time control</i>	8
1.5.	<i>Agrobacterium-mediated transformation and plant cell factors</i>	9
1.6.	<i>Aims of the study</i>	11
2.	MATERIALS AND METHODS.....	14
2.1.	<i>Materials</i>	14
2.1.1.	Chemicals.....	14
2.1.2.	Enzymes.....	14
2.1.3.	Kits.....	14
2.1.4.	Bacterial strains.....	15
2.1.4.1.	<i>E. coli</i> strains.....	15
2.1.4.2.	<i>Agrobacterium</i> strains	15
2.1.5.	Vectors.....	15
2.1.6.	Hormones.....	15
2.1.7.	Oligonucleotides	16
2.1.7.1.	Oligonucleotides for cloning	16
2.1.7.2.	Oligonucleotides for screening of T-DNA insertion mutants in <i>Arabidopsis thaliana</i>	16
2.1.7.3.	Oligonucleotides used for RT-PCR.....	16
2.1.7.4.	Oligonucleotides utilized for Real-time quantitative PCR.....	17
2.1.8.	Small RNAs probes for northern blot analysis.....	26
2.1.9.	Plant materials.....	26
2.2.	<i>Methods</i>	26
2.2.1.	Plant growth conditions.....	26
2.2.2.	Crossing of <i>Arabidopsis</i> plants	26
2.2.3.	Seedling growth assays in different light regimes.....	27
2.2.4.	Phytohormone treatments.....	27
2.2.5.	Hypocotyl tumorigenesis assay.....	27
2.2.6.	<i>Agrobacterium</i> -mediated transformation of <i>Arabidopsis thaliana</i> by vacuum infiltration.....	27
2.2.7.	General molecular biology techniques.....	28
2.2.8.	Construction of bacterial and plant expression vectors	28
2.2.9.	Site-directed mutagenesis.....	28
2.2.10.	Purification of <i>Arabidopsis</i> proteins expressed in <i>E. coli</i>	29
2.2.11.	Immunaffinity purification of HA-VirD2 protein	29
2.2.12.	Protein kinase assays.....	30
2.2.13.	Immunoblotting.....	30
2.2.14.	Two dimensional protein gel electrophoresis	30
2.2.15.	Protein identification and database search.....	31
2.2.16.	Mass spectrometry analysis of CDKF;1 phosphorylated VirD2.....	31
2.2.17.	RT-PCR.....	32
2.2.18.	Real-time quantitative PCR.....	32
2.2.19.	Light microscopy	32
2.2.20.	Confocal-laser-scanning microscopy	32
2.2.21.	Pollen preparation for fluorescence analysis.....	32
2.2.22.	Flow cytometry for ploidy analysis.....	33
2.2.23.	Small RNA detection by northern RNA hybridization.....	33
2.2.24.	Transcript profiling using Affymetrix <i>Arabidopsis</i> ATH1 microarrays	33
3.	RESULTS	35
3.1.	<i>Isolation and molecular characterization of cdkf;1 and cdkd mutations</i>	35
3.1.1.	Mutations in the <i>CDKF;1</i> gene	35
3.1.2.	Insertion mutations in the <i>CDKD</i> genes.....	37
3.1.3.	Transcripts analysis of <i>CDKF;1</i> and <i>CDKD</i> genes in the T-DNA insertion mutants.....	38
3.2.	<i>Analysis of phenotypic characteristics of the cdkf;1 and cdkd mutants</i>	40
3.2.1.	Phenotypic characterization of the <i>cdkd</i> mutants	40
3.2.2.	Characterization of <i>cdkf;1</i> mutants.....	42
3.2.3.	Genetic complementation of the <i>cdkf;1-1</i> mutation	45
3.3.	<i>Phosphorylation targets of CDKF;1 and CDKD protein kinases</i>	46
3.3.1.	CDKF;1 phosphorylates the CDK-activating CDKD kinases.....	46
3.3.2.	The CTD domain of <i>Arabidopsis</i> RNA polymerase II largest subunit is phosphorylated by CDKF;1 and CDKD;2.....	49
3.3.3.	RNA polymerase II CTD phosphorylation in <i>cdkf;1</i> and <i>cdkd;2</i> mutant plants.....	52
3.4.	<i>Transcript profiling of cdkf;1 mutant and wild type seedlings using Affymetrix ATH1 microarray</i>	54
3.4.1.	Data mining – identification of pathways affected by the <i>cdkf;1-1</i> mutation.....	54
3.4.2.	The <i>cdkf;1-1</i> mutation results in transcriptional down-regulation of small RNA biogenesis pathways.....	55

3.4.3.	Altered transcription of genes acting in light perception in the <i>cdkf;1-1</i> mutant.....	58
3.4.4.	Altered regulation of genes in the circadian clock and flowering time pathways in the <i>cdkf;1-1</i> mutant	62
3.4.5.	Effects of <i>cdkf;1-1</i> mutation on genes controlling hormone biosynthesis and signal transduction	63
3.4.6.	The <i>cdkf;1-1</i> mutation has minimal effect on genes in cell cycle control	66
3.4.7.	Inhibition of cell elongation correlates with down-regulation of genes controlling cytoskeleton functions in the <i>cdkf;1-1</i> mutant	67
3.5.	<i>CDKF;1</i> is a <i>VirD2</i> kinase controlling <i>Agrobacterium</i> -mediated tumour formation in plants	68
3.5.1.	<i>CDKF;1</i> phosphorylates the CDKD kinases and <i>VirD2</i> with similar efficiency.....	71
3.5.2.	The <i>cdkf;1</i> and <i>cdkd;2</i> mutants are defective in <i>Agrobacterium</i> -mediated tumorigenesis	71
4.	DISCUSSION	74
4.1.	<i>Arabidopsis CDKF;1</i> phosphorylates CDKDs and RNA polymerase II CTD.....	74
4.2.	<i>CDKF;1</i> is a major regulator of CTD phosphorylation code.....	76
4.3.	Are cyclin-dependent kinases (CDKs) targets of CDKDs/ CAKs?	77
4.4.	Regulation of small RNA pathways by <i>CDKF;1</i> -mediated phosphorylation of Serine-7 position of RNA polymerase II CTD	78
4.5.	Correlations between <i>cdkf;1</i> mutant phenotype, <i>CDKF;1</i> kinase function and transcript profiling data	80
4.6.	Control of <i>VirD2</i> phosphorylation and <i>Agrobacterium</i> -mediated tumorigenesis by <i>CDKF;1</i>	82
5.	REFERENCES	87
6.	ACKNOWLEDGEMENTS	148

FIGURES

Figure 1.	T-DNA junctions in the <i>cdkf;1-1</i> (GABI_315A10) mutant.....	35
Figure 2.	Analysis of T-DNA insert junctions in the <i>cdkf;1-2</i> (SALK_148336) mutant.....	36
Figure 3.	Characterization of T-DNA insert junctions in the <i>cdkd;1-1</i> (SALK_114643) mutant.....	37
Figure 4.	Analysis of T-DNA insert junctions in the <i>cdkd;2-1</i> and <i>cdkd;2-2</i> mutants.....	38
Figure 5.	T-DNA junctions in the <i>cdkd;3</i> mutants.....	39
Figure 6.	RT-PCR detection of transcription of <i>cdkf;1</i> and <i>cdkd</i> alleles.....	40
Figure 7.	The leaky <i>cdkd;3-2</i> mutation causes a significant reduction of plant growth in the <i>cdkf;1-1</i> , <i>cdkd;2-1</i> mutant background.....	41
Figure 8.	Morphological characteristics of the <i>cdkf;1-1</i> knockout mutant.....	43
Figure 9.	Flow cytometric analysis of nuclear DNA content of leaf cells of two and three weeks old wild type and <i>cdkf;1-1</i> mutant seedlings.....	44
Figure 10.	Fluorescence microscopy of DAPI-stained mature pollen grains of wild type and hemizygous <i>cdkf;1-1/+</i> plants.....	45
Figure 11.	Genetic complementation of the <i>cdkf;1-1</i> mutation.....	46
Figure 12.	Multiple alignment of <i>Arabidopsis</i> CDKD protein kinase sequences.....	47
Figure 13.	Purification of CDKF;1 and CDKD protein kinases fused to N-terminal thioredoxin and C-terminal His ₆ tags, and isolation of a GST-CTD fusion protein carrying the C-terminal heptapeptide repeats of <i>Arabidopsis</i> RNAPII largest subunit.....	47
Figure 14.	Phosphorylation of affinity-purified thioredoxin-fused CDK-activating CDKD kinases by the CAK-activating CDKF;1 kinase.....	48
Figure 15.	CDKF;1 and CDKD;2 do not phosphorylate the control glutathione-S-transferase (GST) and thioredoxin proteins.....	48
Figure 16.	CDKF;1 mediates T-loop phosphorylation of CDKD;1 protein kinase.....	49
Figure 17.	CDKF;1 and CDKD;2 phosphorylate the CTD of RNA polymerase II largest subunit.....	50
Figure 18.	CTD phosphorylation specificities of CDKD;2 and CDKF;1 kinases <i>in vitro</i>	51
Figure 19.	Changes in the levels of Serine-7, Serine-5 and Serine-2 specific phosphorylation of RNA polymerase II CTD in <i>cdkf;1</i> and <i>cdkd;2</i> mutant seedlings during early stages of seedling development.....	53
Figure 20.	Comparative analysis of transcript levels of genes acting in small RNA pathways in wild type and <i>cdkf;1-1</i> seedlings 7 DAG.....	57
Figure 21.	Comparison of levels of selected small RNAs in wild type, <i>cdkd;2-1</i> and <i>cdkf;1-1</i> seedlings.....	58
Figure 22.	Hypocotyl elongation responses of <i>cdkf;1-1</i> mutant compared to wild type to different light regimes.....	59
Figure 23.	Comparison of hypocotyl lengths of control wild type and <i>cdkf;1-1</i> mutant seedlings grown under different light conditions.....	59
Figure 24.	CDKF;1 phosphorylates the HA-VirD2 protein <i>in vitro</i>	69
Figure 25.	Resolution of CDKF;1 phosphorylated HA-VirD2 isoforms, carrying different number of phosphorylated residues, by two-dimensional gel electrophoresis.....	70
Figure 26.	CDKF;1 phosphorylates VirD2 and CDKD substrate with similar efficiency <i>in vitro</i>	71
Figure 27.	Comparison of frequency of tumor formation by hypocotyl agroinfection in wild type, <i>cdkf;1</i> and <i>cdkd</i> mutant seedlings.....	72
Figure 28.	The mode of action of CDKF;1 in modulation of phosphorylation of RNA polymerase II CTD during transcription and T-DNA integration through phosphorylation of VirD2.....	86

TABLES

Table 1.	Self pollination of hemizygous <i>cdkf;1-1/+</i> mutant yields a distorted segregation ratio of wild type and <i>cdkf;1-1</i> mutant progeny.	45
Table 2.	Male and female transmission efficiency of <i>cdkf;1-1</i> allele determined by reciprocal crosses.	45
Table 3.	Wild type and mutant variants of consensus CTD heptapeptide used as substrates in kinase assays with CDKF;1 and CDKD;2.	50
Table 4.	Genes showing 1.5-fold alteration in their transcript levels ($p < 0.05$) between the <i>cdkf;1-1</i> mutant and wild type were sorted to significantly overrepresented pathways according to GO-terms.	55
Table 5.	The list of differentially expressed genes involved in light signalling, circadian clock, flowering time and flower development pathways.	60
Table 6.	Differential expression of hormone-related genes in the <i>cdkf;1-1</i> mutant.	65
Table 7.	Altered transcription of genes involved in cell cycle control and regulation of cytoskeleton organization in the <i>cdkf;1-1</i> mutant.	68
Table 8.	List of remaining microarray data showing altered transcript levels of genes in pathways affected by the <i>cdkf;1-1</i> mutation, which have not mentioned in the text.	105

ABBREVIATIONS AND SYMBOLES

%	percentage
°C	degree Celsius
2,4-D	2,4-Dichlorophenoxy acetic acid
3'	3-prime
5'	5-prime
ABA	abscisic acid
ACC	1-aminocyclopropane-1-carboxylic acid
AG	AGAMOUS
AGO1	ARGONAUT 1
AP2	APETALA 2
ATP	adenosine 5'-triphosphate
bp	base pair
BSA	bovine serum albumin
CAK	CDK-activating kinase
CAKAK	CAK-activating kinase
CCA1	CIRCADIAN CLOCK ASSOCIATED 1
CDK	cyclin dependent kinase
cDNA	complementary DNA
CO	CONSTANS
CMT3	CHROMOMETHYLASE 3
CTD	C-terminal domain
DAPI	4',6'-diamidino-2-phenylindole
DAG	day after germination
DCL1	DICER-LIKE RIBONUCLEASE III-1
DMS3	DEFECTIVE IN MERISTEM SILENCING 3
DMSO	dimethyl sulfoxide
DNA	deoxyribonucleic acid
DRM1	DOMAINS REARRANGED METHYLTRANSFERASE 1
DSBR	Double-Strand Break Repair
dsRNA	double-stranded RNA
E2F	ADENOVIRUS E2 PROMOTOR BINDING FACTOR
et al.	<i>et alii</i> / <i>et aliae</i> [Lat.] and others
FLC	FLOWERING LOCUS C
FT	FLOWERING LOCUS T
G1	gap phase between M phase and S phase
G2	gap phase between S phase and M phase

GA	gibberellin
GI	GIGANTEA
GST	glutathione-S-transferase
HEN1	HUA ENHANCER 1
HST	HASTY
HYL1	HYPONASTIC LEAVES 1
IAA	indole-3-acetic acid
i.e.	<i>id est</i> [Lat.] that is
IEF	iso-electeric Focussing
IPTG	isopropyl- β -thiogalactoside
kb	kilobase
kDa	kilo Dalton
KRP	KIP-RELATED PROTEIN
LD	long day
LHY	LONG ELONGATED HYPOCOTYL
M	molar
MBP	maltose binding protein
μ g	microgram
mg	milligram
min	minute
miRNA	micro-RNA
ml	milliliter
μ l	microliter
mM	millimolar
μ M	micromolar
mRNA	messenger RNA
nat-siRNA	natural-antisense transcript-derived siRNA
NHEJ	Non-Homologous End-Joining
Ni-NTA	nickel-nitrilotriacetic acid matrix
nt	nucleotide
OD	optical density
PAGE	polyacrylamide gel electrophoresis
PCR	polymerase chain reaction
pH	negative logarithm of the proton concentration
PHYA	PHYTOCHROME A
PHYB	PHYTOCHROME B
PHYC	PHYTOCHROME C
PHYD	PHYTOCHROME D

PHYE	PHYTOCHROME E
PMF	peptide mass fingerprint
PMSF	phenylmethylsulfonyl fluoride
Pol IV	RNA POLYMERASE IV
pri-miRNA	primary micro-RNA
PTEFb	POSITIVE ELONGATION FACTOR b
PVDF	polyvinylidene difluoride
ra-siRNA	repeat-associated siRNAs
RdRP6	RNA-DEPENDENT RNA POLYMERASE 6
RISC	RNA-induced silencing complex
RITC	RNA-induced transcriptional silencing
RNA	ribonucleic acid
RNAPII	RNA POLYMERASE II
RNAPIIO	hyperphosphorylated RNA POLYMERASE II
RNAPIIA	hypophosphorylated RNA POLYMERASE II
RNase	ribonuclease A
rpm	revolution per minute
RT-PCR	reverse transcription PCR
S-phase	synthetic phase of the cell cycle
SDS	sodium dodecylsulfate
SD	short day
SGS3	SUPRESSOR OF GENE SILENCING 3
siRNA	short interfering RNA
SMZ	SCHLAFMÜTZE
SNZ	SCHNARCHZAPFEN
SOC1	SUPRESSOR OF OVEREXPRESSION OF CONSTANS 1
SPL9	SQUAMOSA PROMOTER BINDING PROTEIN LIKE 9
SSGP	Single-Stranded Gap Repair
T-DNA	transferred DNA
TBP	TATA-box binding protein
ta-siRNA	trans-acting siRNAs
TOE1	TARGET OF EAT 1
Trx	thioredoxin
Thr	threonine
UTR	untranslated region
UV	UV ultraviolet light
VirD2	virulence D2

ZUSAMMENFASSUNG

Cyclin-abhängige Protein Kinasen (CDKs) regulieren wichtige Kontrollpunkte und Übergangphase im Zellzyklus. Die Aktivierung von CDKs erfolgt durch die Phosphorylierung eines in deren T-Schleife lokalisierten, konservierten Threonin-Rests durch CDK-aktivierende Kinasen (CAKs), die ihrerseits auf analoge Weise durch CAK-aktivierende Kinasen (CAKAKs) aktiviert werden. CDKF1, eine pflanzenspezifische CAKAK, phosphoryliert Berichten zufolge zwei der drei in *Arabidopsis* bekannten CAKs (CDKD2 und CDKD3). Im Rahmen unserer Arbeit konnte gezeigt werden, dass in *E. coli* überexprimierte und aufgereinigte CDKF;1 und CDKD Kinase, ohne eine Bindung mit Cyclinen einzugehen, autoaktiviert sind und dass CDKF;1 für die Phosphorylierung aller drei *Arabidopsis* CDKDs (CDKD;1, CDKD;2 und CDKD;3) verantwortlich ist. Weiterhin konnten wir feststellen, dass CDKF;1 und CDKD;2 benötigt sind für die Phosphorylierung der CTD Domäne der grössten *Arabidopsis* RNA POLYMERASE II (RNAP II) Untereinheit, welche aus 15 konsensus und 26 variablen YSPTSPS tandem heptapeptid repeats besteht. Diesbezüglich zeigen unsere Daten, dass CDKD;2 die Phosphorylierung an der Serine-5 Position der CTD Domäne vermittelt, was auf eine mögliche Rolle von CDKD;2 in der Transkriptionsinitiation sowie dem 5' capping naszierender RNAs schliessen läßt. Die Phosphorylierung an der Serine-7 Position der CTD Domäne hingegen wird von CDKF;1 durchgeführt. Darüber hinaus konnten wir feststellen, dass eine Verringerung der Serine-7 CTD Phosphorylierung, wie sie in der *cdkf;1* Mutanten beobachtet wird, verursacht Defekte in der Transkription und während der Entwicklung, und reduziert auch die Produktion kleiner RNAs, wie miR156, miR165, miR172, ta-siRNA1 (*TAS1*), und *COPIA*. Zusätzlich konnte aufgezeigt werden, dass CDKF;1 kann auch das VirD2 Protein *in vitro* phosphorylieren. VirD2 ist kovalent mit dem 5'-Ende von Agrobacterium transferiert einzelsträngiger DNA (T-DNA/T-Strang) verbunden und vermittelt deren Integration in das Genom des Zellkerns der Pflanzenwirtszelle. Es wurde früher gezeigt, dass VirD2 mit der TATA-Box-bindenden Untereinheit (TBP) von RNAPII interagiert, und dass es *in vivo* von einer CTD-assoziierten CAK-ähnlichen Protein Kinase phosphoryliert wird. Andere Studien mit *Arabidopsis* CAKs haben gezeigt, dass CDKF;1 zusammen mit CDKD;2 und cyclin H Teil des TFIIH Komplexes sind, welcher an Genom und transkriptions-gekoppelter Exzisionsreparatur beteiligt ist. Unsere Daten zeigen, dass Mutationen verursachen die Inaktivierung von CDKF;1 oder seines CAK Substrats CDKD;2, zu einer dramatischen Verringerung der Tumorbildung durch *Agrobacterium tumefaciens* C58 führen. Dies läßt den Schluss zu, dass CDKD;2 ein wichtiger Vermittler der VirD2 Phosphorylierung durch CDKF;1 ist. Wir vermuten dass diese Phosphorylierung ist unerlässlich damit VirD2 mit dem TFIIH-komplex interagieren kann, der die Reparatur-Rekombination zwischen 5'-Ende des T-Stranges und der Ziel Sequenz im Wirtchromosom vermittelt.

SUMMARY

Cyclin-dependent protein kinases (CDKs) control checkpoint transitions of the cell cycle. Activation of CDKs requires phosphorylation of a conserved threonine residue in their T-loops by CDK-activating kinases (CAKs) that are analogously activated by CAK-activating kinases (CAKAKs). CDKF;1, a plant specific CAKAK, is reported to phosphorylate two of three known *Arabidopsis* CAKs (CDKD;2 and CDKD;3). Here we show that CDKF;1 and CDKDs purified from *E. coli* are auto-activated without cyclin binding and that CDKF;1 phosphorylates all three *Arabidopsis* CDKDs (CDKD;1, CDKD;2, and CDKD;3). We found that CDKF;1 and CDKD;2 are required for phosphorylation of the CTD domain of *Arabidopsis* RNA POLYMERASE II (RNAPII) largest subunit, which comprises of 15 consensus and 26 variant YSPTSPS tandem heptad repeats. CDKD;2 mediates Serine-5 phosphorylation of the CTD, suggesting its possible role in the control of transcription initiation and 5' capping of nascent RNAs. CDKF;1 phosphorylates the Serine-7 residue of CTD heptapeptide repeats. Reduction of CTD-phosphorylation on Serine-7 in the *cdkf;1* mutant causes overall defects in transcription and development, as well as in the production of small RNAs, including miR156, miR165, miR172, ta-siRNA1 (*TASI*), and *COPIA*. CDKF;1 can also phosphorylate *in vitro* the VirD2 protein, which is covalently bound to the 5'-end of single-stranded intermediate of *Agrobacterium* transferred DNA (T-DNA/T-strand) and mediates its integration into the nuclear genomes of plant host cells. Previous data indicate that VirD2 interacts with the TATA-box-binding subunit of RNAPII and is phosphorylated *in vivo* by a CTD-associated CAK-like protein kinase. Studies of *Arabidopsis* CAKs show that CDKD;2 is found in association with cyclin H and CDKF;1 as part of the TFIIH complex, which is implicated in global genome and transcription-coupled repair. Our data demonstrate that mutations inactivating either CDKF;1 or its CAK substrate CDKD;2 result in dramatic reduction of tumour formation mediated by *Agrobacterium tumefaciens* C58. This suggests that CDKD;2 is an important mediator of VirD2 phosphorylation by CDKF;1, which is likely required for VirD2 recruitment to the TFIIH complex implicated in repair-recombination between the 5'-end of the T-strand and target sequences in the host chromosomes.

1. INTRODUCTION

Plants utilize interconnected regulatory networks for perception and transduction of different external and internal signals. Environmental and hormonal signals play pivotal roles in the regulation of plant homeostatic control systems. When an input signal surpasses a certain threshold, the interconnected signalling networks provide the possibility for appropriate adjustment of specific network balance and corresponding response output. Regulatory proteins that act at the network interfaces (i.e., hubs) are usually capable to modulate multiple pathways. Although, many key regulatory functions in plants are encoded by functionally equivalent duplicated genes or larger gene families, genetic studies have also identified evolutionally conserved single copy genes implicated in multidisciplinary regulatory functions, inactivation of which causes dramatic effects in plant development. One of these in *Arabidopsis* is the *CDKF;1* protein kinase gene, which functions as major signalling hub in coordination of transcription, cell cycle and several signalling pathways. Inactivation of *CDKF;1* gene by T-DNA insertion mutations in this work revealed its important roles in the control of activation of cyclin-dependent kinase-activating kinases (CAKs/CDKDs), phosphorylation of C-terminal heptapeptide repeats RNAPII largest subunit, transcription, biogenesis of small RNAs and T-DNA transformation mediated by the *Agrobacterium* VirD2 protein. The following sections provide a brief overview on our current knowledge on these specific pathways.

1.1. Cell cycle control

Cell growth and division are coordinated by a cyclic series of regulatory events during successive phases (G1, S, G2, and M) of the cell cycle. The exit from cell cycle may also mark the onset of cell differentiation processes indicating that, in addition to controlling cell division, cell cycle regulators play essential roles in the development and growth of multicellular organisms. Due to unique features of plants, such as post-embryonic initiation of organ development and sessile life style, changes in environmental conditions have profound effects on their development and growth. Cell cycle regulators modulate the normal balance between plant growth and development by causing specific structural changes and modifying the growth rate in response to changing environment (Cockcroft et al., 2000; Menges et al., 2002; De Jager et al., 2005).

A great variety of components and mechanisms has been characterized in the regulation of plant cell cycle progression. These include, for example, the cyclin-dependent protein kinases (CDKs) and their noncatalytic cyclin subunits, CDK inhibitors, retinoblastoma tumour suppressors, E2F/DP transcription factors, CDK subunit (CKS) proteins, positive and negative regulatory effects of phosphorylation, and proteolysis of multiple regulatory proteins (Morgan, 1995; Kaldis et al., 1996; De Veylder et al., 1997; Michael et al., 1998; Verkest et al., 2005; Del Pozo et al., 2006). The onset of cell differentiation, accompanied by endoreduplication in plant cells, is concomitant with reduction of the activity of mitotic-phase associated CDK-cyclin complexes. Therefore, the mechanisms coordinating mitosis with transition to endocycle play important roles in plant development (Park et

al., 1995; Cebolla et al., 1999; Sun et al., 1999; De Veylder et al., 2001, 2002; Vinardell et al., 2003; Gonzalez et al., 2004; Verkest et al., 2005a; Vlieghe et al., 2005).

1.1.1. Plant cyclin-dependent protein kinases (CDKs)

Cyclin-dependent protein kinases (CDKs) are evolutionarily conserved and represent the main regulatory core of eukaryotic cell cycle. The catalytic activity of CDKs is regulated by phosphorylation events and binding of noncatalytic partners, including cyclins and CDK inhibitors (Gould et al., 1991; Solomon et al., 1992; Dewitte and Murray, 2003; Shimotohno et al., 2004). In plants, there are seven known classes of CDKs named CDKA to CDKG. Based on our current knowledge CDKAs, CDKBs, CDKDs, and CDKFs are involved in the regulation of cell cycle progression (Vandepoele et al., 2002; Francis, 2007). CDKA, which is closely related to yeast Cdc2/CDC28 and human CDK1/2/3, contains a conserved PSTAIRE motif in the cyclin-binding domain (Colasanti et al., 1991; Hirt et al., 1993; Joubés et al., 2000a) and controls both G1 to S and G2 to M checkpoint transitions (Hemerly et al., 1995; Reichheld et al., 1999; Menges and Murray, 2002). CDKB is a plant specific CDK class that consists of two subgroups, CDKB1 (PPTALRE) and CDKB2 (P(P/S)TTLRE). CDKBs are involved in the control of G2 to M transition (Porceddu et al., 2001; Menges et al., 2002, Francis, 2007).

The first plant CDK-activating protein kinase (CDKD;1/R2) has been isolated from rice and is closely related to human CDK7/p40^{MO15}, fission yeast Mcs6/Crk1/Mop1 and budding yeast Kin28p (Buck et al., 1995; Damagnez et al., 1995; Feaver et al., 1997). The latter CDK-activating kinases (CAKs) interact with cyclin H (i.e., human CycH and yeast Mcs2/Ccl1) subunits that positively regulate their kinase activities through stabilizing the catalytic sites. The cyclin H-kinase complex is further stabilized by a conserved RING finger protein (Pmh1, Rig2p/Tfb3p and MAT1) in yeast and metazoans. Putative MAT1 homologues are also found in *Arabidopsis* and rice. Whereas interaction between rice MAT1 and CDKD;1/R2 is unknown so far (Umeda et al., 2005), CDKD;2 binding of a MAT1 homolog has been reported in *Arabidopsis in vivo* (Leene et al., 2007; Leene et al., 2008).

Similarly to the heterotrimeric human CDK7-CycH-MAT1 and fission yeast Mcs6/Crk1/Mop1-Mcs2-Pmh1 kinases, rice CDKD;1 kinase phosphorylates *in vitro* the C-terminal heptapeptide repeat domain (CTD) of the largest subunit of RNAPII, as well as a conserved threonine residue within the T-loops of CDKs (i.e., CDK2/CDKA), which is necessary for their activation. *Arabidopsis* contains three CAKs (CDKD;1, CDKD;2, and CDKD;3). CDKD;2 and CDKD;3 phosphorylate human CDK2 and the RNAPII CTD with different specificities *in vitro*, while CDKD;1 does not seem to have these kinase activities (Umeda et al., 1998; Shimotohno et al., 2003). *Arabidopsis* CDKDs are also reported to interact with At;CycH;1 and their kinase activities are increased upon binding of cyclin H1 in insect cells as suggested by *in vitro* kinase assays (Shimotohno, 2004).

Homologues of the plant specific kinase CDKF;1 were identified in rice, *Arabidopsis*, leafy spurge, and soybean. *Arabidopsis* CDKF;1 (At;CDKF;1) activates human CDK2 and *Arabidopsis*

CAKs (At;CDKD;2 and At;CDKD;3) through phosphorylation of their T-loops *in vitro*. At;CDKF;1 does not interact with At;CycH;1 and, according to Shimotonho et al. (2003), cannot phosphorylate the CTD of RNAPII. However, interestingly, *Arabidopsis* CDKF;1 suppresses the temperature sensitive *cak^{ts}* mutations in budding yeast (Umeda et al., 1998), while budding yeast Kin28p-Ccl1p-Rig2p/Tfb3p kinase (CAK kinase) phosphorylates RNAPII CTD, but has no CAK activity. Leafy spurge Ee;CDKF;1 has intramolecular autophosphorylation activity, which is suggested to be controlled by phosphorylation of its Thr291 and Thr296 residues (Chao et al., 2006).

1.2. The CTD code

In analogy to human CDK7, *Arabidopsis* CDKD;2 and CDKD;3 may control transcription by phosphorylation of the CTD domain of the RNAPII largest subunit, which consists of highly conserved heptapeptide repeats. The number of CTD heptapeptide repeats and their deviation from the consensus sequence (YSPTSPS) increase evolutionally. *Saccharomyces cerevisiae* has 26 conserved heptapeptide repeats, while human RNAPII CTD carries 52 repeats. Of these, 21 repeats are exactly conserved, whereas the remaining 31 show deviation from the consensus sequence (Chapman et al., 2004). RNAPII CTD of *Arabidopsis thaliana* contains 15 consensus and 26 divergent heptapeptide repeats. The divergent repeats are located in the C-terminal end of the CTD domain, as in the human enzyme (Nawrath et al., 1990). Previous experiments demonstrate that the CTD domain is essential for cell viability (Nonet et al., 1987; Zehring et al., 1988; Corden, 1990; Stiller and Cook, 2004). In addition, the CTD domain has a unique structure that is very hydrophilic and flexible. This disordered nature of CTD provides a possibility for interaction with many proteins according to the induced fit model. This model predicts that changes in the phosphorylation pattern of CTD conferred by various CTD kinases regulate its interaction with binding proteins involved in mRNA processing during the transcription cycle (Cagas and Corden, 1995; Bienkiewicz et al., 2000; Meinhart et al., 2005).

Phosphorylation patterns of RNAPII CTD with pinpoint accuracy orchestrate its association with numerous nuclear factors, which are necessary for transcription initiation, elongation, and termination, as well as co-transcriptional RNA processing, including 5'-capping, 3'-polyadenylation, and splicing. These molecular codes are determined by collaboration of CTD kinases and phosphatases during transcription. The reversible serine phosphorylation sites (Serine-2, Serine-5, and Serine-7) in the heptapeptide repeats are main determinants of activity of RNAPII CTD domain. However, these serine phosphorylation sites are not functionally equivalent (Hemali et al., 2006; Chapman et al., 2007).

Unphosphorylated RNAPII CTD is recruited by the transcription pre-initiation complex to promoter regions of genes. Subsequently, the Serine-5 residues of CTD are phosphorylated in the promoter-proximal regions by Kin28 and CDK7, representing components of the TFIIF complex in yeast and mammals, respectively. A peak of phosphoserine-5 residues on the CTD is detected at the 5'-end of the transcribed gene and is reduced gradually as transcription proceeds along the gene. Phosphorylation of Serine-5 residues of the CTD repeat facilitates promoter clearing, as well as the

recruitment and activation of capping enzymes that attach a methylguanosine cap to the 5'-ends of nascent transcripts when they are about 25 bases long (Jove and Manley, 1984; Ho and Shuman, 1999; Perales and Bentley, 2009; Komarnitsky et al., 2000; Meinhart, 2005; Yu et al., 1997; Cho et al., 1997; Phatnani and Greenleaf, 2006; Lolli, 2009). Interaction of CTD with capping enzymes enhances 5'-capping of pre-mRNA and facilitates the transition to the transcription elongation phase (Schroeder et al., 2000; McCracken et al., 1977a; Gao and Gross, 2008).

Following Serine-5 phosphorylation, CTD heptapeptide repeats of human RNAPII largest subunit undergo Serine-2 phosphorylation by CDK9/CTK-1, a catalytic subunit of POSITIVE ELONGATION FACTOR b (PTEFb), during the elongation phase (Price, 2000; Ahn et al., 2004; Peterlin and Price, 2006; Egloff and Murphy, 2008). Phosphorylation of Serine-2 residues of CTD repeats increases as the RNAPII progresses toward the 3'-end of the transcribed gene. Hyperphosphorylated RNAPII (RNAP IIO), carrying phosphoserine-2 and phosphoserine-5 in its CTD repeats, interacts with components of the spliceosome and strongly stimulates pre-mRNA splicing. By contrast, hypophosphorylated RNAPII (RNAP IIA) negatively regulates splicing (Chabot et al., 1995; Mortillaro et al., 1996; Kim et al., 1997; Hirose et al., 1999; Damgaard et al., 2008). Furthermore, immunohistochemistry experiments demonstrate that truncations of the CTD inhibit the accumulation of spliced pre-mRNA variants (Hirose and Manley, 2000).

In addition to capping and splicing, 3'-end processing of pre-mRNAs and transcription termination are also prevented by truncation of the RNAPII CTD in transient transfection assays (McCracken et al., 1997b). The CTD domain interacts specifically with cleavage-polyadenylation factors and enhances 3'-end processing of pre-mRNAs *in vivo* (McCracken et al., 1997b; Hirose and Manley, 1998; Hirose and Manley, 2000). In yeast, the Pcf11p subunit of cleavage-polyadenylation factor A (CFIA) preferentially binds to heptapeptide repeats containing phosphoserine-2 (Licatalosi et al., 2002; Meinhart and Cramer, 2004). Similarly, the yeast Rtt103 protein, which is co-purified with cleavage-polyadenylation factors, also binds to CTD repeats containing phosphoserine-2. Furthermore, Yhh1p, a subunit of cleavage and polyadenylation specificity factor (CPSF) also binds to phosphorylated CTD using a yet unknown molecular recognition code (Dichtl et al., 2002; Egloff and Murphy, 2008). It is therefore not surprising that inhibition of CDK9 CTD kinase in *Drosophila* cells *in vivo* negatively regulates 3'-end processing of transcribed pre-mRNAs (Ni et al., 2004).

Chapman et al. (2007) demonstrated that heptapeptide repeats of the CTD domain are also phosphorylated at Serine-7 during transcription. They showed that the Serine-7 phosphorylation level is high at promoters and gradually increases along the transcribed genes. Simultaneously, Egloff and Murphy (2007) found that Serine-7 substitution with alanine in either 25 or 48 consensus CTD repeats inhibits proper 3'-end processing and transcription of the small noncoding nuclear RNA U2-globin. However, alanine replacement of CTD Serine-7 residues did not affect the transcription and processing of protein-coding genes, such as the gene encoding the heterogeneous nuclear ribonucleoprotein K. Phosphorylated Serine-7 is required for recruitment of the snRNA specific integrator complex, which mediates 3'-end processing *in vivo*. Interestingly, the CDK7/Kin28 Serine-5

kinases were recently reported to phosphorylate also Serine-7 residues of CTD repeats (Akhtar et al., 2009; Glover-Cutter et al., 2008). This finding is an important milestone in unraveling of the molecular code of CTD.

Phosphorylation of heptapeptide repeats of RNAPII CTD does not always have positive effect on transcription. For example, the CDK8-CyclinC CTD-kinase negatively regulates transcription by phosphorylating Serine-5 residues, which prevents complete assembly of the RNAPII pre-initiation complex at promoter regions of transcribed genes. On the other hand, CDK8-Cyclin C also phosphorylates the cyclin H regulatory subunit of CDK7, and thereby inhibits transcription stimulatory activity of the TFIIF-associated CDK7 CTD-kinase (Akoulitchev et al., 2000).

1.3. *Small RNA biogenesis pathways*

Based on functional similarities between conserved CTD kinases, it is expected that mutations influencing proper maintenance of the CTD code may also affect the biogenesis of certain small RNAs in plants as in mammals. Compared to animals, in plants somewhat diversified pathways have evolved to produce noncoding small RNAs (approximately 18-25 nucleotides). Plant small RNAs post-transcriptionally regulate a broad range of biological functions, including the control of flowering-time and development, chromatin modification, metabolism, and immunity responses (Xie et al., 2004; Voinnet, 2009; Pedersen and David, 2008; Aukerman and Sakai, 2003; Mallory et al., 2004; Schmitz et al., 2007; Fornara and Coupland, 2009).

Two major classes of plant small RNAs are the microRNAs (miRNAs) and short interfering RNAs (siRNAs). Although both groups are intimately similar, their precursors and biogenesis are different. miRNAs are processed from stem-loop precursors transcribed by RNAPII. The siRNA family is comprised of three known classes: trans-acting siRNAs (ta-siRNAs), natural-antisense transcript-derived siRNAs (nat-siRNAs) and repeat-associated siRNAs (ra-siRNAs). The endogenous source of ta-siRNAs are RNAPII transcribed transcripts (e.g., *TASI*, 2 and 3 mRNAs) that are cleaved by an AGO1-bound specific microRNA and converted to double-stranded RNA (dsRNA) by the RNA-dependent RNA polymerase RDR6 prior cleavage by DCL4 (DICER-LIKE 4). In comparison, primary nat-siRNAs represent dsRNA regions of overlapping antisense transcripts cleaved by DCL2 (DICER-LIKE 2), whereas ra-siRNAs are processed from transcribed repeat-derived dsRNAs by DCL3. In addition to these dsRNAs precursors, transcripts from viruses, transgenes and transposons may also be converted to dsRNA precursors and processed to siRNAs (Vaucheret, 2005; Vazquez, 2006; Voinnet, 2009; Mallory et al., 2008).

Primary miRNA transcripts (pri-miRNAs) may undergo splicing, and are polyadenylated in plants before being processed by the DICER-Like RIBONUCLEASE III 1 (DCL1) in the nucleus. The miRNA located in a dsRNA region of pri-miRNA hairpin is cleaved by DCL1 producing a 2-nt overhang at the 3'end of miRNA:miRNA* duplex. Interaction of DCL1 with the dsRNA-binding protein HYPOPLASTIC LEAVES 1 (HYL1) is essential for proper trimming and maturation of miRNAs. In addition, the DCL1-HYL1 complex contains SERRATE, a DCL1-interacting protein,

which appears to control microRNA processing in interaction with the ABH1/CBP80 and CBP20 core subunits of the cap-binding complex. The nuclear RNA-binding protein DWADLE (DDL) is another DCL1-interacting factor, which is likely implicated in pri-miRNAs stabilization. Whereas the *se*, *hyll*, *cbp80*, and *cbp 20* mutants show enhanced pri-miRNAs accumulation and decreased mature miRNA levels, the *ddl* mutant has low levels of pri-miRNAs and mature microRNAs (Bartel, 2004; Kurihara and Watanabe, 2004; Vazquez et al., 2004; Han et al., 2004; Kurihara et al., 2006; Voinnet et al., 2009; Fang and Spector, 2007; Gregory et al., 2008; Laubinger et al., 2008; Voinnet et al., 2009; Allen et al., 2004; Fahlgren et al., 2007; Dunoyer et al., 2007).

The 3'-terminal ribose residue of each miRNA:miRNA* duplex strand is methylated by the HUA ENHANCER 1 (HEN1), a S-adenosyl methionine-methyltransferase providing protection from polyuridylation and degradation (Yu et al., 2005; Li et al., 2005; Yang et al., 2006; Voinnet et al., 2009). Subsequently, HASTY (HST), a plant orthologue of animal miRNA transporter Exportin 5, exports the methylated miRNA:miRNA* duplex into the cytoplasm (Park et al., 2002; Park et al., 2005) where miRNAs are incorporated into the RNA-induced silencing complex (RISC, Boutet et al., 2003; Yu et al., 2005). Previous studies in *Arabidopsis* showed that the RISC complex recognizes near-perfect or perfect complementary targets of miRNAs. ARGONAUTE 1 (AGO1), a RISC component with slicer activity, cleaves the target mRNA in the middle of its miRNA complementary sequence (Llave et al., 2002; Vaucheret et al., 2004; Jones-Rhoades et al., 2006; Vazquez et al., 2006; Baumberger and Baulcombe, 2005; Hutvagner and Zamore, 2002; Song et al., 2004). Moreover, there were few reports, which were indicating that the AGO1-microRNA RISC complex inhibits translation of certain mRNAs in *Arabidopsis*, similarly to RISC complexes in animals (Aukerman and Sakai, 2003; Bari et al., 2006; Chen, 2003; Gandikota et al., 2007). However, recent results show widespread translational repression not only by plant miRNAs, but also siRNAs (Brodersen et al., 2008; Voinnet, 2009, Lanet et al., 2009).

Like miRNAs, ta-siRNAs are originated from non-protein coding genes transcribed by RNAPII. The mRNAs derived from such ta-siRNA source *TAS* genes are processed by miRNA-guided cleavage. Therefore, subunits of the DCL1-complex involved in miRNAs biogenesis are also required for biogenesis of the ta-siRNAs. Cleaved *TAS* transcripts are converted to dsRNAs by RDR6 and SUPPRESSOR OF GENE SILENCING 3 (SGS3; Peragine et al., 2004; Vazquez et al., 2004; Allen et al., 2005; Yoshikawa et al., 2005). DCL4 in interaction with the dsRNA-binding protein DRB4 processes the RDR6-derived dsRNAs into siRNA duplexes (Xie et al., 2005; Adenot et al., 2006; Vazquez, 2006). The mature 21nt ta-siRNAs are then mostly loaded into AGO1 (Baumberger and Baulcombe, 2005; Rubio-Somoza, et al., 2009; Voinnet, 2009). There are four known *TAS* genes in *Arabidopsis*, which yield ta-siRNAs upon cleavage of their transcripts by specific miRNAs. *TAS1* and *TAS2* derived ta-siRNA biogenesis is driven by miR173, ta-siRNA formation from *TAS4* mRNA is guided by miR828, and AGO7-mediated cleavage of *TAS3* transcript requires miR393 (Axtell et al., 2006; Howell et al., 2007; Yoshikawa et al., 2005; Montgomery et al., 2008).

Compared to ta-siRNAs, the natural antisense nat-siRNAs are originated from two convergent and overlapping antisense transcripts. Transcription of the first two nat-siRNAs identified in *Arabidopsis* (nat-siRNA-SRO5 and nat-siRNA-ATGB2) was found to be stress inducible (Borsani et al., 2005; Katiyar-Agarwal et al., 2006). Stress induction of the *SRO5* and *ATGB2* genes results in dsRNA formation with overlapping transcripts of the neighbouring *P5CDH* (for *SRO5*) and *PPRL* (for *ATGB2*) genes, respectively. The dsRNAs segment formed by these transcripts is cleaved by DCL2 into a 24nt primary ta-siRNA, which is targeted by a yet unknown AGO protein to the *P5CDH* or *PPRL* transcripts. Following dsRNA formation catalysed by RDR6, SGS3 and the NRDP1a subunit of Pol IVa, the double-stranded *P5CDH* and *PPRL* RNAs are processed by DCL1 into 21nt siRNAs (Borsani et al., 2005; Katiyar-Agarwal et al., 2006; Herr et al., 2005; Onodera et al., 2005; Vazquez, 2006).

Repeat-associated siRNAs (ra-siRNAs) represent specialized type of siRNAs, which have evolved for maintenance of DNA and histone methylation on certain perfect or imperfect complementary regions of the genome, including transposons, repetitive DNA elements, and transcribed intergenic and noncoding sequences. Although, RNAP IVa/Pol IV is the main DNA polymerase in ra-siRNA production, it appears that primary sources of these siRNAs are transcripts resulting from RNAPII activity. Since DNA sequences encoding ra-siRNAs consist of tandem sequence repeats, the primary source of ra-siRNA biogenesis is likely a hairpin-loop of dsRNA resulting from transcription of an inverted repeat. However, it is also possible that repeat-derived dsRNA formation involves a yet unknown RNA-dependent RNAP. Processing of dsRNA substrates to 24nt ra-siRNAs/heterochromatic-siRNAs requires DCL3 and subsequent 3'-methylation of the products by HEN1. Silencing of complementary loci by ra-siRNAs is mediated by nuclear AGO4-containing RITS (RNA-Induced Transcriptional Silencing) complexes that carry associated components of RNAP IVb/Pol V (e.g., RDM2, NRPD1, NRPE1, NRPD2a) and trigger siRNA-mediated DNA methylation in interplay with components of the Polycomb repressing complex 2 and histone 4 K27 and K4 methylases. Therefore, siRNA-dependent DNA methylation (RdDM) is also dependent on the functions of DNA methylases and associated chromatin factors, including the DOMAINS REARRANGED METHYLTRANSFERASEs DRM1 and DRM2; CHROMOMETHYLASE3 (CMT3), DIRECTED DNA METHYLATION1 (DRD1) and DEFECTIVE IN MERISTEM SILENCING3 (DMS3). Recently, Wierzbicki et al. (2009) proposed that nascent Pol V transcripts are also implicated in driving the AGO4 effector complex to target loci. The current RdDM model suggests that following replication and DNA methylation, the methylated loci are transcribed by Pol IV and the primary transcripts are converted to dsRNAs by RDR2. These dsRNAs are processed into mature 24nt ra-siRNA by DCL3, methylated by HEN1, and loaded into RISC-like RITS complexes containing AGO4 and Pol V, which scan the genomic DNA to drive DNA methylation at target loci carrying complementary sequences. The accumulation of ra-siRNA is dependent on DNA methylation of the target loci that are transcribed by Pol IV. Therefore, RNA-

directed DNA methylation (RdDM) implies a positive feedback loop (Vazquez, 2006; Matzke et al., 2009; Wierzbicki et al., 2008; Cao et al., 2003; Zilberman et al., 2003).

1.4. *Small RNAs and flowering time control*

During their life cycle, plants utilize several complex pathways to coordinate transitions through different developmental phases. Among these, the juvenile to adult and vegetative to reproductive phase transitions are best studied, including genetic dissection of the regulatory pathways. Small RNAs and proteins involved in their biogenesis play important roles throughout the developmental phase transitions. Mutations of *DCLA*, *HST*, *RDR6*, *AGO1*, *AGO7* and *SGS3* accelerate the transition from juvenile to adult phase suggesting that these small RNA biogenesis factors regulate the phase transition during vegetative development (Peragine et al., 2004; Telfer and Poethig, 1998; Xie et al., 2005; Hunter et al., 2003). On the other hand, the *dcl1dcl3* and *hen1* mutations confer late flowering phenotype, which correlates with an increase in the expression of the floral repressor FLC (FLOWERING LOCUS C; Schmitz et al., 2007; Xie et al., 2003; Liu et al., 2004). Moreover, there are three known miRNAs (miR172, 156, and 159) that are directly involved in flowering time regulation. *GIGANTEA* (*GI*), a circadian clock-controlled gene, regulates flowering time by modulating the proteolysis of CDF repressor of *CO* transcription. At the same time, *GI* positively regulates the levels of miR172. Through a *CO*-independent pathway, miR172 negatively controls the expression of a set of AP2-like transcription factors (*TARGET OF EAT1*, *TOE1*; *TOE2*, *TOE3*; *SCHLAFMÜTZE*, *SMZ*, *SCHNARCHZAPFEN*, *SNZ*) that act as flowering time repressors (Jung et al., 2007). *TOE1* to *TOE3*, *SMZ* and *SNZ* inhibit the transcription of floral integrator genes *FLOWERING LOCUS T* (*FT*) and *SUPPRESSOR OF OVEREXPRESSION OF CONSTANTS 1* (*SOC1*). miR172 represses the expression of these AP2-like transcription factors by translational inhibition rather than cleavage of their mRNAs (Schmid et al., 2003; Aukerman and Sakai, 2003; Mathieu et al., 2009; Chen, 2003; Kasschau et al., 2003; Schwab et al., 2005). Intriguingly, *TOE1* and *TOE2* positively regulate the transcription of pri-miR172 precursor, which provides a feedback regulatory loop. In contrast to miR156, miR172 levels are high in adult phase and low during the juvenile phase. Transcription of pri-miR172 precursor is also positively regulated by the transcription factors *SQUAMOSA PROMOTER BINDING PROTEIN LIKE 9* (*SPL9*) and *SPL10*, which are targeted by miRNA156. In *Arabidopsis*, 10 members of the *SPL* family carry complementary sequences with miR156 (*SPL2*, *SPL3*, *SPL4*, *SPL5*, *SPL6*, *SPL9*, *SPL10*, *SPL11*, *SPL13*, and *SPL15*) and most likely repressed through translational inhibition. In contrast to miR172, the abundance of miR156 is high during the juvenile phase, when it represses the *SPL* transcription factors. As the plant ages, the level of miR156 decreases by yet unknown mechanisms (i.e., despite the activation of pri-miR156 transcription by *SPL9* and *SPL10*) and consequently the levels of *SPL* transcription factors are being increased. *SPL9* and *SPL10* also activate the transcription of pri-miRNA172 precursor and thereby enhance *FT* and *SOC1* expression. On the other hand, *SPL3* and *SPL9* enhance the expression of floral homeotic genes *API*, *LEAFY* (*LFY*), *FRUITFUL* (*FUL*), and *AGAMOUS-LIKE 42* (*AGL42*) stimulating flower development.

Thereby, the SPL family facilitates both juvenile to adult and adult to reproductive transition phases (Gandikota et al., 2007; Fornara and Coupland, 2009; Wu et al., 2009; Yamaguchi et al., 2009; Wang et al., 2009).

The plant hormone gibberellin regulates flowering via two independent DELLA-mediated pathways. On one hand, GA targets DELLA proteins [GIBBERELLIN INSENSITIVE (GAI) and REPRESSOR OF *ga1-3* (RGA)] to the proteasomal degradation system and consequently enhances the expression of *LFY* and *SOC1* by a miR159/MYB33-independent pathway. On the other hand, GA inhibits *LFY* expression by enhancing the accumulation of miR159, which represses the *LHY*-activating transcription factor *MYB33* through mRNA cleavage. Overexpression of miR159 creates therefore a late flowering phenotype in short days (Quesada et al., 2005; Mutasa-Göttgens and Hedden, 2009; Achard et al., 2004).

1.5. *Agrobacterium*-mediated transformation and plant cell factors

The results described in this thesis demonstrate that mutations in two CTD kinases have also a dramatic effect on the process of *Agrobacterium*-induced tumour formation in plants. Genetic transformation mediated by *Agrobacterium* is widely studied and used in higher plants (Gelvin, 2003). A conservation of host factors involved in *Agrobacterium*-mediated transformation is suggested by the fact that agrobacteria can also transform other eukaryotes, including fungi (Janyce et al., 2005), sea urchins (Citovsky et al., 2007) and human cells (Ziemenowicz et al., 2000; Tzfira et al., 2004).

During transformation, *Agrobacterium* transfers a well-defined segment of its Ti (tumour-inducing) plasmid, the T-DNA, into eukaryotic cells, where it is stably integrated into the host genome. The mechanism of *Agrobacterium*-mediated transformation is only partially understood. Host-released signals, particularly phenolics and sugar compounds in combination with acidic pH and temperature (Brencic and Winans, 2005), are perceived by *Agrobacterium* through VirA, a transmembrane histidine protein kinase. VirA *trans*-phosphorylates the VirG transcription factor, which acts as response regulator activating the expression of virulence (*vir*) genes by binding to vir-boxes in their promoters (Gao et al., 2006; Stock et al., 2000). Boundaries of the transferred DNA (T-DNA) in the Ti plasmid are defined by specific *cis*-elements corresponding to 25bp direct repeats. The *vir* gene products VirC1 and VirC2 bind to overdrive sequences adjacent to T-DNA borders and help targeting the VirD1/D2 complex that introduces single-stranded nicks at the 25bp border repeats. During this process, VirD2 forms a covalent bond with the 5' end of lower strand of the T-DNA, the T-strand, which is released by a subsequent strand-replacement DNA synthesis proceeding from the right border to the position of similarly nicked left border (Gelvin, 2000; Tzfira et al., 2004). The VirD2-coupled T-strand, as well as the VirE2, VirE3, VirF, and VirD5 proteins are transported into host plant through a VirB/D4 type 4 secretion system (T4SS T-pili). Upon transfer, the single-stranded DNA binding protein VirE2 assembles as polymer on the T-strand, covering it on its entire length and providing effective nuclease protection. Nuclear localization sequences (NLS) in both VirD2 and VirE2 guarantee rapid translocation of the T-strand into the nuclei of host cells (Gelvin, 1998;

Mccullens and Binns, 2006). Additionally, host factors including importin α (Ballas and Citovsky, 1997), the VirE2-binding bZIP transcription factor VIP1 (Tzfira et al., 2002) and several protein kinases (Tao et al., 2004) also play important roles in nuclear import of the T-strand complex (i.e., T-complex). Once inside of the plant cell nucleus, VirF likely forms a SCF^{VirF} E3 ubiquitin ligase complex, which destabilizes the T-complex through targeting VirE2 and VIP1 to proteasomal degradation (Munro et al., 2007; Schrammeijer et al., 2001). Subsequently, the T-strand may be converted to double-stranded DNA and integrated into the host genome by non-homologous end-joining (NHEJ) and illegitimate recombination mechanisms (Chilton and Que, 2003). Several studies indicate that other host factors, such as VIP2 (Anand et al., 2007b), and histones H3 (Anand et al., 2007a) and H2A (Mysore et al., 2000; Li et al., 2005) are also required for T-DNA integration. Nonetheless, the precise mechanism by which the T-DNA is integrated into the host chromosomes is thus far largely unknown.

The analysis of plant chromosomal junctions of T-DNA insertions demonstrated that the 3' end of integrating T-strand features almost always some limited sequence homology (i.e., micro homology) with the pre-insertion target sites, which often suffer deletions during T-DNA integration (Mayerhofer et al., 1991; Tinland et al., 1995). Sequence compilations of 3'-end junctions of T-DNA insertions are completely consistent with formation of the junctions by non-homologous end-joining (NHEJ, Kohli et al., 1999). However, genetic and molecular analyses of knockout mutations in genes encoding *Arabidopsis* NHEJ components indicates that this pathway is not essential for T-DNA integration (Gallego et al., 2003), although the rate of transformation is significantly reduced by the NHEJ mutations. In contrast to the 3'-end, the 5' end junctions of T-DNA insertions in most plant hosts appear to be very precise and well conserved, reflecting the position of covalently bound VirD2 protein (Tinland et al., 1995). Therefore, the available data suggest that the 3' and VirD2-linked 5' ends of the T-DNA are recombined into the host genome probably by different mechanisms. Although VirD2 is expected to play a pivotal role in interaction of the 5'-end of the T-DNA with host target sites, using *in vitro* studies Ziemienowicz et al. (2000) showed that ligation of VirD2-bound oligonucleotides to target sequences by T4 DNA ligase was less efficient than ligation of free oligonucleotides. It is thus likely that the release of covalently bound VirD2 protein from the 5'-end of the T-strand requires some modification of VirD2 by nuclear host factors.

In T-DNA transformed plant populations selected for the expression of T-DNA encoded antibiotic resistance marker genes, T-DNA integration was found to occur preferentially into promoter regions of plant genes (Alonso et al., 2003; Szabados et al., 2002). This suggests that the VirD2 pilot protein can interact with plant host factors that are associated with promoter sequences that carry open chromatin regions accessible to T-DNA integration (Citovsky et al., 2007). Studies by Bakó et al (2003) demonstrated that in fact the VirD2 protein interacts with the TATA-box binding protein TBP *in vivo*, and that VirD2 is phosphorylated by the RNAPII CTD-binding CDK2-activating kinase CAK2Ms in alfalfa cells. The fact that *Arabidopsis* TBP differs only with few non-conserved amino acids from fungal, insect, animal, and human TBPs suggests that interaction of VirD2 with TBP is

probably involved in precise integration of the 5'-end of T-DNA into the genomes of different organisms (Lacroix et al., 2006). TBP is recruited to mismatches and serves as binding platform for TFIIH, which is recognized by other repair and chromatin remodelling factors involved in the removal of lesions present in the DNA strand by a transcription-dependent mechanism called transcription-coupled repair (TCR) or global genome repair (GGR, Laine and Egly, 2006). Interaction of VirD2 with TBP may thus target VirD2 to the nucleotide excision repair complex that assumingly carries an associated CAK VirD2 kinase.

1.6. Aims of the study

Major goal of the present study was to perform functional characterization of the *Arabidopsis* CDKF;1 protein kinase. To achieve this goal, the study included the following genetic and biochemical approaches:

- **Isolation and characterization of T-DNA insertion mutations in the *CDKF;1*, *CDKD;1*, *CDKD;2* and *CDKD;3* genes.**

In these experiments, we have identified at least two T-DNA insertion mutations in *CDKF;1* and each member of the *CDKD* gene family using PCR-based mutant screens and sequencing the junctions of T-DNA insertions in the target genes. Subsequently, we have performed phenotypical characterization of the T-DNA insertion mutants, including the documentation of developmental defects and assays of their altered responses to plant hormones, and metabolic and environmental factors. Mutations inactivating the individual *CDKD* genes permitted normal seedling development due to functional redundancy of three CDKDs in *Arabidopsis*, whereas inactivation of the unique *CDKF;1* gene by insertion mutations lead to dramatic developmental defects. To assess the effects of inactivation of all *CDKD* genes, we have initiated the construction of triple mutants.

- **Biochemical characterization of CDKF;1 protein kinase.**

To identify potential substrates of CDKF;1, first we have performed a series of *in vitro* protein kinase assays. For these purpose, CDKF;1, CDKD;1, CDKD;2 and CDKD;3 have been purified to apparent homogeneity as N-terminal thioredoxin fusion proteins from *E. coli*. We have found that all four kinases underwent partial autophosphorylation and showed various levels of activity *in vitro*. In contrast to Shimothono et al. (2003), we have observed that CDKF;1 phosphorylated not only CDKD;2 and CDKD;3, but also CDKD;1, as well as the CTD domain of the largest subunit of RNAPII. Using wild type and mutated versions of the CTD consensus heptapeptide as kinase substrate, we have determined the specificity of CTD phosphorylation by CDKF;1 and CDKD;2. These assays indicated that CDKD;2 mediates phosphorylation of the Serine-5 residue, whereas CDKF;1 can phosphorylate Serine-7 residues of the CTD heptapeptide repeats. Using monoclonal antibodies against phosphoserine residues of CTD repeats, we have confirmed a reduction of Serine-5 CTD phosphorylation in the *cdkd;2* insertion mutant *in vivo*. Analogously, we have observed that during early seedling development (i.e., until day 7) the *cdkf;1* mutation causes a remarkable reduction

of Serine-7 phosphorylation, whereas during later stages of plant development it also affects the levels of Serine-2 and Serine-5 phosphorylation. This observation has supported our data indicating that CDKF;1 is an upstream activator of CDKD;2 and therefore affects indirectly Serine-5 phosphorylation of the CTD. The fact that the *cdkf;1* mutant exhibits very low level of Serine-2 phosphorylation of CTD repeats suggests a possible involvement of a yet unknown CDKF;1-activated downstream CTD kinase.

• **Analysis of transcriptional changes by Affymetrix microarray profiling in the *cdkf;1* mutant.**

To determine the effect of CDKF;1 mutation on genome-wide transcription and correlate this with the observed dramatic alterations of developmental, light and hormonal regulatory pathways, we have performed a comparative Affymetrix transcript profiling experiment using 7 days old wild type and *cdkf;1-1* mutant seedlings. At this early stage, wild type and *cdkf;1-1* mutant seedlings showed comparable growth and development despite a root elongation defect in the mutant. Standard analysis of the Affymetrix data using the GeneSpring software indicated that at $p > 0.05$ confidence level only 845 genes showed at least 2-fold or higher changes in transcript levels between the mutant and wild type, while by lowering the cut off value to 1.5-fold resulted in 2385 genes showing significant change in transcription in the *cdkf;1-1* mutant. To confirm that the observed changes in transcript levels lower than 2-fold were reproducible and meaningful, we performed confirmatory quantitative real-time (qRT-PCR) assays to measure precisely the mRNA levels of 132 genes from different pathways. This indicated less than 25% variation between 80% of Affymetrix and qRT-PCR data and revealed that the *cdkf;1-1* mutation resulted in down-regulation of genes encoding key enzymes in the biogenesis pathways of microRNAs, ta-siRNAs, nat-siRNAs and ra-siRNAs. This observation has been confirmed by testing the transcript levels of selected representatives of all four small RNA classes using northern RNA hybridizations. All genes showing altered transcription in the *cdkf;1* mutant were sorted to GO terms and pathways by literature mining, to correlate genome-wide transcriptional changes with the reduction of CTD Serine-7 phosphorylation during early seedling development in the *cdkf;1-1* mutant.

• **Determination of effects of *cdkf;1* and *cdkd* mutations on *Agrobacterium* mediated tumour formation.**

Bakó et al. (2003) has demonstrated that a CTD-associated CDKD-like protein kinase mediates the phosphorylation of VirD2 pilot protein of *Agrobacterium* T-DNA in alfalfa cells. Therefore, we were interested to determine how the *cdkd;1*, *cdkd;2*, *cdkd;3*, and *cdkf;1* knockout mutations affect the process of *Agrobacterium*-mediated plant cell transformation. We have found that the *cdkf;1-1* and *cdkd;2-1* mutations dramatically reduce the number of tumours incited by an oncogenic *Agrobacterium tumefaciens* C58 strain in hypocotyls of *Arabidopsis* seedlings. The deficiency of tumorigenesis in these mutants suggested that both CDKF;1 and CDKD;2 play a role in the recognition and modification of VirD2, and thereby in the process of T-DNA integration. In fact, we found that CDKF;1 can phosphorylate the VirD2 protein at multiple positions *in vitro*. This, together

with the finding that *Arabidopsis* and rice CDKF;1 kinases co-purify with CDKD;2 and cyclin H (Van Leene et al., 2007; Ding et al., 2009) provides a basis for further studying how CDKF;1 and CDKD2 regulate the function of VirD2 during the process of T-DNA integration.

2. MATERIALS AND METHODS

2.1. Materials

2.1.1. Chemicals

Chemicals used in the experiments were purchased from Sigma, Bio-Rad, Merck, Roche, Roth, GE Healthcare, PerkinElmer, Duschefa, Biomol, Boehringer, and Gibco, unless otherwise stated. General solutions and buffers were prepared as described by Sambrook and Russell (2001), unless otherwise stated.

2.1.2. Enzymes

All enzymes were used according to the manufacturer's instructions unless otherwise stated.

<i>Taq</i> DNA polymerase, recombinant	Invitrogen, Karlsruhe, Germany
Accuprime™ <i>Taq</i> DNA polymerase High Fidelity	Invitrogen, Karlsruhe, Germany
Platinum <i>Pfx</i> DNA polymerase	Invitrogen, Karlsruhe, Germany
<i>TaKaRa LA Taq</i> ™	TaKaRa Biomedicals, Shiga, Japan
RNase-Free DNase Set	Qiagen, Hilden, Germany
Restriction endonucleases	New England Biolabs, Frankfurt
Gateway BP Clonase Enzyme	Invitrogen, Karlsruhe, Germany
Gateway LR Clonase Enzyme	Invitrogen, Karlsruhe, Germany
T4 polynucleotide kinase	New England Biolabs, Frankfurt
T4 DNA ligase	New England Biolabs, Frankfurt
Antarctic phosphatase	New England Biolabs, Frankfurt
Protease Inhibitor Cocktails for plant cell and tissue extracts	Sigma, St. Louis, MO, USA
RNase A	Boehringer, Mannheim, Germany

2.1.3. Kits

Nucleospin Plasmid QuickPure Kit	Macherey-Nagel, Germany
QIAquick PCR Purification Kit	Qiagen, Hilden, Germany
QIAquick Nucleotide Removal Kit	Qiagen, Hilden, Germany
QIAquick Gel Extraction Kit	Qiagen, Hilden, Germany
RNeasy Plant Mini Kit	Qiagen, Hilden, Germany
Transcriptor First Strand cDNA Synthesis Kit	Roche, Mannheim, Germany
iQ™ Supermix	Bio-Rad, München, Germany

2.1.4. Bacterial strains**2.1.4.1. E. coli strains**

DH10b	Invitrogen, Karlsruhe, Germany
DB3.1	Invitrogen, Karlsruhe, Germany
BL21(DE3)pLysS	Novagen, Madison, WI
XL10-Gold	Stratagene, La Jolla, USA

2.1.4.2. Agrobacterium strains

C58	wild type
GV3101/pMP90RK	rifampicin, gentamicin and kanamycin resistant
GV3101/pPMP90	rifampicin and gentamycin resistant (Koncz and Schell, 1986)

2.1.5. Vectors

pET201	Horváth, M. 2007 (Ph.D. thesis)
pPCV6NFHyg	Koncz et al., 1989
pDONR201	Invitrogen, Karlsruhe, Germany
N-TAPI	Rohila et al., 2004
pER8GW-XVE (Hyg)	Zuo et al., 2000
pBluescript II SK ⁺	Stratagene, La Jolla, USA
pENTR1A	Invitrogen, Karlsruhe, Germany
pGEX4T-2	Amersham Biosciences GmbH, Freiburg, Germany

2.1.6. Hormones

Name	Stock solution
β-estradiol	10 mM in DMSO
1-Aminocyclopropane-1-carboxylic acid (ACC)	1 mM in H ₂ O
Ethephon	50 mg/ml in methanol
Abscisic acid (ABA)	1 mg/ml in methanol
6-Benzylaminopurine (BAP)	1 mg/ml in 1N NaOH
Gibberellin (GA3)	10 mM in ethanol
Indole 3-acetic acid (IAA)	2 mg/ml in 0.5 M HCl, adjusting pH 5.8 with 0.5 M KOH
Kinetin	1 mg/ml in 0.5 M HCl, adjusting pH 3.0 with 0.5 M KOH

1-naphthylacetic acid (NAA) 1 mg/ml in 0.5 M KOH, adjusting pH 7
to 8 with 0.5 M HCl

The hormone stock solutions were filter sterilized and stored at -20°C

2.1.7. Oligonucleotides

2.1.7.1. Oligonucleotides for cloning

D1FE	AGGAGCGCCGAATTCGGGATCCATGGAACAGCCGAAGAAAGTTGCT
D1RB	CCTGCCTGGTCGTCGACGGATCCTAGGAACTCGAGATCAAGTTTCCTCTTCA
D2FN	GAGCGCCGAGCTAGCGGATCCCTCGAGATGTCGAAATCCGGCGATAATCAA
D2RB	TGCCTGGTCGCGGCCGACGGATCCAGTGAATCCTTCAGGACCCATCACTCT
D3FN	GAGCGCCGAGCTAGCGGATCCATGCCGGAGCAGCCAAAGAAAGT
D3RB	CCTGCCTGGTCGTCGACGGATCCCTGGAACCAAGATCGAGTTTCCTCTTC
F1FX	GAGCGCTGACTC GAG ATGGATAAACAACCGGCGACCAG
F1RN	CTGCTCGCGGCCGCGCTAGCATTGGGGAATTCTATTGTAATCCACTACTGGTAG
HFNB	GAGCGCCGAGCTAGCGGATCCATGGCGGATTTTCAGACATCAACA
HRSB	CCTGCCTGGTCGTCGACGGATCCACCTATGGGTGGCGGTGCC
Uni5	GGGACAAGTTTGTACAAAAAAGCAGGCTTCGAAGGAGATAGAACCATG
Uni3	GGGGACCACTTTGTACAAGAAAGCTGGGTCTCCACCTCCGGATC
FFG	GGAGATAGAACCATGGATAAACAACCGGCGACCAG
FRG	TCCACCTCCGGATCTTCAGGGGAATTCTATTGTAATCCACTACT

2.1.7.2. Oligonucleotides for screening of T-DNA insertion mutants in *Arabidopsis thaliana*

FISH1	CTGGGAATGGCGAAATCAAGGCATC
FISH2	CAGTCATAGCCGAATAGCCTCTCCA
SALKLB	TTTGGGTGATGGTTCACGTAGTGGG
GABI RB	TTCCATTGCCAGCTATCTGTAC
CAK1 5'	CAGGAAAGATCCGAAGAAAAGCGAC
CAK1 3'	ATCAAGATGCTCAACCATGGACTCTG
CAK2 5'	GAAAGATGATGACAAGCTATGCGGGAA
CAK2 3'	AGGGCTTGCATGTAAGCACGGTAAGTC
CAK3 5'	TCTGATGATGTGGGCACGAAAGCA
CAK3 3'	GATGTGGCCGTACATTGGTCTTTAGAA
CAK4 5'	GTTGAAAAAAGTGCCGTTAAATGGTCA
CAK4 3'	CCTATACAACAAGATCACTGCTTCCCAAT

2.1.7.3. Oligonucleotides used for RT-PCR

Name	Sequence (5'-3')	Start	Stop
D1FA	TCCGGAGATGGAACAGCCGA	159	178
D1RA	AATGCAGCCAGCAGCCCAA	759	740
D1RB	TGGTTGGTCGTTTTGGTGGC	1306	1287
D1FC	GCTCCAAGACCAGTTTCCAAGC	1071	1093
D1RC	GCACTGGTGATGGTTGGTCCG	1316	1296

Name	Sequence (5'-3')	Start	Stop
D2FA	CCAATGTCGAAATCCGGCGA	58	77
D2RA	CAGCCTGCAGCCAAACATCA	656	636
D2RB	GCTCGGAGGCCTTTGGTTCG	1024	1005
D2FC	CCCGCTCCACCATTACGTACCA	811	832
D2RC	CTCGGAGGCCTTTGGTTCGAG	1023	1003
D3FA	AACCCGAAAATGCCGGAGCA	193	212
D3RA	TGTCGGCGGGTGAGAGGAAA	532	513
D3FB	CGTTGCCTGCATATTCGCCG	786	805
D3RB	ACCCTCCCACGCTCAGGCAT	1226	1207
D3FC	CCGGAGCCGGAGCTCTCAA	34	53
D3RC	CCTCCCACGCTCAGGCATCA	1224	1205
F1FA	CAACCGGCGACCAGTTGGAG	42	61
F1RA	CCGCAGCGAGATCCGACCTA	336	317
F1FB	ATCTCGCTGCGGTGATCCGA	325	344
F1RB	TGCTCAACCATGGACTCTGCCA	1824	1803
F1FC	GCCTTCCAACCATTACAGGGG	1180	1200

2.1.7.4. Oligonucleotides utilized for Real-time quantitative PCR

Gene	AGI	Primer name	Sequence
Ubiquitin	At3g62250	UbiF	CCAGAAGGAATCGACGCTTCATCTC
		UbiR	GAGAAGGATCGATCTACCGCTACAACAG
Phot1	At3g45780	Pho1F	TGATGCCAACATGACACCAGAGG
		Pho1R	TGCAACGACAACCTTGAGCAGCA
Phot2	At5g58140	Phot2F	GGCAGAGGGACAGTTGGGA
		Phot2R	TCTTCGGGCCGCGTATTAGC
TLP1	At2g02710	TLP1E2F	GGATTGGGAACAGTGTGAAGCGAG
		TLPE3RJ	CTGGTAAGCATGGATTGGTTAATACGA
NPH3L1	At3g15570	NPH3L1F	TCTGCAGCGCGGTGTTTGTG
		NPH3L1R	AACCCGAGCCTCTTCCACCG
NPH3L2	At3g19850	NPH3L2F	CAGGTGGGTCAGATGGGTTCG
		NPH3L2R	CGGCGACTGAGAGGAGGCTG
SOB3	At1g76500	SOB3F	CAGCGGCTCATGGGGCAAAT
		SOB3R	TGTCCTTGACCGGCTCCAGATG
PHYA	At1g09570	PHYA1F	CATCCCTCAAGCAGCCCGTT
		PYHA1R	CCCAGTGGAGCATCACGCAT
PHYB	At2g18790	PHYBF	TCCCGCCAATTTTTGCTGCT
		PHYBR	CCCTCGAGGCTAACCCGCTT

Gene	AGI	Primer name	Sequence
PHYC	At5g35840	PHYCF	TGAAGGACCCCGAAAAGGCA
		PHYCR	CTCAATGCAGGCGTGAAGCG
PHYD	At4g16250	PHYDF	GGCCTCGCAGCGAAGTGATT
		PHYDR	TGCAGCTCGGGACTCGGTATC
PHYE	At4g18130	PHYEF	GCGGGATACCCTGGTGCCAT
		PHYER	TTTCCCACGGCAAGCTCCTG
HY2	At3g09150	HY2F	GCGGGTTTCATGGAGCCTGAG
		HY2R	CCCCATGGGAAAGTCTCAGCA
HO2	At2g26550	HO2F	TCGATTTATCGGGAGTTTTGCTGG
		HO2R	CGTCCCGACTCCAGTGCTCC
PIF3	At1g09530	PIF3F	CGTGCCCTGCAAGAACTCATTCC
		PIF3R	CGATGAACCACCACGGCTCA
PIF4	At2g43010	PIF4F	TCGGCTCCGATGATGTTCCC
		PIF4R	GCTGTCCCGCCGGTGAACTA
AAR3	At1g59940	AAR3F	GTCACGGCGGTTGATAGCGG
		AAR3R	CGGCGAATCCACAAGCGAAG
ARR12	At2g25180	AAR12F	TCGGTGTCCGCAGCCTTTCT
		AAR12R	TGTTATGTGCCGGGGGAGGA
ARR14	At2g01760	AAR14F	GTGGTAGCCTCGAGACTGTTGTTGTTTC
		AAR14R	GAAACAGGACGGTTAGAAGCGGA
ARR3	At2g41310	ARR3F	GCCGTCGAATTCGATAGATTGAAGGT
		ARR3R	TAGACAGAGGCGATTCCACCGTAGAG
ARR9	At3g57040	ARR9F	GCAAGAATCAGCAGATGTTTAGAAGAAGG
		ARR9R	GTCGAATCTAGGACGTGCTCTATCAGTTG
PRR5	At5g24470	PRR5F	CAGACGTGGAGGTTAGTGCGAGAGAC
		PRR5R	GGGTTGGCGTAGGGTATGAACTCTG
PRR7	At5g02810	PRR7F	TCCCCATAATCATCGCTCACA
		PRR7R	ACTTCCACTTCCGCTTCCACTACC
APH1	At3g21510	APH1F	GGGATTTTGGACAGCCAGTTCTTG
		APH1R	GCCGGGATCATTCCACCAGAAG
CCA1	At2g46830	CCA1F	CAATGCACGCCGCAGTAGAATC
		CCA1R	TTGAGTTTCCAACCGCATCCGT

Gene	AGI	Primer name	Sequence
LHY1	At1g01060	LHYE8F	CACGGGCACGCAAATCTTCA
		LHYE8R2	TTTGAGCCACAGGATGAGCGG
CCR2	At2g21660	CCR2E1F	TGGCGTCCGGTGATGTTGAG
		CCR2E1R	GCCACCGCTTCCTCGTGACT
CCR1	At4g39260	CCR1F	CTGAAGTTGAGTACCGGTGCTTTGTC
		CCR1R	CGTTCATCTCTTCAATCGCATCCC
GI	At1g22770	GIE12F	TCTTCTTCTGCGGGCAACTGATG
		GIE14R	TGAGGCGGCGTTGAAGAATCG
WNK2	At3g22420	WNK2E7F	CATGGAGTGTAGCGGTTGAGATGG
		WNK2E7R	ACCCGTTTGAAGCACACTCTCCA
WNK6	At3g18750	WNK6E9F	ACCCACCTGGAAAACCGATGTCA
		WNK6E9R	CTTTGGTGGCATCGACGCATTG
CIR1	At5g37260	CIR1F	CCATTGAGATCCCGCCTCCA
		CIR1R	CTCATGTTGTTTCATCTCAGTCACCGAC
PAP2	At4g29080	PAP2F	GTGATGTCGGCTCGGGTCTG
		PAP2R	CCCAAGGGACATCTCCGACCAG
PAP1	At3g16500	PAP1F	GCCTCCGGTTCGTTTCGTTCA
		PAP1R	ATGGAACATCCCCAACAAAGCATCT
AFR1	At2g24540	ARF1F	GCACGTGGCGAGAGATGAG
		ARF1R	AGCCAGTGAAAAGGGTTTTAGTGAA
PKS1	At2g02950	PKS1F	CGTCGACTCGAAGCAGAGCG
		PKS1R	GCATGCGCATTTACACCCCA
PKS2	At1g14280	PKS2F	CGCGCCTCAGAGACGGAAATC
		PKS2R	GGCGATTGCGTGTGAGAAACAG
HY5	At5g11260	HY5E1F	CATCAAGCAGCGAGAGGTCATCAAG
		HY5E3R	GTCTAAGCATCTGGTTCTCGTTCTGAAG'
HYH	At3g17609	HYHE1F	GAACTCGAGTTCGTCTTCTTCCCACA
		HYHc4R	GCTGCTTAGAACACATGTTGATCCAGCT
CIP1	At5g41790	CIP1F	GAGGAGAGGGGTAAGGAAGTGACATC
		CIP1R	CCCAATTCGTCGCAGTCCACA
LZF1	At1g78600	LZF1F	GCAGCAGCAGGAACAGCAGG
		LZF1R	CGCCCATGATGTCTCACCTCCC
STH	At2g31380	STHF	CCCTCCCTGCGACATCTGCC
		STHR	GCAGCGGGTTGCTGAGTTGG

Gene	AGI	Primer name	Sequence
DCL1	At1g01040	E16F	GGTTCACCTTATCCGAGGTGCTCAGAG
		E17R	CACCCTCTAGTTCACCATCTCCATC
DCL2	At3g03300	DCL2E23F	GCAAACCTGCACAAACACATCCTG
		DCL2E24R	ACTCAACTCGAACTGCCACTTCTGAC
DCL3	At3g43920	DCL3E20F	CGTAAAACCTCGCTCGGGGATA
		DCL3E22R	CACGATTGGGTATCCTTAGGGTTATGG
DCL4	At5g20320	DCL4E22F	AGCAGCAAAACCGCAAAATCCC
		DCL4E22R	CCTTTCTTCGTTGCTCTAGCCTCACC
AGO1	At1g48410	AGO1E21F	CACTTCTCGACCTGCTCATTACCAC
		AGO1 3'	CGTGTGCTTCTACCAGCCATTC
AGO4	At2g27040	AGO4E15F	CATTATCCTTGGGATGGATGTTTCAC
		AGO4E23R	CCAAGCTGAGCAGCTGCCAAGTG
AGO6	At2g32940	AGO6F	TCATGGGCCTCCAGGTCGGG
		AGO6R	TTCCGTGCCCTGCTTGTCGG
AGO7	At1g69440	AGO7E2F	GAACTTGCCGTGTCTGCAAATCAGTAG
		AGO7E3R	CTGCCTCCAATACTCATCAAAGCCC
RDR2	At4g11130	RDR2E2F	GACGAAAAACCCATGTCTTACCCT
		RDR2E4R	GGCTTTTTTCAGGGTCACGGTCTG
RDR6	At3g49500	RDR 5'	GGACCTGTACTTTGTGGCTTGGGA
		RDR3'	ACCCGTCTGTAAAGCCGACCCA
HYL	At1g09700	HYLE1F	GCTCGTGAAAATGACCTCCACTGATG
		HYLE3R	GGTTCTTGCATAATCCCGTTTCGTG
HASTY	At3g05040	HSTE1F	GCGGTCCAATTCCTGGATTCTGTA
		HSTE6R	GAGTAAGTCCCCGCAACAATAGCCT
HEN1	At4g20910	HENE5F	GATACTGTGAGAATCCGCTCGCTCC
		HENE9R	GACAATCAGGAGCTTGGGGTGGAAC
DRD1	At2g16390	DRDF	TGGCTGACGATCCTGGTGGCT
		DRDR	CAGCTGCTGTGCCCGGTTCT
miR162a	At5g08185	162a5'	TAGTTGGAAGAAGAGTGAGAGTCGCTG
		162a3'	AAGAAAGATACAAGAGGCAAACGCTGG
miR165a	At1g01183	Pri165a5'	CTGCTAAGATCGATTATCATGAGGGTTAAG
		Pri165a3'	AATGTAACAATAAATGGTGATCAGAGGCAAT

Gene	AGI	Primer name	Sequence
miR172a	At2g28056	Pri172a5'	CTGTTTTTGCTTCCCCTCTGCCA
		Pri172a3'	GTGGATCTATTAATGTCTTGATAAAGACTGCC
miR172b	At5g04275	Pri172b5'	TTGCACCTCTCACTCCCTTTCTCTAACTA
		Pri172b2R	CAAGGGCTGACGTGTCAACTTATAAGTG
miR172c	At3g11435	Pri172c5'	TTCCAGCAAAATGGTGCCGTCTT
		Pri172c3'	CCTCCGATCTGTGAATTCCTACAAAAAG
TAS1a	At2g27400	TAS1AF	TGAGCGCCGTCAAGCTCTGC
		TAS1AR	ACAGAGAGGGCGACGGGAGG
TAS1b	At1g50055	TAS1bF	GAGATAGGTTCTTAGATCAGGTTCCGCTGT
		TAS1bR	GTAATTGGCGGTAGACTTCATGACACATC
TAS2	At2g39681	TAS2F	GTTGGGTTTGGGAGTGAGTTTACGAG
		TAS2R	TTACAAGTGCAAAAGTGATGAACGCTC
TAS3	At3g17185	TAS3E1F	TTAGCGAGACCGAAGTTTCTCCAAG
		TAS3E2R	GCTCAGGAGGGATAGACAAGGTAGGAG
KRP2	At3g50630	KRPF	ACGACGACGACGGTGAAACGA
		KRPR	TCGTCTCCGACGCTCCTGCT
SIM	At5g04470	SIMF	CCGCAGAAACCCCGTCCACC
		SIMR	GGCCACCGTGATAGCCGTCG
ZWI	At5g65930	ZWIF	ACCACAGTGTCTGATGCTGTTGAGGA
		ZWIR	TGTGCAGCATCGTCCCTCCCA
AS1	At2g37630	AS1-1F	ATGGAAGTTGCTCTTGAGTTTGGGATTA
		AS1-2R	CCTGAAGACGGATCACAAGCCTCTG
AS2	At1g65620	AS2-F1	CCATCGAGAGCCTCAAAACCCAA
		AS2-R2	GGCTTCTGTTGCTCAGAGGGGAAATA
CO	At5g15840	COE1F	GCTCAAGTTCACTCTGCCAATCGC
		COE1R	AGGGAACAGCCACGAAGCAACC
FLC	At5g10140	FLCE1F	GGCAAGCTCTACAGCTTCTCCTCCG
		FLCE4R	CACGGAGAGGGCAGTCTCAAGGTG
FT	At1g65480	FT-F	CACCAGGGTGGCGCCAGAAC
		FT-R	TCCTCCGCAGCCACTCTCCC
SOC1	At2g45660	SOC1E6F	GAGAAAGCTCTAGCTGCAGAAAACGAG
		SOC1E7R	GGTAACCCAATGAACAATTGCGTCTCT

Gene	AGI	Primer name	Sequence
COL1	At5g15850	COL1E1F	TCAACGAGTTCCAATTCTGCCCA
		COL1E1R	ACAACCATGAAGCCGCCTCTGC
COL2	At3g02380	COL2E1F	CGATGAGGATGATCGAGAGGTTGCTT
		COL2E1R	GACCCTAGCCTCCCTCTCCATTG
COL9	At3g07650	COL9E4F	CAATGCCTGCTCACATTTCAGTAACCC
		COL9E5R	TGGTTGGGGTGAGAGGGTTCGT
CDF2	At5g39660	CDF2E1F	CGGTTTAGGACGAGAAGAAGGTGATG
		CDF2E2R	GCTGTTACATCGCGGACACGG
AP2	At4g36920	AP2E10F	TTCCGGCGGCTGAGAACCAC
		AP2R	GAGAGGAGGTTGGAAGCCATTTGTCT
SMZ	At3g54990	SMF1	CCGTGGAAGACAGTCACTGGTTGAA
		SME5R	CCTAAGTGTTTGCACGAACTCCACC
SNZ	At2g39250	SNZF1	CAAGAAGCTCTCATTATCGTGCGT
		SNZE5R	AGCTTGCACTCGCTCGTCTAAGAGAT
TOE1	At2g28550	TOE1F1	GGAGAGGACCAAGGTCTAGAAGTTCACA
		TOE1E5R	GCGAAAACCCCGTGCTCTGTCTAC
TOE2	At5g60120	TOE2F1	ATAGGTAGCGGGAGCGGTGGTG
		TOE2E6R	GCAGCTTCCCTTCCCTTCCATTG
TOE3	At5g67180	TOE3F1	GATAAAGAAGAGCCGACGTGGTCCTC
		TOE3E6R	CTAGCAGCTTCAATCTCGGTATCAAAGAG
AP3	At3g54340	AP3E4F	GTGAGTGTTTGGACGAGCTTGACATTC
		AP3E7R	GAGCGTAAGCACGTGACCCTTCG
PI	At5g20240	PIE3F	TGTCGAGCACGCCATTGAACA
		PIE6R	CCTGAAGATTTGGCTGAATCGGTTG
AGL24	At4g24540	AGL24E1F	GAAGAGGAATCTTCAAGAAAGCCGAT
		AGL24E4R	CTCCAGCCGCTGCAACTCTTCT
AG	At4g18960	AGE5F	GCAATTGATGGGTGAGACGATAGGG
		AGE8R	CTGGAGAGCGGTTTGGTCTTGG
SVP	At2g22540	SVPE1F	GTTCTCTGCGACGCCGATGTC
		SVPE3R	CAATTTCTTTACTCATTCGGGCGTG
SEP3	At1g24260	SEP3E7R	AGATGCCACTCCAGCTGAACCCT
		SEP3E8R	CCATTCATCTTGTTGCCCTG

Gene	AGI	Primer name	Sequence
SEP4	At2g03710	SEP3E7R	GGACAGTGATGCAGCACTTACTCAATC
		SEP3E8R	GTTGGTTGCATTTGCAGGATTGTG
ATC	At2g27550	ATCE4F	AGAGATAATCGGGTACGAGATGCCTC
		ATCE4R	CGGTCTCACGCTGGCAGTTGAAG
ULT1	At4g28190	ULT1E2F	GGTTATCATTGGGGGCGAAAAGG
		ULT1E3R	GTGAAGTCGACACAAGTCTGGCAAGT
SPL2	At5g43270	SPL2E4F	CCAAAACCGCAAGAGCCGAGT
		SPL2E5R	GGGTTGGAGGTTGCTTGAGGG
MYB33	At5g06100	MYB3E3F	CCCTCCTCGAAGCGACTTTGG
		MYB3E4R	GGTGAATGTCGGTTTCCATAGAGAGG
MYB101	At2g32460	MYB1E3F	CCTAAACCCGATCCCCGATTCTTC
		MYB1E3R	CCTCGAGACAAGGCTTGAGACTCC
MAX1	At2g26170	MAX1E4F	TGCAAGGGAAACTGCTAAAGAAGTGG
		MAX1E5R	ATCTCTGTCCAACACAGGCTCGTG
MYB88	At2g02820	MYB8E9F	GGCAACCTGATCTCCATGATTCACC
		MYB8E9R	CCAGTTGAGAGTAAACCCACTTGTTC
FLP	At1g14350	FLPE9F	GCTCGTCCCGAAAAATCCTGATG
		FLPE10R	GGACTCTTTTGCAAGGGGGTGG
TRN2	At5g46700	TRN2E1F	TGTACTIONTTTTGGGTTGCCTTGTCGG
		TRN2E2R	ATCCACATTTTGTGGGGGCTTG
TRN1	At5g55540	TRN1E2F	CATGTTATGCGAATTTAGGCGGG
		TRN1E2R	ACCCAATGCAGCAGCGACCC
ATH1	At4g32980	ATH1E2F	GTTTCGGTCTACGGAATTGGATGTTC
		ATH1E4R	ATGCATTGCTTGGCTCATCATAACAG
BEL1	At5g41410	BEL1E2F	GACTCTTGTTGACGCTCATCCTTGG
		BEL1E3R	TCGTTCCATGGGTTGAGTTGTGAC
BLH3	At1g75410	BLH3E3F	TCTCTCGCCATTTCCGCTGTTTAC
			TCGTGTTTGAGCTGAGATGTTTCCTG
OFP16	At2g32100	OFP16F	GTCCAATGCAATCACCGACTCACC
		OFP16R	GGAGAAAGCCCTGATGACGAACTTG
RIK1	At3g29390	RIK1E5F	CACATATCTGCCGCTGCCAGT
		RIK1E7R	CGAGCAGCAACATTAGATGATGGGTC

Gene	AGI	Primer name	Sequence
ZAT6	At5g04340	ZAT6F	AGAAACCGTGACCTTGACCTGCC ACACTTCCTCCCCGCCACC
SHR	At4g37650	SHRF SHRR	GAAGTCTTGCCATTAAGTGCCTAGG CCACGCACTAGCCCAAACCACC
LPR1	At1g71040	LPR1E2F LPR1E3R	GACGTGTCAAACGCCGTTCTCAC CTGAGTCGGATCGAATGGGTAAGATG
SCL3	At1g50420	SCL3F SCL3R	GCAGCTGAGGCACGTGAGAATG TCTATACCCATCAAACCAGCACCT
CRF5	At2g46310	CRF5F CRF5R	CTCTGGCTTGGGACTTTTGCGAC GTGGAATTCGTCGAGAAACAAAGGG
CRF6	At3G61630	CRF6F CRF6R	TTCCTAACTCCGCCGACGCC ACACCAAACCCGCCGACGAT
CGA1	At4g26150	CGA1F CGA1R	ACCACCAGCGACAGCAGCAA ATGACCGGTGGGGATACGCC
ST1	At2g03760	ST1F ST1R	CATATCGCATCTTTCGCTCCCC TCTCGCGCTTGCATACCAGTA
CIPK20	At5g45820	CIPK20F CIPK20R	TGTTTGGTCTTGCGGGGTTGTG TCTTCACTCCTACATCGCTCTTCGTC
ABA1	At5g67030	ABI1E13F ABI1E15R	GCGCATTGTGATCCCTTCGTCTC GCGGGAAAATTCGGTGTGCTC
NCED4	At4g19170	NCED4F NCED4R	ACGTTTACGCGGCGATTGGAG GGCGATTTAGCGTCCATCACCAG
CIPK14	At5g01820	CIPK14F CIPK14R	GCATTCCCAAGTGGACCTCACC CGCCGACACGATCTCCTCCA
CIPK6	At2g17290	CIPK6E6F CIPK6E7F	CAGCGAGTTTATTGCAGCGACGA GGAAACATTTGCATCCTCACC GA
ATDR4	At1g73330	ATDR4F ATDR4R	CTTTGGCCGCACCCTCCCTA GGTAGGCCCAAGTCAAGCGGA
ABF1	At1g49720	ABF1E1F ABF1E4R	GAATCCGCTGCTAGATCAAGGGCTC TGACTTCACCTTCTTACCACGGACC
RHA2A	At1g15100	RHA2AF RHA2AR	GACTAGCCAACATAATCGTTCTCGCC AATCCCTCCCAACGCTACGCTG

Gene	AGI	Primer name	Sequence
RHA2B	At2g01150	RHA2BF	GTACCGCTACTCCGACAACGCAG
		RHA2BR	TCACTGCCATGTCCCTGATGATG
AFP2	At1g13740	AFP2E1F	ACCGGCGGAGATGGAAGAGG
		AFP2E2R	GTTCCCTGGCTTCCGCTGTTC
AFP3	At3g29575	AFP3E1F	TGGTGGTCAACGATAGGTCAGGG
		AFP3E2R	TCTCGGGCTGAGATTGGGCAC
SWEETIE	At1g67140	SWEE39F	TTGCTGTGCTTCCAGTAACACACC
		SWEE40R	CCGGCTCCTCTTCAGCAACACT
ADH1	At1g77120	ADH1E5F	CGGATGGTGGGGTGGACAGG
		ADH1E7R	CCCATGGTGATGATGCAACGAATAC
GBF3	At2g46270	GBF3E10F	AGGAAAGTGGAAGCCTTGACAGCC
		GBF3E11R	TGCGGGGACTCTCTTTTCGGG
AHB1	At2g16060	AHB1E2F	TCCAAAGCTCAAGCCTCACGCA
		AHB1E4R	GCCTGACCCCAAGCCACCTTC
SLAH1	At1g62280	SLAH1E1F	CCAGTGGTTCACAACGGAGAAGAGA
		SLAH1E2R	AAGCCCACCACGCGACATTGA
ASA1	At5g05730	ASA1E8F	GGCAGGAACCAGCAAGAGAGGG
		ASA1E9R	CTGTTCCCACTGGTAAAGCCGCAC
CYP79B2	At4g39950	CYP79E1F	TGCCGATGCTCACTGGACTTGA
		CYP79E2R	ACGGCGTTTGATGGATTGTCTGG
ESM1	At3g14210	ESM1E4F	TGGGAGCGAGTAAATTCGTGGTTC
		ESM1E5R	GCAACCATATGCATTGTGTGTCCC
PLA2A	At2g26560	PLA2AE5F	ACTGGGGATGCTGCTTCTGTTGA
		PLA2AE6R	CTTTTGCATGAGGTGAACGAATGTCTC
LOX1	At1g55020	LOX1E7F	AAAACCACTGGACCTTCCCTGACC
		LOX1E8R	ACCAAACCTCAAGCCCATCCACTG
OPR3	At2g06050	OPR3E2F	GGAAGCAAGTTGTGGAAGCAGTTCAC
		OPR3E3R	ACGTGGGAACCATCGGGCAA
AOC4	At1g13280	AOC4E1F	GAGCAAGATCCACCACTTCCTCCAC
		AOC4E2R	CATGTTGGATCAAAACGCAGAGACC
JAZ1	At1g19180	JAZ1E2F	CCGACAACAACCATGAGTTTATTCCC
		JAZ1E2R	TTGGGGAGGATTGGATTGGCTC

Gene	AGI	Primer name	Sequence
ST2A	At5g07010	ST2AF	CGACGTCCCGAAAGCCGAAG
		ST2AR	GGTTGCGAACGTTCTTGGACTGG
PBS3	At5g13320	PBS3E3F	CCGTTGTCACTGGTTCAATGGGAC
		PBS3E4R	GTTGAGGTGTCAGCATAACTGGTGAAG
EDS1	At3g48090	EDS1E4F	GAATACAAGCCAAAGTGTCAAGCCC
		EDS1E4R	CATATATGTAGCGGGTTGGTCTTCCTC

2.1.8. *Small RNAs probes for northern blot analysis*

U6	GCTAATCTTCTCTGTATCGTTCC
COPIA	TTATTGGAACCCGGTTAGGA
TAS1	TACGCTATGTTGGACTTAGAA
miR156	GTGCTCTCTCTCTCTGTCA
miR165	GGGGGATGAAGCCTGGTCCGA
miR172	ATGCAGCATCATCAAGATCT

2.1.9. *Plant materials*

All *Arabidopsis thaliana* lines used in this study were in the Columbia (Col-0) background. The different alleles of T-DNA insertion mutations in the *CDKD;1*, *CDKD;2*, and *CDKD;3* genes were isolated from the SALK SiGNAL collection (<http://signal.salk.edu>). T-DNA insertion mutations in the *CDKF;1* were collected from the SALK and GABI-Kat (<http://www.gabi-kat.de>) collections.

2.2. *Methods*

2.2.1. *Plant growth conditions*

Arabidopsis plants were grown in MSAR medium (Koncz et al., 1994) in a controlled culture room at 22°C with 120 mol/m²s light intensity and a photoperiod of 8 h light and 16 h dark. Seedlings from *in vitro* cultures were transferred into soil and grown under standard greenhouse conditions (long day: 16h light/8 h of dark period; 22-24°C day temperature and 18°C night temperature, 80 to 120 mol/m²s light intensity). For crosses and *Agrobacterium*-mediated transformation, *Arabidopsis* seeds were sown in soil and plants were grown under short day condition (8h light/16h dark) for 14-16 days and then transferred to long day condition to induce flowering and produce seed.

2.2.2. *Crossing of Arabidopsis plants*

Upon removal all open flowers and young siliques from the inflorescence axis selected for crossing, the sepals and petals of 3 to 5 unopened flower buds were removed, and then these flowers were emasculated by dissecting the anthers a using magnifying glass headset and fine pair of forceps. The

stigma of the recipient flower was pollinated with pollen grains from open mature flowers of the donor plant.

2.2.3. Seedling growth assays in different light regimes

Seeds were sterilized by 5% calcium hypochlorite solution for 10 min, washed with sterile H₂O and plated on MSAR medium. To induce seed germination, plates kept for 1 day at 4°C in the dark, followed by 1h exposure to red light. The germinating seedlings were either grown in complete darkness or subjected to constant red (12 mol/ m²s), far-red (6 mol/m²s), or blue light (2.5 mol/m²s) illumination for 7 days. As white light source, cool-white fluorescent tubes (photon irradiance of 400 to 700 nm) were used at a fluence rate of 80 mol/m²s. Red, far-red, and blue lights were provided by light-emitting diodes (LEDs). To compare light responses of wild type control and mutant plants, hypocotyls lengths of at least 100 seedlings were measured.

2.2.4. Phytohormone treatments

Sterilized seeds were plated on MSAR medium containing different hormones, including: 50mg/l ethephon (ethylene generating chemical), 10 µM 1-aminocyclopropane-1-carboxylic acid (ACC, ethylene precursor), 0.1 µM brassinolide, 1 µM ABA (abscisic acid), 10 µM GA3 (gibberellin), 0.5 mg/l 6-benzylaminopurine (BAP, cytokinin) with 0.05 mg/L 1-naphtaleneacetic acid (NAA) or 0.1 BAP with 0.5 mg/l of NAA. Similarly, plant growth responses were also assayed in MSAR media containing either 5% sucrose or 3% glucose. In case of ethephon and ACC treatments, the germination assays were performed in the darkness at 22 °C for 7 days, while all other hormone assays were carried out by growing seedlings in the culture room (see: 2.2.1) for 7 days.

2.2.5. Hypocotyl tumorigenesis assay

Young seedlings of *cdkf;1*, *cdkd;1*, *cdkd;2*, and *cdkd;3* mutant and wild type plants carrying four expanded leaves were used in hypocotyls tumorigenesis assays. The oncogenic *Agrobacterium tumefaciens* C58 strain was grown in YEB liquid medium to an OD₆₀₀ 0.6. The *Agrobacterium* culture was supplemented with 50 µM acetosyringone (pH 5.5) and injected into each hypocotyl by Femtotip (Eppendorf).

2.2.6. Agrobacterium-mediated transformation of Arabidopsis thaliana by vacuum infiltration

Arabidopsis plants were transformed by *Agrobacterium* using the vacuum infiltration method (Bechtold et al., 1993; Clough and Bent, 1998) with minor modifications. From bolting *Arabidopsis* plants grown in the greenhouse the siliques were removed, to reduce the background of untransformed seeds. *Agrobacterium* cultures grown in 500 ml YEB medium at 28°C to an OD₆₀₀ of 0.8 to 1.0 were harvested by centrifugation (4°C, 10,000g) and resuspended in infiltration medium containing 4.3g/l

MS basal salt mixture, 1X B5 vitamin, 3% sucrose, 5 mM MES, 0.05 μ M BAP, and 0.005%(v/v) Silwet L-77. *Arabidopsis* plants were submerged in the *Agrobacterium* suspension followed by application of vacuum for 3 minutes. Subsequently, the plants were covered with plastic bags for 2 days to secure for slow adaptation to lower humidity. Seeds were collected in paper bags, dried and subjected to selection for the *Agrobacterium* T-DNA encoded antibiotics resistance markers by germination on MSAR agar medium.

2.2.7. General molecular biology techniques

Standard molecular biological techniques, such as PCR amplification, agarose gel separation of DNA and RNA, restriction enzyme digestions, genomic DNA extraction, preparation of *E. coli* competent cells and purification of plasmid DNAs by CsCl-ethidium bromide equilibrium density gradient centrifugation were performed according to standard protocols described by Sambrook and Russell (2001).

2.2.8. Construction of bacterial and plant expression vectors

The cDNA fragments carrying CDKD coding sequences (i.e., both wild and T-loop mutated versions), as well as coding regions of CDKF;1 and CycH;1 cDNAs, were obtained by PCR amplification using plasmid clones of full-length cDNAs as templates. The full-length cDNA constructs were donated by Arp Schnittger, Strasburg. The PCR products were cloned in pET201, a bacterial expression vector providing a polylinker between coding sequences for an N-terminal thioredoxin and a C-terminal His6 tag, by *EcoRI-XhoI* (CDKD;1), *NheI-NotI* (CDKD;2), *NheI-XhoI* (CDKD;3), *SalI-NotI* (CDKF;1), and *NheI-XhoI* (CycH;1) respectively. For expression of CDKF;1 kinase in plants, a PCR amplified cDNA sequence flanked by *attB1* and *attB2* sites was inserted by BP recombination into pDONR201 (Invitrogen) and then by LR reaction cloned into the TAP-tagging expression vector N-TAPI (Rohila et al., 2004).

2.2.9. Site-directed mutagenesis

Site-directed mutagenesis of coding sequences was performed using a Quick Change Multi Site-Directed Mutagenesis Kit (Stratagene) according to manufacture's instructions. The mutagenesis procedure was based on PCR reactions that were carried out using either pET201-CDKD;1 or pDONR201-VirD2 DNAs as templates and one of more mutagenesis primers combined with the indicator primer provided by the manufacturer. Typically, the PCR reactions of 25 μ l contained 50 ng plasmid DNA template, 100 ng of each mutagenesis primer, 1 μ l of dNTP mixture, 2.5 μ l of 10x QuickChange Multi reaction buffer, and 1 μ l of QuickChange Multi enzyme blend. The PCR product was digested by *DpnI* at 37°C for 1 hour to digest the double-stranded non-mutated template DNA. After dialysis against ddH₂O, the PCR products were transformed into XL-10 Gold Ultra Competent *E. coli* (Stratagene) cells, which were then plates on selective LB medium containing appropriate

antibiotics. From each transformation, plasmid DNA was purified from three independent recombinant clones and correct positions of the designed mutations (i.e., excluding any other change in the target sequences) were verified by sequencing.

2.2.10. Purification of *Arabidopsis* proteins expressed in *E.coli*

E.coli BL21 (DE3) pLysS cells carrying GST-CTD (Umeda et al., 1998) were grown at 28°C to OD₆₀₀ of 0.4-0.6. Expression of the GST-CTD protein expression was induced by 1mM IPTG for 4h at 37°C. The cells were harvested by centrifugation and then resuspended and sonicated in lysis buffer (50 mM NaH₂PO₄, 300 mM NaCl, 1mM PMSF, 0.1 mM benzamidine, 10 µg/ml aprotinin, 10 µg/ml leupeptin, pH 8.0). The cell lysate was subjected to centrifugation (Sorvall HB-4 rotor, 11000 rpm for 30min at 4°C) and the cleared extract was used for protein purification. Affinity purification was carried out on glutathione-Sepharose 4B (Amersham Biosciences) as described (Bakó et al, 2003). *E.coli* BL21 (DE3) pLysS cells carrying pET201-thioredoxin-CDKDs-His₆, pET201-thioredoxin-CDKF;1-His₆, and pET201-thioredoxin-CycH;1-His₆ were disrupted by sonication in lysis buffer and upon centrifugation (see above) the cleared extracts were applied on Ni-NTA agarose (Qiagen) according to the manufacturer instruction. Elution of matrix-bound proteins was performed by increasing the imidazol concentration in stepwise manner from 60 to 250 using 20 mM intervals. The protein profiles of fractions were visualized by SDS-PAGE and the fractions carrying the purified target proteins were collected.

Lysis buffer (1 liter):

50 mM NaH ₂ PO ₄	6.90 g NaH ₂ PO ₄ ·H ₂ O (MW 137.99 g/mol)
300 mM NaCl	17.54 g NaCl (MW 58.44 g/mol)
10 mM imidazole	0.68 g imidazole (MW 68.08 g/mol)

Adjust pH to 8.0 using NaOH.

Wash buffer (1 liter):

50 mM NaH ₂ PO ₄	6.90 g NaH ₂ PO ₄ ·H ₂ O (MW 137.99 g/mol)
300 mM NaCl	17.54 g NaCl (MW 58.44 g/mol)
20 mM imidazole	1.36 g imidazole (MW 68.08 g/mol)

Adjust pH to 8.0 using NaOH.

Elution buffer (1 liter):

50 mM NaH ₂ PO ₄	6.90 g NaH ₂ PO ₄ ·H ₂ O (MW 137.99 g/mol)
300 mM NaCl	17.54 g NaCl (MW 58.44 g/mol)
250 mM imidazole	17.00 g imidazole (MW 68.08 g/mol)

Adjust pH to 8.0 using NaOH.

2.2.11. Immunaffinity purification of HA-VirD2 protein

To purify the HA-VirD2 protein described by Bakó et al., 2003), an anti-HA Affinity Matrix (Roche) was used. *E.coli* BL21 (DE3) pLysS cells carrying the pET28a-HA-VirD2 plasmid were grown and induced by IPTG as described in 2.2.10 and then harvested cells by centrifugation, resuspended and sonicated in lysis buffer (20 mM Tris-HCl [pH 7.5], 0.1 mM EDTA; 150 mM NaCl; 1mM PMSF; 0.1 mM benzamidine; 10 µg/ml aprotinin; 10 µg/ml leupeptin). The cleared extract was applied on HA matrix in a disposable chromatographic column and incubated on a rocker for 1h at 4°C. The flow through was collected for further analysis and the matrix was washed by 10 volumes of washing buffer (20 mM Tris-HCl [pH 7.5] 50 mM NaCl; 1mM PMSF; 0.1 mM benzamidine; 10 µg/ml aprotinin; 10

$\mu\text{g/ml}$ leupeptin). During washing, the flow through was also collected for protein analysis. Lysis buffer containing 1mg/ml HA peptide was utilized as elution buffer. The eluted HA-VirD2 protein fraction was further purified by anion-exchange chromatography on a 1ml pre-packed HiTrap DEAE-Sepharose FF anion exchange column (GE Healthcare). The column was equilibrated with Tris-HCl pH 8.0. Elution was carried out by increasing NaCl concentration ($40\text{--}260\text{ mM}$) in stepwise manner using 20mM intervals. The SDS-PAGE profile showed that fractions eluting with $80\text{--}120\text{ mM}$ NaCl contained the purified HA-VirD2 protein.

2.2.12. Protein kinase assays

Affinity purified wild type and mutant thioredoxin-CDKDs-His₆, thioredoxin-CDKF;1-His₆, thioredoxin-CycH;1-His₆, and GST-CTD proteins were used in *in vitro* protein kinase assays. The kinase reactions contained $1\text{--}2\mu\text{g}$ substrate (i.e., CDKD;1, or CDKD;2 or CDKD;3 or GST-CTD or alternatively one of the CDKDs together with GST-CTD) and $0.25\text{--}0.5\ \mu\text{g}$ thioredoxin-CDKF;1-His₆ protein in kinase-buffer (50 mM Tris-HCl [pH 8.0], 15 mM MgCl₂, 1mM DTT, and $5\ \mu\text{Ci}$ [$\gamma\text{-}^{32}\text{P}$]ATP). The kinase reactions were incubated for 90 min at room temperature. The reactions were separated by SDS-PAGE and subsequently the dried gel was placed into an autoradiography cassette with a X-ray film and exposed for 15 min up to 4 h .

2.2.13. Immunoblotting

For western blot analysis, total protein extracts were prepared in protein extraction-buffer containing 50 mM Tris-HCl (pH 7.5), 10% glycerol, 1 mM EDTA, 150 mM NaCl, and 0.2% Igepal. Protein concentration of tissue extracts were determined by Bradford assay (Bio-Rad) using a BSA dilution series as standard. The protein samples were subjected to size separation by SDS-PAGE electrophoresis and electro-transferred onto PVDF membranes (Millipore). Primary antibodies used for detection of various target proteins were: a mouse monoclonal antibody 4H8 (Abcam, ab5408), RNAPII mouse monoclonal antibody H14 (Covance), rat monoclonal antibody (rmAb) 3E10, rmAb 3E8, and rmAb 4E12 (Chapman et al., 2007; Egloff et al., 2007). Protein detection was performed by autoradiography of Enhanced Chemoluminescence ECL (ECL) generated by horseradish peroxidase-coupled secondary antibodies: goat anti-rat IgG (Sigma, A 9037), anti-mouse IgM (Sigma, A8786), and goat anti-mouse IgG (Thermo Scientific Pierce).

2.2.14. Two dimensional protein gel electrophoresis

IEF (iso-electric focussing) and SDS-PAGE were carried out according to Görg et al. (1998) with minor modifications. For IEF with a linear gradient (pH 3–10), IPG strips of 11 cm were rehydrated using rehydration buffer (8 M w/v urea, 2% w/v CHAPS, 0.28% w/v DTT, 2% v/v IPG buffers) in a rehydration tray at room temperature for 16h . For IPG strip of 11 cm , $40\ \mu\text{g}$ protein was loaded and conducted at 20°C with Protean IEF Cell (Bio-Rad). The first equilibration was performed in a

solution containing 50 mM Tris-HCl (pH 8.8), 6 M urea, 30%(v/v) glycerol, 2% (w/v) SDS, and 1% (w/v) DTT, with a few grains of bromophenol blue. The second equilibration was performed as the first one, except that DTT was replaced with 2.5% (w/v) iodoacetamide. The second dimension was developed with a NuPAGE 4-12% Bis-Tris ZOOM gel (Invitrogen). The protein spots were stained using a phosphor-staining kit (Pro-Q Diamond Phosphoprotein gel stain, Invitrogen) followed by Coomassie PAGEBlue (Fermentas) staining according to the manufacturer's protocols.

2.2.15. Protein identification and database search

The protein spots separated by two dimensional gel electrophoresis were selected and robotically punched from Coomassie stained gels using a Proteineer SPII system (Bruker Daltonics). The punched spots were then digested with trypsin and spotted on AnchorChip™ targets by a Proteineer dp robot (Bruker Daltonics). Peptide mass fingerprint (PMF) data were collected on an UltraflexIII MALDI ToF/ToF spectrometer (Bruker Daltonics) and used for database searches as described below. Following on-target recrystallization of the sample spots, MS/MS spectra were collected on selected precursors as described (Suckau, 2003) for verification of PMF identifications and for further sample elucidation. Both MS and MS/MS data were used to search against the May 2007 release of NCBI non-redundant database (<http://www.ncbi.nlm.nih.gov>) and version 8 of the TAIR *Arabidopsis* Protein database (www.arabidopsis.org) using MASCOT (<http://www.matrixscience.com>).

2.2.16. Mass spectrometry analysis of CDKF;1 phosphorylated VirD2

After kinase assay and two dimensional gel electrophoresis, the VirD2 spots were excised and subjected to the following treatment: The gel-plugs were rinsed with an ammonium bicarbonate buffer/acetonitrile 1:1 mixture to eliminate the CBB and the SDS. The proteins were reduced with DTT and alkylation of sulfhydryl groups was performed with iodoacetamide. Then the proteins were incubated with Promega side-chain protected porcine trypsin for approximately 4h. The resulting peptides were extracted. Phosphopeptides were enriched by TiO₂. The digest was dried down and redissolved in 1 % TFA in 50 % acetonitrile and loaded on TiO₂ beads suspended in the same solvent. After a few minutes of vortexing, the supernatant was discarded and the TiO₂ beads were washed five times with the loading solvent. Phosphopeptides were eluted with 1% NH₄OH. Samples were subjected before and after phosphopeptide enrichment to MALDI-TOF MS (Reflex III, Bruker) analysis using 2,5-dihydroxybenzoic acid (DHB) as matrix, and to LC-MS/MS analysis on an ion trap (XCT Plus, Agilent Technologies) equipped Q-TOF (Waters) mass spectrometer. Data were processed using the softwares XMass 5.1.5 (MALDI-TOF), Mascot Distiller 2.1.1.0 (Q-TOF) and DataAnalysis 5.2 (for ion trap). Database searches were performed by Mascot v2.1 (<http://www.matrixscience.com>) on the NCBI 20071130 database (5678482 sequences). For MALDI-TOF MS data, monoisotopic masses with mass tolerance of ± 200 ppm, for Q-TOF data, monoisotopic masses with peptide mass tolerance of ± 50 ppm and fragment mass tolerance of ± 0.1 Da, and for ion trap data monoisotopic

masses with peptide mass tolerance of ± 1 Da and fragment mass tolerance of ± 0.8 Da were considered. No species restriction was used and two missed cleavages were permitted. Fixed modifications were: Cys carbamidomethylation; whereas variable modifications parameters were: acetylation of protein N-termini, methionine oxidation, pyroglutamic acid formation from N-terminal Gln residues and phosphorylation of amino acid residues. Subsequently, all data were also manually inspected.

2.2.17. RT-PCR

Total RNA was extracted by RNeasy Mini kit supplied with RNase-Free DNase set (Qiagen). Two micrograms of total RNA template was reverse-transcribed using a Transcriptor First Strand cDNA Synthesis Kit (Roche Applied Science) with gene-specific primer sets (primer sequences, see: 2.1 Materials). The resulting cDNA:RNA hybrids were applied as templates to PCR amplify *CDKD* and *CDKF;1* cDNAs. The PCR products were fractionated using agarose gel electrophoresis and stained with ethidium bromide.

2.2.18. Real-time quantitative PCR

Total RNA samples were prepared using RNeasy columns (QIAGEN) and treated with RNase-Free DNase according to the manufacturer's instructions. RNA (1 μg) was then reverse transcribed into cDNA using Transcriptor First Strand cDNA Synthesis Kit (Roche). The reaction mixture was diluted to 100 μl , and a 2.5 μl aliquot was used for each real-time PCR reaction performed with iQ Supermix (Bio-Rad) in a Bio-Rad iCycler iQ5. Ubiquitin UBQ5 (At3g62250) primers were used to generate a standard curve for quantification. The applied PCR conditions were 10 min at 95°C for enzyme activation, followed by 38 cycles: 95°C for 45 s, 60°C for 30 s, 72 for 3 min.

2.2.19. Light microscopy

Light microscopy was performed with Leica MZFLIII microscope and images were captured and processed with Diskus version 4.30.102 program.

2.2.20. Confocal-laser-scanning microscopy

Confocal-laser-scanning microscopy was performed with Leica TCS SP2 AOBS (Leica, Wetzlar, Germany) or LSM 510 META (Zeiss, Heidelberg, Germany).

2.2.21. Pollen preparation for fluorescence analysis

Anthers carrying mature pollen grains were collected from flowers and put in a droplet (15 μl) of DAPI solution (2.5 $\mu\text{g}/\text{ml}$ of 4',6-diamidino-2-phenylindole (DAPI); 0.01 % Tween; 5 % DMSO; 50 mM PBS buffer, pH 7.2) on a microscopy slide. Cover slip was used to squash anthers in order to

release pollens. The slides were then kept in darkness until the rim of the cover slip was dry, and then sealed with nail polish. After 4-12 hours incubation at 4 °C in darkness, the preparations were inspected for DAPI fluorescence with UV filter.

2.2.22. Flow cytometry for ploidy analysis

Fluorescence-activated cell sorting (FACS) analysis was performed with leaf tissues of 2 to 3 weeks old wild type and *cdkf;1-1* mutant seedlings. The samples were sliced with a razor blade in nuclear extraction buffer of the CyStain UV-Precise kit (Partec). All preparations were subsequently filtered through a 30µm filter and stained with nuclear staining solution (CyStain UV-precise kit by Partec) containing DAPI. We used a Partec flow cytometer with 405nm solid state laser for excitation and a 440/40 band pass filter for recording of DAPI fluorescence. Data were evaluated using the Flomax software (Partec GmbH).

2.2.23. Small RNA detection by northern RNA hybridization

Detection of small RNAs was performed by northern blot analysis as described (Pall and Hamilton, 2008). Total RNA extracts were prepared from 7 days old young seedlings using Trizol extraction (Sigma, T9424) according to manufacturer's instructions. For comparison of expression levels of small RNAs in wild type and *cdkf;1-1* mutant seedlings, 40 µg of total RNA was size separated in 15% polyacrylamide gels with 7M urea under denaturing condition and transferred to Hybond-NX membrane (Amersham Biosciences) by electroblotting. The RNA samples were cross-linked to the membrane using a EDC (1-ethyl-3-(3-dimethylaminopropyl)-carbodiimide (0.373g) in 10ml H₂O containing 122.5 µl 1-methylimidazole for 1h at 60°C. Hybridization was carried out at 37°C using oligonucleotides complementary to specific small RNAs, which were labelled with γ^{32} ATP using T4 polynucleotide kinase (New England Biolabs).

2.2.24. Transcript profiling using Affymetrix Arabidopsis ATH1 microarrays

Comparative microarray transcript profiling of *cdkf;1* mutant and wild type was performed with Affymetrix ATH1 GeneChip microarrays. Short day-grown seedlings (7 DAG) were used for total RNA extraction using RNeasy Mini Kit (Qiagen). The hybridization probes were prepared and processed by the Affymetrix hybridization service at the MPIZ by generating three independent microarray datasets for both wild type and *cdkf;1-1* samples. The microarray data analysis was performed using the GeneSpring GX10 (Agilent) software. According to MIAME standards, the data were first summarized using the RMA algorithm using a baseline to the median of all samples followed by quality control with principal component analysis (PCA). The raw data were filtered for expression by percentile (upper cut-off 100, lower cut-off 20) and then filtered for error at a coefficient variation <50%. Subsequent statistical analysis with TTest for unpaired samples included asymptotic p value computation using 100 permutations and Benjamin-Hochberg multiple testing for

false-discovery rate (FRD). Subsequently, the data were filtered allowing either 1.5 or 2-fold difference between control wild type and mutant transcript levels and subjected to further statistical analysis of Gene Ontology (GO) terms using a cut-off value <0.1 . To assist proper annotation of data to pathways, the Significant Pathway analysis tool with a cut-off value of p-value <0.01 was used from the GeneSpring package, and then the data on pathway allocation of functions were combined with updated information obtained by mining the latest literature references in the PubMed and TAIR databases.

3. RESULTS

3.1. Isolation and molecular characterization of *cdkf;1* and *cdkd* mutations

In a reverse genetic approach, different T-DNA insertion mutations identified in the SALK and GABI collections were used to study the roles of *CDKF;1* and *CDKD* genes in plant development. Exact positions of the insertion mutations in the *CDKF;1* and *CDKD* genes have been determined by PCR amplification of T-DNA boundaries using T-DNA border and gene specific primers and sequencing the obtained PCR products.

3.1.1. Mutations in the *CDKF;1* gene

We have identified two independent T-DNA insertion mutations in the *CDKF;1* gene. In both *cdkf;1* mutant alleles, *cdkf;1-1* (GABI_315A10) and *cdkf;1-2* (SALK_148336), the T-DNA insertion has been localized in exon2 of *CDKF;1* gene.

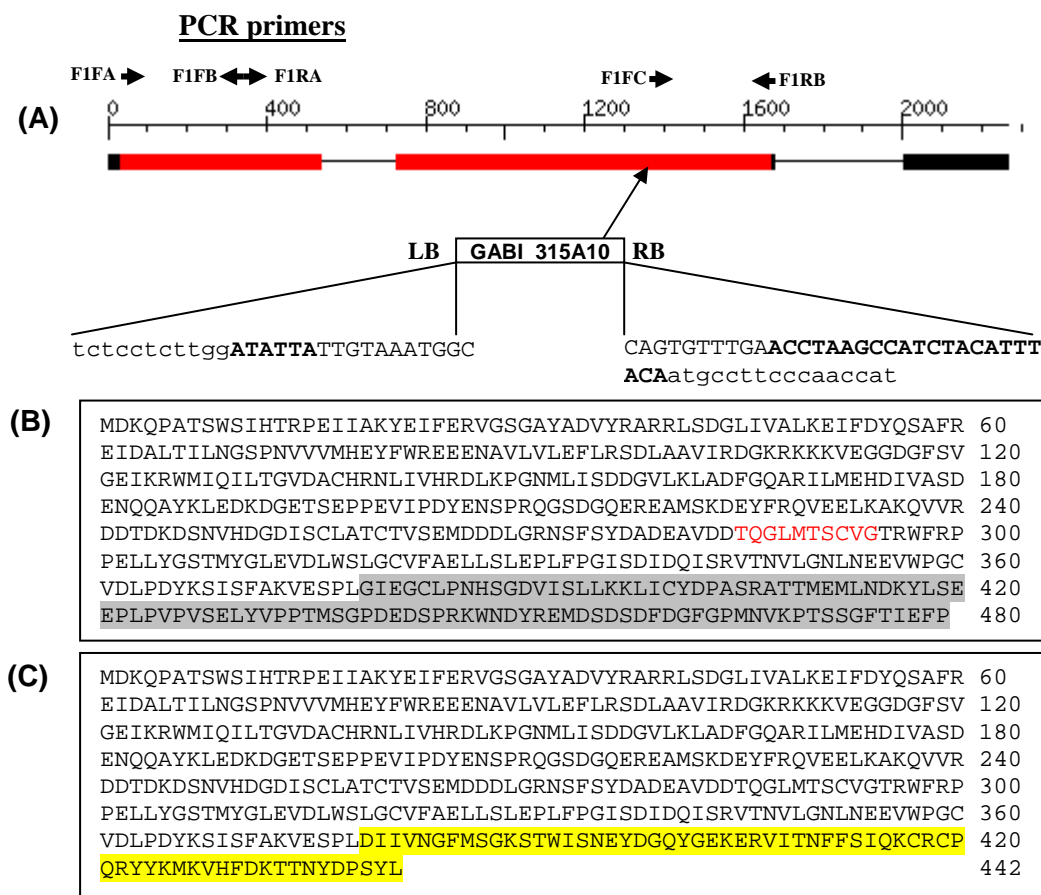


Figure 1. T-DNA junctions in the *cdkf;1-1* (GABI_315A10) mutant.

(A) An arrow shows the position of the integrated T-DNA. Black and red blocks depict untranslated and exon regions, respectively. Intron sequences are marked by black lines. Capital, small and bold capital letters represent border sequences, coding sequences, and filler DNA, respectively. (B) Amino acid sequence of CDKF;1 protein. The region shaded in grey is not translated due to interruption of the gene by the T-DNA insertion. Red letters indicate the position of the T-loop region. (C) Predicted sequence of C-terminally truncated CDKF;1 protein, which is fused to a T-DNA-encoded C-terminal peptide (highlighted in yellow) and possibly expressed due to transcription of the *cdkf;1-1* allele from its native promoter. Positions of PCR primers used for RT-PCR analysis of transcribed regions of mutant allele are shown above the scale bar.

In the *cdkf;1-1* (GABI_315A10) mutant a single T-DNA insertion was located in exon2. The T-DNA used for generation of GABI insertion mutants carries a promoter of mannopine synthase 2' gene in close vicinity of the left border (LB). Therefore, plant sequences in junction with LB are transcribed in the mutants. In the *cdkf;1-1* allele this event may generate an antisense transcript from the 5'-coding domain of *CDKF;1*, whereas the T-DNA insertion prevents transcription of 3'-coding sequences as the right border (RB) region of the T-DNA does not carry promoter elements (Figures 1A and B). Theoretically, transcription of the *cdkf;1-1* allele from its native promoter could result in the translation of an N-terminally truncated protein in fusion with a C-terminal peptide domain encoded by the LB segment of the T-DNA. If synthesized, this C-terminally truncated fusion protein is predicted to carry the catalytic domain of the kinase, including the T-loop sequences (Figure 1C).

Sequencing of T-DNA border junctions in the *cdkf;1-2* mutant revealed integration of an inverted T-DNA repeat flanked by LB junctions in exon 2. Sequences of T-DNA border junctions, illustrating the generation of short filler DNA sequences during T-DNA integration, are shown in Figure 2A.

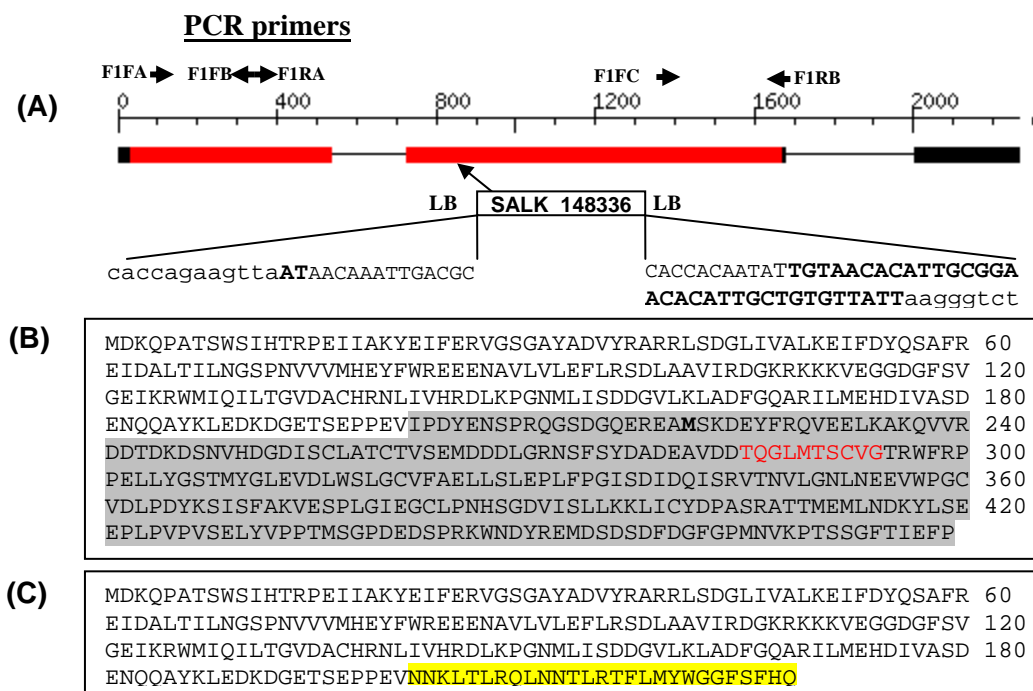


Figure 2. Analysis of T-DNA insert junctions in the *cdkf;1-2* (SALK_148336) mutant.

(A) An arrow shows the position of T-DNA insertion in exon2. Black and red blocks mark untranslated and exon sequences, respectively, whereas introns are labelled by black lines. Capital letters, small letters and bold capital letters represent T-DNA border sequences, coding sequences, and filler DNA, respectively. (B) Amino acid sequence of CDKF;1 protein. The region shaded in grey represents the predicted C-terminal domain, which is predicted to be transcribed and possibly translated from an internal start codon (highlighted by bold M) in the *cdkf;1-2* mutant. Red letters indicate the T-loop region of CDKF;1 kinase. (C) Predicted sequence of the N-terminal kinase domain, which could potentially be expressed in fusion with C-terminal T-DNA encoded peptide sequences (highlighted by yellow colour) in the *cdkf;1-2* mutant. Positions of PCR primers used for RT-PCR analysis of transcribed regions of mutant allele are shown above the scale bar.

The T-DNA used for generation of SALK insertion mutants carries promoter and enhancer sequences from the Cauliflower Mosaic Virus 35S RNA gene near the left border (LB). Sequences of the tagged genes located downstream of the T-DNA left border junctions are therefore transcribed in the SALK mutants. This predicts that coding sequences located at 3'-downstream of the T-DNA integration site

in the *cdkf;1-2* mutant are transcribed by the 35S promoter and possibly translated from an internal methionine start codon, resulting in an N-terminally truncated segment of CDKF;1 protein lacking the kinase catalytic domain (Figure 2B). On the other hand, transcription of the *cdkf;1-2* allele from its native promoter could result in a translational gene fusion between 5'-coding sequences and the 5' T-DNA LB junction, and yield a fusion between part of the N-terminal kinase domain and a small C-terminal T-DNA encoded peptide (Figure 2C).

Despite these theoretical considerations, characterization of the *cdkf;1-1* and *cdkf;1-2* mutants revealed (see: 3.4.1) that both SALK and GABI T-DNA insertions in the *CDKF;1* gene resulted in fully identical phenotypes. This excluded the possibility that predicted expression of a C-terminally truncated kinase from the *cdkf;1-2* allele could confer a partial loss of function phenotype.

3.1.2. Insertion mutations in the *CDKD* genes

In public insertion mutant collections only a single T-DNA insertion (SALK_114643) was identified in the *CDKD;1* gene. In the *cdkd;1-1* mutant, integration of an inverted T-DNA repeat flanked by LB junctions has been identified in exon 5 (Figure 3A).

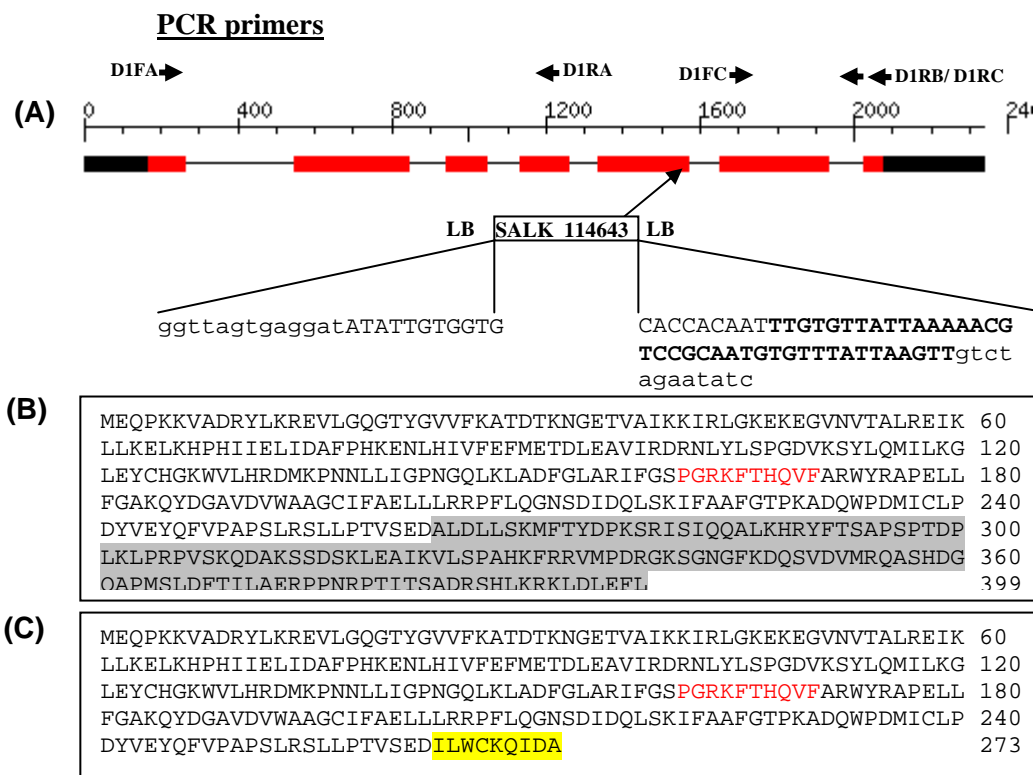


Figure 3. Characterization of T-DNA insert junctions in the *cdkd;1-1* (SALK_114643) mutant.

(A) An arrow shows the position of integrated T-DNA. Black and red blocks depict untranslated and exon sequences, respectively. Introns are marked by black lines. Capital, small and bold capital letters indicate T-DNA border sequences, coding sequences, and filler DNA, respectively. (B) Amino acid sequence of the CDKD;1 protein. The T-loop region is indicated by red letters. The truncated 3' coding region could be transcribed by a 35S promoter located upstream of LB in the T-DNA. (C) Transcription of the *cdkd;1-1* allele from its native promoter could lead to the synthesis of a fusion protein carrying the N-terminal kinase catalytic domain in fusion with a small T-DNA encoded C-terminal peptide marked in yellow. Positions of PCR primers used for RT-PCR analysis of transcribed regions of mutant allele are shown above the scale bar.

Due to transcription from 35S promoters of the T-DNA LB regions, an antisense 5'-transcript and a truncated 3'-transcript encoding the C-terminal cyclin-binding domain of CDKD;1 could be theoretically generated in the *cdkd;1-1* mutant (Figure 3B). On the other hand, transcription of the *cdkd;1-1* allele from its native promoter may lead to translation of a C-terminally truncated CDKD;1 kinase, which carries the catalytic domain with the T-loop, but lacks the cyclin-binding regulatory domain (Figure 3C).

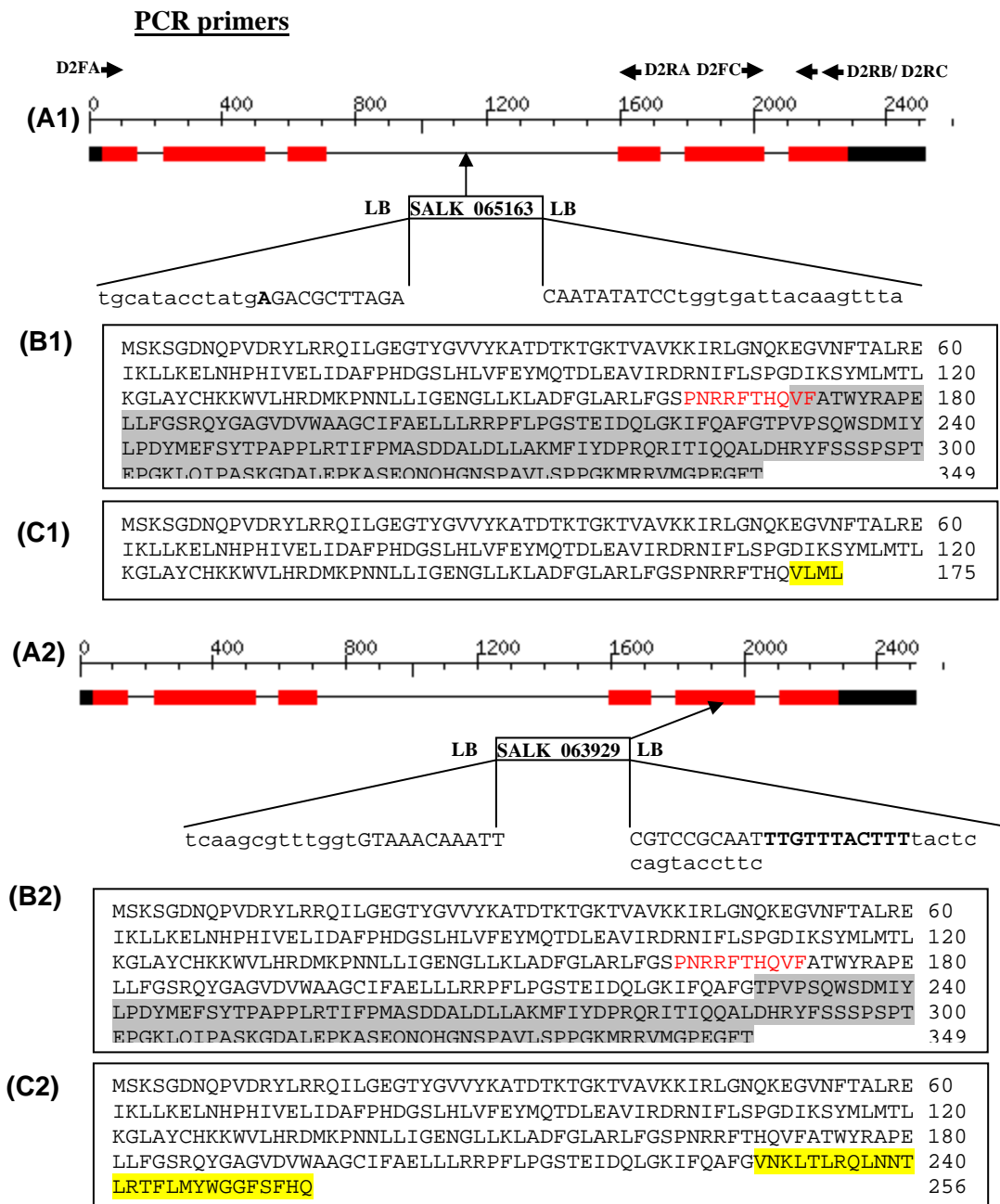


Figure 4. Analysis of T-DNA insert junctions in the *cdkd;2-1* and *cdkd;2-2* mutants.

(A1/A2) Arrows indicate the positions of integrated T-DNAs. Black and red blocks mark untranslated and exon sequences, whereas introns are shown by black lines. Capital, small and bold capital letters represent T-DNA border sequences, coding sequences, and filler DNAs, respectively. (B1/B2) Amino acid sequence of CDKD;2 protein kinase. Red letters show the T-loop region. Regions shaded in grey represent C-terminal cyclin-binding domains of CDKD;2 that could theoretically be synthesized due to transcription of 3' coding sequences in the *cdkd;2-1* and *cdkd;2-2* mutants. (C1/C2) Sequences of N-terminal kinase domains in fusion to T-DNA encoded peptides that may be expressed from truncated 5'-coding domains transcribed by the native CDKD;2 promoter in the *cdkd;2-1* and *cdkd;2-2* mutants. Positions of PCR primers used for RT-PCR analysis of transcribed regions of mutant allele are shown above the scale bar in A1.

In the *CDKD;2* gene two mutations were identified. Both *cdkd;2-1* (SALK_065163) and *cdkd;2-2* (SALK_063929) mutations were caused by insertions of inverted T-DNA repeats flanked by LB junctions that were mapped in intron 2 and exon 5, respectively (Figure 4). In both *cdkd;2* mutants, bidirectional transcription from 35S promoters of LB regions is expected to generate 5' antisense and 3' sense transcripts. Analogously, transcription from the native *CDKD;2* promoter is theoretically expected to generate 5'-truncated transcripts that encode a truncated N-terminal kinase catalytic domain without intact T-loop sequences in *cdkd;2-1* and a full-length T-loop containing kinase domain in *cdkd;2-2* in fusion with T-DNA encoded C-terminal peptides of different lengths.

We have also obtained two independent T-DNA insertion mutations in the *CDKD;3* gene (Figure 5). In the *cdkd;3-1* (SALK_120536) mutant a single T-DNA insertion was mapped to the beginning of exon 3. As downstream of exon 3 the right border (RB) region of T-DNA (i.e., which lacks promoter elements) is found in junction with 3' coding sequences of the *cdkd;3-1* allele, transcription of these sequences is unlikely (Figure 5A1). Consequently, the *cdkd;3-1* allele is expected to represent a genuine knockout mutation as the T-DNA insertion interrupts the coding region of kinase catalytic domain. By contrast, in the *cdkd;3-2* mutant a single T-DNA insertion has replaced the translational stop codon by adding two new codons to the 3'-end of the coding sequence (Figure 5A2). This sequence change is not expected to influence the protein function, but interruption of 3'-untranslated sequences of *CDKD;3* by the T-DNA insertion could potentially alter the stability of mRNA. This latter possibility was tested by a RT-PCR assay.

3.1.3. *Transcripts analysis of CDKF;1 and CDKD genes in the T-DNA insertion mutants*

To examine transcription of mutant *cdkf;1* and *cdkd* alleles, RT-PCR assays were performed with cDNA templates synthesized from RNA samples of homozygous T-DNA insertion mutant lines. In these assays, we have tested the transcription of 5' and 3' coding regions flanking the T-DNA insertions, as well as monitored the lack of full-length transcripts by designing specific oligonucleotide primers to the 5' and 3' ends of transcribed sequences (see: Figure 5A2). The results confirmed nearly predictions described above, indicating the activities of native promoters and transcription of truncated gene sequences through the activity of 35S promoter of SALK T-DNA LB junctions. The *cdkd;1-1* allele represented the only exception, where transcription of sequences located 3'-downstream of the right T-DNA LB junction in *cdkd;1-1* (Figure 6, third panel, primers D1FC-D1RC) could not be detected. As transcribed 5'-domains of *cdkd;1-1* allele could potentially be translated to truncated protein carrying the kinase domain with an intact T-loop, the assessment whether this mutation result only in a partial loss of function has to be delayed while suitable antibody become available.

In the predicted leaky *cdkd;3-2* (SALK_007756) mutant, the RT-PCR assay detected transcription of both 5' and 3' segments, as well as full-length sequences of the coding region, as expected (Figs. 5 and 6). However, the levels of all three PCR amplified transcript segments were less in the *cdkd;3-2* mutant compared to wild type, indicating that the T-DNA insertion in the 3' UTR lead indeed to some reduction in the amount of mRNA.

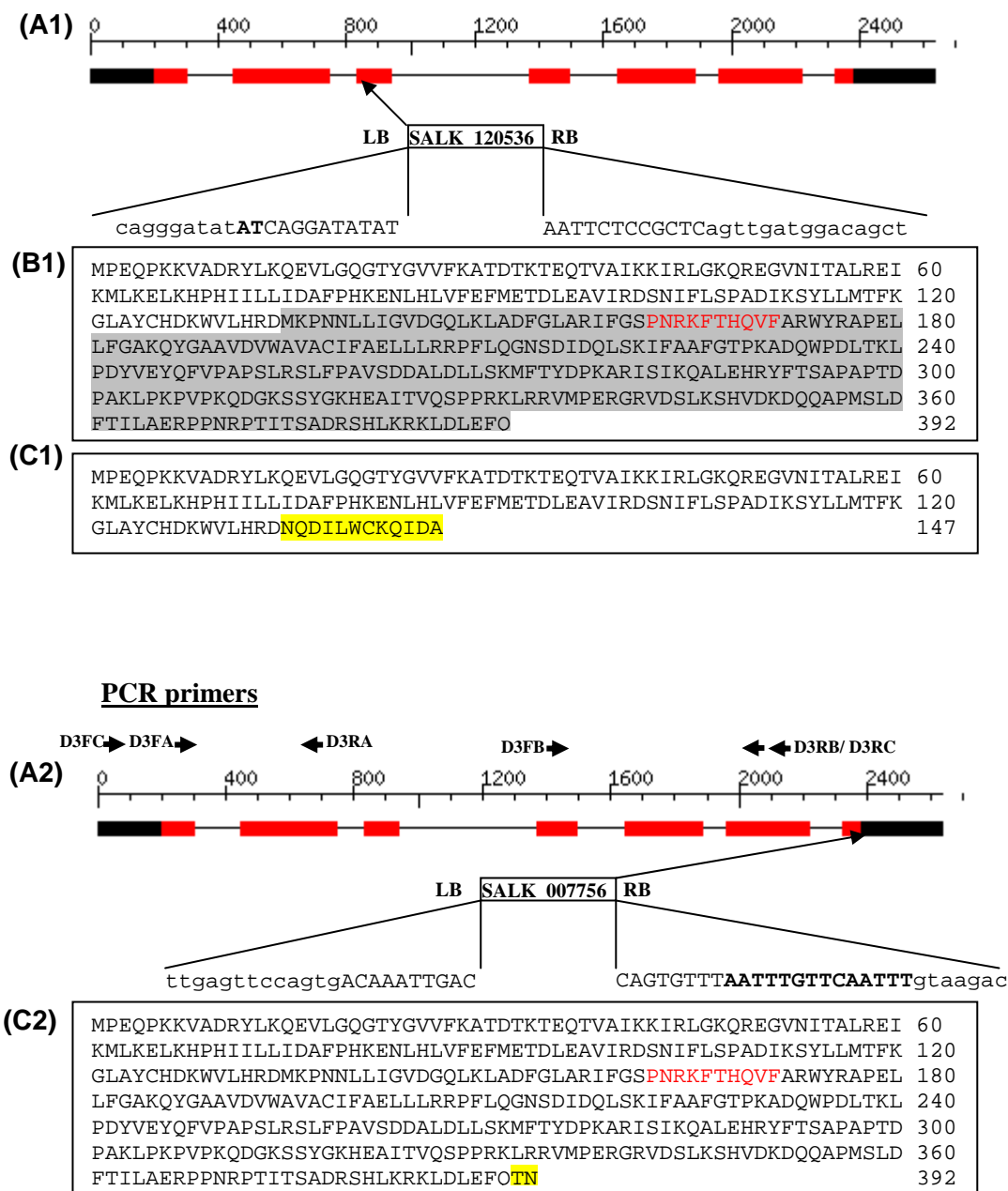


Figure 5. T-DNA junctions in the *cdkd;3* mutants.

(A1/A2) An arrow shows the position of integrated T-DNA. The positions of oligonucleotide primers used in PCR assays described in Figure 6 are shown above the scheme. The black and red blocks depict untranslated and exon regions, respectively. The intron regions are marked by black lines. Capital, small and bold capital letters represent border sequences, coding sequences, and filler DNA, respectively. **(B1)** The sequence of CDKD;3 protein. The region shaded in grey is not translated because of T-DNA insertion. The red letters show T-loop region. **(C1/C2)** The sequence of CDKD;3 recombinant protein after T-DNA insertion. The highlighted yellow part is additional fused polypeptide to the first part of CDKF;1 protein. Positions of PCR primers used for RT-PCR analysis of transcribed regions of mutant allele are shown above the scale bar in A2.

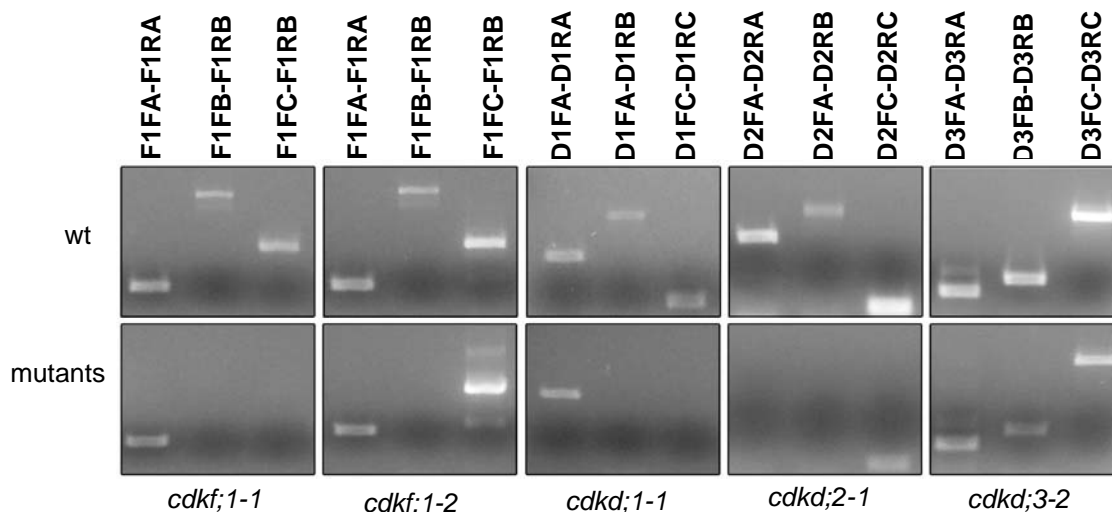


Figure 6. RT-PCR detection of transcription of T-DNA insertion mutant *cdkf;1* and *cdkd* alleles.

The first panels from the left show RT-PCR assays of transcription regions 5' upstream (first lanes: primers F1FA-F1RA), 3'-downstream (third lanes: primers F1FC-F1RB), and overlapping the position (second lanes: primers F1FB-F1RB) of *cdkf;1-1* T-DNA insertion in the wild type and mutant alleles. Next to the right, the same primer combinations were used to detect transcribed regions of *cdkf;2-1* allele. The third and fourth panels show RT-PCR detection of transcription 5' upstream (first lanes: primers D1FA-D1RA and D2FA-D2RA), 3'-downstream (third lanes: primers D1FC-D1RC and D2FC-D2RC), and overlapping the position (second lanes: primers D1FA-D1RB and D2FA-D2RB) of T-DNA insertions in *cdkd;1-1* and *cdkd;2-2* using cDNA templates prepared from RNAs of wild type and *cdkd* mutants. The last panel to the right shows an RT-PCR assay of transcription 5' upstream (first lane: primers D3FA-D3RA), 3'-downstream (second lanes: primers D3FB-D3RB), and overlapping the position (third lane: primers D3FC-D3RC) of *cdkd;3-2* T-DNA insertion in the wild type *cdkd;3-2* mutant alleles.

3.2. Analysis of phenotypic characteristics of the *cdkf;1* and *cdkd* mutants

3.2.1. Phenotypic characterization of the *cdkd* mutants

To assist the study of functional importance of the CDKD1, CDKD2, and CDKD3, protein kinases in *Arabidopsis*, we performed a preliminary characterization of *cdkd* knockout mutants. Different properties were surveyed including flowering time, root length, hypocotyls length, site shoots, and auxiliary shoots. There were no recognizable phenotypic changes in the individual *cdkd* mutants compared to wild type. The seeds of *cdkd* mutants germinated as wild type in the presence of 0.5% sucrose, 3% glucose, 50mg/l ethephon, 10 μ M ACC, 0.1 μ M brassinolide, 1 μ M ABA, 10 μ M GA3, and 0.5 mg/l 6-benzylaminopurine (BAP) plus 0.05 mg/L 1-naphthaleneacetic acid (NAA; i.e., shoot inducing hormone combination, which inhibits root formation), and 0.1 BAP plus 0.5 mg/l NAA (i.e., root/callus inducing hormone combination; data not shown). The lack of alterations in developmental, sugar and hormonal responses in the single *cdkd* mutants indicated that none of the three CDKD genes alone plays a distinguished role in these processes. Rather, the CDKD protein kinases appear to perform redundant and/or overlapping functions, where inactivation of one of the CDKDs by a T-DNA insertion mutation is compensated by complementary function of another CDKD.

To confirm this conclusion, we have constructed *cdkd;1-1, cdkd;2-1* (SALK_114643 and SALK_065163), *cdkd;1-1, cdkd;3-2* (SALK_114643 SALK_007756), and *cdkd;2-1, cdkd;3-2* (SALK_065163 SALK_007756) double mutants and compared their developmental and hormonal responses. Again, we failed to find any recognizable phenotypic difference compared to wild type. However, the triple mutant *cdkd;1-1, cdkd;2-1, cdkd;3-2* (SALK_114643, SALK_065163, SALK_007756), which carried the weak *cdkd;3-2* allele, showed a significant reduction in seedling growth compared to wild type (Figure 7). This suggested that the *cdkd;1-1* and *cdkd;2-1* mutations are possibly null mutations as a slight reduction in *CDKD;3* transcript levels by the *cdkd;3-2* mutation in this background resulted in a clear retardation of growth and development. Whether or not *cdkd;1-1* is indeed a genuine knockout mutation, will be soon determined by characterization of an alternative *cdkd;1-1, cdkd;2-1, cdkd;3-1* (SALK_114643, SALK_065163, SALK_120536) triple mutant, which carries the putative *cdkd;2-1* and *cdkd;3-1* null mutations. In addition, there is a second, likely null *cdkd;1-2* (MPI8258) allele available, which carries a T-DNA insertion in exon 2.



Figure 7. The leaky *cdkd;3-2* mutation causes a significant reduction of plant growth in the *cdkd;1-1, cdkd;2-1* mutant background.

The size of leaves and inflorescence stems of *cdkd;1-1, cdkd;2-1, cdkd;3-2* (SALK_114643 SALK_065163 SALK_007756) triple mutant seedlings (two pots to the left) are about 30-40% smaller compared to wild type.

This allele has been previously identified by screening the insertion mutant collection of our laboratory (Shimotono et al., 2006) and can now be used for construction of a third combination of a *cdkd;1-2*, *cdkd;2-1*, *cdkd;3-1* (MPI8258, SALK_065163, SALK_120536) triple mutant, in order to generate a complete allelic series. Preliminary characterization of *cdkd* mutations summarized above provides a basis for further dissection of CDKF;1-CDKD kinase regulatory circuit, from which the CDKF;1 function is characterized in detail in this work.

3.2.2. Characterization of *cdkf;1* mutants

Seedlings carrying either the *cdkf;1-1* (SALK_148336) or *cdkf;1-2* (GABI_315A10) mutant allele showed completely identical alterations in all performed assays. Both *cdkf;1* mutants were characterized by highly retarded development producing tiny plants with twisted and serrated leaves. Furthermore, the loss of CDKF;1 function resulted in inhibition of root elongation and reduction of the number of root hairs (Figure 8). The mutant plants have started to initiate flowering upon 56 ± 10 days of vegetative development in long days, but this could be accelerated and achieved within 27 ± 4 days using gibberellin treatment. The mutant inflorescences carried petalless, fully sterile male and female organs. Cross pollination with wild type failed to yield any seed.

Scanning electron microscopic measurement of cell size showed that leaf epidermal cells of *cdkf;1* mutants were 40-50% smaller compared to wild type. In addition, the cell numbers per leaf were also less in *cdkf;1* compared to than wild type seedlings, indicating a lack of compensatory mechanism described for some cell cycle mutants (Inzé and De Veylder, 2006). Furthermore, instead of developing normal trichomes carrying three branches, most of the trichomes possessed only 2 branches or remained unbranched (i.e., stichel-like) in both *cdkf;1* mutants. These observations suggested that upon exit from the cell cycle the normal endoreduplication process, determining the final size distribution of leaf cells, could be affected by the *cdkf;1* mutations. To test this possibility, a FACS analysis was performed. The results of DNA profiling indicated identical relative percentage of 2C, 4C, 8C, and 16C cells in the *cdkf;1* mutants compared to wild type. This observation demonstrated that the *cdkf;1* mutations caused no endoreduplication defect. Nevertheless, the reduction of cell number in various organs (e.g., leaves, hypocotyls etc.) suggested a cell proliferation defect in the *cdkf;1* mutants (Figure 9).

To test possible effects of the *cdkf;1-1* mutation on gametogenesis, the offspring of self pollinated hemizygous *cdkf;1-1/+* T2 mutant families was examined. Instead of the expected 3:1 Mendelian segregation of wild type and *cdkf;1-1* mutant progeny, a distorted 4:1 segregation ratio was observed (Table 1). Therefore, male and female transmission efficiency of the *cdkf;1-1* mutant allele, carrying a T-DNA encoded sulfadiazine resistance marker gene, was analyzed using reciprocal crosses between hemizygous *cdkf;1-1/+* mutant and wild type plants. The efficiencies of female and male transmissions of *cdkf;1-1* allele were 113% and 68%, respectively, which indicated a partial male transmission defect, as in case of pollination with the *cdkf;1-1/+* parent the observed segregation ratio (0.68: 1) differed significantly from the expected 1:1 ratio (Table 2).

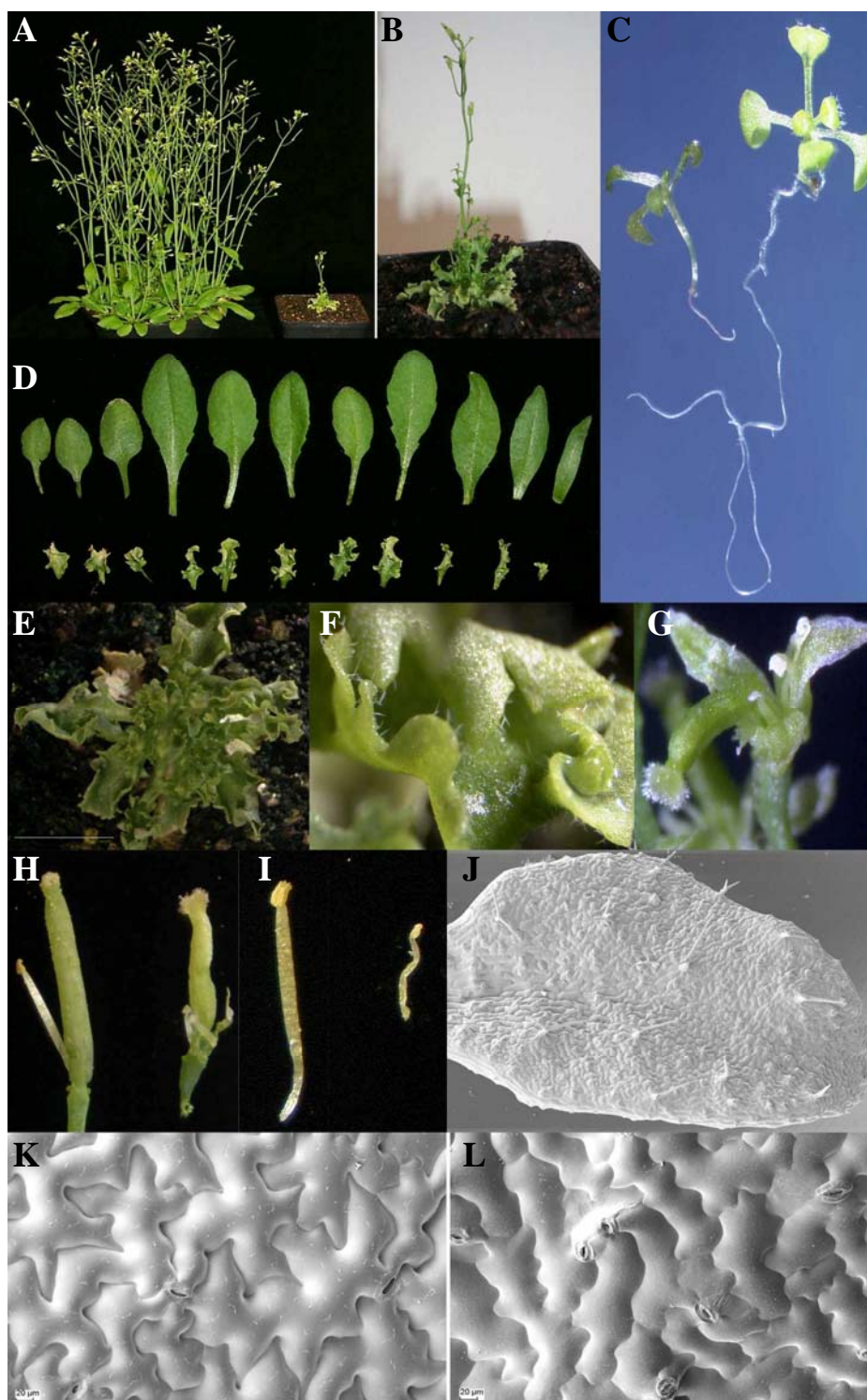


Figure 8. Morphological characteristics of the *cdkf;1-1* knockout mutant.

(A) Wild type (left) and *cdkf;1-1* mutant (right) plants 18 days and one month after germination (gibberellin-mediated flowering in *cdkf;1-1*), respectively. The mutant shows extremely reduced growth and development (B) A magnified picture of *cdkf;1-1* mutant after induction of its flowering by gibberellin treatment. (C) Wild type and *cdkf;1-1* mutant seedlings 12 days after germination. The mutant seedling displays significantly shorter root and retarded development. (D) Comparison of leaves of wild type (top row) and *cdkf;1-1* mutant (bottom row) plants shown in (A). (E) One month old *cdkf;1-1* mutant without gibberellin treatment (F) Trichomes with reduced branch number on serrated leaves of the *cdkf;1-1* mutant. (G) The aberrant flower of *cdkf;1-1* mutant. There are no real petals. (H) and (I) Comparison of carpels and stamens of wild type (left side) and *cdkf;1-1* mutant, respectively. (J) Scanning electron micrographs of *cdkf;1-1* mutant leaf showing single and double branched trichomes. (K) and (L) Scanning electron micrographs of cotyledons of wild type and *cdkf;1-1* mutant seedlings. The size of epidermal cells in the mutant leaves is smaller compared to wild type.

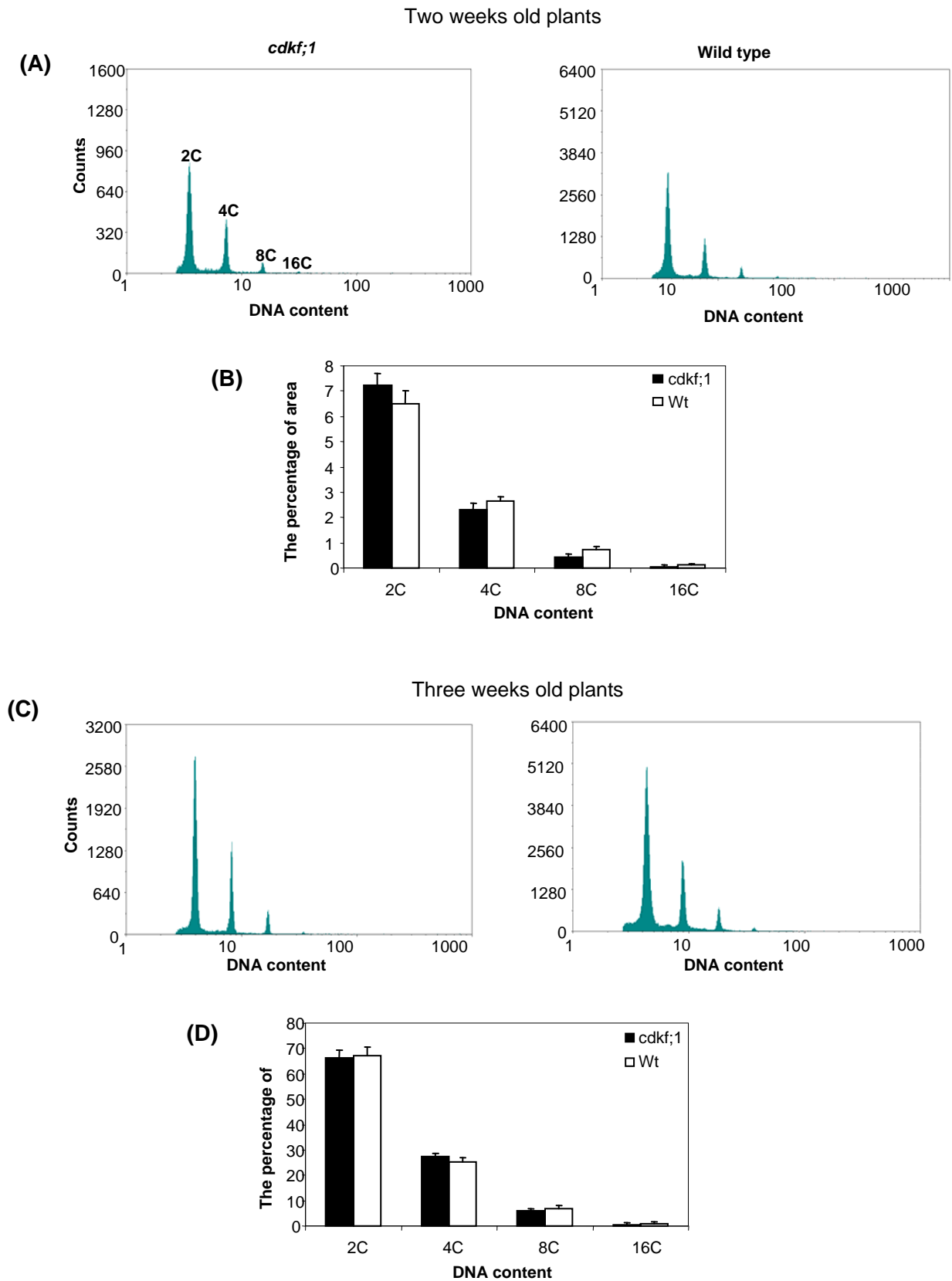


Figure 9. Flow cytometric analysis of nuclear DNA content of leaf cells of two and three weeks old wild type and *cdkf;1-1* mutant seedlings.

(A) Ploidy profiles of leaf cells of two weeks old wild type and *cdkf;1-1* mutant seedlings. (B) Calculation of percentage of nuclear DNA content for each C-value class. (C) Nuclear DNA content of leaf cells of three weeks old wild type and *cdkf;1-1* seedlings. (D) Calculation of percentage of nuclear DNA content for each C-value class. The error bars show the standard deviations of measurements.

Table 1. Self pollination of hemizygous *cdkf;1-1/+* mutant yield a distorted segregation ratio of wild type and *cdkf;1-1* mutant progeny.

	wt and <i>cdkf;1/+</i>	<i>cdkf;1/cdkf;1</i>	Ratio
Expected ratio	753	251	3:1
Observed ratio	804	201	4:1

Table 2. Male and female transmission efficiency of *cdkf;1-1f* allele determined by reciprocal crosses.
TE (transmission efficiency) = Sulfadiazine^R/Sulfadiazine^S x 100.

	Crosses	Sulfadiazine ^R	Sulfadiazine ^S	TE
Female	<i>cdkf;1-1/+</i> x wt	87	76	113%
Male	wt x <i>cdkf;1-1/+</i>	77	113	68%

DAPI staining of pollens from hemizygous *cdkf;1-1/+* plants indicated that some mature pollen grains had significantly smaller size compared to wild type but carried clearly recognizable generative cells (Figure 10). However, we could not detect a cell division defect in the abnormal pollen grains.

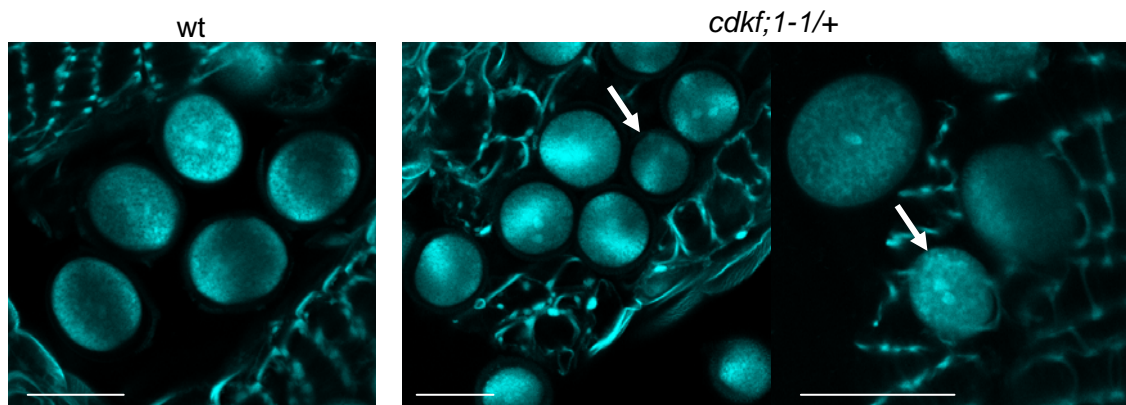


Figure 10. Fluorescence microscopy of DAPI-stained mature pollen grains of wild type and hemizygous *cdkf;1-1/+* plants.

The white arrows show smaller pollen grains in the hemizygous *cdkf;1-1/+* anthers.

3.2.3. Genetic complementation of the *cdkf;1-1* mutation

To confirm that all observed phenotypic changes were indeed caused by the *cdkf;1-1* T-DNA insertion mutation, a genetic complementation test was performed with a full-length *CDKF;1* cDNAs cloned in pER8-GW and pN-TAPI vectors. The constructs were transferred into *Agrobacterium* GV3101 (pMP90) and transformed by vacuum infiltration into sulfadiazine resistant hemizygous *cdkf;1-1/+* (GABI_315A10) plants. The transformed T1 generation was selected on MSAR media containing

either hygromycin (pER8-GW marker) or BASTA (pN-TAPI marker). Subsequently, all resistant seedlings were transferred onto sulfadiazine containing medium, in order to select for the antibiotic resistance marker of the *cdkf;1-1* allele. T2 generation was analogously germinated on either hygromycin or BASTA containing medium, and then resistant plants were subjected to sulfadiazine selection and screened by PCR for homozygous status of the *cdkf;1-1* mutation. Subsequent growth of seedlings carrying the pN-TAPI construct, conferring expression of *CDKF;1* cDNA in fusion with coding sequences of an N-terminal TAP tag, revealed wild type phenotype indicating genetic complementation of the *cdkf;1-1* mutation. Surprisingly, few lines carrying the *CDKF;1* cDNA under the control of an estradiol-inducible promoter in the T-DNA of pER8-GW expression vector also yielded wild type homozygous *cdkf;1-1* progeny, indicating leaky expression in the absence of estradiol induction (Figure 11). In any case, these assays demonstrated that expression of the *CDKF;1* cDNA by the CaMV 35S promoter is sufficient to confer genetic complementation of the *cdkf;1-1* mutation.

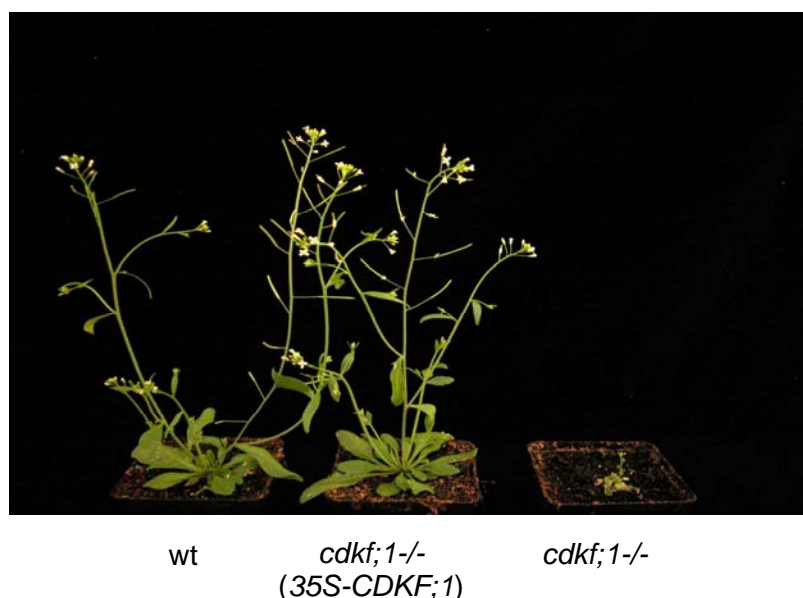


Figure 11. Genetic complementation of the *cdkf;1-1* mutation.

Comparison of phenotypes of wild type (wt), pER8-GW -*CDKF;1*-cDNA containing homozygous *cdkf;1-1* mutant, and untransformed homozygous *cdkf;1-1* mutant plants. Wild type phenotype of *cdkf;1-1* homozygous plants expressing the *CDKF;1* cDNA under the control of a CaMV 35S promoter in the pER-GW vector indicates successful genetic complementation of the mutation.

3.3. Phosphorylation targets of *CDKF;1* and *CDKD* protein kinases

3.3.1. *CDKF;1* phosphorylates the CDK-activating *CDKD* kinases

Shimotonho et al., (2004) have previously found that *CDKF;1* phosphorylates the T-loop of *CDKD;2*, and *CDKD;3* *in vitro*, but failed to detect phosphorylation of *CDKD;1* by *CDKF;1*. However, the fact that both T-loop sequences and predicted protein structures of all three *Arabidopsis* *CDKD* kinases are very similar (Figure 12) suggested a possible inconsistency in these results.

```

CDKD1 M- EQP- - KKVADRYLKREVLGGQTYGVVFKATDTKNGETV 37
CDKD2 M- SKSGDNGPVDRYLRRQI LGEGTYGVVYKATDTKTGKTV 39
CDKD3 MPEQP- - KKVADRYLKQEVLGGQTYGVVFKATDTKTEQTV 38

CDKD1 AI KKI RLKGEKEGVNVTALREI KLLKELKHPHI I ELI DAF 77
CDKD2 AVKKI RLGNQKEGVNFTALREI KLLKELNHPHI V ELI DAF 79
CDKD3 AI KKI RLGKQREGVNI TALREI KMLKELKHPHI I LLI DAF 78

CDKD1 PHKENLHLVFEF METDLEAVI RDRNLYLSPGDIKSYLQMI 117
CDKD2 PHDGS LHLVFEYMQTDLEAVI RDRNI FLSPGDI KSYMLMT 119
CDKD3 PHKENLHLVFEF METDLEAVI RDSNI FLSPA DI KSYLLMT 118

CDKD1 LKGL EYCHGKWWLHRDMKPNLLI GPNGQLKLADFGLARI 157
CDKD2 LKGLAYCHKQWWLHRDMKPNLLI GENGLKLADFGLARL 159
CDKD3 FKGLAYCHDKWWLHRDMKPNLLI GVDGQLKLADFGLARI 158

CDKD1 FGS PGRKF THQVFARWYRAPELLFGAKQYDGAVDVWVAAGC 197
CDKD2 FGS PNRRF THQVFATWYRAPELLFGBRQYGAQVDVWVAAGC 199
CDKD3 FGS PNRKF THQVFARWYRAPELLFGAKQYGAQVDVWVAAC 198

CDKD1 IFAELLRRPFLQGNSDI DQLSKI FAAF GTPKADQWPDMI 237
CDKD2 IFAELLRRPFLPGSTEI DQLGKI FAAF GTPVPSQMSDMI 239
CDKD3 IFAELLRRPFLQGNSDI DQLSKI FAAF GTPKADQWPDLT 238

CDKD1 CLPDYVEYQFVPAPSLRSLPTVSEADLDDLKMFITYDPK 277
CDKD2 YLPDYMEFSYTPAPPLRTIFPMSDDALDLLAKMFITYDPR 279
CDKD3 KLPDYVEYQFVPAPSLRSLFPAWSDDALDDLKMFITYDPK 278

CDKD1 SRI SI QQALKHRYFTSAPSPTDPLKLRPVSQKQDA---KS 314
CDKD2 QRI TI QQALDHRYFSSPSPTEPGKLIQIPASKGDALPEKA 319
CDKD3 ARI SI QQALEHRYFTSAPAPTDRAPKLRKVPKQDQ---KS 315

CDKD1 SDSK L- EAI KVLSPA H K FRRVMPDRGKSGNGFKDQSVDV 352
CDKD2 SEQNGHGNSPAVLSPPGKMRVMGPEG----- 346
CDKD3 SYGKH- EAI TVGSPPRKLRVMMPERGRVDS-----L 345

CDKD1 MRQASHDQAPMSLDFTI LAERPPNRPTI TSADRSHLKRK 392
CDKD2 ----- 346
CDKD3 KSHVDK DQAPMSLDFTI LAERPPNRPTI TSADRSHLKRK 385

```

Figure 12. Multiple alignment of *Arabidopsis* CDKD protein kinase sequences. Conserved regions are depicted by black shading, whereas red rectangle frames the T-loop sequences.

Therefore, we have repeated the CDKF;1 kinase assays with the CDKD substrates. We have used a N-terminal thioredoxin and C-terminal His₆ sandwich tagging technology for isolation of soluble and intact kinase proteins from *E. coli* BL 21. Recombinant CDKDs/CAKs (Trx-CDKD;1-His, Trx-CDKD;2-His, and Trx-CDKD;3-His) were purified to apparent homogeneity (Figure 13) and used subsequently as substrates in kinase assays with [γ -³²P]ATP and similarly purified CDKF;1/CAKAK.

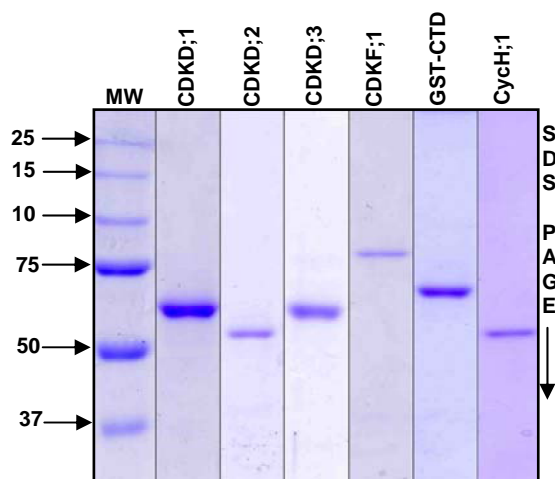


Figure 13. Purification of CDKF;1 and CDKD protein kinases fused to N-terminal thioredoxin and C-terminal His₆ tags, and isolation of a GST-CTD fusion protein carrying the C-terminal heptapeptide repeats of *Arabidopsis* RNAPII largest subunit.

The thioredoxin-His₆ sandwich tagged CDKF;1 and CDKD protein kinases (Trx-CDKD;1-His, Trx-CDKD;2-His, Trx-CDKD;3-His, and Trx-CDKF;1-His) were isolated by nickel affinity chromatography using the His₆-tag, whereas the GST-CTD kinase substrate was purified by glutathione-Sepharose affinity chromatography. The proteins were size separated on 10% SDS-PAGE and stained by Coomassie blue to control their purity.

We found that in these assays CDKF;1 underwent partial autoactivation by self-phosphorylation, as described for the leafy spurge *Ee*;CDKF;1 by Chao et al. (2006), and phosphorylated all three *Arabidopsis* CDKDs (CDKD;1, CDKD;2, and CDKD;3; Figure 14), but not the negative control thioredoxin protein (Figure 15). Subsequently, we used a T-loop mutated variant of CDKD;1 (T166A) as substrate for CDKF;1. Phosphorylation of the CDKD;1 (T166A) substrate was clearly lower compared to wild type CDKD;1, which suggested that CDKF;1 phosphorylates the threonine 166 residue in the T-loop of CDKD;1 (Figure 16). Nevertheless, residual labelling of CDKD;1 (T166A) by ^{32}P indicated that the Thr166Ala substitution did not fully abolish CDKD;1 phosphorylation by CDKF;1.

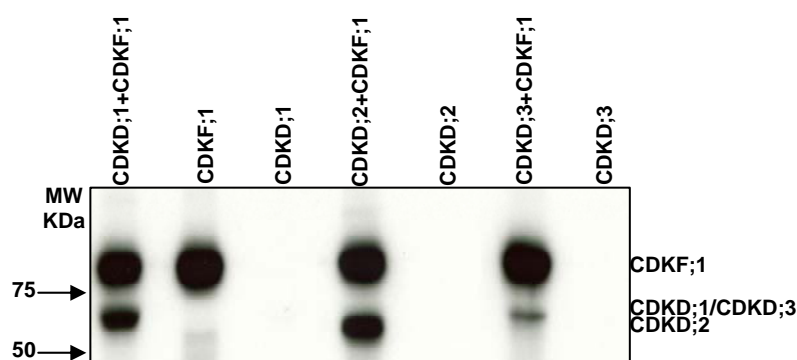


Figure 14. Phosphorylation of affinity-purified thioredoxin-fused CDK-activating CDKD kinases by the CAK-activating CDKF;1 kinase.

Control assays were performed with CDKF;1 and each CDKD kinase independently, to exclude possible contamination with *E. coli* derived kinases. Following size separation of proteins from the kinase assays on 10% SDS-PAGE, the phosphorylated kinases were detected by autoradiography. Due to a short exposure time optimized for monitoring CDKF;1-mediated phosphorylation, lower levels of autophosphorylation of CDKDs were not detected under this condition.

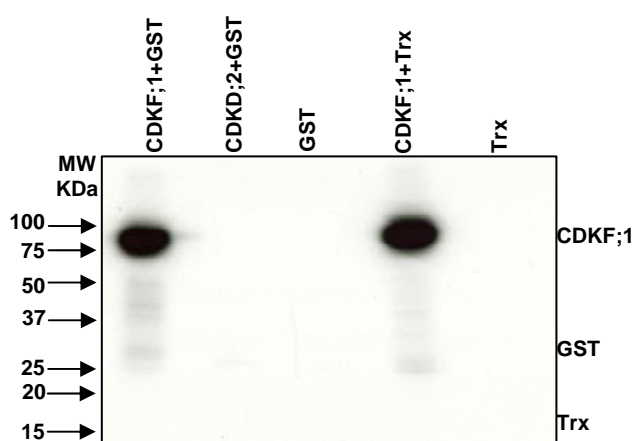


Figure 15. CDKF;1 and CDKD;2 do not phosphorylate the control glutathione-S-transferase (GST) and thioredoxin proteins.

Purified GST and thioredoxin were subjected to kinase assays to test possible contamination with *E. coli* derived kinases and demonstrate specificity of CDKF;1-mediated phosphorylation of Thx-CDKD-His₆ and GST-CTD (see: 3.3.2) substrates.

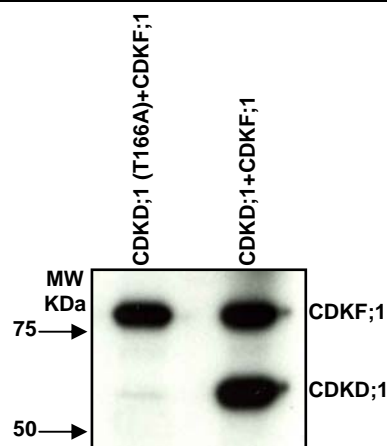


Figure 16. CDKF;1 mediates T-loop phosphorylation of CDKD;1 protein kinase.

CDKF;1 phosphorylates only very weakly the T-loop mutated variant of CDKD;1 (T166A) kinase compared to wild type CDKD;1.

This low level phosphorylation of CDKD;1 (T166A) is consistent with some previous reports suggesting that CDKF;1 could also phosphorylate partially the Ser168 residue preceding the T-loop sequences (Shimotohno et al., 2004, Umeda et al., 2005). Based on these data it was concluded that the previous studies of CDKF;1 substrates were not fully reliable concerning CDKF;1-mediated phosphorylation of CDKD;1, perhaps because in those experiments a maltose-binding protein (MBP) fusion was used for secretion and purification of CDKF;1, which in our hands results in a kinase with lower *in vitro* activity.

3.3.2. *The CTD domain of Arabidopsis RNA polymerase II largest subunit is phosphorylated by CDKF;1 and CDKD;2*

Previously, Bakó et al (2003) found that the alfalfa CAK2Ms kinase phosphorylates and co-immunoprecipitates with the CTD of the largest subunit of RNAPII. Shimotohno et al. (2004) confirmed this observation by showing that *Arabidopsis* CDKD;2, an ortholog of alfalfa CAK2Ms, was also capable of phosphorylating CTD after co-immunoprecipitation from plant extracts with cyclin H. To characterize the CTD kinase activity of CDKF;1 and all three CDKD kinases, we first performed *in vitro* phosphorylation assays with a GST-CTD fusion protein as substrate (Figure 17). In addition to CDKD;2, we also found that CDKF;1 is also capable of phosphorylating the GST-CTD substrate, whereas neither CDKF;1 nor CDKD;2 phosphorylated the control glutathione-S-transferase protein (Figure 15). Using each protein kinase without substrate, as well as the GST-CTD substrate without kinase, in control assays demonstrated that all three purified CDKD kinases were able to undergo autophosphorylation and autoactivation *in vitro* (Figure 17). Autophosphorylation of CDKDs was however weak compared to CDKF;1. In any case, these results indicated that the CDKD protein kinases have some basic activity in the absence of their phosphorylation by CDKF;1 *in vitro*, and suggested that this may be the case also in the *cdkf;1* mutants *in vivo*.

The CTD domain of *Arabidopsis* RNAPII largest subunit consists of 15 consensus (YSPTSPS) and 26 variant tandem heptad repeats (Nawrath et al., 1990).

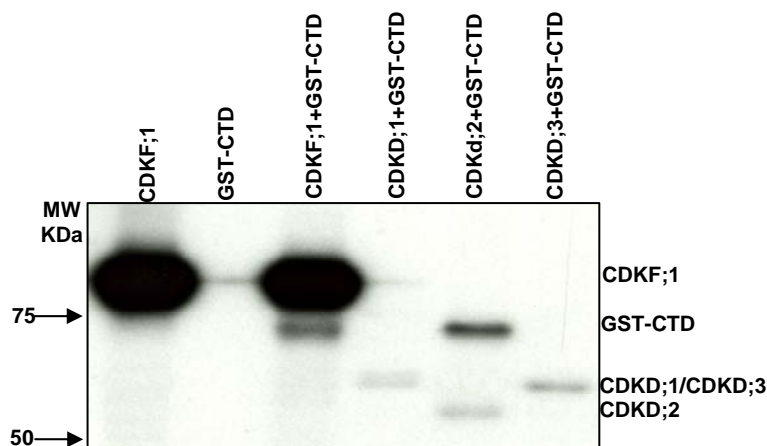


Figure 17. CDKF;1 and CDKD;2 phosphorylate the CTD of RNAPII largest subunit.

The kinase assays were performed with purified CDKF;1 and CDKD protein kinases using GST-CTD as substrate and $[\gamma\text{-}^{32}\text{P}]\text{ATP}$. To monitor autophosphorylation of the kinases, separate assays were performed with GST-CTD alone and each protein kinase in the absence of substrate (shown here only for CDKF;1).

In mammals, the predominant phosphorylation occurs at serine residues Serine-2, Serine-5, and Serine-7 of CTD heptapeptide motives (Phatnani and Greenleaf, 2006; Chapman et al., 2007). To determine which serine positions of the consensus CTD heptapeptide are phosphorylated by the CDKD;2 and CDKF;1 kinases, we have used four different synthetic peptides as substrates (Table 3).

Table 3. Wild type and mutant variants of consensus CTD heptapeptide used as substrates in kinase assays with CDKF;1 and CDKD;2.

Peptide “a” corresponds to the wild type heptapeptide, peptide “b” carries alanine exchanges of Serine-2 and Serine-5; in peptide “c” Serine-5 is exchanged for alanine, and in peptide “d” Serine-2 is replaced by alanine. Note that phosphorylation of peptide “b” specifically detects Serine-7 kinase activity.

a	Y	S2	P	T	S5	P	S7
b	Y	A	P	T	A	P	S7
c	Y	S2	P	T	A	P	S7
d	Y	A	P	T	S5	P	S7

Compared to the wild type consensus heptapeptide sequence in peptide (a), alanine substitutions of either Serine-5, or Serine-2, and both Serine-2 and Serine-5 residues were introduced into peptides (c), (d), and (b), respectively. In comparison to phosphorylation of wild type peptide (a), CDKD;2 phosphorylated peptide (d) more efficiently than peptide (c), but did not recognize peptide (b) as substrate (Figure 18A). These results showed that CDKD;2 phosphorylated both Serine-2 and Serine-5 residues, but preferred Serine-5 over Serine-2. However, CDKD;2 was not capable to phosphorylate the Serine-7 residue of CTD heptapeptide.

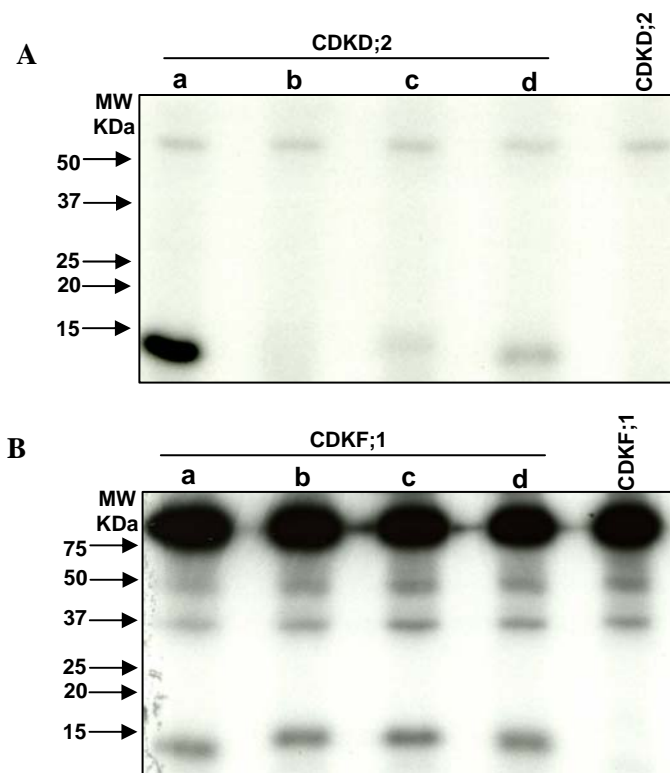


Figure 18. CTD phosphorylation specificities of CDKD;2 and CDKF;1 kinases *in vitro*.

CDKD;2 phosphorylates Serine-5 of CTD heptapeptide repeats at higher efficiency compared to the Serine-2 residue. (A) Kinase assay was performed with CDKD;2 and four different synthetic heptapeptides. CDKD;2 phosphorylation of peptide “d” carrying Serine-2 to alanine replacement is more efficient compared to peptide “c”, which carries Serine-5 to alanine replacement. By contrast, peptide “b” carrying alanine replacement of both Serine-2 and Serine-5 residues is not phosphorylated by CDKD;2. (B) CDKF;1 phosphorylates with similar efficiency all four heptapeptide substrates, including peptide “b”, indicating that CDKF;1 is also capable to phosphorylate the Serine-7 residue of the CTD heptapeptide repeats.

Moreover, CDKD;2 phosphorylated peptides (d) and (c) at significantly lower levels than the wild type peptide (a). This indicated that phosphorylation of one of the serine residues could have a positive effect on phosphorylation of another serine position. This observation supports the results of Jones et al. (2004) who showed that partially phosphorylated CTD heptapeptides were more efficient substrates for budding yeast *CTDK-I* compared to unphosphorylated heptapeptide substrates.

Unlike CDKD;2, CDKF;1 appeared to phosphorylate all four heptapeptide substrate variants with comparable efficiency (Figure 18B). Consequently, this result did not indicate the exact target(s) of CDKF;1 phosphorylation in the heptapeptide sequence. CDKF;1 is a serine/threonine kinase, there are two possible additional target residues (Thr4 and Ser7) for CDKF;1 in the mutated peptides. Since Serine-7 is one of the major CTD phosphorylation site *in vivo*, phosphorylation of peptide “b” carrying alanine replacement of both Serine-2 and Serine-5 residues suggested that CDKF;1 is likely a CTD Serine-7 kinase. In contrast to the report of Shimotohno et al. (2004), who failed to detect CTD phosphorylation by CDKF;1, our data strongly suggested that CDKF;1 is an important CTD kinase, in addition to its downstream CDKD;2 kinase target.

3.3.3. RNA polymerase II CTD phosphorylation in *cdkf;1* and *cdkd;2* mutant plants

To verify that CDKF;1 and CDKD;2 indeed play important roles in CTD phosphorylation *in vivo*, we performed western blot analysis of proteins extracted from wild type control, *cdkf;1* and *cdkd;2* mutant seedlings using primary rat monoclonal antibodies 3E10, 3E8/H14, and 4E12 (Chapman et al., 2007; Egloff et al., 2007) that exclusively detect phosphoserine-2, phosphoserine-5, and phosphoserine-7 in the heptapeptide repeats of RNAPII CTD domain, respectively. The amount of RNAPII largest subunits was adjusted in the samples to equal using mouse a monoclonal antibody 8WG16 (abcam, ab817).

Whereas the *cdkf;1* mutation caused a progressive delay in vegetative development after seed germination, the phenotype of the *cdkd;2* mutant was indistinguishable from wild type. To standardize the CTD phosphorylation assay, therefore, proteins extracts were prepared from 7 days old wild type and mutant seedlings when, despite inhibition of root elongation, the size and development of *cdkf;1-1* mutant was fully comparable to those of wild type and *cdkd;2-1* mutant seedlings that carried no leaves but only two fully expanded cotyledons. At this developmental stage, western blotting with the CTD phosphoserine-7 specific 4E12 antibody revealed that phosphorylation at Serine-7 residues of CTD heptapeptide repeats was specifically reduced in the *cdkf;1-1* mutant, whereas the levels of CTD phosphoserine-7 were comparable in wild type and *cdkd;2-1* mutant seedlings (Figure 19). In support of *in vitro* kinase assays, this data demonstrated that the CDKF;1 protein kinase is required *in vivo* for phosphorylation of Serine-7 residues of CTD heptapeptide repeats of RNAPII.

To determine whether CTD phosphorylation levels would change during further seedling development, we have also performed western blot analysis of protein extracts that were prepared from 12 days old seedlings that carried four fully expanded leaves. At this developmental stage, the *cdkf;1-1* mutant showed some slight but clearly recognizable delay in elongation growth compared to *cdkd;2-1* and wild type seedlings (see: Figure 8C). In addition to maintenance of largely reduced phosphoserine-7 levels in the *cdkf;1-1* mutant, we have observed a dramatic reduction of phosphoserine-5 levels in both *cdkd;2-1* and *cdkf;1-1* seedlings (Figure 19). In accordance with the results of *in vitro* kinase assays, this observation showed that the CDKD;2 protein kinase is required for *in vivo* phosphorylation of CTD Serine-5 residues. Reduction of CTD-Serine-5 phosphorylation in *cdkf;1-1* mutant seedlings confirmed the notion that CDKF;1 may indeed act *in vivo* as upstream activating kinase (CAKAK) of CAKs/CDKs. In fact, the T-loop phosphorylation of CDKD;2 and CDKD;3 by CDKF;1 *in vitro* has been reported by (Shimothono et al; 2004), and we found that CDKD;1 is also an *in vitro* substrate of CDKF;1 (Figure 16). Furthermore, CDKF;1 is detected in association with CDKD;2 *in vivo* (Van Leene et al., 2007). Therefore, CDKF;1/CAKAK is likely to mediate the activation of CDKs/CAKs in their complexes with cyclins *in vivo* (Umeda et al., 1998; Shimothono et al., 2006).

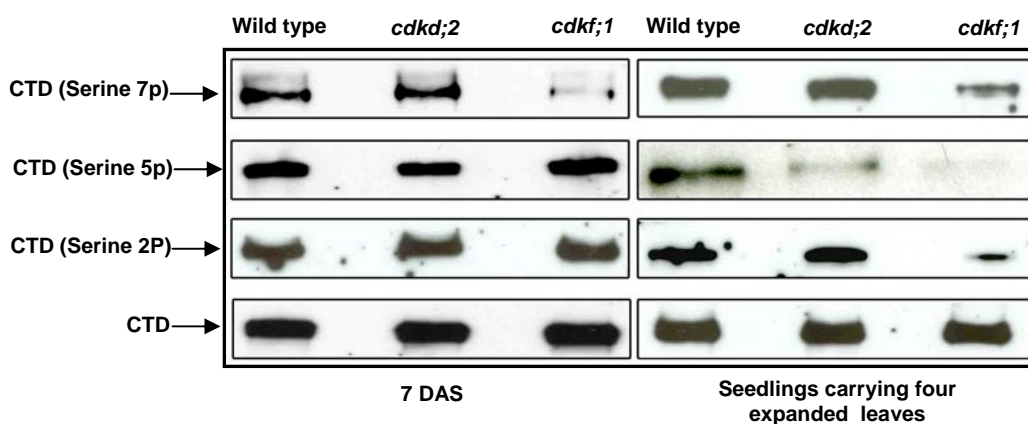


Figure 19. Changes in the levels of Serine-7, Serine-5 and Serine-2 specific phosphorylation of RNAPII CTD in *cdkf;1* and *cdkd;2* mutant seedlings during early stages of seedling development

Protein extracts were prepared from seedlings with fully expanded cotyledons but no leaves harvested at day 7 after sowing, and from 12 days old seedlings carrying four expanded primary leaves. Western blot analyses of protein extracts (50 μ g/lane) prepared from wild type, *cdkf;1* and *cdkd;2* seedlings were performed with antibodies recognizing specifically the phosphorylated Serine-7, Serine-5, and Serine-2 residues of RNAPII CTD heptapeptide repeats. The samples were standardized using an antibody, which recognizes the CTD independently of its phosphorylation status.

Lower level of phosphoserine-5 in *cdkf;1* compared to *cdkd;2* mutant seedlings thus indicates CDKD;2 is not the only CDKF;1-activated kinase, which is involved in CTD-Serine-5 phosphorylation. The CDKD;3 and CDKD;1 protein kinases are likely candidates for being responsible for residual phosphorylation of Serine-5 position of CTD in the *cdkd;2* mutant. This should be further examined using the available double and triple *cdkd* mutants. Low level of Serine-5 phosphorylation in the *cdkf;1-1* mutant, on the other hand, suggests that the CDKD kinases have some basic activity even in the absence of CDKF;1. Therefore, it will be interesting to examine the effect of gradual inactivation of CDKDs in the *cdkf;1* mutant background.

Remarkable, neither Serine-5 nor Serine-2 residue of CTD show any reduction in their phosphorylation level in the *cdkf;1-1* mutant seedlings 7 days after germination and prior initiation of leaf development. As CDKD;2 without its regulatory cyclin (CycH;1) subunit and CDKF;1-mediated activation showed *in vitro* phosphorylation of Serine-5 and at lower level Serine-2 residues of the CTD, it is possible that a gradual decline of the threshold of CDKD;2 kinase activity with together other unknown kinases in developing seedlings contribute to gradual manifestation of defective Serine-5 and Serine-2 phosphorylation in the *cdkf;1-1* mutant. Thus, reduction of Serine-2 and Serine-5 phosphorylation is not immediately detectable in *cdkf;1-1* mutant seedlings 7 DAG. As at that stage only a reduction of CTD phosphoserine-7 levels is observed in the *cdkf;1-1* mutant, the use of these very young seedlings provided an ideal tools to determine the regulatory effects of CTD Serine-7 phosphorylation on the control of transcription. Therefore, we have performed an Affymetrix GeneChip transcript profiling experiment with RNA samples prepared from *cdkf;1-1* mutant and wild type seedlings 7 DAG.

3.4. Transcript profiling of *cdkf;1* mutant and wild type seedlings using Affymetrix ATH1 microarray

Comparative microarray transcript profiling of *cdkf;1* mutant and wild type was performed by Affymetrix ATH1 GeneChip microarrays as described in section 2.2.24 to obtain three independent microarray datasets for both wild type and *cdkf;1-1* samples. Analysis of the microarray data with the GeneSpring GX10 (Agilent) program using a cut-off value of 2.0-fold difference between transcript levels at a p value <0.05 in control wild type and *cdkf;1-1* mutant samples resulted in 845 genes. From these 367 showed down-regulation and 478 upregulation in *cdkf;1-1* seedlings. Subsequent statistical analysis of gene list has identified 37 Gene Ontology (GO) terms, which showed overrepresentation at a cut-off value <0.1. Testing the dataset for significant pathways compiled in the GeneSpring package has identified 42 pathways overrepresented at a p-value <0.01. Because some regulatory factors in the identified pathways showed changes in their transcript levels lower than 2-fold, but higher than 1.5-fold, we have repeated the statistical analyses allowing 1.5-fold difference at p-value <0.05 between wild type and *cdkf;1-1* transcript levels. This resulted in 2383 genes (in *cdkf;1-1* down-regulated 1258 and upregulated: 1125) corresponding to 42 GO-terms (p<0.1) and the same 35 significantly overrepresented pathways, which were obtained by using a cut-off of 2-fold change in the altered expression levels.

3.4.1. Data mining – identification of pathways affected by the *cdkf;1-1* mutation

The analysis of GO-terms (Table 4) suggested that the *cdkf;1-1* mutation primarily affected several stress response and redox-regulatory pathways and their coordinated control with a wide-range of metabolic and nuclear encoded chloroplast functions. Subsequent manual annotation of the gene list to pathways compiled in the Annex and following sections helped to allocate precisely the gene functions to better defined pathways involved in the regulation of: light responses, circadian clock, flowering time; shoot-, root-, flower-, gametophyte-, embryo- and seed development; plant hormone (cytokinin, brassinosteroid, ABA, auxin, jasmonate and salicylic acid) biosynthesis and signalling; pathogen defence responses, senescence, cell death, synthesis of phenylpropanoids and anthocyanines, osmotic (salt and drought), cold and oxidative stress responses; mitochondrial and chloroplast function, including chlorophyll biosynthesis; RNA processing and biogenesis of small RNAs; cell cycle, DNA repair and replication, chromatin conformation and modifications, nuclear import, cytoskeleton organization, phospholipid and Ca²⁺ signalling, vesicular transport, protein folding and proteolysis, carbohydrate metabolism (glycolysis, gluconeogenesis, sugar transport), fatty acid-, cell wall- and amino acid metabolism and transport; glutathione-transferases, cytochrome P450 families, and metabolism and transport of ammonia, sulphate, phosphate, iron, and potassium. In addition, the *cdkf;1-1* mutation affected the expression levels of 48 yet uncharacterized protein kinases, 76 transcription factors and numerous other genes of unknown function.

Table 4. Genes showing 1.5-fold alteration in their transcript levels ($p < 0.05$) between the *cdkf;1-1* mutant and wild type were sorted to significantly overrepresented pathways according to GO-terms.

The majority of GO-terms are related to pathways controlling plant responses to abiotic and biotic stimuli and oxidative stress indicating that transcription of many stress regulated genes are altered by the *cdkf;1-1* mutation.

GO ACCESSION	GO Term	p-value	% Count in Total
GO:0003824	catalytic activity	4.66E-06	43.2428
GO:0050896	response to stimulus	4.14E-15	18.9136
GO:0009536	Plastid	6.63E-08	16.481775
GO:0009507	Chloroplast	1.97E-08	16.11017
GO:0006950	response to stress	1.88E-14	10.962348
GO:0042221	response to chemical stimulus	6.17E-09	10.006011
GO:0016491	oxidoreductase activity	9.59E-18	7.776381
GO:0055114	oxidation reduction	3.17E-17	6.19706
GO:0005576	extracellular region	1.16E-14	4.568556
GO:0006952	defense response	6.83E-07	3.9510355
GO:0030312	external encapsulating structure	1.65E-12	3.4755998
GO:0005618	cell wall	2.87E-12	3.4318814
GO:0005506	iron ion binding	8.01E-11	3.4154873
GO:0009055	electron carrier activity	4.29E-08	3.2132905
GO:0009607	response to biotic stimulus	5.72E-06	3.076671
GO:0019748	secondary metabolic process	5.49E-17	2.3443904
GO:0005509	calcium ion binding	1.58E-05	2.1367288
GO:0046906	tetrapyrrole binding	1.44E-08	2.0984752
GO:0020037	heme binding	5.94E-08	1.9563911
GO:0009605	response to external stimulus	6.72E-10	1.8744193
GO:0006725	aromatic compound metabolic process	1.14E-05	1.7924477
GO:0006979	response to oxidative stress	3.82E-16	1.5683917
GO:0009505	plant-type cell wall	1.10E-10	1.4645609
GO:0050660	FAD binding	5.03E-06	0.87436473
GO:0009611	response to wounding	5.09E-07	0.86343515
GO:0009698	phenylpropanoid metabolic process	1.24E-05	0.84157604
GO:0015979	Photosynthesis	4.12E-06	0.83611125
GO:0016209	antioxidant activity	5.32E-14	0.73228043
GO:0000302	response to reactive oxygen species	5.65E-16	0.7104213
GO:0004601	peroxidase activity	5.97E-14	0.6612383
GO:0016684	oxidoreductase activity, acting on peroxide as acceptor	5.97E-14	0.6612383
GO:0042542	response to hydrogen peroxide	2.66E-15	0.6393792
GO:0006800	oxygen and reactive oxygen species metabolic process	3.09E-15	0.595661
GO:0042743	hydrogen peroxide metabolic process	4.40E-17	0.4809006
GO:0042744	hydrogen peroxide catabolic process	8.68E-18	0.46450627
GO:0004364	glutathione transferase activity	8.86E-09	0.273239
GO:0019757	glycosinolate metabolic process	1.10E-05	0.25684464
GO:0016137	glycoside metabolic process	1.10E-05	0.25684464
GO:0019760	glucosinolate metabolic process	1.10E-05	0.25684464
GO:0009404	toxin metabolic process	5.37E-08	0.25137985
GO:0009407	toxin catabolic process	5.37E-08	0.25137985
GO:0043295	glutathione binding	4.00E-06	0.060112573

3.4.2. *The cdkf;1-1 mutation results in transcriptional down-regulation of small RNA biogenesis pathways*

As shown in Figure 8D, in addition to other severe developmental defects, the *cdkf;1-1* mutation resulted in alteration of leaf development characterized by upward curling serrated leaves. Similar leaf phenotype has been shown to be conferred by mutations affecting key enzymes in the microRNA biogenesis pathway, including DICER-LIKE 1 (DCL1), SERRATE (SE) and HYPONASTIC LEAF (HYL1) (for review see: Voinnet, 2009). Analysis of the microarray hybridization data in fact indicated that the *cdkf;1-1* mutation caused 1.8-fold reduction in the transcript level of *DCL1* encoding a key enzyme involved in pri-microRNA processing and microRNA-mediated cleavage of ta-siRNA precursors. In addition, a similar reduction was observed in the transcript levels of *DCL2* involved in the nat-siRNA pathways and AGO1, a major component of RISC complexes catalysing microRNA and ta-siRNA mediated cleavage of target transcripts in *Arabidopsis*. As several critical functions in the small RNA pathways are not represented on the *Arabidopsis* ATH1 microarray, and because we have lowered the cut-off value of altered transcript levels from standard 2-fold to 1.5-fold (i.e., which could increase the false discovery rate), we have measured the mRNA levels of a set of genes acting in the four known *Arabidopsis* small RNA (miroRNA, ta-siRNA, nat-siRNA and ra-siRNA) pathways by quantitative real-time PCR (qRT-PCR). This has revealed 1.5 to 6-fold decrease in the transcript levels of four *DICER-LIKE* (*DCL1*, *DCL2*, *DCL3*, and *DCL4*), four *ARGONAUTE* (*AGO1*, *AGO4*, *AGO6*, and *AGO7*), and two *RNA-dependent RNA polymerase II* genes (*RDR2* and *RDR6*), in addition to the *HYL1*, *HEN1* (HUA ENHANCER 1), *HST1* (HASTY), and *DRD1* (DEFECTIVE IN RNA-DIRECTED DNA METHYLATION 1) genes, in the *cdkf;1-1* mutant (Figure 20). These results thus indicated that the *cdkf;1-1* mutation most likely negatively affects all four small RNA pathways (i.e., DCL1, HYL1, HEN1, HST1 and AGO1 in microRNA processing and action; DCL1, RDR6, DCL4, HEN1, AGO1 and AGO7 in ta-siRNA processing and action; DCL1, DCL2, RDR6 and HEN1 in nat-siRNA biogenesis; and DCL3, RDR2, HEN1, DRD1 and AGO4 in the ra-siRNA pathway, Voinnet, 2009). These results also predicted that through down-regulation of *AGO4* and *AGO6*, which are effectors of siRNA-mediated DNA methylation, the *cdkf;1-1* mutation could also affect the regulation of gene silencing (Zheng et al., 2007; He et al., 2009).

To confirm that down-regulation of genes controlling the processing of small RNA precursors indeed leads to a reduction of mature small RNA levels, we have compared the amounts of microRNAs miR156, miR165 and miR172, as well as ta-siRNA 1 and ra-siRNA COPIA by northern blot hybridization in 7 days old wild type, *cdkf;1-1* and *cdkd;2-1* seedlings (Figure 21). Equal amount of input RNA samples was standardized by hybridization with an U6 snRNA probe. The hybridization data demonstrated that the levels of tested microRNAs, tas-siRNA 1 and ra-siRNA COPIA were indeed remarkably lower in the *cdkf;1-1* mutant compared to wild type. On the other hand, the *cdkd;2-1* mutant displayed wild type levels of all tested mature small RNAs. As we showed that at day 7 of seedling development the *cdkd;2-1* mutation does not result in any detectable alteration of RNAPII CTD phosphorylation, these data also indicated that reduced phosphorylation of Serine-7 CTD residue in the *cdkf;1-1* mutant correlates with the observed down-regulation of small RNA biogenesis

pathways. To determine whether negative regulation of genes involved in small RNA processing results in the accumulation of small RNA precursors, we have compared the amounts of unprocessed microRNA and ta-siRNA precursors, including pri-miR162a, pri-miR165a, pri-miR172a/b/c, TAS1a/b, TAS2 and TAS3 in wild type and *cdkf;1-1* mutant seedlings by qRT-PCR measurements (Figure 20).

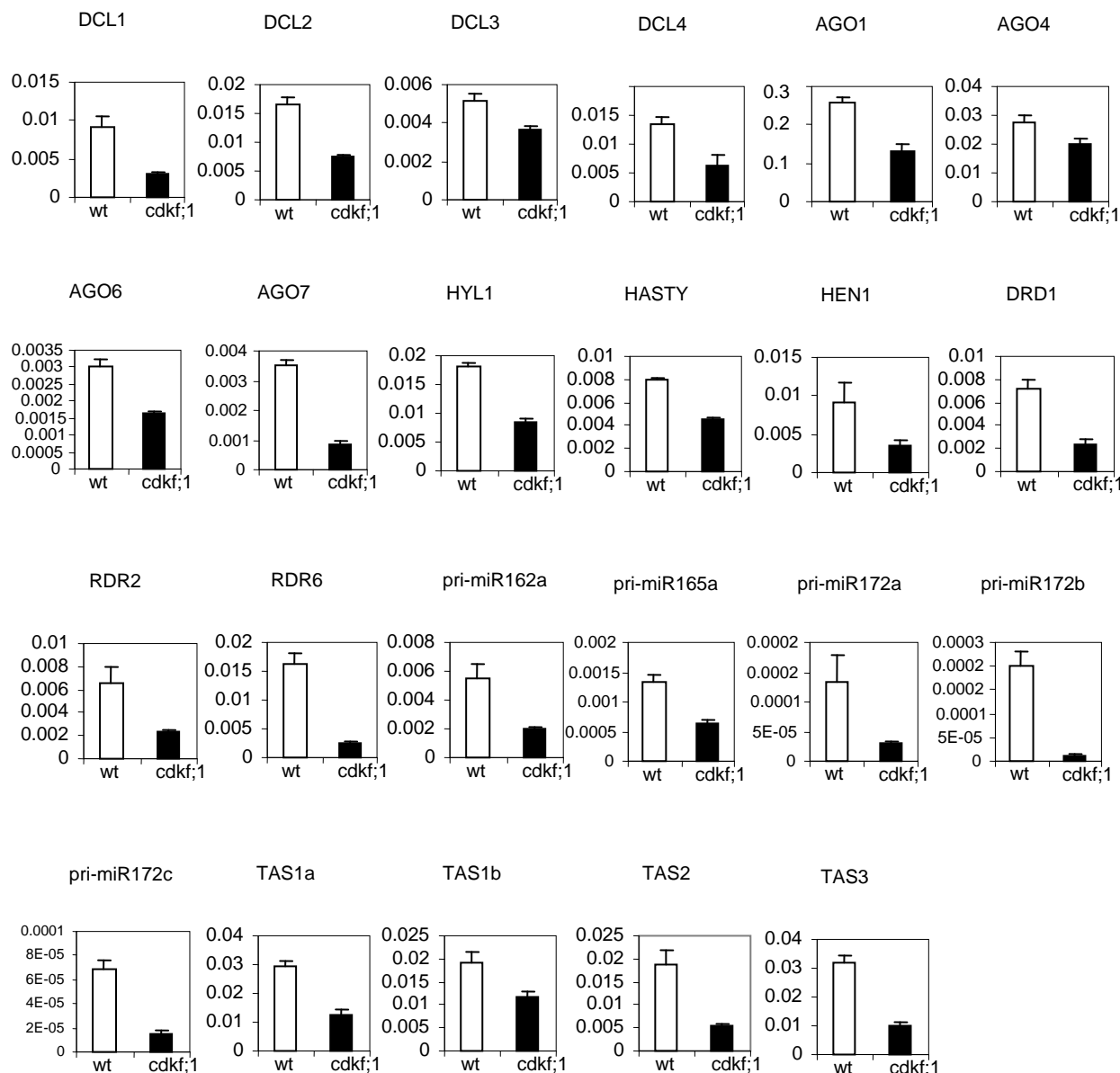


Figure 20. Comparative analysis of transcript levels of genes acting in small RNA pathways in wild type and *cdkf;1-1* seedlings 7DAG.

Transcript levels of genes involved in the biogenesis and action of small RNAs, as well as those of selected pri-miRNAs and TAS source genes of ta-siRNAs were compared by qRT-PCR measurement using ubiquitin UBI5 (At3g62250) as standard. Each measurement was performed in triplicates. Bars indicate standard deviations.

Surprisingly, the data indicated that transcription of tested small RNA genes was also reduced by 2 to 6-fold in the *cdkf;1-1* mutant. This indicated that deficiency of Serine-7 phosphorylation of RNAPII CTD during early seedling development in the *cdkf;1-1* mutant results in coordinate down-regulation

of transcription of small RNA source genes, as well as genes involved in processing of their primary transcripts to mature small RNAs.

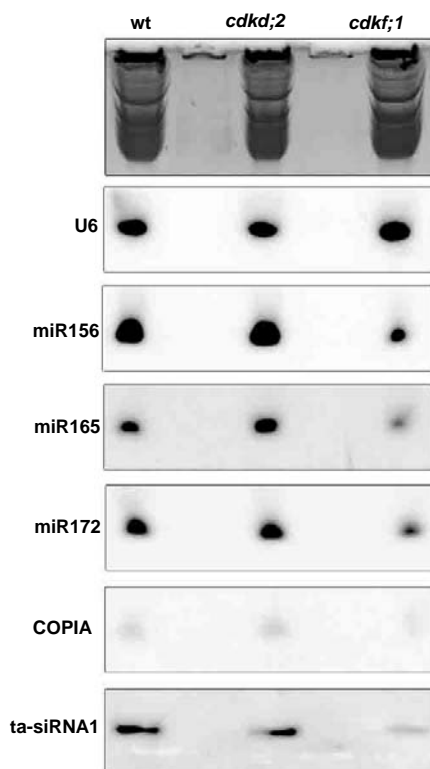


Figure 21. Comparison of levels of selected small RNAs in wild type, *cdkd;2-1* and *cdkf;1-1* seedlings.

Northern RNA hybridization of RNA samples from 7 days old wild type, *cdkd;2-1* and *cdkf;1-1* seedlings was performed with oligonucleotide probes complementary to miR156, miR165, miR172, ra-siRNA COPIA and ta-siRNA 1 as described in section 2.2.25. The first panel shows ethidium bromide stained image of RNA samples separated in a 15% PAGE containing 7M urea. The amount of samples was standardized by hybridization with an U6 snRNA probe.

3.4.3. Altered transcription of genes acting in light perception in the *cdkf;1-1* mutant

The microarray and confirmatory qRT-PCR data (Table 5) indicated simultaneous down-regulation of transcript levels several genes encoding photoreceptors and their signalling partners in the *cdkf;1-1* mutant. These included the blue-light receptor *PHOT2*, *twin LOV/ PLPB* (PAS/LOV PROTEIN B), two members of the phototropic-responsive NPH3 family protein, and phytochromes *PHYA*, *PHYC*, *PHYD*, and *PHYE*, which showed 1.5 to 2.9-fold lower expression in the *cdkf;1-1* mutant compared to wild type. The decrease in the transcript levels of phytochromes correlated with a reduction of expression of *HEME OXYGANASE 2 (HO2)* and *ELONGATED HYPOCOTYL 2 (HY2)* genes that code for enzymes involved in the biosynthesis of phytochrome chromophore required for light perception (Davis et al., 2001). As a possible feedback mechanism compensating down-regulation of phytochrome expression, genes encoding the PHYTOCHROME KINASE SUBSTRATE 1 (PKS1) and PKS2, which fine-tune the *PHYA* activated state, root phototropism, and gravitropism (Boccalandro et al., 2008; Lariguet et al., 2003), were up-regulated in the *cdkf;1* mutant. Despite a marginal decrease in *PHYA* transcript levels, preliminary testing of different light responses of the

cdkf;1-1 mutant indicated an enhanced sensitivity to far-red light and slightly reduced sensitivity to blue light (Figure 22). Hypocotyl elongation of the *cdkf;1-1* is reduced to about 50% of wild type in the darkness, and this defect is not compensated by plant hormones, such as 0.1 μM Brassinolide and 10 μM GA3. Remarkably, inhibition of hypocotyl elongation of *cdkf;1-1* seedlings is highly enhanced by even low dose of far-red light that induces hypocotyl thickening, which is accompanied by formation of leaf-primordium-like structures appearing in addition to the cotyledons and enhanced anthocyanin formation. This suggests the potential enhancement of PHYA signalling pathway. By contrast, in low dose of blue light, causing incomplete inhibition of hypocotyl elongation of wild type, the difference in hypocotyl length between wild type and mutant is diminished. Whether or not this reflects some decrease in blue light sensitivity remains to be established.

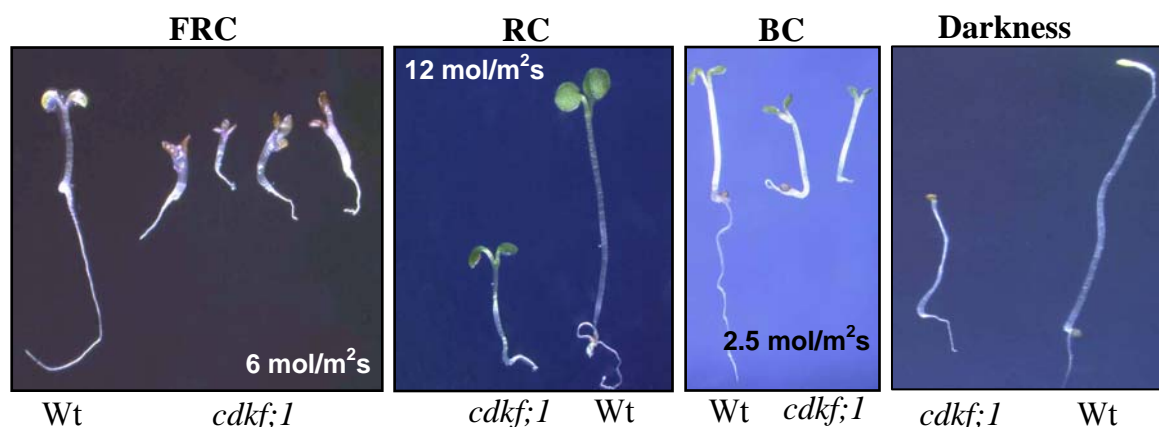


Figure 22. Hypocotyl elongation responses of *cdkf;1-1* mutant compared to wild type to different light regimes.

Seedlings were grown for 7 days under FRC – constant far-red, RC – constant red, BC – constant blue illumination.

Remarkably, hypocotyl lengths of wild type and *cdkf;1-1* mutant were similar when seedlings were grown under short day conditions in white light (Figure 23). In contrast, similar light conditions in long days resulted in enhanced inhibition of *cdkf;1-1* hypocotyl elongation compared to wild type. This suggests a day-length dependent regulation of hypocotyl growth by the CDKF;1 function.

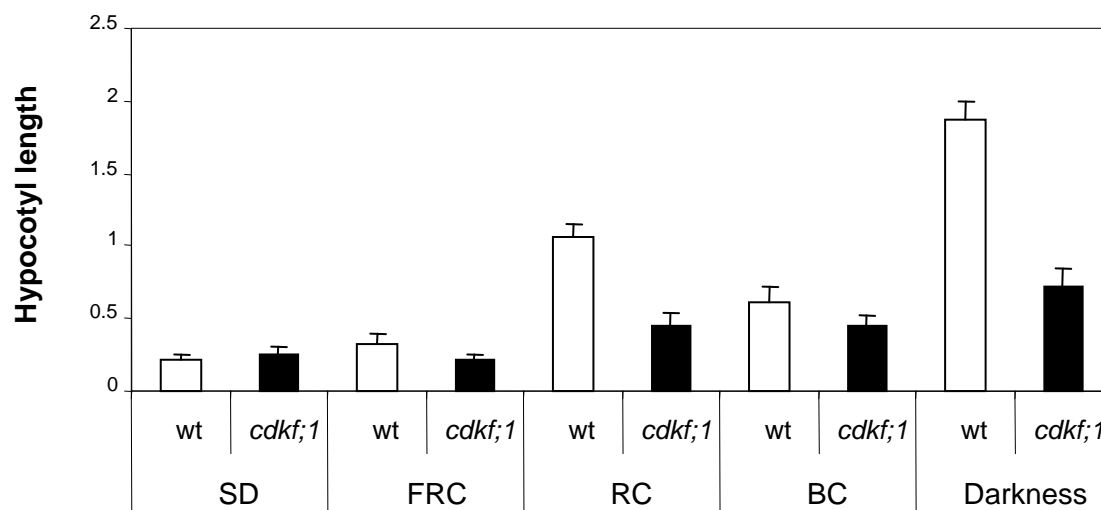


Figure 23. Comparison of hypocotyl lengths of control wild type and *cdkf;1-1* mutant seedlings grown under different light conditions.

Hypocotyl lengths of seedlings grown in white light under short day (SD, 8g light/16h darkness) condition, constant far-red (FRC), constant red (RC), constant blue (BC) illumination and darkness for 7 days.

In potential relationship with this, our transcript profiling data indicated 2 to 4-fold upregulation of transcription of two central positive regulators of photomorphogenesis, ELONGATED HYPOCOTYL5 (HY5) and HY5 HOMOLOG (HYH) in the *cdkf;1-1* mutant (Table 5). Activation of HY5 controlling anthocyanin biosynthesis is also consistent with higher level of transcription of numerous genes acting in the anthocyanin/flavonoid pathways in the *cdkf;1-1* mutant (Vandenbussche et al., 2007; Table 5).

Table 5. The list of differentially expressed genes involved in light signaling, circadian clock, flowering time and flower development pathways.

Reproducibility of differences observed in transcript levels by microarray hybridization between wild type and *cdkf;1-1* mutant was verified by qRT-PCR measurements. Green colour indicates down-regulated genes, purple marks up-regulated transcripts.

AGI	Short /Full name	Fold change	
		Affymetrix Chip Data	RT-qPCR
Light signaling			
AT5G58140	PHOT2	1.71846	1.07698
AT2G02710	PLPB	1.978388	1.63074
AT1G75100	JAC1	1.524982	
AT3G19850	phototropic-responsive NPH3 family protein	1.74752	1.304647
AT3G15570	phototropic-responsive NPH3 family protein	3.007502	3.04997
AT1G76500	SOB3	2.068157	1.63776
AT1G09570	PHYA		1.437115
AT5G35840	PHYC	2.090195	2.95653
AT4G16250	PHYD		1.617621
AT4G18130	PHYE	1.608125	1.548439
AT3G09150	HY2	1.649175	2.02203
AT2G26550	HEME OXYGENASE 2	1.71529	2.17184
AT2G02950	PKS1	2.118433	3.43448
AT1G14280	PKS2		1.737654
AT1G18810	phytochrome kinase substrate-related	2.035439	
AT2G24540	ATTENUATED FAR-RED RESPONSE	2.191512	2.84612
AT4G29080	PAP2	1.842162	1.19394
AT1G09530	PIF3	2.040161	2.13754
AT2G43010	PIF4	2.256505	2.70038
AT5G41790	CIP1	2.316819	1.91121
AT5G11260	HY5	2.13102	3.46212
AT3G17609	HYH	3.671373	4.73602
AT1G78600	LZF1	3.271578	2.0358
AT2G31380	STH	1.85505	1.7009
Circadian clock			
AT2G46830	CCA1	3.019413	1.50248
AT1G01060	LHY	3.650038	1.94039
AT5G24470	APRR5	1.532648	1.36116
AT5G02810	PRR7	4.774467	4.589

AGI	Short /Full name	Fold change	
		Affymetrix Chip Data	RT-qPCR
AT1G22770	GIGANTEA	2.191684	1.81519
AT5G37260	CIR1	5.292889	4.31392
AT4G39260	CCR1		1.420341
AT2G21660	CCR2 AtGPR7	1.636161	2.08296
AT3G22420	WNK2	1.662158	1.42562
AT3G18750	WNK6	2.403382	2.79786
Flowering time			
AT5G10140	FLOWERING LOCUS C	2.247264	2.19343
AT5G15850	constans-like 1	3.158363	2.22442
AT3G02380	constans-like 2	2.910838	1.74536
AT3G07650	CONSTANS-LIKE 9	1.711383	1.92767
AT5G15840	CO		1.540962
AT5G39660	CDF2 (CYCLING DOF FACTOR 2)	2.099515	1.45951
AT1G51700	ADOF1	1.724686	
AT5G62940	Dof-type zinc finger domain-containing protein	1.764011	
AT2G28510	Dof-type zinc finger domain-containing protein	1.821603	
AT1G26790	Dof-type zinc finger domain-containing protein	3.950895	
AT3G54990	SMZ (SCHLAFMUTZE)	2.377229	2.5202
AT2G39250	SNZ		1.364241
AT5G67180	TOE3		3.797919
AT1G65480	FLOWERING LOCUS T		10.52798
AT2G22540	SVP (SHORT VEGETATIVE PHASE)	2.99947	4.78543
AT2G45660	SOC1	3.333172	13.5992
AT5G06100	MYB33	1.863911	2.98583
At2g32460	MYB101		2.2737855
AT1G13260	RAV1	2.650737	
Flower development			
AT5G13790	AGAMOUS-LIKE 15	1.517282	
AT2G21060	ATGRP2B	2.474226	
AT2G27550	ATC	2.233745	1.16389
AT1G06180	ATMYB13	2.294585	
AT5G15230	GASA4	1.664284	
AT3G25655	IDL1	1.514651	
AT1G06520	GPAT1	1.572195	
AT4G24540	AGL24		2.238488
AT4G18960	AGAMOUS		4.156866
AT4G36920	APETALA 2	1.609219	3.03772
AT3G54340	APETALA 3		5.227593
AT5G20240	PISTILLATA		2.109287
AT1G24260	SEPALLATA3	2.344792	4.2779
AT2G03710	SEPALLATA 4	2.341351	5.74995
AT4G37940	AGL21	1.842394	
AT4G28190	ULTRAPETALA1	1.767913	3.52046
AT5G43270	SPL2	2.105046	1.76612
AT1G27370	SPL10	1.594298	
AT2G45830	DTA2	1.588151	
AT2G22310	ATUBP4	1.652804	
AT3G02130	RECEPTOR-LIKE PROTEIN KINASE 2	1.675311	
Phenylpropanoid/Flavonoid/Anthocyanin			

AGI	Short /Full name	Fold change	
		Affymetrix Chip Data	RT-qPCR
AT1G71030	MYBL2	2.735058	
AT5G04230	PAL3	1.607179	
AT3G51240	F3H	2.1829	
AT5G42800	DFR	2.254091	
AT5G13930	TT4 (TRANSPARENT TESTA 4)	2.839279	
AT4G39230	isoflavone reductase, putative	1.616363	
AT5G19440	cinnamyl-alcohol dehydrogenase	1.621758	
AT1G80820	CINNAMOYL COA REDUCTASE	1.735608	
AT2G30490	CINNAMATE-4-HYDROXYLASE	1.616198	
AT4G37970	CAD6	2.123842	
AT3G21240	4CL2	1.611799	
AT1G65060	4CL3 (4-coumarate-CoA ligase)	1.791232	
AT5G61160	AACT1	2.772888	
AT5G54060	UF3GT	1.692318	
AT2G22990	SNG1 (SINAPOYLGLUCOSE 1	2.614454	

3.4.4. Altered regulation of genes in the circadian clock and flowering time pathways in the *cdkf;1-1* mutant

In *Arabidopsis*, four major genetic pathways, the photoperiodic, vernalization, autonomous, and gibberellin pathways, control flowering time. Control of the timing of floral induction by the photoperiodic pathway involves the central regulator *CONSTANS* (*CO*), which promotes flowering by activating the transcription of flowering time integrators genes *FLOWERING LOCUS T* (*FT*) and *SUPPRESSOR OF OVEREXPRESSION OF CONSTANS1* (*SOCI*) (Yoo et al., 2005).

Transcription of *CO* is regulated by the circadian clock together with the stability of *CO* protein, and therefore also by the photoreceptors *PHYA*, *PHYB*, *CRY1*, and *CRY2*. Regulation of *CO* represents thus a key mechanism of day-length measurement and flowering time regulation (Valverde et al., 2004; Corbesier and Coupland, 2006; Más, 2008). Our microarray and qRT-PCR data indicated simultaneous upregulation of two core genes of the circadian clock, *CIRCADIAN CLOCK-ASSOCIATED PROTEIN 1* (*CCA1*) and *LATE ELONGATED HYPOCOTYL* (*LHY*) (Table 5). Enhancement of *CCA1* and *LHY1* transcription is consistent with an increase of transcript level of *PHYTOCHROME-INTERACTING FACTOR 3* (*PIF3*) and decrease of *PRR5* and *PRR7* expression, which is negatively regulated by *CCA1* and *LHY1* (Nakamichi et al., 2007). *PIF3* is proposed to recruit the active form of *PHYB* to G-box containing promoters and it is functionally required for *PHYB*-induced transcription of *CCA1* and *LHY* (Alabadi et al., 2001; Martinez-Garcia et al., 2000). *GIGANTEA* (*GI*), which is repressed by *CCA1* and *LHY* but required for *CO* activation (Quail, 2002), is also down-regulated in the *cdkf;1* mutant (Table 5). In the GI-dependent but *CO*-independent flowering pathway, in which miR172 negatively regulates the functions of *TOE1* homologues, the transcription of *SCHLAFMÜTZE* (*SMZ*) encoding a floral repressor is down-regulated but other *TOE1*-related repressors are unaffected or upregulated, such as *TOE3*.

In addition to alterations in the regulation of genes acting in the photoperiodic pathway, the expression of *FLC* encoding a central repressor of floral integrator genes (Lee et al., 2000), is upregulated in the *cdkf;1-1* mutant. In accordance, transcript levels of floral integrator genes *FT* and *SOC1* show 10- and 13-fold decrease in *cdkf;1-1* compared to wild type seedlings (Table 5). Despite the fact that these data derived from short day grown (7 DAG), some of the observed regulatory changes seem to be relevant as they are consistent with the *cdkf;1-1* flowering phenotype. Unless treated with gibberellin, the *cdkf;1-1* mutant never blooms in short days, and in long days develops flower buds only after 56±10 days.

From the framework of genes controlling flower development downstream of the flowering time pathways *ULTRAPETALA 1 (ULT1)*, *AGAMOUS LIKE 24 (AGL24)*, *AGAMOUS (AG)*, *APETALA 2 (AP2)*, *APETALA 3 (AP3)*, *SEPALLATA 3 (SEP3)*, and *SEPALLATA 4 (SEP4)* showed reduced expression in the *cdkf;1-1* mutant (Table 5). *SHORT VEGETATIVE STAGE (SVP)*, which is an interacting partner of *FLC* in a co-repressor complex showing direct binding to the *SOC1* promoter (Li et al., 2008), is down-regulated in *cdkf;1-1*. Thus, *SVP* cannot account for strong repression of *SOC1* in the mutant. *SVP* together with *AGL24* are direct repressors of *APETALA1 (AP1)* and *CAULIFLOWER (CAL)*, and the *ap1 agl24 svp* triple mutants produces inflorescence meristems in place of flowers (Gregis et al., 2008). This is fully consistent with that the *cdkf;1-1* mutant produces only single terminal flowers on side branches of inflorescence stem (see Figure 8). Nevertheless, it is clear that for establishment of further correlations between flowering traits and altered gene regulation in the *cdkf;1-1* mutant it will be necessary to examine plants in a later developmental stage exposed to induction of flowering. A huge difference between development of wild type and *cdkf;1-1* mutant at flowering would however prevent reaching meaningful conclusions. Therefore, this experiment can only be performed using the estradiol-inducible vector pER8-GW described in 3.2.3 to obtain a genetically complemented *cdkf;1-1* mutant grown on estradiol, and subsequent depletion of *CDKF;1* transcript levels by withdrawing estradiol before induction of flowering.

3.4.5. *Effects of cdkf;1-1 mutation on genes controlling hormone biosynthesis and signal transduction pathways*

The microarray data indicated altered the expression of several genes acting in the cytokinin signal transduction pathway in the *cdkf;1-1* mutant (Table 6). Cytokinin signal transduction is mediated by a two-component system, in which cytokinin perception and autophosphorylation of a conserved His residue takes place in *Arabidopsis* HISTIDIN KINASEs (AHKs). Subsequently, the phosphoryl group is transferred to a conserved Asp residue within the receiver domain of AHKs. Transphosphorylation of HISTIDINE-CONTAINING PHOSPHOTRANSFERASEs (AHPs) by AHKs triggers their import into the nucleus, where they transmit the phosphoryl group to type-B *Arabidopsis* RESPONSE REGULATORS (ARRs), which activate the expression of cytokinin-responsive genes and type-A ARR. In turn, type-A ARR mediate negative feedback regulation of cytokinin signaling (Lohrmann and Harter, 2002; Hwang, et al., 2002; Kakimoto, 2003). In the *cdkf;1* mutant, *HP (AHP1)*, one out of

6 *AHPs*, two from 12 type-B *ARRs* (*ARR12* and *ARR14*) and four from 11 type-A *ARRs* (*ARR3*, *ARR4*, *ARR8*, and *ARR9*) are down-regulated. A potential clue to further understanding of these changes is provided by the observations that *ARR4* can directly interact with *PHYB* and that loss of *ARR3* and *ARR4* functions directly affect the circadian clock by lengthening the normal period (Salomé et al., 2006). The fact that transcription of *ARR7* (type-A), the *Cytokinin RESPONSE FACTORS* *CRF5* and *CRF6*, and the *Cytokinin-RESPONSIVE GATA FACTOR1* (*CGA1*), which positively regulate a large fraction of cytokinin-responsive genes (Rashotte et al., 2006; Naito et al., 2007; Table 6), are up-regulated in the mutant indicates that cytokinin responses are not completely compromised by the *cdk;1-1* mutation.

Down-regulation of the *HY2* and *HO2* genes involved in phytochrome chromophore biosynthesis has been demonstrated to trigger overproduction of jasmonic acid (JA) and activation of JA-induced genes (Zhai et al., 2007). This is also indicated by upregulation of JA-responsive PHOSPHOLIPASE A 2A(*PLA2*), LYPOXIGEASE (*LOX2*), CORONATINE INDUCED 1 (*CORI1*), JASMONATE RESPONSIVE 1 (*JR1*), PDF2.1 etc. target genes in the mutant (see Annex). Among these, the activation of JA-induced *ANTHRANILATE SYNTHASE ALPHA SUBUNIT 1* (*ASA1*) gene, which encodes a rate-limiting enzyme of tryptophan biosynthesis is accompanied by upregulation of *TRYPTOPHAN SYNTHASE BETA SUBUNIT 2* (*TSB2*) and *TRYPTOPHAN AMINOTRANSFERASE OF ARABIDOPSIS 1*, and several genes involved in the biosynthesis of indole glucosinolates (*CYTOCHROME P450 83A1*, *CYP83A1*; *CYTOCHROME P450 81F2*, *CYP81F2*; *INDOLE-3-ACETATE BETA-D-GLUCOSYLTRANSFERASE*, *IAGLU*; *EPITHIOSPECIFIER MODIFIER 1*, *ESMI*) (Niyogi and Fink, 1992; Bak et al., 2001; Teale et al., 2006; Chandler, 2009). As only few auxin-responsive genes showed altered regulation in the mutant, this data suggested that upregulation of tryptophan-derived IAA synthesis channels the IAA pool into the glucosinolate biosynthesis.

The *cdk;1-1* mutation caused also changes in the transcription of numerous genes controlling ABA biosynthesis and signalling, and downstream targets in the ABA-dependent osmotic stress response pathways (Table 6; Annex; Niyogi et al., 1998). The first step of ABA biosynthesis is regulated by ABA DEFICIENT 1 (*ABA1*), which showed around 3-fold reduction in expression in the mutant. In addition, *NINE-CIS-EPOXYCAROTENOID DIOXYGENASE 4* (*NCDE4*) and *ALDEHYDE OXIDASE 2* (*AAO2*), which encode close homologues of two key enzymes of ABA biosynthesis *NCDE3* and *AAO3* (Nambara and Marion-Poll, 2005), showed 7- and 2-fold down-regulation, respectively. Partial deregulation of ABA-responses is also indicated by a decrease in transcript levels of GLUTAMATE RECEPTOR 1.1 (*GLR1.1*; regulates ABA biosynthesis and signalling; Kang et al., 2004), the ABA-responsive transcription factor *ABSCISIC ACID RESPONSIVE ELEMENT-BINDING FACTOR 1* (*ABF1*), and several ABA-inducible target genes encoding the *CALCIUM-DEPENDENT PROTEIN KINASE 6* (*CPK6*), *CBL-INTERACTING PROTEIN KINASE 20* (*CIPK20*), *DELAY OF GERMINATION 1* (*DOG1*), *PLANT U-BOX 9* (*PUB9*), and *ATDR4*. On the other hand, as part of a potential compensatory mechanism, several genes acting in ABA signalling showed higher transcript levels in the *cdk;1-1* mutant. These included the *NUCLEAR FACTOR Y SUBUNIT C2* (*NF-YC2*),

Arabidopsis thaliana SERINE/THREONINE PROTEIN KINASE 1 (ATSR1), RING-H2 FINGER PROTEIN 2B (RHA2B), and ABI FIVE BINDING PROTEIN 2 (AFP2). Activation of the hypoxia-linked ABA response pathway was indicated by simultaneously elevated transcript levels of ALCOHOL DEHYDROGENASE (ADH1) and its activating bZIP transcription factor GBF3. Furthermore, transcript level of the TWO OR MORE ABRES-CONTAINING GENE 2 (TMAC2) gene, which is highly ABA-inducible, was 2-fold higher in the *cdkf;1-1* mutant compared to wild type. This gene negatively regulates ABA signalling and its overexpression reduces the expression level of *SOC1* and *SEP3* genes (Huang and Wu, 2006), which is fully consistent both microarray data and the observed *cdkf;1* phenotype.

The *cdkf;1-1* mutation causes only minor changes in the expression of genes controlling the ethylene and gibberellin pathways. Among the five genes showing differential expression in the ethylene biosynthesis and signalling pathways, transcript level of the ETHYLENE-FORMING ENZYME (EFE) gene, encoding a key enzyme of ethylene biosynthesis, shows a marginal 1.7 increase in *cdkf;1-1* seedlings (Table 6).

Table 6. Differential expression of hormone-related genes in the *cdkf;1-1* mutant.

Comparison of differences in transcript levels between wild type and *cdkf;1-1* mutant observed by microarray hybridization and qRT-PCR. Green colour indicates down-regulated genes, purple marks up-regulated transcripts.

AGI	Short /Full name	Fold change	
		Affymetrix Chip Data	RT-qPCR
Cytokinin			
AT1G19050	ARR7 (RESPONSE REGULATOR 7)	2.005949	
AT1G59940	ARR3 (RESPONSE REGULATOR 3)	1.570101	7.7204
AT1G10470	ARR4 (RESPONSE REGULATOR 4)		1.843903
AT3G57040	ARR9 (RESPONSE REGULATOR 9)	1.933676	2.36305
AT2G25180	ARR12 (RESPONSE REGULATOR 12)	1.720893	2.49203
AT2G01760	ARR14 (RESPONSE REGULATOR 14)	1.595503	2.48388
AT2G41310	ATRR3/ARR8 (RESPONSE REGULATOR 3)	2.109085	4.47897
AT3G21510	AHP1	2.43281	2.70815
AT4G29740	CKX4 (CYTOKININ OXIDASE 4)	1.716478	
AT2G46310	CRF5 (CYTOKININ RESPONSE FACTOR 5)	1.787357	2.12204
AT3G61630	CRF6 (CYTOKININ RESPONSE FACTOR 6)	2.551048	2.70008
AT4G26150	CGA1 (CYTOKININ-RESPONSIVE GATA FACTOR 1)	2.09657	5.93395
Auxin/tryptophan			
AT5G05730	ASA1	1.896081	1.76674
AT4G27070	TSB2	1.930539	
AT4G39950	CYP79B2	2.08635	1.05275
AT5G57220	CYP81F2	2.605483	
AT4G13770	CYP83A1	1.641514	
AT4G15550	IAGLU	1.578305	
AT2G47000	ABCB4	1.805203	
AT3G14210	ESM1 (epithiospecifier modifier 1)	1.751925	2.72782
AT1G70560	TAA1	1.834745	

AGI	Short /Full name	Fold change	
		Affymetrix Chip Data	RT-qPCR
AT4G24670	TAR2	1.882579	
AT3G59900	ARGOS	1.848169	
AT2G46990	IAA20	1.63337	
AT2G46530	ARF11 (AUXIN RESPONSE FACTOR 11)	2.915711	
AT3G04730	IAA16	1.543862	
AT4G32280	IAA29	1.592003	
AT4G12550	AIR1	3.601185	
AT3G07390	AIR12	1.712879	
AT3G25290	auxin-responsive family protein	1.55307	
AT4G12410	auxin-responsive family protein	1.600831	
AT1G16510	auxin-responsive family protein	1.624749	
AT3G12830	auxin-responsive family protein	1.787623	
AT3G60690	auxin-responsive family protein	2.084724	
AT4G34770	auxin-responsive family protein	2.347394	
AT1G75590	auxin-responsive family protein	3.571218	
AT4G36110	auxin-responsive protein, putative	3.482878	
AT4G00880	auxin-responsive family protein	2.572448	
AT2G37030	auxin-responsive family protein	2.810369	
AT1G76520	auxin efflux carrier family protein	1.705095	
ABA			
AT3G02140	TMAC2	2.014552	
AT1G56170	NF-YC2	1.512972	
AT1G13740	AFP2 (ABI FIVE BINDING PROTEIN 2)	1.967505	1.57501
AT3G29575	AFP3 (ABI FIVE BINDING PROTEIN 3)	1.767525	1.02929
AT4G38530	ATPLC1	1.500047	
AT5G01540	LECRKA4.1	1.583252	
AT1G15100	RHA2A;	2.543912	1.33174
AT2G01150	RHA2B	2.550761	1.71894
AT5G01820	ATSR1 (CIPK14)	1.881711	1.74123
AT2G17290	CPK6	1.87901	2.80004
AT5G45820	CIPK20/PKS18	9.525643	5.14657
AT3G04110	GLR1.1	1.934274	
AT5G67030	ABA1 (ABA DEFICIENT 1)	2.432254	2.92544
AT4G19170	NCED4	4.18439	6.8079
AT3G43600	AAO2 (ALDEHYDE OXIDASE 2)	1.992733	
AT1G49720	ABF1	1.615398	3.59847
AT5G45830	DOG1 (DELAY OF GERMINATION 1)	1.567339	
AT3G07360	PUB9 (PLANT U-BOX 9)	1.656021	
AT1G73330	ATDR4	10.53311	20.4879
Ethylene			
AT3G24500	MBF1C	1.940762	
AT4G26200	ACS7	2.136188	
AT1G05010	EFE (ETHYLENE-FORMING ENZYME)	1.707715	
AT1G12010	ACC oxidase, putative	1.766575	
AT5G43850	ARD4	1.549809	
GA			
AT5G14920	gibberellin-regulated family protein	2.762983	
AT2G14900	gibberellin-regulated family protein	2.969134	

3.4.6. *The cdkf;1-1 mutation has minimal effect on genes in cell cycle control*

Unexpectedly, the *cdkf;1-1* mutation resulted only in very modest changes in the transcription of genes involved in cell cycle control (Table 7). As a unique case, we have observed an about 10-fold difference between our Affymetrix microarray hybridization and qRT-PCR measurements of *KRP2* transcript levels, which showed a remarkable 13-fold increase by qRT-PCR in the *cdkf;1-1* mutant. This indicated that measurement of transcript levels of *KRP* homologues is likely not accurate using the Affymetrix chip. Overexpression of *KRP2* was reported to decrease the number of lateral roots and the rate of cell division through the reduction of CDKA;1 activity, leading to the onset of endoreduplication and increase of DNA ploidy level (Verkes et al., 2005). During phenotypic characterization of the *cdkf;1-1* mutant (section 3.3.2) we have observed a reduction in the number and size of leaf epidermal cells and a dramatic decrease in formation of lateral roots, which is consistent with upregulation of *KRP2* expression. However, in contrast to the results of Verkes et al. (2005), we found no enhancement of endoreduplication, which suggests that despite remarkable overexpression at the level of transcription, the *KRP2* protein could be efficiently degraded (e.g., due to marginal overexpression of the mitosis specific CDKB;1 kinase in *cdkf;1-1*). Further immunoblotting studies are therefore required to clarify this discrepancy.

3.4.7. *Inhibition of cell elongation correlates with down-regulation of genes controlling cytoskeleton functions in the cdkf;1-1 mutant*

In addition to potential defects in light signalling discussed in 3.4.3, cell elongation defects observed in the *cdkf;1-1* mutant also correlated with a general reduction in the transcription of genes encoding cytoskeleton-related proteins (Table 7). These included *ACTIN 11 (ACT11)*, *ACTIN DEPOLYMERIZING FACTORS ADF8* and *ADF11*; *FORMIN HOMOLOGY proteins AFH1* and *AtFIM1*; *RHO-RELATED PROTEIN FROM PLANTS 2 (ROP2I)*; *TONNEAU 1A (TON1A)*; *MICROTUBULE-ASSOCIATED PROTEINS AtMAP65-1* and *AtMAP70-4*; *ZWICHEL (ZWI)*; two *MYOSIN HEAVY CHAIN-RELATED* and three *KINESIN MOTOR PROTEIN-RELATED* genes.

ACTIN 11 (ACT11) is a structural constituent of cytoskeleton, which is expressed in young and developing tissues, including elongating hypocotyls, expanding leaves, floral organ primordia, emerging floral buds, and developing ovules (Huang et al., 1997). *AFH1* plays a key role in initiation and organization of actin cables (Michelot et al., 2005). Both *ADF8* and *ADF11* are specifically expressed in root trichoblast cells, developing root hairs and mature pollens (Kandasamy et al., 2007). The latter actin depolymerizing factors together with actin bundling proteins play crucial roles in the regulation of cytoskeleton organization and dynamics, and thereby cell division and intracellular trafficking in the root hair. *AtFIM1*, an actin filament cross-linking protein stabilizes actin filaments (Kovar et al., 2000). The *Arabidopsis* *ROP2* GTPase positively regulates different stages of root hair development (Jones et al., 2002). Loss of function of *TONNEAU 1* leads to an extreme dwarf phenotype; the *ton1* mutants have defects in random orientation, cell elongation and cell division. *AtMAP65-1* bundles microtubules during the cell cycle (interphase, anaphase, and telophase, but not

in prometaphase and metaphase). This event is probably mediated by phosphorylation and inactivation of AtMAP65-1, and required for metaphase to anaphase transition (Smertenko et al., 2006). ZWICHEL, a kinesin-like protein, is expressed in root hairs, trichomes, and pollen grains, as well as dividing cells. The *zwichel* mutant develops trichomes with only two branches showing a defect in trichome morphogenesis (Oppenheimer, 1997; Reddy and Reddy, 2004). The above described functional defects, including deficiency of root elongation, lack of root hairs, development of aberrant trichomes with single or two branches, the defect of epidermal cell expansion and extreme dwarf phenotype represent major phenotypic characteristics of the *cdkf;1-1* mutant.

Table 7. Altered transcription of genes involved in cell cycle control and regulation of cytoskeleton organization in the *cdkf;1-1* mutant.

Green colour indicates down-regulated genes, purple marks up-regulated transcripts.

AGI	Short /Full name	Fold change	
		Affymetrix Chip Data	RT-qPCR
Cell Cycle			
AT5G04470	SIAMASE	1.966066	1.416683
AT3G50630	KRP2	1.620258	13.44091
AT4G37490	CYCB1;1	1.613603	
AT1G47210	cyclin family protein	1.521937	
AT3G21870	CYCP2;1 (cyclin p2;1)	1.792875	
AT5G67260	CYCD3;2	1.60564	
AT3G19650	cyclin-related	1.814348	
AT1G27630	CYCT1;3	1.529668	
Cytoskeleton			
AT3G53760	tubulin family protein	1.614687	
AT3G12110	ACT11 (actin-11)	1.651488	
AT1G01750	ADF11	3.861768	
AT4G00680	ADF8	4.741093	
AT3G25500	AFH1	1.531936	
AT4G26700	ATFIM1	1.719208	
AT1G20090	ROP2	1.54212	
AT3G55000	TON1A (TONNEAU 1)	2.288211	
AT5G55230	ATMAP65-1	1.755587	
AT1G14840	ATMAP70-4	1.735414	
AT5G27950	kinesin motor protein-related	1.622855	
AT5G10470	kinesin motor protein-related	1.782079	
AT2G21380	kinesin motor protein-related	1.892213	
AT2G37080	myosin heavy chain-related	1.564108	
AT3G13190	myosin heavy chain-related	1.661566	
AT5G65930	ZWI (ZWICHEL)	2.099097	2.09174

3.5. *CDKF;1* is a *VirD2* kinase controlling *Agrobacterium*-mediated tumour formation in plants

Bakó et al. (2003) have found that CAK2Ms, an alfalfa orthologue of *Arabidopsis* CDKD;2/CAK4 kinase phosphorylates the *VirD2* protein that plays a pivotal role in *Agrobacterium*-mediated transformation of plants. During processing of the T-DNA borders in bacteria, the *VirD2* protein

covalently binds to the 5'-end of the single-stranded T-DNA intermediate (T-strand) and aids its transfer into plant host cells through T4SS T-pili assembled from components of the VirB/D4 type 4 secretion system. Genetic studies show that *virD2* mutations dramatically reduce nuclear import of the T-strand, as well as the frequency of T-DNA integration into plant chromosomes, and result in the formation of deletions at the right border (RB) junctions of T-DNA insertions (Mysore et al., 1998; Michielse et al., 2004). Therefore, VirD2 is thought to mediate precise linking the 5'-end of the T-strand to free 3'-ends in the integration target sites of host chromosomes.

Bakó et al. (2003) showed that upon its α -importin mediated nuclear import (Ziemiencowicz et al., 2001), VirD2 interacts through its N-terminal domain with the TATA-binding protein TBP, which can be co-immunoprecipitated with the CTD of RNA polymerase II largest subunit. Bakó et al. also purified and identified a VirD2 kinase as CAK2Ms, and showed that HA-CAK2Ms immunoprecipitated from plant extracts phosphorylates the CTD domain of RNA polymerase II and the VirD2 protein *in vitro*. However, CAK2Ms expressed in and purified from *E. coli* has not been tested for VirD2 phosphorylation. To determine, whether *Arabidopsis* CDKD2 and any other member of the CDKD kinase family would phosphorylate VirD2 *in vitro*, we have performed kinase assays with purified thioredoxin-His₆-tagged fusions of CDKD;1, CDKD;2 and CDKD;3, and purified HA-VirD2 as substrate. Unexpectedly, we found that none of the *Arabidopsis* CDKD kinases was capable to phosphorylate the HA-VirD2 protein.

CDKD2 kinases purified from both *Arabidopsis* and rice have been detected in tight association with the CDKF;1 (Van Leene et al., 2007; Ding et al., 2009) and the *cdkf;1-1* mutation was found to reduce dramatically the level of CDKD2 protein in *Arabidopsis* (Takatsuka et al., 2009). Therefore, it appeared to be plausible that in the experiments of Bakó et al. (2003) CAK2Ms was immunoprecipitated with an alfalfa orthologue of CDKF;1, which was responsible for the observed VirD2 kinase activity. To test this possibility, we performed an *in vitro* kinase assay with purified thioredoxin-His₆-tagged *Arabidopsis* CDKF;1 and the HA-VirD2 substrate (Figure 24).

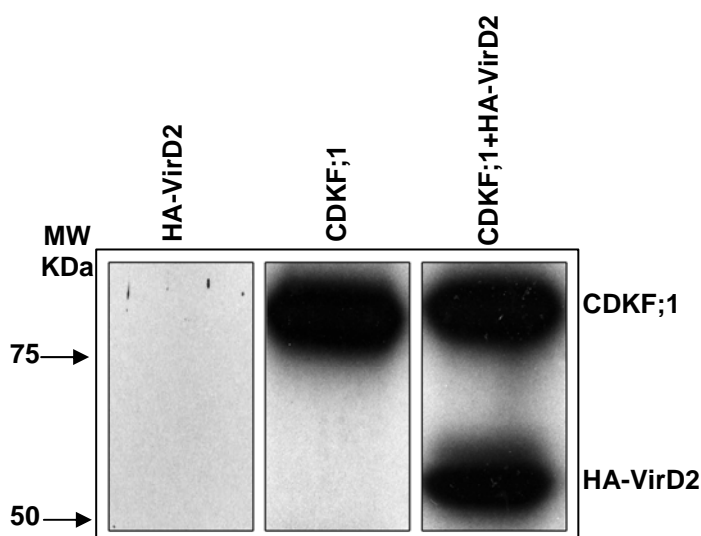


Figure 24. CDKF;1 phosphorylates the HA-VirD2 protein *in vitro*.

Phosphorylation of HA-VirD2 substrate was performed with purified CDKF;1 kinase in the presence of [γ -³²P]ATP). Control phosphorylation assays contained either CDKF;1 or HA-VirD2 alone.

This experiment demonstrated that in fact CDKF;1 could efficiently phosphorylate HA-VirD2 *in vitro*. To examine the biological relevance of CDKF;1 phosphorylation sites in the VirD2 protein and study the effects of their mutations on T-DNA integration, we have initiated mapping of the phosphorylated VirD2 residues. The phosphorylated VirD2 protein isoforms were separated by 2D electrophoresis, and then the phosphoprotein spots were visualized by phosphostaining, and subsequent CBB staining (Figure 25). The phosphorylated VirD2 spots were excised from gel, to identify the phosphorylation sites followed affinity capture of phosphopeptides and their identification by MALDI Q-TOF degradation. This approach has led to the identification of 6 phosphorylation sites in the VirD2 protein in close vicinity of the C-terminal nuclear localization signals (data not shown).

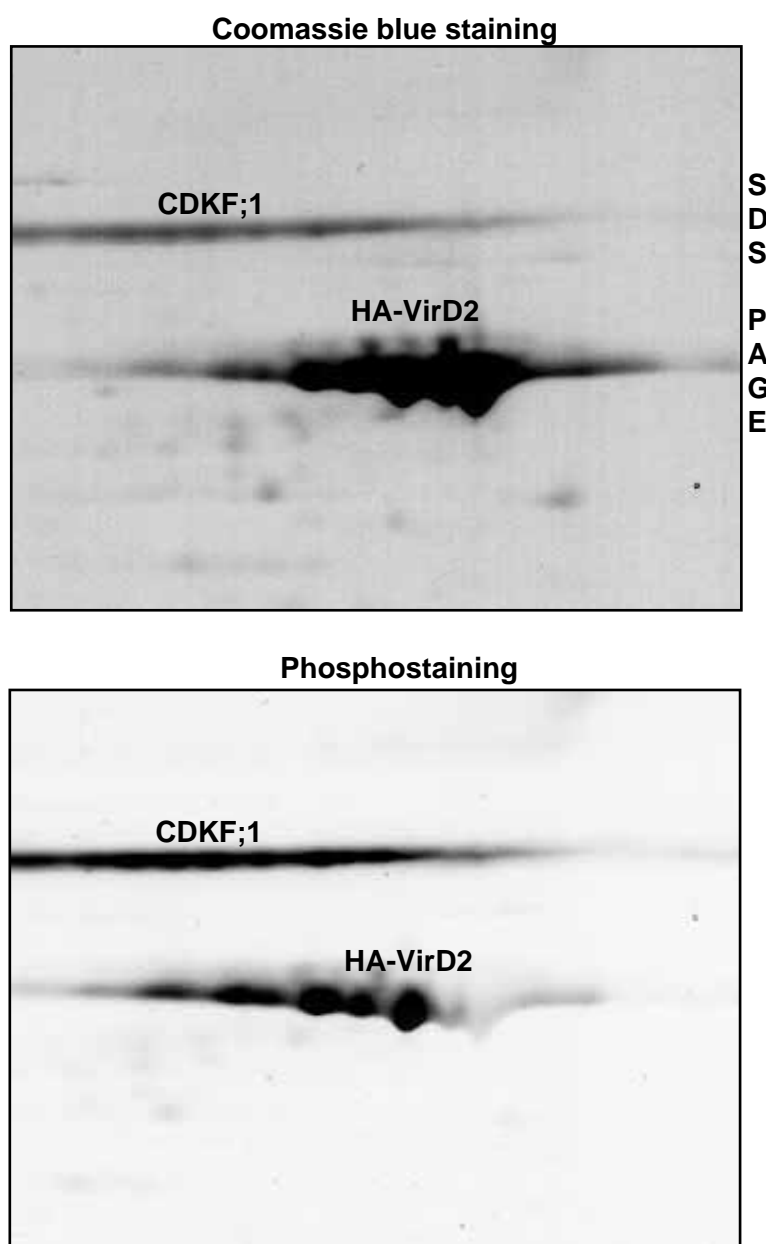


Figure 25. Resolution of CDKF;1 phosphorylated HA-VirD2 isoforms, carrying different number of phosphorylated residues, by two-dimensional gel electrophoresis.

In the first dimension, isoelectric focusing was performed on an IPG strip using a linear gradient of pH 4-7. In the second dimension, the proteins were separated on a 12% SDS-PAGE along with phosphorylated molecular

mass markers. The autophosphorylated CDKF;1 kinase and phosphorylated HA-VirD2 substrate were visualized by phosphoprotein stain. Arrows indicate protein bands subjected to analysis by iontrap MALDI mass spectrometry.

3.5.1. *CDKF;1 phosphorylates the CDKD kinases and VirD2 with similar efficiency*

To compare the CDKD and VirD2 substrate specificity of CDKF;1, we performed standardized comparative kinase assays by combining purified CDKF;1 and HA-VirD2 with different CDKD substrates. CDKF;1 phosphorylated all three CDKDs and the HA-VirD2 protein with very similar efficiency (Figure 26).

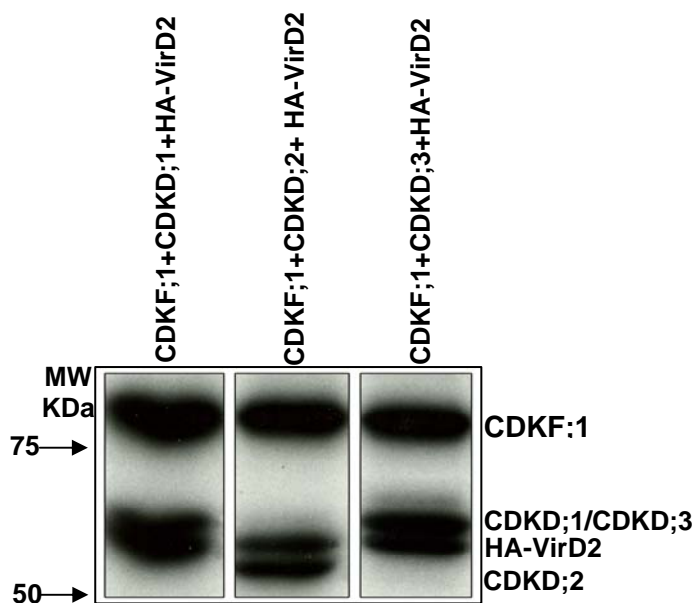


Figure 26. CDKF;1 phosphorylates VirD2 and CDKD substrate with similar efficiency *in vitro*. The kinase assays contained CDKF;1 and HA-VirD2 in combination with either CDKD;1; CDKD;2 or CDKD;3.

3.5.2. *The cdkf;1 and cdkd;2 mutants are defective in Agrobacterium-mediated tumorigenesis*

Whereas we failed to demonstrate that CDKD;2, a likely functional orthologue of alfalfa CAK2Ms (Bako et al., 2003), is a VirD2 kinase, we have observed efficient phosphorylation of VirD2 by CDKF;1 in our assays. Because CDKF;1 is an upstream activator of CDKD;2 *in vivo*, our data does not exclude a potential role of CDKD;2 in VirD2 phosphorylation. To test possible involvement of CDKF;1 and CDKD kinases in the control of *Agrobacterium*-mediated transformation, the oncogenic *Agrobacterium tumefaciens* C58 strain was used for hypocotyl tumorigenesis assay with *cdkd;1-1*, *cdkd;2-1*, *cdkd;3-1*, and *cdkf;1-1* mutant and wild type plants. The number of infected plants was 150 ± 4 in each experiment (Figure 27). The overall efficiency of tumour formation was 81% in wild type, 83% in *cdkd;1-1* and 82% in *cdkd;3-1* plants. By contrast, the frequency of tumour formation was reduced to 7% in *cdkf;1-1* and 18% in *cdkd;2-1* mutants indicating that both CDKF;1 and CDKD;2 play a role in the control of *Agrobacterium*-mediated plant transformation. These results strongly suggest that the CDKD;2 kinase is most likely required for recruitment of VirD2 to the CDKF;1 kinase. In fact Bakó et al. (2003) noted a close similarity between N-terminal VirD2

sequences and the histidine-triad protein interaction domain of HINT proteins that mediate their interactions with yeast Kin28 and human CDK7 orthologues of *Arabidopsis* CDKDs (Korsisaari and Mäkelä, 2000).

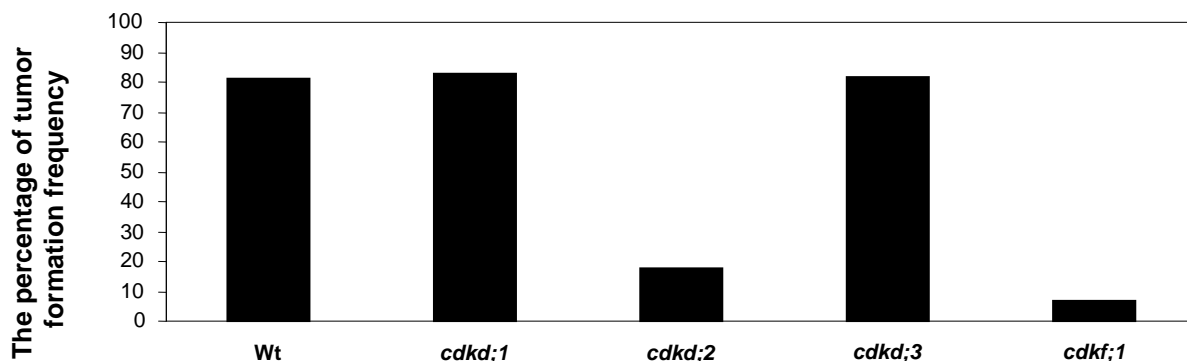


Figure 27. Comparison of frequency of tumour formation by hypocotyl agroinfection in wild type, *cdkf;1* and *cdkd* mutant seedlings.

The hypocotyl tumorigenesis assays were performed with an oncogenic *Agrobacterium tumefaciens* C58 strain by infection of 15 days old plants.

As the structures of eukaryotic CAKs are remarkably similar, it is likely that the histidine-triad domain plays a role in recruitment of VirD2 by CDKD;2, which is associated with the VirD2 kinase CDKF;1. The observation that inactivation of CDKF;1 leads to enhanced proteolysis of CDKD;2, as proposed by Takatsuka et al. (2009), suggests that the CDKD;2-cyclinH complex is stable only in the presence of CDKF;1. Thus, mutations affecting both CDKF;1 and CDKD;2 could destabilize the complex preventing the recognition of VirD2 protein. Further purification of CDKF;1-CDKD;2-cyclin-(TFIIH) complex and studying its *in vivo* interaction with VirD2 should help to confirm this model. In any case, our current data show that the CDKF;1 function mediating VirD2 phosphorylation is necessary together with CDKD;2 for *Agrobacterium*-mediated tumour formation in *Arabidopsis*.

4. DISCUSSION

4.1. *Arabidopsis* CDKF;1 phosphorylates CDKDs and RNA polymerase II CTD

C-terminal heptapeptide repeats of the largest subunit of RNAPII are known to provide a scaffold for assembly of numerous factors that regulate the initiation, elongation, and termination of transcription, mRNA processing (5' capping, 3' polyadenylation, and splicing) and histone methylation in yeast and mammals (Belostotsky and Rose, 2005; Xiao et al., 2003). Overall conservation of CTD and many of its binding factors suggests that the CTD is implicated in similar processes also in plants. This is indicated by the fact that CTD kinases, including the TFIIH-associated CAKs that represent key regulators of the CTD code during transcription, are evolutionarily conserved in higher plants. *Arabidopsis* CDKD;2 and rice R2/CDKD;1 are closely related to human CDK7 and therefore thought to play important roles in transcription initiation and 5' capping of nascent RNAs (Leene et al., 2008; Rohila et al., 2006). As human CDK7, rice R2 was shown to interact with cyclin H, which stimulates its kinase activity on *Arabidopsis* RNAPII CTD and heterologous human CDK2 substrates *in vitro* (Yamaguchi et al., 1998).

In *Arabidopsis* three CAKs (CDKD;1, CDKD;2, and CDKD;3) were identified, which are closely related to rice R2 and human CDK7. When co-expressed in insect cells, cyclin H-binding was shown to increase the activity of *Arabidopsis* CDKD;2, which phosphorylates the human GST-CDK2 and *Arabidopsis* GST-CTD substrates *in vitro* (Shimotono et al., 2006). In contrast to CDKD;2, CDKD;3 appears to phosphorylate both GST-CDK2 and GST-CTD in the absence of cyclin H binding. Nevertheless, the activity of CDKD;3 is also enhanced by co-expression of cyclin H;1 in insects cells. Compared to CDKD;2, CDKD;3 has low CTD-kinase activity but phosphorylates human CDK2 with higher efficiency. The third member of the CDKD family, CDKD;1 purified in fusion with the maltose-binding protein MBP, was reported to show no kinase activity with GST-CTD and GST-CDK2 substrates.

In *Arabidopsis*, rice, soybean and leafy spurge (*Euphorbia esula* L.) a fourth plant specific CAK-like kinase, CDKF;1, was identified, which suppresses the temperature sensitive *cak^{ts}* mutations in budding yeast (Umeda et al., 1998, 2005; Chao et al., 2007). It was reported that *Arabidopsis* CDKF;1 does not bind cyclin H and cannot phosphorylate the CTD of RNAPII (Shimotono et al., 2004). In addition, it was shown that CDKF;1 phosphorylates human CDK2, as well as the *Arabidopsis* CDKD;2 and CDKD;3 kinases on a highly conserved Thr residue in their T-loops, and that CDKF;1-mediated phosphorylation enhances the CTD kinase activity of CDKD;2 (Shimotono et al., 2004). However, the same authors reported that CDKF;1 does not phosphorylate CDKD;1, the third member of *Arabidopsis* CDKD/CAK family, which apparently cannot phosphorylate the CTD and human CDK2, and is therefore thought to be an inactive kinase. These observations defined CDKF;1 as a novel CAK-activating kinase (CAKAK), which has not been so far identified in mammals. In their model, Umeda et al., (2005) suggested that CDKF;1 can control in two independent ways the activity of cyclin-dependent CDK kinases acting in cell cycle control: either by direct

phosphorylation of CDKs (i.e., either CDKA or CDKB or both) or by activation of CDK-activating CDKD kinases. This model predicts that inactivation of CDKF;1 should lead to lethality due to complete block of the cell cycle, as the lack of CDKF;1 should also prevent the activation of CDKDs and hence activation of CDKs through the second pathway. However, identification of *cdkf;1* insertion mutants (sections 3.1.1 and 3.2.2) clearly demonstrated that the loss of CDKF;1 function reduces but does not completely block cell division activity. Nevertheless, the *cdkf;1* mutations cause dramatic developmental effects characterized by reduction of cell number and cell elongation, hypersensitivity to sucrose, glucose and far-red light, aberrant root, leaf and flower development, extremely delayed flowering and male and female sterility. A further discrepancy in the proposed model has stemmed from the fact that members of the *Arabidopsis* CDKD kinase family show remarkable sequence conservation, including their activating T-loop regions, which serve as CDKF;1 phosphorylation site. This has predicted that conserved T-loop sequences of CDKD;1 should serve as CDKF;1 substrate, analogously those of CDKD;2 and CDKD;3 kinases. In addition, conservation of CDKD sequences suggested potential functional similarity of these kinases.

To clarify these discrepancies, we have repeated the CDKF;1 phosphorylation assays with purified CDKD kinases and have initiated functional characterization of the *cdkd* T-DNA insertion mutants. Instead of using fusions with the maltose binding protein of 42 kDa as Shimotohno et al. (2004; 2006), we exploited a sandwich tagging technology by generating CDKF and CDKD fusions to an N-terminal thioredoxin (Trx) tag of 12 kDa and a small C-terminal His₆ tag. This technology allowed the purification of highly soluble forms of intact CDKF and CDKD kinases to apparent homogeneity. As expected, purified CDKF;1 proved to be active in the absence of a cyclin subunit as indicated by its high levels of autophosphorylation. Repetition of *in vitro* CDKF;1 kinase assays with purified Trx-CDKD-His₆ substrate revealed that in contrast to the data of Shimotohno et al. (2004) CDKF;1 phosphorylated CDKD;1, as well as the CDKD;2 and CDKD;3 kinases. Control kinases assay with the (T166A) T-loop mutant version of CDKD;1 revealed as expected that CDKF;1 mediated phosphorylation of the T-loop of this CAK, similarly to CDKD;2 and CDKD;3.

Unexpectedly, we also found that all three *Arabidopsis* CDKD kinases showed low levels of autophosphorylation in the absence of cyclin subunit, which allowed testing their phosphorylation specificity using the GST-CTD substrate that carries the CTD repeats of *Arabidopsis* RNAPII largest subunit. These assays revealed that in addition to CDKD;2, CDKF;1 functioned *in vitro* as a CTD kinase in contrast to the observations of Shimotohno et al. (2004). In our assays, however, monomeric CDKDs and CDKF;1 failed to phosphorylate *Arabidopsis* CDKA;1, which suggested that recognition of the CDK substrates may require their association with cyclin or the formation of CDKD-cyclin complexes. Recently, Takatsuka et al. (2009) found that CDKF;1 cannot phosphorylate human CDK2 even *in vitro* correcting the previous data from Shimotohno et al. (2004, 2006). This, together with the phosphorylation of CDKD;1 by CDKF;1 indicated that CDKF;1 is a likely upstream activating kinase (CAKAK) of all three CDKDs/CAKs, but cannot alone function as an independent CDK-activating kinase (CAK).

The fact that CDKD;1 showed a low level autophosphorylation in our assays indicates that is an active kinase. This observation directs further attention to the functional characterization of CDKD;1, the expression of which peaks at both G1-S and G2-M checkpoint boundaries (Menges et al., 2005). Data from the *in vitro* kinase assays should however be handled with necessary caution. The fact that CDKD;1 and CDKD;3 showed no CTD kinase activity *in vitro* would suggest that in this respect the function of these kinases cannot be redundant with that of CDKD;2. However, we found that phenotypes of *cdkd;1* and *cdkd;3* insertion mutants is indistinguishable from wild type and that of the *cdkd;2* single mutant, which suggests that if CDKD;1 is an active kinase, its functions should be overlapping with that of either CDKD;2 or CDKD;3. Functional similarity between the three *Arabidopsis* CDKD kinases is also indicated by the fact that all three combinations of double mutants (*cdkd;1cdkd;2*, *cdkd;1cdkd;3*, *cdkd;2cdkd;3*) show no developmental defect and any alteration compared to wild type. By contrast, minor decrease of *CDKD;3* transcript level by combination of the leaky *cdkd;3-2* mutation with both *cdkd;1-1* and *cdkd;2-1* mutations caused a significant delay in plant development. This suggests that all CDKDs, including CDKD;1, are active kinases and perform largely overlapping functions. Further characterization of various allelic combinations of triple *cdkd* mutants and well as detailed biochemical characterization of CDKD complexes isolated from *Arabidopsis* is expected to provide more insight into *in vivo* roles of CDKDs in the activation of CDKs and phosphorylation of RNAPII CTD.

4.2. *CDKF;1 is a major regulator of CTD phosphorylation code*

Our data show that the CTD domain of the largest subunit of RNAPII is phosphorylated by both CDKF;1 and CDKD;2 protein kinases. To determine their phosphorylation target sites within the consensus CTD heptapeptide repeat, we conducted a series of kinase assays using wild type and mutated heptapeptide substrates. These assays indicated that CDKD;2 phosphorylates both Serine-2 and Serine-5 residues of the CTD, but prefers the Serine-5 position over Serine-2. In comparison, CDKF;1 could equally phosphorylate mutant heptapeptides that carried alanine replacements of either Serine-2, or Serine-5 or both, indicating that this kinase phosphorylates either the Serine-7 residue or, which is less likely, Thr-4. To confirm the CTD-code specificity of CDKD;2 and CDKF;1, we have examined the phosphorylation levels of specific CTD serine residues by western blotting using CTD phosphoSerine-2, phosphoSerine-5 and phosphoSerine-7 specific monoclonal antibodies in *cdkf;1-1* and *cdkd;2-1* mutant seedlings compared to wild type. In this experiment, we have considered that fact that the *cdkf;1-1* mutation causes a gradually manifesting general developmental defect soon after seed germination. Therefore, we have examined two subsequent developmental stages: i) seedlings carrying two cotyledons but no leaves at day 7 after germination, which showed retarded root growth but no difference of hypocotyl elongation and cotyledon expansion in the *cdkf;1-1* mutant compared to wild type and *cdkd;2-1* seedlings; and ii) 12 days old seedlings, showing a clear retardation of hypocotyl growth, leaf development and root elongation of *cdkf;1-1* mutant. During early stage of seedling development, we have observed a reduction of CTD phosphorylation only at the Serine-7

position in the *cdkf;1-1* mutant compared to wild type CTD phosphorylation in the *cdkd;2-1* mutant. This clearly demonstrated that the *cdkf;1-1* mutation affects specific phosphorylation of Serine-7 position of CTD heptapeptide repeats. Five days later in seedling development, the *cdkf;1-1* mutant showed a deficiency of both Serine-5 and Serine-7 CTD phosphorylation, whereas reduced phosphorylation of only Serine-5 CTD position was observed in the *cdkd;2* mutant. This indicated that CDKD;2 is primarily responsible for phosphorylation of the Serine-5 residue. Reduction of Serine-5 CTD phosphorylation in the *cdkf;1-1* mutant is likely due to absent activation of CDKD;2 by CDKF;1 *in vivo*.

At day 12 after germination, a significant reduction of Serine-2 CTD phosphorylation was also observed in the *cdkf;1-1* mutant, which suggests a likely involvement of a yet unknown Serine-2 specific CTD kinase, which represents a putative substrate for CDKF;1 mediated activation. Nevertheless, based on our *in vitro* kinase assays we cannot exclude that CDKF;1 could also phosphorylate the Serine-2 and/or Serine-5 position. Combination of *in vitro* kinase assays with antibodies, which are able to differentiate different phosphorylation on the CTD domain, when GST-CTD is substrate of CDKF;1 could uncover/exclude possible direct phosphorylation of Serine-2 and/or Serine-5 by CDKF;1. Alternatively, further characterization of CTD phosphorylation patterns in the double and triple *cdkd* mutants will help to verify that CDKF;1 is solely responsible for phosphorylation of the Serine-7 CTD position. Our current data is however fully consistent with the conclusion that CDKF;1 acts as upstream activating kinase (CAKAK) of CDKD;2 *in vivo*, and probably this conclusion can also be extended to the other CAK/CDKD kinases.

Residual phosphorylation of Serine-5 CTD residue in the *cdkd;2-1* mutant indicates the existence of another Serine-5 kinase. CDKD;3 is a likely candidate for Serine-5 CTD phosphorylation, as it is very closely related to CDKD;2 and because Shimotohno et al. (2004) observed that CDKD;3 immunoprecipitated from *Arabidopsis* cell culture is able to phosphorylate the GST-CTD substrate *in vitro* (Shimotohno et al., 2004). In metazoans, Serine-2 phosphorylation is catalysed by CDK9. In *Arabidopsis*, CDKC;1 and CDKC;2 represent potential functional orthologues of CDK9 and additional targets for activation by CDKF;1. Taken together, these results demonstrate CDKF;1 is responsible for fine-tuning of RNAPII CTD phosphorylation in *Arabidopsis* and thereby it is involved in different steps of transcription regulation that have dramatic effect on plant development.

4.3. Are cyclin-dependent kinases (CDKs) targets of CDKDs/ CAKs?

As human CDK7, *Arabidopsis* CDKF;1, CDKD;2, and CDKD;3 have been reported to mediate phosphorylation of human CDK2 *in vitro*. Therefore, Umeda et al. (2005) suggested that CDKF;1 and CDKDs are directly involved in the activation of CDKs, such as CDKA;1, in *Arabidopsis*. More remarkably, Shimotohno et al. (2006) also found that CDKF;1 is capable of activating *Arabidopsis* CDKA;1 *in vivo*, when these two kinases are co-expressed in *Arabidopsis* cell culture. As mentioned above, these results have been recently revised by the same group showing that CDKF;1 is not involved in T-loop phosphorylation of the *Arabidopsis* CDKA;1, CDKB;1 and CDKB;2 kinases

(Takatsuka et al., 2009). Our *in vitro* kinase assays also indicate CDKF;1 and CDKDs are not able to phosphorylate CDKA;1 *in vitro* (data not shown).

As cyclin dependency of CDKs and CAKs may largely influence the results of *in vitro* kinase assays, these discrepancies should rather be clarified by genetic means. One evident option is to express site-specifically mutated *CDKD* kinase genes, in which the codon of phosphorylated Thr in the T-loop is exchanged for either Asn or Gln. As these amino acid exchanges mimic phosphorylation of the T-loop, the products of these mutant genes will be dominantly activated (i.e. being phosphatase resistant) CDKD kinases, which can be tested for suppression of the *cdkf;1* mutant phenotype. Analogously activated CDKA and CDKB kinases can be used for testing suppression of cell cycle defects caused by *cdkf;1* and triple *cdkd* mutations.

Our microarray data revealed little effect of *cdkf;1-1* mutation on transcriptional regulation of cell cycle related genes. The only change, which may deserve attention is a 13-fold upregulation of *KRP2* transcript levels in the *cdkf;1-1* mutant. KRP2 interacts with CDKA;1 and reduces CDKA;1 activity, which leads to onset of endoreduplication and increase of cell's DNA ploidy level (Verkes et al., 2005), as well as to inhibition of lateral root formation (Himanen et al., 2002). The abundance of KRP2 protein is regulated through phosphorylation by CDKB1;1, which targets KRP2 to proteosomal degradation. Although viable, the *cdkf;1* mutant has a cell division defect, as characterization of the mutant seedlings indicates a reduction of cell number in the epidermal layers of leaves and hypocotyls. Although this defect is also accompanied by a significant reduction of cell elongation, we have found no evidence for change in the level of endoreduplication. Although root elongation and defect of lateral root development in the *cdkf;1-1* mutant show similarities to *KRP2* overexpressing plants, it remains to be necessary to confirm KRP2 overproduction in the *cdkf;1-1* mutant by western blotting and demonstrate its effect of the regulation of CDKA;1 activity. On the other hand, to determine whether CDKF;1 plays a direct role in cell cycle regulation, it will be necessary to generate synchronisable cell cultures from our conditionally complemented *cdkf;1-1* mutant, which expresses *CDKF;1* under an estradiol-inducible promoter in the mutant background. Depletion of CDKF;1 expression in actively dividing synchronized cells is expected to provide information on whether *CDKF;1* has any effect on the control of cell cycle progression and the activity of phase specific CDKA and CDKB kinases.

4.4. Regulation of small RNA pathways by CDKF;1-mediated phosphorylation of Serine-7 position of RNA polymerase II CTD

The observation that the *cdkf;1-1* mutation specifically reduces the CTD phosphoserine-7 levels in very young seedlings (7 DAG) provided us a unique tool to examine the role played by Serine-7 CTD phosphorylation in the control of transcription. Comparative Affymetrix ATH1 microarray hybridization analysis of RNA samples from wild type and *cdkf;1-1* mutant seedlings demonstrated that reduced CTD Serine-7 phosphorylation does not cause overall down-regulation of transcription. From a total of 2383 genes, 1258 showed reduced and 1125 at least 1.5-fold increased transcript levels

in the *cdkf;1-1* mutant. As CTD Serine-7 phosphorylation has been reported to affect specifically the 3'-end processing and transcription of small noncoding nuclear RNA U2G in mammalian cells (Egloff and Murphy, 2007), we have first searched for changes, which could affect the functions involved in RNA processing and/or biogenesis of small RNAs. Among the RNA processing functions affected by the *cdkf;1-1* mutation, we found that transcript levels of *DICER-LIKE DCL1* and *DCL2*, as well as *ARGONAUTE 1 (AGO1)* and *RNA-DEPENDENT RNA POLYMERASE 6 (RDR6)* acting in the microRNA and ta-siRNA pathways showed 1.7 to 1.8 reduction in the *cdkf;1-1* mutant. As these changes appeared to be decent, and because we reduced the cut-off value of filtering of expression differences from standard 2-fold change to 1.5, we performed a series of confirmatory qRT-PCR experiments by measuring the transcript levels of these genes, as well as other genes acting in the four known small RNA pathways characterized in *Arabidopsis*.

Remarkably, the observed data revealed a general down-regulation of expression of key genes involved in all four small RNA biogenesis pathways and associated DNA methylation/silencing functions. These included DCL1, HYL1, HEN1, HST1 and AGO1 in the microRNA and, RDR6, DCL4, HEN1, AGO1 and AGO7 in the ta-siRNA pathway; DCL1, DCL2, RDR6 and HEN1 in nat-siRNA and DCL3, RDR2, HEN1, DRD1 and AGO4 in ra-siRNA biogenesis (Voinnet, 2009). As down-regulation of small RNA biogenesis pathways predicted a consequent decrease in the levels of processed mature small RNAs, we have performed northern RNA hybridizations with probes detecting some representatives of three small RNA classes, including miR156, miR165, miR172, ta-siRNA, and rai-siRNA COPIA. All tested mature small RNAs showed remarkably reduced levels in the *cdkf;1-1* mutant compared to wild type. Because mutations abolishing key functions in the small RNA processing pathways result in the accumulation of unprocessed pri-microRNAs and source transcripts of ta-siRNAs and ra-siRNAs, we have determined the levels of unprocessed polyadenylated transcripts of pri-miR156, pri-miR165, pri-miR172, TAS1a and COPIA genes. Surprisingly, we found that also the levels of small RNA precursors have been reduced in the *cdkf;1-1* mutant, indicating that alteration of Serine-7 phosphorylation of RNAPII CTD has a direct effect on their transcription. Overall reduction of transcription of noncoding small RNA genes and protein coding genes involved in their processing indicates the existence of a highly coordinated control mechanism by which synthesis of small RNA precursors and their processing is regulated by an RNAPII modulating function. As CDKF;1 is an upstream activating kinase of CDKD;2 which is a TFIIH-associated protein kinase controlling transcription and DNA repair (Leene et al., 2008), compromised CDKD;2 activity could represent a reason for the observed transcription regulatory defect in the *cdkf;1-1* mutant. However, this possibility can be excluded as at the examined early developmental stage the levels of CDKD;2-mediated Serine-5 CTD phosphorylation is comparable to wild type in the *cdkf;1-1* mutant, which suggests that the CDKD;2-TFIIH complex is fully active. Therefore, taken together, these data demonstrate that Serine-7 phosphorylation of the CTD domain by the CDKF;1 protein kinase is required for proper transcription and processing of small RNAs in *Arabidopsis*.

4.5. *Correlations between cdkf;1 mutant phenotype, CDKF;1 kinase function and transcript profiling data*

In contrast to the single *cdkd* mutants, which result in no alteration of wild type phenotype, the *cdkf;1* insertion mutants display dramatic morphological alterations and develop to extreme dwarf plants that fail to flower in short days. Even in long days, the *cdkf;1* mutants flower only after two months, twice the generation time of control wild type plants. Flowers of the *cdkf;1-1* mutant lack petals, develop petal-like sepals, varying number of aberrant and sterile pistils, and short similarly aberrant and sterile carpels. Single terminal flowers appear on side-branches of inflorescence, which correspond to elongated receptacle structures. Despite very early developmental stage of seedlings used in our transcript profiling experiments, some of the observed changes in transcript levels show logical correlation with the observed phenotypic traits. Thus, both confirmatory qRT-PCR and Affymetrix transcript profiling data indicate that transcript levels of *FT* and *SOC1* floral integrator genes are reduced by 10- to 13-fold in the *cdkf;1-1* mutant.

The alteration of *FT* and *SOC1* transcript levels reflect much more complex underlying changes, including upregulation of flowering time repressor *FLC* and changes in the expression of numerous key genes in the circadian clock and photoperiod dependent flowering time pathways. In *cdkf;1-1* seedlings, the expression level of all phytochromes except *PHYB* is marginally down-regulated along with coordinate increase of *PIF3*, *CCA1* and *LHY*, transcript levels. This data is consistent with the notion that *PIF3* is functionally required for transcription of *CCA1* and *LHY* (Alabadi et al., 2001; Martinez-Garcia et al., 2000). Furthermore, *GIGANTEA* (*GI*), another clock function which is repressed by *CCA1* and *LHY* (Quail, 2002), shows down-regulation in the *cdkf;1-1* mutant analogously to the *PRR5* and *PRR7* genes, which are positively controlled by *CCA1* and *LHY*, and known activate *CO* transcription (Nakamichi et al., 2007). Thus, up-regulation of *CCA1* and *LHY*, together with down-regulation of *GI*, *PRR5* and *PRR7* well correlates with extreme late flowering phenotype of *cdkf;1* mutants.

As *CO*, which acts in the central core of photoperiodic pathway shows slight up-regulation (1.54-fold) rather than decrease in the *cdkf;1-1* mutant, it appears that down-regulation of *FT* and *SOC1* at this early stage of development is regulated through a *CO*-independent pathway. Based on current knowledge, *GI* is capable of enhancing *FT* and *SOC1* expression by stimulating the production of miR172 (Jung et al., 2007; Mathieu et al., 2009), which inhibits the translation of a set of AP2-like flowering time repressor genes (*TOE1*, *TOE2*, *TOE3*, *SMZ*, and *SNZ*). These AP2-like transcription factors repress the transcription of *FT* and *SOC1* and consequently delay the time of flower formation (Schmid et al., 2003; Aukerman and Sakai, 2003; Mathieu et al., 2009; Chen, 2003; Kasschau et al., 2003; Schwab et al., 2005). Intriguingly, the *cdkf;1-1* mutation down-regulates both *GI* transcription and the whole miRNA pathway, hence decreasing the level of mature miR172, which consequently predicts up-regulation of protein levels of AP2-like flowering time repressors of *FT* and *SOC1* genes. On the other hand, the *cdkf;1-1* mutation also down-regulates the expression of several genes (e.g., *DCLA*, *HST*, *RDR6*, *AGO1*, and *AGO7*), which are involved in phase transition from juvenile to adult stage. Although down-regulation of these genes and low abundance of miR156 is predicted to

accelerate juvenile to adult transition (Peragine et al., 2004; Telfer and Poethig, 1998; Xie et al., 2005; Hunter et al., 2003; Fornara and Coupland, 2009), this is accompanied by aberrant leaf development and failure in proper induction of flowering in the *cdkf;1-1* mutant.

A reduction of miR156 level is concomitant with an increase in the expression of SPL transcription factor genes, including *SPL9* and *SPL10*, which would activate the transcription of miRNA172 precursor and thereby enhance *FT* and *SOC1* expression (Fornara and Coupland, 2009). However, this pathway is inhibited by down-regulation of microRNA biogenesis and *pri-miR172* expression in the mutant. Reduction of *FT* and *SOC1* transcription could also reflect the enhanced *FLC* expression in *cdkf;1-1*, although functions in the autonomous and vernalization-dependent pathways and FLC enhancers (SWR1 complex, Paf1 complex, and FRIGIDA) are apparently unaffected by the mutation. Therefore, upregulation of *FLC* could reflect a silencing/epigenetic defect due to lower transcription of *DCL1*, *DCL3*, and *HEN1* in the *cdkf;1* mutant (Schmitz et al., 2007; Xie et al., 2003; Liu et al., 2004). As key genes acting in all four small RNA biogenesis pathways, including RNA-directed DNA methylation, are down-regulated in *cdkf;1-1*, DNA methylation and thereby H3K9 methylation of the *FLC* locus could be specifically affected.

Interestingly, the *TMAC2* gene, which is highly inducible by ABA shows elevated transcript levels in the mutant. *TMAC2* negatively regulates ABA signalling and its overexpression reduces the expression levels of the *SOC1* and *SEP3* genes (Huang and Wu, 2006). Taken together, these data suggests that the observed reduction in *FT* and *SOC1* expression is likely caused by overexpression of FLC and very low abundance of miR172.

As described in section 3.4.3, our preliminary data indicate that the *cdkf;1-1* mutation results in enhanced sensitivity to far-red (FR) light, which triggers aberrant hypocotyl thickening and enhanced anthocyanin pigment accumulation in developing seedlings. The transcript profiling data indicate that the expression levels of *HY5* and *PIF3* are increased in the *cdkf;1-1* mutant when grown in short days under normal white light conditions. Activation of *HY5* and *PIF3* controlling anthocyanin biosynthesis is consistent with significantly increased transcription of numerous genes acting in the anthocyanin/flavonoid pathways (Shin et al., 2007; Vandenbussche et al., 2007). *PHYA* as FR light photoreceptor promotes *HY5* protein stability and probably enhances *PIF3* expression (Quail, 2002; Shin et al., 2007). Therefore, hypersensitivity of *cdkf;1-1* to constant FR could reflect higher activity of *HY5* and *PIF3*, despite marginal down-regulation of *PHYA* in the mutant. Interestingly, *ARR4* which inhibits dark conversion of Pfr form of *PHYB* to its Pr form shows lower transcript level in *cdkf;1-1* seedlings compared to wild type (Martinez-Garcia et al., 2000; Hanano et al., 2006). Moreover, negative regulators of *PHYB*-connected light-signalling pathways, including *PIF3*, *CCA1*, and *LHY*, are simultaneously upregulated in the mutant, which is consistent with lower expression of *PRR5* and *PRR7* that are positive regulators of *PHYB*-mediated light-signal transduction pathway (Ito et al., 2000). These data suggest that the activity of *PHYB* signalling could also be compromised by the *cdkf;1-1* mutation.

The *cdkf;1* mutations results in dramatic developmental defects characterized by inhibition of root elongation, reduction of number of root hairs, development of few and aberrantly short lateral roots, appearance of trichomes carrying single or two branches, defect of epidermal cell expansion, reduction of cell number in epidermal layers of leaves, hypocotyls and roots. In addition, at early developmental stages *cdkf;1* seedlings can be easily recognized based on their short hypocotyls length in different constant light regimes (FRC, RC, and BC), as well as in darkness. Interestingly, the hypocotyl length of *cdkf;1-1* mutant is similar to wild type under short day conditions in white light. This suggests a day length dependent (and possibly light quality dependent) control of hypocotyl elongation, as this defect cannot be compensated by either 0.1 μ M brassinolide or 10 μ M GA3 treatments in the *cdkf;1* mutants.

In potential relevance to the cell elongation defects, the microarray profiling data indicate a general reduction in the expression of *ADF8*, *ADF11*, *AFH1*, *AtFIM1*, *ROP2*, *TONIA*, *AtMAP65-1*, *AtMAP70-4*, and *ZWI* genes encoding important cytoskeleton constituents and cytoskeleton-related proteins in the *cdkf;1-1* mutant. Actin depolymerizing factors (ADF8 and ADF11) regulate cell division and intracellular trafficking in the root hair through cytoskeleton, modulating the actin bundling proteins. Both ADF8 and ADF11 are highly expressed in the root trichoblast cells and developing root hairs (Kandasamy et al., 2007), thus their down-regulation may contribute to root developmental defects of the *cdkf;1* mutants. The initiation and organization of actin cables is regulated by AFH1 (Michelot et al., 2005), whereas AtFIM1, an actin filament crosslinking protein, stabilizes actin filaments (Kovar et al., 2000). The *Arabidopsis* ROP2 GTPase positively regulates different stages of root hair development (Jones et al., 2002), while TONA1 controls cell elongation and cell division, and its mutation confers a dwarf phenotype. AtMAP65-1 binds to microtubules during the cell cycle (interphase, anaphase, and telophase) and its inactivation, which probably takes place by phosphorylation, is required for metaphase to anaphase transition (Smertenko et al., 2006). ZWICHEL is one of the major regulators of trichome morphogenesis and its mutation reduces the number of trichome branches from three to two (Oppenheimer, 1997; Reddy and Reddy, 2004). Finally, *ACT11*, encoding a structural constituent of cytoskeleton, plays an important role in root hair development and cell elongation (Kandasamy et al., 2009), and is highly expressed in young and developing tissues, including elongating hypocotyls, expanding leaves, floral organ primordia, emerging floral buds, and developing ovules (Huang et al., 1997). Taken together, coordinate down-regulation of these genes correlates with the observed cell elongation, root hair and trichome developmental defects and, in addition to deregulation of small RNA pathways, contribute to the observed developmental aberrations in the *cdkf;1* mutant.

4.6. Control of *VirD2* phosphorylation and *Agrobacterium*-mediated tumorigenesis by *CDKF;1*

Current models of *Agrobacterium*-mediated T-DNA integration into host chromosomes are based on previous studies of the effects of host mutations on the T-DNA integration process in yeast and

Arabidopsis, and analysis of sequence junctions formed during illegitimate recombination of the T-DNA ends with chromosomal target sites in fungal and plant host genomes. These studies show that the 3'-end of the T-strand, which corresponds to T-DNA left border junctions, frequently suffers deletions during the integration process. By contrast, the 5'-end of the T-strand, which defines the right T-DNA junctions, corresponds in the majority of cases to the position of VirD2-mediated cleavage site that is protected by the covalently bound VirD2 protein during T-DNA transfer (Mayerhofer et al., 1991; Tinland et al., 1995). Mutations of VirD2 largely prevent T-DNA integration, but in those few cases where mutant VirD2 assisted the integration process, larger deletions were identified also in the right T-DNA border junctions. T-DNA sequences covered by the single-stranded DNA-binding protein VirE2, but lacking VirD2, can be imported into host nuclei where they integrate into the host genome by illegitimate recombination. This process is mediated by the host non-homologous end-joining recombination system (NHEJ), which likely mediates also the formation of linkage between the unprotected 3'-end of the T-strand and host DNA forming the T-DNA LB junctions. Mutations affecting various components of the NHEJ recombination pathway reduce but do not fully abolish T-DNA integration and their effects are less dramatic compared those of *virD2* mutations (van Attikum et al., 2001). These data suggest that the VirD2 protein, which is covalently bound to the 5'-end of the T-strand and responsible for efficient nuclear import of this T-DNA transfer intermediate, plays also a distinguished role in the T-DNA integration process (Gelvin, 2000). Based on this assumption, it is also evident that the VirD2-mediated linkage of 5'-end of the T-strand must involve VirD2-interacting host factors, which may differ from those that mediate stabilization of the 3'-end of the T-strand.

Current reviews discuss two slightly different models describing the proposed mode of T-DNA integration: the Single-Stranded-Gap-Repair (SSGR) and Double-Strand-Break-Repair (DSBR) models (Tinland et al., 1995; Tzfira et al., 2004). In the SSGR model, first the 3'-end of T-strand is annealed to the target sequence by finding short complementary sequence (i.e., microhomology). This is followed by nicking and partial degradation of the target sequence in the plant DNA, and finally the 3'-end is integrated in to the genome by NHEJ. A clear weakness of the SSGR model from Tinland et al (1995) is that it assumes that annealing of the VirD2 protected 5' end of the T-strand is mediated by pairing of a single base, which is highly unrealistic because terminal nucleotides in the 5'-end of T-strand are covered by the VirD2 protein, which is covalently bound by phosphotyrosine bound between its Tyr29 residue and the last T-strand nucleotide. The SSGR model suggests that the latter electrophilic center contributes to the generation of a nick in the target sequence generating a free 3'-OH group as nucleophilic center. Subsequently, these electrophilic and nucleophilic centers attract each other and finally create a new bond there. Thus, according to the SSGR model, the two ends of the T-DNA are integrated into the genome based on different mechanisms, but the integration of the 5'-end is largely based on promiscuous action of the VirD2 protein in the absence of any plant factor. In fact, Pansegrau et al. (1993) showed that VirD2 has ligase like activity *in vivo*, whereas

Ziemienowicz et al., (2000) failed to observe VirD2-mediated ligation of the T-strand to model nucleotides in the absence of added DNA ligase.

The second DSBR model proposed for T-DNA integration assumes that on its way to the nucleus through the cytoplasm the single-stranded T-DNA (T-strand) is protected by the VirD2 protein on its 5'-end and along its full length by the VirE2 protein. This model attributes the various deletions observed at the 3'-end to insufficient nuclease protection during the transfer process. Upon nuclear import, the DSBR model assumes that the T-strand is converted to double-stranded T-DNA, which is prerequisite for T-DNA integration by the NHEJ system. Unfortunately, the DSBR model fails to answer the critical questions how DNA synthesis is primed on the T-strand and where is the putative replication origin for bidirectional DNA synthesis on the T-DNA.

In their study, aiming at the identification of a nuclear receptor for the T-strand linked VirD2 protein, Bakó et al. (2003) found that VirD2 can specifically interact with the TATA-binding protein TBP *in vivo* and demonstrated that TBP co-immunoprecipitates from *Arabidopsis* with the CTD of RNAPII. Furthermore, Bakó et al. (2003) purified a protein kinase, which phosphorylates VirD2, from alfalfa and found that this protein kinase cross-reacts with an antibody recognizing *Arabidopsis* CDKD;2. Using this antibody, a cDNA clone encoding CAK2Ms was isolated and used for overexpression of a HA-epitope tagged version of the CAK2Ms kinase in alfalfa protoplasts, in order to combine it with its native cyclin subunit. Following immunoprecipitation with anti-HA antibody, the pulled down HA-CAK2Ms kinase was demonstrated to phosphorylate GST-VirD2, as well as GST-CTD. Subsequently, CAK2Ms was shown to co-immunoprecipitate with the CTD of RNAPII.

To follow up these studies, we performed kinase assays to identify which of the *Arabidopsis* CDKD kinases correspond to functional orthologue of the CAK2Ms VirD2 kinase. To our surprise, we have found that none of the CDKD kinases, including the CTD kinase CDKD;2, could phosphorylate the GST-VirD2 substrate *in vivo*. As Bakó et al. (2003) used an immunoprecipitated CAK2Ms kinase from alfalfa cells for GST-VirD2 phosphorylation and, at the meanwhile purified *Arabidopsis* CDKD;2 was found in a tight complex with cyclin H and CDKF;1 by mass spectrometry studies (van Leene et al., 2007), we have assumed that the immunoprecipitated CAK2Ms complex carried an associated CDKF;1 subunit. Therefore, we have assayed phosphorylation of the GST-VirD2 substrate with purified *Arabidopsis* CDKF;1 and indeed found that CDKF;1 can phosphorylate VirD2 with similar efficacy as its three CDKD substrates.

Subsequently, we have shown by 2D PAGE analysis that CDKF;1 phosphorylates VirD2 at multiple positions, and by mass spectrometry analysis of purified VirD2 phosphopeptides we have identified 6 phosphorylated Thr residues located close to the critical C-terminal nuclear localization signal in VirD2. This experiment has identified the *bona fide* VirD2 kinase and suggested that the nuclear receptor involved in the recognition of T-strand-associated VirD2 in plants is likely a TFIIF complex carrying the interacting CDKF;1 and CDKD;2 kinases. While this latter assumption is being verified by future characterization of the CDKD;2-cyclin H-CDKF;1 complex, we have set out to test the biological significance of our finding by performing *Agrobacterium*-induced hypocotyl

tumorigenesis assays with the *cdkf;1-1* and *cdkd;2-1* insertion mutants. These assays indicated that both *cdkf;1-1* and *cdkd;2-1* mutations drastically reduced the frequency of *Agrobacterium*-mediated plant transformation and subsequent tumorigenesis.

As mentioned above, the absence of VirD2 in the presence of all other components of T-DNA transfer apparatus hugely reduces but does not abolish completely *Agrobacterium*-mediated transformation and tumour formation. Therefore, if CDKF;1 and CDKD;2 kinases only affect the role of VirD2 in T-DNA integration, their absence can be expected to reduce dramatically, but not completely, *Agrobacterium*-mediated T-DNA transformation and tumorigenesis. Our data show that compared to *cdkf;1-1* the *cdkd;2-1* mutation is somewhat less efficient in reducing the frequency of tumour formation. This appears to be logical since VirD2 is not phosphorylated by CDKD;2, but this kinase may just act as a mediator stabilizing the CDKF;1-CDKD;2 complex. Alternatively, as noted by Bakó et al. (2003), CDKD;2 may mediate direct recognition of a histidine triad motif in the N-terminal domain of VirD2, which has also been identified in several CAK-binding HINT proteins (Korsisaari and Mäkelä, 2000). More severe effect of *cdkf;1-1* mutation on the frequency of tumour formation can also be explained by recent observation of Takatsuka et al. (2009), who found that the CDKD;2 protein levels are dramatically decreased by the *cdkf;1-1* mutation.

Assuming that the CDKF;1/CAKAK-CDKD;2/CAK complex is similarly part of TFIID in *Arabidopsis* as in other eukaryotes, our data suggest that the nuclear VirD2 receptor is the RNAPII associated TFIID complex, which is a central regulator of DNA repair. Interaction of VirD2 with TBP shown by Bakó et al. (2003) is relevant in the light of data demonstrating that TBP is capable to recognize different DNA lesions, such as kinked DNA, and recruit to these subsequently the TFIID DNA repair complex. Therefore, our data suggest a new model for VirD2-mediated T-DNA integration. This predicts that linkage of the VirD2 protein to the 5'-end of the T-strand mimics a DNA lesion which recruits the VirD2-interacting TBP protein and, through CDKD;2, the CDKF;1-associated TFIID complex. Subsequently, CDKF;1-mediated phosphorylation of VirD2 probably deactivates the covalent bond between the 5'-end of the T-strand and VirD2, which leads to the release of VirD2 and TFIID-mediated repair-ligation of free 5' end of the T-strand to a TBP recruited 3' end in the chromosomal target sequence. Ultimately, the phosphorylated VirD2 could be targeted for proteasomal degradation. Whereas many steps in this model should be confirmed by further experimentation, the available data already demonstrate that CDKF;1 also plays a pivotal role in the control of DNA repair mechanism mediating *Agrobacterium*-mediated T-DNA transformation and subsequent tumour formation in *Arabidopsis*.

In analogy to recent models of co-transcriptional modifications of RNAPII CTD and concerning TFIID-associated nucleotide excision repair activity, Figure 28 depicts a schematic view of major functions of CDKF;1 and CDKD;2 kinases discussed above.

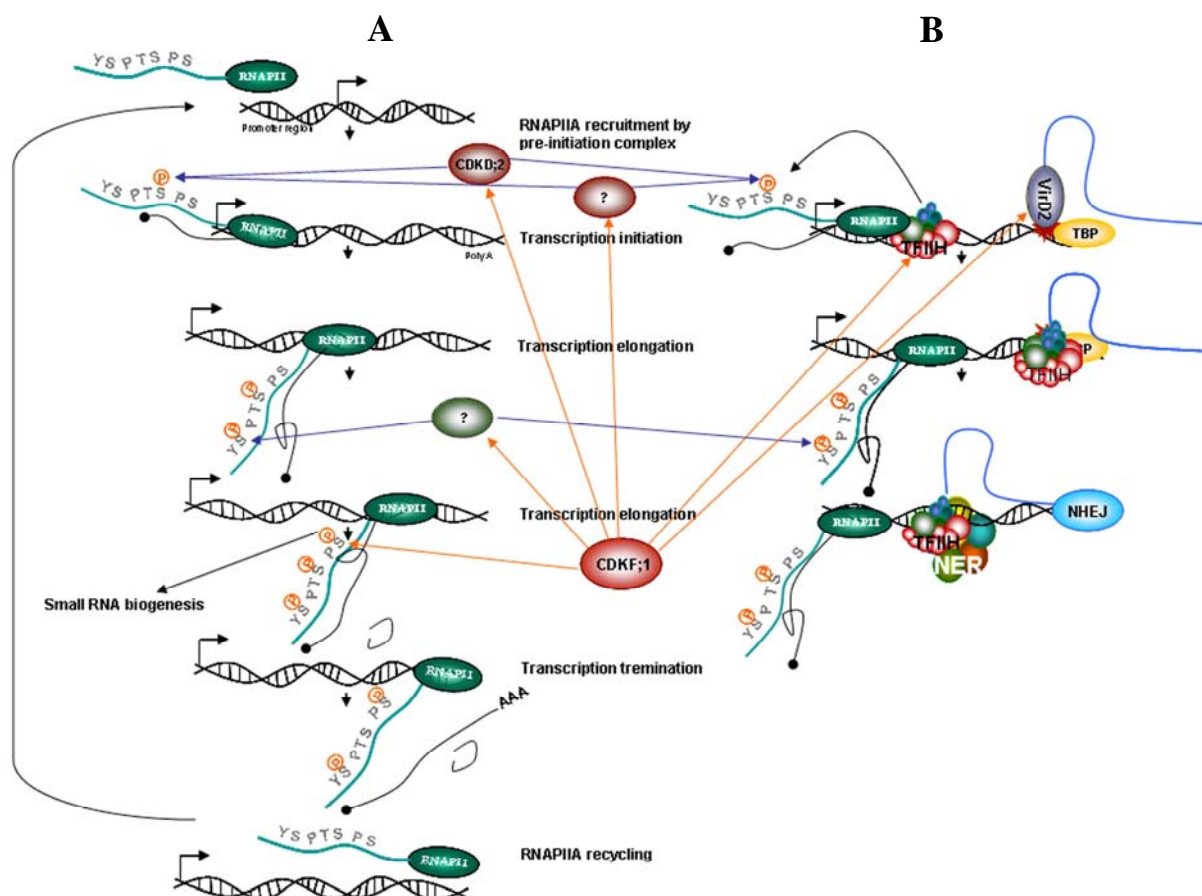


Figure 28. The mode of action of CDKF;1 in modulation of phosphorylation of RNAPII CTD during transcription (A) and T-DNA integration through phosphorylation of VirD2 (B).

(A) Unphosphorylated form of RNAPII CTD (RNAPIIA) is recruited by pre-initiation complex to the promoter region. Subsequently, Serine-5 phosphorylation of the CTD domain probably takes place by CDKD;2, a subunit of TFIIH and unknown kinase(s), the functions of which are positively regulated by the CAK-activating CDKF;1 kinase. Serine-5 phosphorylation is required for transcription initiation and 5'-capping. In a later step, Serine-2 is phosphorylated by another unknown kinase(s), which represent putative target(s) of CDKF;1. Serine-2 phosphorylation activates transcription elongation and it is required for splicing and polyadenylation in yeast and mammals. CDKF;1 phosphorylates Serine-7 residues of the CTD and thereby fine-tunes miRNA and siRNA biogenesis. At the end of transcription cycle, after dephosphorylation of the CTD, the RNAPII is recycled for initiation of a new round of transcription. (B) The VirD2 protein covalently linked to the 5'-end of the T-strand mimics a type of DNA lesion and recruits TBP, which is able to recognize different DNA lesions. Subsequently, TBP recruits TFIIH with the associated CDKF;1 and CDKD;2 kinases. CDKF;1 attached to TFIIH complex phosphorylates the VirD2 protein. The covalent bond between T-strand and VirD2 is deactivated and then the phosphorylated VirD2 protein is released and likely targeted for proteasomal degradation. In later step, the NER (i.e., nucleotide excision repair) machinery is also recruited and integrates the free 5' end of the T-strand in to the genome, while the 3' end is integrated by NHEJ system.

5. REFERENCES

- Achard, P., Herr, A., Baulcombe, D.C., and Harberd, N.P.** (2004). Modulation of floral development by a gibberellin-regulated microRNA. *Development*. **131**: 3357–3365.
- Adenot, X., Elmayan, T., Laressergues, D., Boutet, S., Bouché, N., Gascioli, V., and Vaucheret, H.** (2006). DRB4-dependent TAS3 trans-acting siRNAs control leaf morphology through AGO7. *Curr. Biol.* **16**: 927–932.
- Ahn, S.H., Kim, M., and Buratowski, S.** (2004). Phosphorylation of serine 2 within the RNA polymerase II C-terminal domain couples transcription and 30 end processing. *Mol. Cell.* **13**: 67–76.
- Akhtar, M., Heidemann, M., Tietjen, J., Zhang, D., Chapman, R.D., Eick, D., and Ansari, A.** (2009). TFIIF kinase places bivalent marks on the carboxy-terminal domain of RNA polymerase II. *Mol. Cell.* **34**: 387–393.
- Akoulitchev, S., Chuikov, S., and Reinberg, D.** (2000). TFIIF is negatively regulated by cdk8-containing mediator complexes. *Nature*. **407**: 102–106.
- Alabadi, D., Oyama, T., Yanovsky, M.J., Harmon, F.G., Más, P., and Kay, S.A.** (2001). Reciprocal regulation between TOC1 and LHY/CCA1 within the *Arabidopsis* circadian clock. *Science*. **293**: 880–883.
- Allen, E., Xie, Z., Gustafson, A.M., and Carrington, J.C.** (2005). microRNA-directed phasing during trans-acting siRNA biogenesis in plants. *Cell*. **121**: 207–221.
- Allen, E., Xie, Z., Gustafson, A.M., Sung, G.H., Spatafora, J.W., and Carrington, J.C.** (2004). Evolution of microRNA genes by inverted duplication of target gene sequences in *Arabidopsis thaliana*. *Nat. Genet.* **36**: 1282–1290.
- Alonso, J.M., Stepanova, A.N., Leisse, T.J., Kim, C.J., Chen, H., Shinn, P., Stevenson, D.K., Zimmerman, J., Barajas, P., Cheuk, R., Gadrinab, C., Heller, C., Jeske, A., Koesema, E., Meyers, C.C., Parker, H., Prednis, L., Ansari, Y., Choy, N., Deen, H., Geralt, M., Hazari, N., Hom, E., Karnes, M., Mulholland, C., Ndubaku, R., Schmidt, I., Guzman, P., Aguilar-Henonin, L., Schmid, M., Weigel, D., Carter, D.E., Marchand, T., Risseuw, E., Brogden, D., Zeko, A., Crosby, W.L., Berry, C.C., and Ecker, J.R.** (2003). Genome-wide insertional mutagenesis of *Arabidopsis thaliana*. *Science*. **301**: 653–657.
- Anand, A., Krichevsky, A., Schornack, S., Lahaye, T., Tzfira, T., Tang, Y., Citovsky, V., and Mysore, K.S.** (2007). *Arabidopsis* VIRE2 INTERACTING PROTEIN2 is required for *Agrobacterium* T-DNA integration in plants. *Plant Cell*. **19**: 1695–1708.
- Anand, A., Vaghchhipawala, Z., Ryu, C.M., Kang, L., Wang, K., del-Pozo, O., Martin, G.B., and Mysore, K.S.** (2007). Identification and characterization of genes involved in *Agrobacterium*-mediated plant transformation by virus-induced gene silencing. *MPMI*. **20**: 41–52.
- Aukerman, M.J., and Sakai, H.** (2003). Regulation of flowering time and floral organ identity by a microRNA and its APETALA2-like target genes. *Plant Cell*. **15**: 2730–2741.
- Axtell, M.J., Jan, C., Rajagopalan, R., and Bartel, D.P.** (2006). A two-hit trigger for siRNA biogenesis in plants. *Cell*. **127**: 565–577.

- Bak, S., Tax, F.E., Feldmann, K.A., Galbraith, D.W., and Feyereisen, R. (2001).** CYP83B1, a cytochrome P450 at the metabolic branch point in auxin and indole glucosinolate biosynthesis in *Arabidopsis thaliana*. *Plant Cell*. **12**: 101-111.
- Bakó, L., Umeda, M., Tiburcio, A.F., Schell, J., and Koncz, C. (2003).** The VirD2 pilot protein of *Agrobacterium*-transferred DNA interacts with the TATA box-binding protein and a nuclear protein kinase in plants. *Proc. Natl. Acad. Sci. USA*. **100**: 10108-10113.
- Ballas, N., and Citovsky, V. (1997)** Nuclear localization signal binding protein from *Arabidopsis* mediates nuclear import of *Agrobacterium* VirD2 protein. *Proc. Natl. Acad. Sci. USA*. **94**: 10723-10728.
- Bari, R., Datt Pant, B., Stitt, M., and Scheible, W-R. (2006).** PHO2, microRNA399, and PHR1 define a phosphate-signaling pathway in plants. *Plant Physiol*. **141**: 988–999.
- Bartel, D. (2004).** MicroRNAs: genomics, biogenesis, mechanism, and function. *Cell*. **116**: 281–297.
- Baumberger, N. and Baulcombe, D.C. (2005).** *Arabidopsis* ARGONAUTE1 is an RNA slicer that selectively recruits microRNAs and short interfering RNAs. *Proc. Natl. Acad. Sci. USA*. **102**: 11928–11933.
- Bechtold, N., Ellis, J. and Pelletier, G. (1993)** *In planta Agrobacterium* mediated gene transfer by infiltration of adult *Arabidopsis thaliana* plants. *C. R. Acad. Sci. Paris, Life Sciences*. **316**: 1194–1199.
- Bienkiewicz, E.A., Moon Woody, A., and Woody, R.W. (2000).** Conformation of the RNA polymerase II C-terminal domain: Circular dichroism of long and short fragments. *J. Mol. Biol*. **297**: 119–133.
- Boccalandro, H.E., De Simone, S.N, Bergmann-Honsberger, A., Schepens, I., Fankhauser, C., and Casal, J.J. (2008).** PKS1 regulates root phototropism and gravitropism. *Plant Physiol*. **146**: 108–115.
- Borsani, O., Zhu, J., Verslues, P.E., Sunkar, R., Zhu, J.K. (2005).** Endogenous siRNAs derived from a pair of natural *cis*-antisense transcripts regulate salt tolerance in *Arabidopsis*. *Cell*. **123**: 1279–1291.
- Boutet, S., Vazquez, F., Liu, J., Beclin, C., Fagard, M., Gratias, A., Morel, J-S., Crete, P., **Chen, X., and Vaucheret, H. (2003).** *Arabidopsis* Hen1: A genetic link between endogenous miRNA controlling development and siRNA controlling transgene silencing and virus resistance. *Curr. Biol*. **13**: 843–848.
- Brencic, A., Winans, S. (2005).** Detection and response to signals involved in host-microbe interactions by plant-associated bacteria. *Microbiol. Mol. Biol. Rev.* **69**: 155–94.
- Brodersen, P., Sakvarelidze-Achard, L., Bruun-Rasmussen, M., Dunoyer, P., Yamamoto, Y.Y., Sieburth, L., and Voinnet, O. (2008).** Widespread translational inhibition by plant miRNAs and siRNAs. *Science*. **320**: 1185–1190.
- Buck, V., Russell, P., and Millar, J.B. (1995).** Identification of a CDK-activating kinase in fission yeast. *EMBO J*. **14**: 6173–6183.

- Cagas, P.M., and Corden, J.L.** 1995. Structural studies of a synthetic peptide derived from the carboxyl-terminal domain of RNA polymerase II. *Proteins*. **21**: 149–160.
- Cao, X., Aufsatz, W., Zilberman, D., Mette, M.F., Huang, M.S., Matzke, M., and Jacobsen, S.E.** (2003). Role of the DRM and CMT3 methyltransferases in RNA-directed DNA methylation. *Curr. Biol.* **13**: 2212–2217.
- Cebolla, A., Vinardell, J.M., Kiss, E., Oláh, B., Roudier, F., Kondorosi, A., and Kondorosi, E.** (1999). The mitotic inhibitor *ccs52* is required for endoreduplication and ploidy-dependent cell enlargement in plants. *EMBO J.* **18**: 4476–4484.
- Chabot B, Bisotto S, and Vincent, M.** (1995). The nuclear matrix phosphoprotein p255 associates with splicing complexes as part of the [U4/U6.U5] tri-snRNP particle. *Nucleic Acids Res.* **23**: 3206–3213.
- Chandler, J.W.** (2009). Local auxin production: a small contribution to a big field. *BioEssays*. **31**: 60-70.
- Chao, W.S., Serpe, M.D., Jia, Y., Shelver W.L., Anderson, J.V., and Umeda, M.** (2006). Potential roles for autophosphorylation, kinase activity, and abundance of a CDK-activating kinase (Ee;CDKF;1) during growth in leafy spurge. *Plant Mol. Biol.* **63**: 365–379.
- Chapman, R.D., Heidemann, M., Albert, T.K., Mailhammer, R., Flatley, A., Meisterernst, M., Kremmer, K., and Eick, D.** (2007). Transcribing RNA polymerase II is phosphorylated at CTD residue serine-7. *Science*. **318**:1780-1782.
- Chapman, R.D., B. Palancade, A. Lang, O. Bensaude, and D. Eick.** (2004). The last CTD repeat of the mammalian RNA polymerase II large subunit is important for its stability. *Nucleic Acids Res.* **32**: 35–44.
- Chen, X.** (2003). A microRNA as a translational repressor of APETALA2 in *Arabidopsis* flower development. *Science*. **303**: 2022-2025.
- Chilton, M-D.M., and Que, Q.** (2003). Targeted integration of T-DNA into the tobacco genome at double-stranded breaks: New insights on the mechanism of T-DNA integration. *Plant Physiol.* **133**: 956–9.
- Cho, E.J., Takagi, T., Moore, C.R., and Buratowski, S.** (1997). mRNA capping enzyme is recruited to the transcription complex by phosphorylation of the RNA polymerase II carboxy-terminal domain. *Genes Dev.* **11**: 3319–3326.
- Citovsky, V., Kozlovsky, S.V., Lacroix, B., Zaltsman, A., Dafny-Yelin, M., Vyas, S., Tovkach, A., and Tzfira, T.** (2007) Biological systems of the host cell involved in *Agrobacterium* infection. *Cell Microbiol.* **9**: 9–20.
- Clough, S.J., and Bent, A.F.** (1998). Floral dip: a simplified method for *Agrobacterium*-mediated transformation of *Arabidopsis thaliana*. *Plant J.* **16**: 735-743.
- Cockcroft, C.E., den Boer, B.G., Healy, J.M., and Murray, J.A.** (2000). Cyclin D control of growth rate in plants. *Nature*. **405**: 575–579.

- Colasanti, J., Tyers, M., and Sundaresan, V.** (1991). Isolation and characterization of cDNA clones encoding a functional p34^{cdc2} homologue from *Zea mays*. *Proc. Natl. Acad. Sci. USA*. **88**: 3377–3381.
- Corbesier, L., and Coupland, G.** (2006). The quest for florigen: A recent review of recent progress. *J. Exp. Bot.* **57**: 3395–3403.
- Corden, J.L.** (1990). Tails of polymerase II. *TIBS*. **15**: 383–387.
- Damagnez, V., Makela, T., and Cottarel, G.** (1995). *Schizosaccharomyces pombe* Mop1-Mcs2 is related to mammalian CAK. *EMBO J.* **14**: 6164–6172.
- Damgaard, C.K., Kahns, S., Lykke-Andersen, S., Nielsen, A.L., Jensen, T.H., and Kjems, J.** (2008). A 50 splice site enhances the recruitment of basal transcription initiation factors in vivo. *Mol. Cell.* **29**: 271–278.
- Davis, S.J., Kurepa, J., and Vierstra, R.D.** (1999). The *Arabidopsis thaliana* *HY1* locus, required for phytochrome-chromophore biosynthesis, encodes a protein related to heme oxygenases. *Proc. Natl. Acad. Sci. USA*. **96**: 6541–6546.
- De Jager, S.M., Maughan, S., Dewitte, W., Scofield, S., and Murray, J.A.** (2005). The developmental context of cell-cycle control in plants. *Seminars in Cell. Dev Biol.* **16**: 385–396.
- De Veylder, L., Beeckman, T., Beemster, G.T., De Almeida Engler, J., Ormenese, S., Maes, S., Naudts, M., Van Der Schueren, E., Jacquard, A., Engler, G., and Inze, D.** (2002). Control of proliferation, endoreduplication and differentiation by the *Arabidopsis* E2Fa-DPa transcription factor. *EMBO J.* **21**: 1360–1368.
- De Veylder, L., Beemster, G.T., Beeckman, T., and Inzé, D.** (2001). CKS1At overexpression in *Arabidopsis thaliana* inhibits growth by reducing meristem size and inhibiting cell-cycle progression. *Plant J.* **25**: 617–626.
- De Veylder, L., Segers, G., Glab, N., Casteels, P., Van Montagu, M., and Inzé, D.** (1997). The *Arabidopsis* Cks1At protein binds to the cyclin-dependent kinases Cdc2aAt and Cdc2bAt. *FEBS Lett.* **412**: 446–452.
- Del Pozo, J.C., Diaz-Trivino, S., Cisneros, N., and Gutierrez, C.** (2006). The balance between cell division and endoreplication depends on E2FC-DPB, transcription factors regulated by the ubiquitin-SCFSKP2A pathway in *Arabidopsis*. *Plant Cell.* **18**: 2224–2235.
- Dewitte, W., and Murray J.A.**, (2003). The plant cell cycle. *Annu. Rev. Plant. Biol.* **54**: 235–264.
- Dichtl, B., Blank, D., Sadowski, M., Hübner, W., Weiser, S., and Keller, W.** (2002) Yhh1p/Cft1p directly links poly(A) site recognition and RNA polymerase II transcription termination. *EMBO J.* **21**: 4125–4135.
- Ding, X., Richter, T., Chen, M., Fujii, H., Seo, Y.S., Xie, M., Zheng, X., Kanrar, S., Stevenson, R.A., Dardick, C., Li, Y., Jiang, H., Zhang, Y., Yu, F., Bartley, L.E., Chern, M., Bart, R., Chen, X., Zhu, L., Farmerie, W.G., Gribskov, M., Zhu, J.K., Fromm, M.E., Ronald, P.C., and Song, W.Y.** (2009) A rice kinase-protein interaction map. *Plant Physiol.* **149**: 1478–1492.

- Dunoyer, P., Himber, C., Ruiz-Ferrer, V., Alioua, A., and Voinnet, O.** (2007). Intra- and intercellular RNA interference in *Arabidopsis thaliana* requires components of the microRNA and heterochromatic silencing pathways. *Nat. Genet.* **39**: 848–856.
- Egloff, S., and S. Murphy.** (2008). Cracking the RNA polymerase II CTD code. *Trends Genet.* **24**: 280–288.
- Egloff, S., O'Reilly, D., Chapman, R.D., Taylor, A., Tanzhaus, K., Pitts, L., Eick, D., and Murphy, S.** (2007). Serine-7 of the RNA polymerase II CTD is specifically required for snRNA gene expression. *Science.* **318**: 1777–1779.
- Fahlgren, N., Howell, M.D., Kasschau, K.D., Chapman, E.J., Sullivan, C.M., Cumbie, J.S., Givan, S.A., Law, T.F., Grant, S.R., Dangl, J.L., and Carrington, J.C.** (2007). High-throughput sequencing of *Arabidopsis* microRNAs: Evidence for frequent birth and death of MIRNA genes. *PLoS ONE.* **2**: e219.
- Fang, Y., and Spector, D.L.** (2007). Identification of nuclear dicing bodies containing proteins for microRNA biogenesis in living *Arabidopsis* plants. *Curr. Biol.* **17**: 818–823.
- Feaver, W.J., Henry, N.L., Wang, Z., Wu, X., Svejstrup, J.Q., Bushnell, D.A., Friedberg, E.C., and Kornberg, R.D.** (1997). Genes for Tfb2, Tfb3, and Tfb4 subunits of yeast transcription/repair factor IIIH. Homology to human cyclin-dependent kinase activating kinase and IIIH subunits. *J. Biol. Chem.* **272**: 19319–19327.
- Fornara, F., and Coupland, G.** (2009) Plant phase transitions make a SPLash. *Cell.* **138**: 625–627.
- Francis, D.** (2007). The plant cell cycle-15 years on. *New Phytologist.* **174**: 261–278.
- Gallego, M.E., Bleuyard, J-Y., Daoudal-Cotterell, S., Jallut, N., and White, C.I.** (2003). Ku80 plays a role in non-homologous recombination but is not required for T-DNA integration in *Arabidopsis*. *Plant J.* **35**: 557–565
- Gandikota, M., Birkenbihl, R.P., Hohmann, S., Cardon, G.H., Saedler, H., and Huijser, P.** (2007). The miRNA156/157 recognition element in the 3' UTR of the *Arabidopsis* SBP-box gene SPL3 prevents early flowering by translational inhibition in seedlings. *Plant J.* **49**: 683–693.
- Gao, L, and Gross, D.S.** (2008). Sir2 silences gene transcription by targeting the transition between RNA polymerase II initiation and elongation. *Mol. Cell. Biol.* **28**: 3979–3994.
- Gao, R., Mukhopadhyay, A., Fang, F., and Lynn, D.G.** (2006) Constitutive activation of two-component response regulators: Characterization of VirG activation in *Agrobacterium tumefaciens*. *J. Bacteriol.* **188**: 5204–5211.
- Gelvin, S.B.** (1998). *Agrobacterium* VirE2 proteins can form a complex with T-strands in the plant cytoplasm. *J. Bacteriol.* **180**: 4300–4302.
- Gelvin, S.B.** (2000) *Agrobacterium* and plant genes involved in T-DNA transfer and integration. *Annu. Rev. Plant Physiol. Plant Mol. Biol.* **51**: 223–56.
- Gelvin, S.B.** (2003). *Agrobacterium*-mediated plant transformation: the biology behind the "Gene-Jockeying" Tool. *Microbiol. Mol. Biol. Rev.* **67**: 16–37.

- Glover-Cutter, K., Kim, S., Espinosa, J., and Bentley, D.L.** (2008). RNA polymerase II pauses and associates with pre-mRNA processing factors at both ends of genes. *Nat. Struct. Mol. Biol.* **15**: 71-78.
- Gonzalez, N., Hernould, M., Delmas, F., Gevaudant, F., Duffe, P., Causse, M., Mouras, A., and Chevalier, C.** (2004). Molecular characterization of a WEE1 gene homologue in tomato (*Lycopersicon esculentum* Mill.). *Plant Mol. Biol.* **56**: 849-861.
- Gould, K.L., and Nurse, P.** (1991). Tyrosine phosphorylation of the fission yeast *cdc2*⁺ protein kinase regulates entry into mitosis. *Nature.* **342**: 39-45.
- Gregis, V., Sessa, A., Colombo, L., and Kater, M.M.** (2008) AGAMOUS-LIKE24 and SHORT VEGETATIVE PHASE determine floral meristem identity in *Arabidopsis*. *Plant J.* **56**: 891-902.
- Gregory, B.D., O'Malley, R.C., Lister, R., Urich, M.A., Tonti-Filippini, J., Chen, H., Millar, A.H., and Ecker, J.R.** (2008). A link between RNA metabolism and silencing affecting *Arabidopsis* development. *Dev. Cell.* **14**: 1-13.
- Han, J., Lee, Y., Yeom, K.H., Kim, Y.K., Jin, H., and Kim, V.N.** (2004). The Drosha-DGCR8 complex in primary microRNA processing. *Genes Dev.* **18**: 3016-3027.
- Hanano, S., Domagalska, M., Nagy, F., and Davis, S.J.** (2006). Multiple phytohormones regulate the plant circadian clock. *Genes Cells.* **11**: 1381-1392.
- He, X.J., Hsu, Y.F., Zhu, S., Wierzbicki, A.T., Pontes, O., Pikaard, C.S., Liu, H.L., Wang, C.S., Jin, H., and Zhu, J.K.** (2009) An effector of RNA-directed DNA methylation in *Arabidopsis* is an ARGONAUTE 4- and RNA-binding protein. *Cell.* **137**: 498-508.
- Hemerly, A., De Almeida Engler, J., Bergounioux, C., Van Montagu, M., Engler, G., Inzé, D., and Ferreira, P.** (1995). Dominant negative mutants of the Cdc2 kinase uncouple cell division from iterative plant development. *EMBO J.* **14**: 3925-3936.
- Herr, A.J., Jensen, M.B., Dalmay, T., and Baulcombe, D.C.** (2005). RNA polymerase IV directs silencing of endogenous DNA. *Science.* **308**: 118-120.
- Hirose, Y., Tacke, R., and Manley, J.L.** (1999). Phosphorylated RNA polymerase II stimulates pre-mRNA splicing. *Genes Dev.* **13**: 1234-1239.
- Hirose, Y., and Manley, J.L.** (1998). RNA polymerase II is an essential mRNA polyadenylation factor. *Nature.* **395**: 93-96.
- Hirose, Y., and Manley, J.L.** (2000). RNA polymerase II and the integration of nuclear events. *Genes Dev.* **14**: 1415-1429.
- Hirt, H., Pay, A., Bogre, L., Meskiene, I., and Heberle-Bors, E.** (1993). *cdc2MsB*, a cognate *cdc2* gene from alfalfa, complements the G1/S but not the G2/M transition of budding yeast *cdc28* mutants. *Plant J.* **4**: 61-69.
- Ho, C., and Shuman, S.** (1999). Distinct effector roles for Ser2 and Ser5 phosphorylation of the RNA polymerase II CTD in the recruitment and allosteric activation of mammalian capping enzyme. *Mol. Cell.* **3**: 405-411.

- Horváth, M.** (2007). *Arabidopsis* AMP-activated protein kinases in proteasomal complexes and their role in cell signalling. Inaugural-Dissertation, Mathematisch-Naturwissenschaftlichen Fakultät der Universität zu Köln.
- Howell, M.D., Fahlgren, N., Chapman, E.J., Cumbie, J.S., Sullivan, C.M., Givan, S.A., Kasschau, K.D., Carrington, J.C.** (2007). Genome-wide analysis of the RNA DEPENDENT RNA POLYMERASE6/DICER-LIKE4 pathway in *Arabidopsis* reveals dependency on miRNA- and tasiRNA-directed targeting. *Plant Cell*. **19**: 926–942.
- Huang, M.D., and Wu, W.L.** (2006). Overexpression of TMAC2, a novel negative regulator of abscisic acid and salinity responses, has pleiotropic effects in *Arabidopsis thaliana*. *Plant Mol. Biol.* **63**: 557-569.
- Huang, S., An, Y.-Q., McDowell, J.M., McKinney, E.C., and Meagher, R.B.** (1997). The *Arabidopsis ACT11* actin gene is strongly expressed in tissues of the emerging inflorescence, pollen, and developing ovules. *Plant Mol. Biol.* **33**: 125–139.
- Hunter, C., Sun, H., and Poethig, R.S.** (2003). The *Arabidopsis* heterochronic gene ZIPPY is an ARGONAUTE family member. *Curr. Biol.* **13**: 1734-1739.
- Hutvagner, G., and Zamore, P.D.** (2002). RNAi: nature abhors a double-strand. *Curr. Opin. Genet. Dev.* **12**: 225-232.
- Hwang, D., Chen, H.C., and Sheen, J.** (2002). Two-component signal transduction pathways in *Arabidopsis*. *Plant Physiol.* **129**: 500–515.
- Ito, S., Nakamichi, N., Nakamura, Y., Niwa, Y., Kato, T., Murakami, M., Kita, M., Mizoguchi, T., Niinuma, K., Yamashino, T., and Mizuno, T.** (2007). Genetic linkages between circadian clock-associated components and phytochrome-dependent red light signal transduction in *Arabidopsis thaliana*. *Plant Cell Physiol.* **48**: 971–983.
- Janyce, A., Sugui, Yun., C, Chang., and Kwon-Chung, K.J.** (2005) *Agrobacterium tumefaciens*-mediated transformation of *Aspergillus fumigatus*: an efficient tool for insertional mutagenesis and targeted gene disruption. *Appl. Environ. Microbiol.* **71**: 1798-1802.
- Jones, J.C., Phatnani, H.P., Haystead, T.A., MacDonald, J.A., Alam, S.M., and Greenleaf, A.L.** (2004). C-terminal repeat domain kinase I phosphorylates Ser2 and Ser5 of RNA Polymerase II C-terminal domain repeats. *J. Biol. Chem.* **279**: 24957-24964.
- Jones, M.A., Shen, J.J., Fu, Y., Li, H., Yang, Z., and Grierson, C.S.** (2002). The *Arabidopsis* Rop2 GTPase is a positive regulator of both root hair initiation and tip growth. *Plant Cell*. **14**: 763–776.
- Jones-Rhoades, M.W. Bartel, D. P., and Bartel, B.** (2006). MicroRNAs and their regulatory roles in plants. *Annu. Rev. Plant Biol.* **57**: 19–53.
- Joubès, J., Chevalier, C., Dudits, D., Heberle-Bors, E., Inzé, D., Umeda, M., Renaudin, J.P.,** (2000) Cyclin-dependent kinase-related protein kinases in plants. *Plant Mol. Biol.* **43**: 607-620.
- Jove, R., and J.L. Manley.** (1984). *In vitro* transcription from the adenovirus 2 major late promoter utilizing templates truncated at promoter-proximal sites. *J. Biol. Chem.* **259**: 8513-8521.

- Jung, J.H., Seo, Y.H., Seo, P.J., Reyes, J.L., Yun, J., Chua, N.H., and Park, C.M.** (2007). The GIGANTEA-regulated microRNA172 mediates photoperiodic flowering independent of CONSTANS in *Arabidopsis*. *Plant Cell*. **19**: 2736–2748.
- Kakimoto, T.** (2003). Perception and signal transduction of cytokinins. *Annu. Rev. Plant. Biol.* **54**: 605–627.
- Kaldis, P., Sutton, A., and Solomon, M.J.** (1996). The Cdk-activating kinase (CAK) from budding yeast. *Cell*. **86**: 553–564.
- Kandasamy, M.K., Burgos-Rivera, B., McKinney, E.C., Ruzicka, D.R., and Meagher, R.B.** (2007). Class-specific interaction of profilin and ADF isoforms with actin in the regulation of plant development. *Plant Cell*. **19**: 3111–3126.
- Kang, J., Mehta, S., and Turano, F.J.** (2004). The putative GLUTAMATE RECEPTOR 1.1 (AtGLR1.1) in *Arabidopsis thaliana* regulates abscisic acid biosynthesis and signaling to control development and water loss. *Plant Cell Physiol*. **45**: 1380–1389.
- Kasschau, K.D., Xie, Z., Allen, E., Llave, C., Chapman, E.J., Krizan, K.A., and Carrington, J.C.** (2003). P1/HC-Pro, a viral suppressor of RNA silencing, interferes with *Arabidopsis* development and miRNA function. *Dev. Cell*. **4**: 205–217.
- Katiyar-Agarwal, S., Morgan, R., Dahlbeck, D., Borsani, O., Villegas, A.Jr., Zhu, J.K., Staskawicz, B.J., and Jin, H.** (2006). A pathogen-inducible endogenous siRNA in plant immunity. *Proc. Natl. Acad. Sci. USA*. **103**: 18002–18007.
- Kim, E., Du, L., Bregman, D.B., and Warren, S.L. (1997). Splicing factors associate with hyperphosphorylated RNA polymerase II in the absence of pre-mRNA. *J. Cell Biol.* **136**: 19–28.
- Kim, S.T., Cho, K.S., Jang, Y.S., and Kang, K.Y.** (2001). Two-dimensional electrophoretic analysis of rice proteins by polyethylene glycol fractionation for protein arrays. *Electrophoresis*. **22**: 2103–2109.
- Kohli, A., Griffiths, S., Palacios, N., Twyman, R.M., Vain, P., Laurie, D.A., and Christou, P.** (1999). Molecular characterization of transforming plasmid rearrangements in transgenic rice reveals a recombination hotspot in the CaMV 35S promoter and confirms the predominance of microhomology mediated recombination. *Plant J.* **17**: 591–601.
- Komarnitsky, P., Cho, E.J., and Buratowski, S.** (2000). Different phosphorylated forms of RNA polymerase II and associated mRNA processing factors during transcription. *Genes Dev.* **14**: 2452–2460.
- Koncz, C., and Schell, J.** (1986). The promoter of TL-DNA gene 5 controls the tissue specific expression of chimaeric genes carried by a novel type of *Agrobacterium* binary vector. *Mol. Gen. Genet.* **204**: 383–396.
- Koncz, C., Martini, N., Mayerhofer, N., Koncz-Kálmán, Z., Körber, H., Rédei, G.P., and Schell, J.** (1989). High-frequency T-DNA-mediated gene tagging in plants. *Proc. Natl. Acad. Sci. USA*. **86**: 8467–8471.

- Koncz, C., Martini, N., Szabados, L., Hroudá, M., Bachmair, A., and Schell, J.** (1994). Specialized vectors for gene tagging and expression studies. In: *Plant Molecular Biology Manual*, Gelvin, S., and Schilperoort, B. (eds.), Kluwer Academic Publishers, Dordrecht-Boston-London, **B2**: 1-22.
- Korsisaari, N., and Mäkelä, T.P.** (2000) Interactions of Cdk7 and Kin28 with Hint/PKCI-1 and Hnt1 histidine triad proteins. *J. Biol. Chem.* **275**: 34837-34840.
- Kovar, D.R., Drobak, B.K., and Staiger, C.J.** (2000). Maize profilin isoforms are functionally distinct. *Plant Cell.* **12**: 583–598.
- Kurihara, Y., and Watanabe, Y.** (2004). *Arabidopsis* micro-RNA biogenesis through Dicer-like 1 protein functions. *Proc. Natl. Acad. Sci. USA.* **101**: 12753–12758.
- Kurihara, Y., Takashi, Y., and Watanabe, Y.** (2006). The interaction between DCL1 and HYL1 is important for efficient and precise processing of pri-miRNA in plant microRNA biogenesis. *RNA.* **12**: 206–212.
- Lacroix, B., Tzfira, T., Vainstein, A., and Citovsky, V.** (2006). A case of promiscuity: *Agrobacterium*'s endless hunt for new partners. *Trends Genet.* **22**: 29–37.
- Laine, J.-P., and Egly, J.-M.** (2006). When transcription and repair meet: a complex system. *TRENDS Genet.* **22**: 430-436.
- Lanet, E., Delannoy, E., Sormani, R., Floris, M., Brodersen, P., Crété, P., Voinnet, O., and Robaglia, C.** (2009). Biochemical evidence for translational repression by *Arabidopsis* microRNAs. *Plant Cell.* **21**: 1762-1768.
- Lariguet, P., Boccalandro, H., Alonso, J., Ecker, J., Chory, J., Casal, J. and Fankhauser C.** (2003). The balance between PKS1 and PKS2 provides homeostasis for phytochrome A signaling in *Arabidopsis*. *Plant Cell.* **15**: 2966-2978.
- Laubinger, S., Sachsenberg, T., Zeller, G., Busch, W., Lohmann, J.U., Raetsch, G., and Weigel, D.** (2008). Dual roles of the nuclear cap-binding complex and SERRATE in pre-mRNA splicing and microRNA processing in *Arabidopsis thaliana*. *Proc. Natl Acad. Sci. USA.* **105**: 8795–8800.
- Lee, H., Suh, S.-S., Park, E., Cho, E., Ahn, J.H., Kim, S.-G., Lee, J.S., Kwon, Y.M., and Lee, I.** (2000). The AGAMOUS-LIKE 20 MADS domain protein integrates floral inductive pathways in *Arabidopsis*. *Gene Dev.* **14**: 2366-2376.
- Li, J., Vaidya, M., White, C., Vainstein, A., Citovsky, V., and Tzfira T.** (2005). Involvement of KU80 in T-DNA integration in plant cells. *Proc. Natl. Acad. Sci. USA.* **102**: 19231-19236.
- Li, J., Yang, Z., Yu, B., Liu, J., and Chen, X.** (2005). Methylation protects miRNAs and siRNAs from a 3'-end uridylation activity in *Arabidopsis*. *Curr. Biol.* **15**: 1501–1507.
- Li, D., Liu, C., Shen, L., Wu, Y., Chen, H., Robertson, M., Helliwell, C.A., Ito, T., Meyerowitz, E., and Yu, H. (2008) A repressor complex governs the integration of flowering signals in *Arabidopsis*. *Dev. Cell.* **15**: 110-120.

- Licalatosi, D.D., Geiger, G., Minet, M., Schroeder, S., Cilli, K., McNeil, J.B., and Bentley, D.L.** (2002). Functional interaction of yeast pre-mRNA 3' end processing factors with RNA polymerase II. *Mol. Cell.* **9**: 1101–1111.
- Liu, J., He, Y., Amasino, R., and Chen, X.** (2004). siRNAs targeting an intronic transposon in the regulation of natural flowering behaviour in *Arabidopsis*. *Genes Dev.* **18**: 2873–2878.
- Llave, C., Xie, Z., Kasschau, K.D., and Carrington, J.C.** (2002). Cleavage of Scarecrow-like mRNA targets directed by a class of *Arabidopsis* miRNA. *Science.* **297**: 2053–2056.
- Lohrmann, J., and Harter, K.** (2002). Plant two-component signaling systems and the role of response regulators. *Plant Physiol.* **128**: 363–369.
- Lolli, G.** (2009). Binding to DNA of the RNA-polymerase II C-terminal domain allows discrimination between Cdk7 and Cdk9 phosphorylation. *Nucleic Acids Res.* **37**: 1260–1268.
- Mallory, A.C., and Bouche, N.** (2008). MicroRNA-directed regulation: to cleave or not to cleave. *Trends Plant Sci.* **13**: 359–367.
- Mallory, A.C., Reinhart, B.J., Jones-Rhoades, M.W., Tang, G., Zamore, P.D., Barton, M.K., and Bartel, D.P.** (2004). MicroRNA control of *PHABULOSA* in leaf development: Importance of pairing to the microRNA 5' region. *EMBO J.* **23**: 3356–3364.
- Marion, J., Bach, L., Bellec, Y., Meyer, C., Gissot, L., and Faure, J.D.** (2008). Systematic analysis of protein subcellular localization and interaction using high-throughput transient transformation of *Arabidopsis* seedlings. *Plant J.* **56**: 169–179.
- Martinez-Garcia, J.F., Huq, E., Quail, P.H.** (2000). Direct targeting of light signals to a promoter element-bound transcription factor. *Science.* **288**: 859–863.
- Mas, P.** (2008) Circadian clock function in *Arabidopsis thaliana*: time beyond transcription. *Trends Cell Biol.* **18**, 966–977.
- Mathieu, J., Yant, L.J., Mürdter, F., Küttner, F., and Schmid, M.** (2009) Repression of flowering by the miR172 Target SMZ. *PLoS Biol.* **7**: e1000148. doi:10.1371/journal.pbio.1000148.
- Matzke, M., Kanno, T., Daxinger, L., Huettel, B. and Matzke A.J.** (2009). RNA-mediated chromatin-based silencing in plants. *Curr. Opin. Cell Biol.* **21**: 367–376.
- Mayerhofer, R., Koncz-Kalman, Z., Nawrath, C., Bakkeren, G., Cramer, A., Angelis, A., Redei, G.P., Schell, J., Hohn, b., and Koncz, C.** (1991). T-DNA integration: a mode of illegitimate recombination in plants. *EMBO J.* **10**: 697–704.
- McCracken, S., Fong, N., Rosonina, E., Yankulov, K., Brothers, G., Siderovski, D., **Hessel, A., Foster, S., Shuman, S., and Bentley D.L.** (1997). 5'-Capping enzymes are targeted to pre-mRNA by binding to the phosphorylated carboxy-terminal domain of RNA polymerase II. *Genes Dev.* **11**: 3306–3318.
- McCracken, S., Fong, N., Yankulov, K., Ballantyne, S., Pan, G.H., Greenblatt, J., Patterson, S.D., Wickens, M., and Bentley, D.L.** (1997). The C-terminal domain of RNA polymerase II couples messenger RNA processing to transcription. *Nature.* **385**: 357–361.

- McCullen C.A., and Binns, A.N.** (2006) *Agrobacterium tumefaciens* and plant cell interactions and activities required for interkingdom macromolecular transfer. *Annu. Rev. Cell Dev. Biol.* **22**: 101-127.
- Meinhart A, Kamenski T, Hoepfner S, Baumli S, Cramer P.** (2005). A structural perspective of CTD function. *Genes Dev.* **19**: 1401–1415.
- Meinhart, A., and Cramer, P.** (2004). Recognition of RNA polymerase II carboxy-terminal domain by 30-RNA-processing factors. *Nature.* **430**: 223–226.
- Menges, M., and Murray, J.A.** (2002). Synchronous *Arabidopsis* suspension cultures for analysis of cell-cycle gene activity. *Plant J.* **30**: 203–212.
- Menges, M., De Jager, S. M., Gruissem, W., and Murray, J.A.** (2005). Global analysis of the core cell cycle regulators of *Arabidopsis* identifies novel genes, reveals multiple and highly specific profiles of expression and provides a coherent model for plant cell cycle control. *Plant J.* **41**: 546-566.
- Menges, M., Hennig, L., Gruissem, W., and Murray, J.A.** (2002). Cell cycle-regulated gene expression in *Arabidopsis*. *J. Biol. Chem.* **277**: 41987–42002.
- Michael, W.M., and Newport, J.** (1998). Coupling of mitosis to the completion of S phase through Cdc34-mediated degradation of Wee1. *Science.* **282**: 1886–1889.
- Michelot, A., Guerin, C., Huang, S., Ingouff, M., Richard, S., Rodiuc, N., Staiger, C.J., and Blanchoin, L.** (2005). The formin homology 1 domain modulates the actin nucleation and bundling activity of *Arabidopsis* FORMIN1. *Plant Cell.* **17**: 2296-2313.
- Michielse, C.B., Ram, A.F., Hooykaas, P.J., and van den Hondel, C. A.** (2004) *Agrobacterium*-mediated transformation of *Aspergillus awamori* in the absence of full-length VirD2, VirC2, or VirE2 leads to insertion of aberrant T-DNA structures. *J. Bacteriol.* **186**: 2038-4205.
- Montgomery, T.A., Howell, M.D., Cuperus, J.T., Li, D., Hansen, J.E., Alexander, A.L., Chapman, E.J., Fahlgren, N., Allen, E., and Carrington, J.C.** (2008). Specificity of ARGONAUTE7-miR390 interaction and dual functionality in TAS3 trans-acting siRNA formation. *Cell.* **133**: 128–141.
- Morgan, D.O.** (1995). Principles of CDK regulation. *Nature.* **374**: 131–134.
- Mortillaro, M.J., Blencowe, B.J., Wei, X., Nakayasu, H., Du, L., Warren, S.L., Sharp, P.A., and Berezney, R. A.** (1996). Hyperphosphorylated form of the large subunit of RNA polymerase II is associated with splicing complexes and the nuclear matrix. *Proc. Natl. Acad. Sci. USA.* **93**: 8253–8257.
- Munro, P., Flatau, G., and Lemichez, E.** (2007). Bacteria and the ubiquitin pathway. *Curr. Opin. Microbiol.* **10**: 39-46.
- Mutasa-Göttgens, E., and Hedden, P.** (2009). Gibberellin as a factor in floral regulatory networks. *J. Exp. Bot.* **60**: 1979-1989.
- Mysore, K.S., Bassuner, B., Deng, X.B., Darbinian, N.S., Motchoulski, A., Ream, W., and Gelvin, S.B.** (1998) Role of the *Agrobacterium tumefaciens* VirD2 protein in T-DNA transfer and integration. *Mol. Plant Microbe Interact.* **11**: 668-683.

- Mysore, K.S., Nam, J., and Gelvin, S.B.** (2000). An *Arabidopsis* histone H2A mutant is deficient in *Agrobacterium* T-DNA integration. *Proc. Natl. Acad. Sci. USA.* **97**: 948-953.
- Naito, T., Yamashino, T., Kiba, T., Koizumi, N., Kojima, M., Sakakibara, H., and Mizuno, T.** (2007). A link between cytokinin and ASL9 (ASYMMETRIC LEAVES 2 LIKE 9) that belongs to the AS2/LOB (LATERAL ORGAN BOUNDARIES) family genes in *Arabidopsis thaliana*. *Biosci. Biotechnol. Biochem.* **71**: 1269–1278.
- Nakamichi, N., Kita, M., Niinuma, K., Ito, S., Yamashino, T., Mizoguchi, T., and Mizuno, T.** (2007). *Arabidopsis* clock-associated pseudo-response regulators PRR9, PRR7 and PRR5 coordinately and positively regulate flowering time through the canonical CONSTANS-dependent photoperiodic pathway. *Plant Cell Physiol.* **48**: 822–832.
- Nambara, E., and Marion-Poll, A.** (2005). Abscisic acid biosynthesis and catabolism. *Annu. Rev. Plant Biol.* **56**: 165-185.
- Nawrath, C., Schell, J. and Koncz, C.** (1990) Homologous domains of the largest subunit of eucaryotic RNA polymerase II are conserved in plants. *Mol. Gen. Genet.* **223**: 65-75.
- Ni, Z., Schwartz B.E., Werner, J., Suarez, J.-R., and Lis, J.T.** (2004). Coordination of transcription, RNA processing, and surveillance by P-TEFb kinase on heat shock genes. *Mol. Cell.* **13**: 55–65.
- Niyogi, K.K., and Fink, G.R.** (1992). Two anthranilate synthase genes in *Arabidopsis*: defense-related regulation of the tryptophan pathway. *Plant Cell.* **4**: 721–733.
- Niyogi, K.K., Grossman, A.R., and Bjorkman, O.** (1998). *Arabidopsis* mutants define a central role for the xanthophyll cycle in the regulation of photosynthetic energy conversion. *Plant Cell.* **10**: 1121–1134.
- Nonet, M., Sweetser, D., and Young, R.A.** (1987). Functional redundancy and structural polymorphism in the large subunit of RNA polymerase II. *Cell.* **50**: 909-915.
- Onodera, Y., Haag, J.R., Ream, T., Nunes, P.C., Pontes, O., and Pikaard, C.S.** (2005) Plant nuclear RNA polymerase IV mediates siRNA and DNA methylation-dependent heterochromatin formation. *Cell.* **120**: 613–622.
- Oppenheimer, D.G., Pollock, M.A., Vacik, J., Szymanski, D.B., Ericson, B., Feldmann, K., and Marks, M.D.** (1997). Essential role of a kinesin-like protein in *Arabidopsis* trichome morphogenesis. *Proc. Natl. Acad. Sci. USA.* **94**: 6261–6266.
- Pansegrau, W., Schoumacher, F., Hohn, B., and Lanka, E.** (1993). Site specific cleavage and joining of single-stranded DNA by VirD2 protein of *Agrobacterium tumefaciens* Ti plasmids: analogy to bacterial conjugation. *Proc. Natl. Acad. Sci. USA.* **90**: 11538–11542.
- Park, J.-A., Ahn, J.-Woo., Kim, Y.-K., Kim, S.-J., Kim, J.-K., Kim, W.T., and Pai, H.-S.** (2005). Retinoblastoma protein regulates cell proliferation, differentiation, and endoreduplication in plants. *Plant J.* **42**: 153–163.
- Park, M.Y., Wu, G., Gonzalez-Sulser, A., Vaucheret, H., and Poethig, R.S.** (2005). Nuclear processing and export of micro-RNAs in *Arabidopsis*. *Proc. Natl. Acad. Sci. USA.* **102**: 3691–3696.

- Park, W., Li, J., Song, R., Messing, J., and Chen, X.** (2002). CARPEL FACTORY, a Dicer homolog, and HEN1, a novel protein, act in microRNA metabolism in *Arabidopsis thaliana*. *Curr. Biol.* **12**: 1484–1495.
- Pedersen, I., and David, M.** (2008). MicroRNAs in the immune response, *Cytokine*. **43**: 391–394.
- Peragine, A., Yoshikawa, M., Wu, G., Albrecht, H.L., and Poethig, R.S.** (2004). SGS3 and SGS2/SDE1/RDR6 are required for juvenile development and the production of trans-acting siRNAs in *Arabidopsis*. *Genes Dev.* **18**: 2368–2379.
- Perales, R., and Bentley, D.** (2009). “Cotranscriptionality”: The transcription elongation complex as a nexus for nuclear transactions. *Mol. Cell.* **36**: 178–191.
- Peterlin, B.M., and Price, D.H.** (2006). Controlling the elongation phase of transcription with P-TEFb. *Mol. Cell.* **23**: 297–305.
- Phatnani, H.P., and Greenleaf, A.L.** (2006). Phosphorylation and functions of the RNA polymerase II CTD. *Genes Dev.* **20**: 2922–2936.
- Porceddu, A., Stals, H., Reichheld, J-P., Segers, G., De Veylder, L., De Pinho Barrôco, R., Casteels, P., Van Montagu, M., Inzé, D., and Mironov, V.** (2001). A plant-specific cyclin-dependent kinase is involved in the control of G2/M progression in plants. *J. Biol. Chem.* **276**: 36354–36360.
- Price, D.H.** (2000). P-TEFb, a cyclin-dependent kinase controlling elongation by RNA polymerase II. *Mol. Cell. Biol.* **20**: 2629–2634.
- Quail, P.H.** (2002). Phytochrome photosensory signalling networks. *Nat. Rev. Mol. Cell Biol.* **3**: 85–93.
- Quesada, V., Dean, C., and Simpson, G.G.** (2005). Regulated RNA processing in the control of *Arabidopsis* flowering. *Int. J. Dev. Biol.* **49**: 773–780.
- Rashotte, A.M., Mason, M.G., Hutchison, C.E., Ferreira, F.J., Schaller, G.E., and Kieber, J.J.** (2006). A subset of *Arabidopsis* AP2 transcription factors mediates cytokinin responses in concert with a two-component pathway. *Proc. Natl Acad. Sci. USA.* **103**: 11081–11085.
- Reddy, V.S., and Reddy, A.S.N.** (2004). Developmental and cell-specific expression of ZWICHEL is regulated by the intron and exon sequences of its upstream protein-coding gene. *Plant Mol. Biol.* **54**: 273–293.
- Reichheld, J.P., Vernoux, T., Lardon, F., Van Montagu, M., and Inze, D.** (1999). Specific checkpoints regulate plant cell cycle progression in response to oxidative stress. *Plant J.* **17**: 647–56.
- Rohila, J.S., Chen, M., Cerny, R., and Fromm, M.E.** (2004). Improved tandem affinity purification tag and methods for isolation of protein heterocomplexes from plants. *Plant J.* **38**: 172–181.
- Rubio-Somoza I, Cuperus, J.T., Weigel, D., and Carrington, J.C.** (2009). Regulation and functional specialization of small RNA–target nodes during plant development, *Curr Opin Plant Biol.* **12**: 622–627.

- Salomé, P.A., To, J.P., Kieber, J.J., and McClung, C.R.** (2006) *Arabidopsis* response regulators ARR3 and ARR4 play cytokinin-independent roles in the control of circadian period. *Plant Cell*. **18**: 55-69.
- Sambrook, J., and Russell, D.W.** (2001). *Molecular Cloning: A Laboratory Manual* Cold Spring Harbor Laboratory Press.
- Schmid, M., Uhlenhaut, N.H., Godard, F., Demar, M., Bressan, R., Weigel, D. And Lohmann, J.U.** (2003). Dissection of floral induction pathways using global expression analysis. *Development*. **130**: 6001–6012.
- Schmitz, R.J., Hong, L., Fitzpatrick, K.E., and Amasino, R.M.** (2007). DICER-LIKE 1 and DICER-LIKE 3 redundantly act to promote flowering via repression of FLOWERING LOCUS C in *Arabidopsis thaliana*. *Genetics*. **176**: 1359–1362.
- Schrammeijer, B., Risseuw, E., Pansegrau, W., Regensburg-Tuïnk, T.J., Crosby, W.L., and Hooykaas, P.J.** (2001). Interaction of the virulence protein VirF of *Agrobacterium tumefaciens* with plant homologs of the yeast Skp1 protein. *Curr. Biol*. **11**: 258–262.
- Schroeder, S.C., Schwer, B., Shuman, S., and Bentley, D.** (2000). Dynamic association of capping enzymes with transcribing RNA polymerase II. *Genes Dev*. **14**: 2435–2440.
- Schwab, R., Palatnik, J.F., Riester, M., Schommer, C., Schmid, M., and Weigel, D.** (2005). Specific effects of microRNAs on the plant transcriptome. *Dev Cell*. **8**: 517–527.
- Shimotohno, A., Matsubayashi, S., Yamaguchi, M., Uchimiya, H., and Umeda, M.** (2003). Differential phosphorylation activities of CDK-activating kinases in *Arabidopsis thaliana*. *FEBS Lett*. **534**: 69–74.
- Shimotohno, A., Ohno, R., Bisova, K., Sakaguchi, N., Huang, J., Koncz, C., Uchimiya, H., and Umeda, M.** (2006). Diverse phosphoregulatory mechanisms controlling cyclin-dependent kinase-activating kinases in *Arabidopsis*. *Plant J*. **47**: 701–710.
- Shimotohno, A., Umeda-Hara, C., Bisova, K., Uchimiya, H. and Umeda, M.** (2004). The Plant-specific kinase CDKF;1 is involved in activating phosphorylation of cyclin-dependent kinase-activating kinases in *Arabidopsis*. *Plant Cell*. **16**: 2954–2966.
- Shin, J., Park, E., and Choi, G.** (2007). PIF3 regulates anthocyanin biosynthesis in an HY5-dependent manner with both factors directly binding anthocyanin biosynthetic gene promoters in *Arabidopsis*. *Plant J*. **49**: 981–994.
- Smertenko, A.P., Chang, H.Y., Sonobe, S., Fenyk, S.I., Weingartner, M., Bogre, L., and Hussey, P.** (2006). Control of the AtMAP65-1 interaction with microtubules through the cell cycle. *J. Cell Sci*. **119**: 3227–3237.
- Solomon, M.J., Lee, T., and Kirschner, M.W.** (1992). Role of phosphorylation in p34^{cdc2} activation: identification of an activating kinase. *Mol. Biol. Cell*. **3**: 13-27.
- Song, J.J., Smith, S.K., Hannon, G.J., Joshuaor, L.** (2004). Crystal structure of Argonaute and its implications for RISC slicer activity. *Science*. **305**: 1434–1437.

- Stiller, J.W., and Cook, M.S.** (2004). Functional unit of the RNA polymerase II C-terminal domain lies within heptapeptide pairs. *Eukaryot. Cell.* **3**: 735–740.
- Stock, A.M., Robinson, V.L., and Goudreau, P.N.** (2000). Two-component signal transduction. *Annu. Rev. Biochem.* **69**: 183–215.
- Sun, Y., Dilkes, B.P., Zhang, C., Dante, R.A., Carneiro, N.P., Lowe, K.S., Jung, R., Gordon-Kamm, W.J., and Larkins, B.A.** (1999). Characterization of maize (*Zea mays* L.) Wee1 and its activity in developing endosperm. *Proc. Natl. Acad. Sci. USA.* **96**: 4180–4185.
- Szabados, L., Kovács, I., Oberschall, A., Ábrahám, E., Kerekes, I., Zsigmond, L., Nagy, R., Alvarado, M., Krasovskaja, I., Gál, M., Berente, A., Rédei, G.P., Ben Haim, A., and Koncz, C.** (2002). Distribution of 1000 sequenced T-DNA tags in the *Arabidopsis* genome. *Plant J.* **32**: 233–242.
- Takatsuka, H., Ohno, R., and Umeda M.** (2009) The *Arabidopsis* cyclin-dependent kinase-activating kinase CDKF1 is a major regulator of cell proliferation and cell expansion but is dispensable for CDKA activation. *Plant J.* **59**: 475–487.
- Tao, Y., Rao, P.K., Bhattacharjee, S., and Gelvin, S.B.** (2004). Expression of plant protein phosphatase 2C interferes with nuclear import of the *Agrobacterium* T-complex protein VirD2. *Proc. Natl. Acad. Sci. USA.* **101**: 5164–5169.
- Teale, W.D., Paponov, I.A., and Palme, K.** (2006). Auxin in action: Signalling, transport and the control of plant growth and development. *Nat. Rev. Mol. Cell Biol.* **7**: 847–859.
- Telfer, A., and Poethig, R. S.** (1998). HASTY: a gene that regulates the timing of shoot maturation in *Arabidopsis thaliana*. *Development.* **125**: 1889–1898.
- Tinland, B., Schoumacher, F., Gloeckler, V., Bravo-Angel, A.M., and Hohn, B.** (1995). The *Agrobacterium tumefaciens* virulence D2 protein is responsible for precise integration of T-DNA into the plant genome. *EMBO J.* **14**: 3585–3595.
- Tzfira, T., and Citovsky, V.** (2002). Partners-in-infection: host proteins involved in the transformation of plant cells by *Agrobacterium*. *Trends Cell Biol.* **12**: 121–129
- Tzfira, T., J, Li., B, Lacroix., and Citovsky, V.** (2004). *Agrobacterium* T-DNA integration: molecules and models. *Trends Genet.* **20**: 375–383.
- Umeda, M., Bhalerao, R.P., Schell, J., Uchimiya, H., and Koncz, C.** (1998). A distinct cyclin-dependent kinase-activating kinase of *Arabidopsis thaliana*. *Proc. Natl. Acad. Sci. USA.* **95**: 5021–5026.
- Umeda, M., Shimotohno, A., and Yamaguchi, M.** (2005). Control of cell division and transcription by cyclin-dependent kinaseactivating kinases in plants. *Plant Cell Physiol.* **46**: 1437–1442.
- Valverde, F., Mouradov, A., Soppe, W., Ravenscroft, D., Samach, A., and Coupland, G.** (2004). Photoreceptor regulation of CONSTANS protein in photoperiodic flowering. *Science.* **303**: 1003–1006.
- van Attikum, H., Bundock, P., and Hooykaas, P.J.** (2001) Non-homologous end-joining proteins are required for *Agrobacterium* T-DNA integration. *EMBO J.* **20**: 6550–6558.

- Vandenbussche, F., Habricot, Y., Condiff, A.S., Maldiney, R., Van der Straeten, D., and Ahmad, M.** (2007). HY5 is a point of convergence between cryptochrome and cytokinin signalling pathways in *Arabidopsis thaliana*. *Plant J.* **49**: 428–441.
- Vandepoele, K., Raes, J., De Veylder, L., Rouzé, P., Rombauts, S., and Inzé, D.** (2002). Genome-wide analysis of core cell cycle genes in *Arabidopsis*. *Plant Cell.* **14**: 903–916.
- Van Leene, V.J., Stals, H., Eeckhout, D., Persiau, G., Slijke, V.E., Isterdael, V.G., Clercq, D.A., Bonnet, E., Laukens, K., Remmerie, N., Hendrickx, K., Vijlder, D.T., Abdelkrim, A., Pharazyn, A., Onckelen, V.H., Inze, D., Witters, E., and Jaeger, D.G.** (2007). A tandem affinity purification-based technology platform to study the cell cycle interactome in *Arabidopsis thaliana*. *Mol. Cell. Proteomics.* **6**: 1226–1238.
- Vaucheret, H.** (2005). MicroRNA-dependent trans-acting siRNA production. *Sci STKE.* 2005(300): pe43.
- Vaucheret, H., Vazquez, F., Crété P., and Bartel, D.P.** (2004) The action of ARGONAUTE1 in the miRNA pathway and its regulation by the miRNA pathway are crucial for plant development. *Genes Dev.* **18**: 1187–1197.
- Vazquez, F.** (2006). *Arabidopsis* endogenous small RNAs: highways and byways. *Trends Plant Sci.* **11**: 460–468.
- Vazquez, F., Gascioli, V., Crete, P., and Vaucheret, H.** (2004) The nuclear dsRNA binding protein HYL1 is required for microRNA accumulation and plant development, but not posttranscriptional transgene silencing. *Curr. Biol.* **14**: 346–351.
- Verkest, A., Manes, C.L., Vercruyse, S., Maes, S., Van Der Schueren, E., Beekman, T., Genschik, P., Kuiper, M., Inze, D., and De Veylder, L.** (2005). The cyclin-dependent kinase inhibitor KRP2 controls the onset of the endoreduplication cycle during *Arabidopsis* leaf development through inhibition of mitotic CDKA;1 kinase complexes. *Plant Cell.* **17**: 1723–1736.
- Vinardell, J.M., Fedorova, E., Cebolla, A., Kevei, Z., Horvath, G., Kelemen, Z., Tarayre, S., Roudier, F., Mergaert, P., Kondorosi, A., and Kondorosi, E.** (2003). Endoreduplication mediated by the anaphase-promoting complex activator CCS52A is required for symbiotic cell differentiation in *Medicago truncatula* nodules. *Plant Cell.* **15**: 2093–2105.
- Vlieghe, K., Boudolf, V., Beemster, G.T.S., Maes, S., Magyar, Z., Atanassova, A., De Almeida Engler, J., Inzé, D., and De Veylder, L.** (2005). The DP-E2F-like *DELI* gene controls the endocycle in *Arabidopsis thaliana*. *Curr. Biol.* **15**: 59–63.
- Voinnet, O.** (2009). Origin, biogenesis, and activity of plant microRNAs. *Cell.* **136**: 669–687.
- Wang, J-W., Czech, B., and Weigel, D.** (2009). miR156-Regulated SPL Transcription Factors Define an Endogenous Flowering Pathway in *Arabidopsis thaliana*. *Cell.* **138**: 738–749.
- Wierzbicki, A.T., Ream, T.S., Haag, J.R., and Pikaard, C.S.** (2009). RNA polymerase V transcription guides ARGONAUTE4 to chromatin. *Nat. Genet.* **41**: 630–634.

- Wu, G., Park, M.Y., Conway, S.R., Wang, J.-W., Weigel, D., and Poethig, R.S.** (2009). The sequential action of miR156 and miR172 regulates developmental timing in *Arabidopsis*. *Cell*. **133**: 3539–3547.
- Xie, Z., Allen, E., Wilken, A., and Carrington, J. C.** (2005). *DICER-LIKE 4* functions in trans-acting small interfering RNA biogenesis and vegetative phase change in *Arabidopsis thaliana*. *Proc. Natl. Acad. Sci. USA*. **102**: 12984-12989.
- Xie, Z., Johansen, L.K., Gustafson, A.M., Kasschau, K.D., Lellis, A.D., Zilberman, D., Jacobsen, S.E., Carrington, J.C.** (2004). Genetic and functional diversification of small RNA pathways in plants. *PLoS Biol*. **2**: 642–652.
- Xie, Z., Kasschau, K.D., and Carrington, J.C.** (2003). Negative feedback regulation of Dicer-like 1 (DCL1) in *Arabidopsis* by microRNA-guided mRNA degradation. *Curr. Biol*. **13**: 784–789.
- Yamaguchi, A., Wu, M.F., Yang, L., Wu, G., Poethig, R.S., and Wagner, D.** (2009). The microRNA-regulated SBP-box transcription factor SPL3 is a direct transcriptional activator of LEAFY, FRUITFULL, and APETALA1. *Dev Cell*. **17**: 268-278.
- Yang, Z., Ebright, Y.W., Yu, B., and Chen, X.** (2006). HEN1 recognizes 21–24 nt small RNA duplexes and deposits a methyl group onto the 2' OH of the 3' terminal nucleotide. *Nucleic Acids Res*. **34**: 667–675.
- Yoo, S.K., Chung, K.S., Kim, J., Lee, J.H., Hong, S.M., Yoo, S.J., Yoo, S.Y., Lee, J.S., and Ahn, J.H.** (2005). CONSTANS activates suppressor of overexpression of CONSTANS 1 through FLOWERING LOCUS T to promote flowering in *Arabidopsis*. *Plant Physiol*. **139**: 770-778.
- Yoshikawa, M., Peragine, A., Park, M.Y., Poethig, R.S.** (2005). A pathway for the biogenesis of trans-acting siRNAs in *Arabidopsis*. *Genes Dev*. **19**: 2164–2175.
- Yu, B., Yang, Z., Li, J., Minakhina, S., Yang, M., Padgett, R.W., Steward, R., and Chen, X.** (2005). Methylation as a crucial step in plant microRNA biogenesis. *Science*. **307**: 932–935.
- Yue, Z., Maldonado, E., Pillutla, R., Cho, H., Reinberg, D., and Shatkin, A.J.** (1997). Mammalian capping enzyme complements mutant *Saccharomyces cerevisiae* lacking mRNA guanylyltransferase and selectively binds the elongating form of RNA polymerase II. *Proc. Natl. Acad. Sci. USA*. **94**: 12898–12903.
- Zehring, W.A., Lee, J.M., Weeks, J.R., Jokerst, R.S., and Greenleaf, A.L.** (1988). The C-terminal repeat domain of RNA polymerase II largest subunit is essential in vivo but is not required for accurate transcription initiation in vitro. *Proc. Natl. Acad. Sci. USA*. **85**: 3698–3702.
- Zhai, Q., Li, C.B., Zheng, W., Wu, X., Zhao, J., Zhou, G., Jiang, H., Sun, J., Lou, Y., and Li, C.** (2007) Phytochrome chromophore deficiency leads to overproduction of jasmonic acid and elevated expression of jasmonate-responsive genes in *Arabidopsis*. *Plant Cell Physiol*. **48**: 1061-1071.
- Zheng, X., Zhu, J., Kapoor, A., and Zhu, J.K.** (2007) Role of *Arabidopsis* AGO6 in siRNA accumulation, DNA methylation and transcriptional gene silencing. *EMBO J*. **26**: 1691-1701.

-
- Ziemienowicz, A., Merkle, T., Schoumacher, F., Hohn, B., and Rossi, L.** (2001) Import of *Agrobacterium* T-DNA into plant nuclei: two distinct functions of VirD2 and VirE2 proteins. *Plant Cell*. **13**: 369-383.
- Ziemienowicz, A., Inland, B., Bryant, J., Gloeckler, V., and Hohn, B.** (2000) Plant enzymes but not *Agrobacterium* VirD2 mediate T-DNA ligation in vitro. *Mol. Cell. Biol.* **20**: 6317–6322.
- Zilberman, D., Cao, X., and Jacobsen, S.E.** (2003). ARGONAUTE4 control of locus-specific siRNA accumulation and DNA and histone methylation. *Science*. **299**: 716–719.
- Zuo, J., Niu, Q.W., and Chua, N.H.** (2000). An estrogen receptor-based trans-activator XVE mediates highly inducible gene expression in transgenic plants. *Plant J.* **24**: 265-273.

Table 8. List of remaining microarray data showing altered transcript levels of genes in pathways affected by the *cdkf;1-1* mutation, which have not mentioned in the text.

Green colour indicates down-regulated genes, purple colour marks up-regulated transcripts.

Probe Set ID	AGI	Short/Full name	Fold change	RT-qPCR
Gametophyte, embryo & seed development				
260716_at	AT1G48130	ATPER1	1.5171459	
253414_at	AT4G33050	EDA39	2.3444316	
253274_at	AT4G34200	EDA9	1.5678797	
247410_at	AT5G62990	embryo defective 1692	1.7676998	
263899_at	AT2G21710	embryo defective 2219	1.5491735	
249462_at	AT5G39680	EMBRYO DEFECTIVE 2744	1.5104511	
249404_at	AT5G40160	embryo defective 506	1.5177532	
266392_at	AT2G41280	M10	3.213478	
266393_at	AT2G41260	M17	4.8909497	
260814_at	AT1G43710	embryo defective 1075	1.6492357	
249900_at	AT5G22640	embryo defective 1211	1.5246706	
258149_at	AT3G18110	embryo defective 1270	1.508755	
254427_at	AT4G21190	embryo defective 1417	1.7842361	
264224_at	AT1G67440	embryo defective 1688	2.6102033	
256613_at	AT3G29290	embryo defective 2076	2.9803932	
263220_at	AT1G30610	embryo defective 2279	2.8456154	
255328_at	AT4G04350	EMBRYO DEFECTIVE 2369	1.6819196	
265896_at	AT2G25660	embryo defective 2410	2.3018644	
252904_at	AT4G39620	embryo defective 2453	1.946124	
260523_at	AT2G41720	EMBRYO DEFECTIVE 2654	1.8424145	
253758_at	AT4G29060	embryo defective 2726	1.6786925	
263593_at	AT2G01860	EMBRYO DEFECTIVE 975	1.6491799	
253061_at	AT4G37610	BT5	1.5798665	
263305_at	AT2G01930	BPC1	1.8067896	
262848_at	AT1G14685	BPC2	1.6872642	
267461_at	AT2G33830	dormancy/auxin associated family protein	2.48564	
265478_at	AT2G15890	maternal effect embryo arrest 14	4.53966	
256715_at	AT2G34090	maternal effect embryo arrest 18	1.6517748	
251936_at	AT3G53700	maternal effect embryo arrest 40	1.5911878	
259328_at	AT3G16440	ATMLP-300B	1.5908215	
251642_at	AT3G57520	AtSIP2	1.8636701	
258136_at	AT3G24560	RASPBERRY	1.9350811	
257127_at	AT3G20070	TTN9 (TITAN9)	1.5399364	
255695_at	AT4G00080	unfertilized embryo sac 11	2.3878458	
Apical meristem & shoot development				
257600_at	AT3G24770	CLE41 (CLAVATA3/ESR-RELATED 41)	1.8970978	
254761_at	AT4G13195	CLE44 (CLAVATA3/ESR-RELATED 44)	2.003524	
267380_at	AT2G26170	CYP711A1	2.1980453	2.0933478
256099_at	AT1G13710	CYP78A5	1.7315377	
263285_at	AT2G36120	DOT1	1.9534844	
267485_at	AT2G02820	MYB88 (myb domain protein 88)	1.6811703	2.1265517
248861_at	AT5G46700	TRN2 (TORNADO 2) (TETRASPANNIN)	1.9384732	1.7855305
248059_at	AT5G55540	TRN1 (TORNADO 1); LOP1	1.8210139	3.4932781
266797_at	AT2G22840	AtGRF1	1.8893403	
263914_at	AT2G36400	AtGRF3 (GROWTH-REGULATING FACTOR 3)	1.5839064	
253411_at	AT4G32980	ATH1	2.3988056	1.9032154
249309_at	AT5G41410	BEL1 (BELL 1)	1.8528721	1.9552852
261120_at	AT1G75410	BLH3 (BEL1-LIKE HOMEODOMAIN 3)	1.7001191	2.7946142

Probe Set ID	AGI	Short/Full name	Fold change	RT-qPCR
265724_at	AT2G32100	OFPI6	2.417903	3.4330189
256734_at	AT3G29390	RIK (RS2-Interacting KH protein)	1.5768218	1.8939216
263598_at	AT2G01850	EXGT-A3;XTH27 hydrolase	1.8724773	
265545_at	AT2G28250	NCRK; kinase	1.5091894	
Root development				
245711_at	AT5G04340	ZAT6	1.7659798	1.5386741
259961_at	AT1G53700	WAG1	1.5346467	
265337_at	AT2G18390	TTN5/ARL2 (TITAN 5)	1.7527206	
253056_at	AT4G37650	SHR (SHORT ROOT)	2.154016	1.772481
264752_at	AT1G23010	LPR1 (Low Phosphate Root1)	1.920951	
245113_at	AT2G41660	MIZ1 (mizu-kussei 1)	1.5070195	
260097_at	AT1G73220	AtOCT1	2.2212842	
255698_at	AT4G00150	scarecrow-like transcription factor 6 (SCL6)	1.6455067	
261866_at	AT1G50420	SCL3	1.9253527	2.8049471
247707_at	AT5G59450	SCL11	1.633932	
256199_at	AT1G58250	SAB (SABRE)	1.5897368	
264029_at	AT2G03720	MRH6 (morphogenesis of root hair 6)	1.9323962	
261953_at	AT1G64440	ROOT HAIR DEFECTIVE 1	1.7259554	
261505_at	AT1G71696	SOL1 (SUPPRESSOR OF LLPI 1)	1.5239848	
Brassinosteroid/sterols				
266996_at	AT2G34490	CYP710A2	2.612973	
251321_at	AT3G61460	BRH1	1.7820951	
254333_at	AT4G22753	SMO1-3	2.053144	
249775_at	AT5G24160	SQE6	2.1477501	
264042_at	AT2G03760	ST; brassinosteroid sulfotransferase	4.0453663	5.7641329
259388_at	AT1G13420	ST4B (SULFOTRANSFERASE 4B)	1.5820786	
249773_at	AT5G24140	SQP2	1.5277069	
266831_at	AT2G22830	SQE2	1.7715586	
261076_at	AT1G07420	SMO2-1	1.5662668	
266495_at	AT2G07050	CAS1 (cycloartenol synthase 1)	1.6527143	
Sugar regulation				
263202_at	AT1G05630	SPTASE13	1.514334	
264472_at	AT1G67140	SWEETIE	1.956425	3.0382622
Hypoxia/CO2				
264953_at	AT1G77120	ADH1 (ALCOHOL DEHYDROGENASE 1)	2.1709154	2.3071211
266555_at	AT2G46270	GBF3 (G-BOX BINDING FACTOR 3)	1.6148728	1.3030978
263096_at	AT2G16060	AHB1 (<i>ARABIDOPSIS</i> HEMOGLOBIN 1)	6.327405	5.5222335
252401_at	AT3G48030	hypoxia-responsive family protein	1.5307045	
264734_at	AT1G62280	SLAH1 (SLAC1 HOMOLOGUE 1); transporter	3.1680465	4.0004441
253828_at	AT4G27970	SLAH2 (SLAC1 HOMOLOGUE 2); transporter	1.5702078	
Dark regulated				
252265_at	AT3G49620	DIN11 (DARK INDUCIBLE 11)	2.9445071	
251428_at	AT3G60140	DIN2 (DARK INDUCIBLE 2)	2.2731857	
246114_at	AT5G20250	DIN10 (DARK INDUCIBLE 10)	2.2377107	
Glucosinolate-nonauxin				
265121_at	AT1G62560	FMO GS-OX3	1.7285726	
265119_at	AT1G62570	FMO GS-OX4	1.5539628	
248713_at	AT5G48180	NSP5 (NITRILE SPECIFIER PROTEIN 5)	1.5501223	
257021_at	AT3G19710	BCAT4	1.8383998	
255773_at	AT1G18590	SOT17 (SULFOTRANSFERASE 17)	1.6149743	
260385_at	AT1G74090	SOT18	1.6743921	
260993_at	AT1G12140	FMO GS-OX5	1.7042922	
255438_at	AT4G03070	AOP1	2.0027516	

Probe Set ID	AGI	Short/Full name	Fold change	RT-qPCR
Jasmonate				
245038_at	AT2G26560	PLA2A (PHOSPHOLIPASE A 2A)	6.2667813	6.0841451
256321_at	AT1G55020	LOX1; lipoxygenase	1.6868287	1.0086607
265530_at	AT2G06050	OPR3 (OPDA-REDUCTASE 3)	1.5712544	1.0812224
259366_at	AT1G13280	AOC4 (ALLENE OXIDE CYCLASE 4)	2.2661138	1.2569037
246236_at	AT4G36470	S-adenosyl-L-methionine	1.9207426	
256017_at	AT1G19180	JAZ1	2.0314522	1.4166325
250292_at	AT5G13220	JAZ10	1.5389376	
260205_at	AT1G70700	TIFY7	1.5986685	
254232_at	AT4G23600	COR13	2.0143182	
259383_at	AT3G16470	JR1	1.7075812	
246225_at	AT4G36910	LEJ2	1.7360142	
260429_at	AT1G72450	JAZ6	1.5137014	
255786_at	AT1G19670	ATCLH1	2.4289212	
250662_at	AT5G07010	ST2A (SULFOTRANSFERASE 2A)	3.2196193	1.3258419
250657_at	AT5G07000	ST2B (SULFOTRANSFERASE 2B)	1.7866082	
249645_at	AT5G36910	THI2.2 (THONIN 2.2); toxin receptor binding	1.8420254	
256527_at	AT1G66100	thionin, putative	2.2041745	
Salicylic acid				
250286_at	AT5G13320	PBS3 (AVRPPHB SUSCEPTIBLE 3)	3.2876549	28.492686
Pathogenic responses				
264647_at	AT1G09090	ATRBO	1.9695027	
248719_at	AT5G47910	RBOHD	1.5924876	
252373_at	AT3G48090	EDS1	1.5372425	2.1603046
246510_at	AT5G15410	DND1 (DEFENSE NO DEATH 1)	1.5857527	
267191_at	AT2G44110	MLO15	2.303784	
245845_at	AT1G26150	PERK10	1.982029	
262254_at	AT1G53920	GLIP5	2.0244954	
252485_at	AT3G46530	RPP13	2.1109254	
245448_at	AT4G16860	RPP4	4.5284386	
245456_at	AT4G16950	RPP5	2.1889265	
252210_at	AT3G50410	OBP1	1.5500985	
251806_at	AT3G55370	OBP3	1.5631398	
248270_at	AT5G53450	ORG1	1.5141984	
247199_at	AT5G65210	TGA1	1.6765685	
255953_at	AT1G22070	TGA3	1.931243	
250463_at	AT5G10030	TGA4	1.8354293	
245258_at	AT4G15340	ATPEN1	1.6683017	
258277_at	AT3G26830	PAD3	5.551125	
257751_at	AT3G18690	MKS1 (MAP kinase substrate 1)	1.6468377	
247038_at	AT5G67160	EPS1	1.7517453	
263065_at	AT2G18170	ATMPK7	1.6121398	
254241_at	AT4G23190	CRK11	1.9614013	
258002_at	AT3G28930	AIG2	2.5425074	
249754_at	AT5G24530	DMR6	1.7103013	
256497_at	AT1G31580	ECS1	2.020975	
259071_at	AT3G11650	NHL2	1.583974	
250676_at	AT5G06320	NHL3	2.0663536	
261135_at	AT1G19610	PDF1.4	2.611171	
266141_at	AT2G02120	PDF2.1	4.694844	
250670_at	AT5G06860	PGIP1	1.6090173	
250669_at	AT5G06870	PGIP2	1.5472852	
256576_at	AT3G28210	PMZ	2.0096269	

Probe Set ID	AGI	Short/Full name	Fold change	RT-qPCR
258791_at	AT3G04720	PR4	2.637618	
247205_at	AT5G64890	PROPEP2	1.5030729	
247215_at	AT5G64905	PROPEP3	1.6278282	
259925_at	AT1G75040	PR5	1.5272574	
245041_at	AT2G26530	AR781	1.6181748	
246099_at	AT5G20230	ATBCB	2.328329	
251895_at	AT3G54420	ATEP3	1.5635811	
256243_at	AT3G12500	ATHCHIB	3.7629106	
260560_at	AT2G43590	chitinase, putative	2.197413	
260568_at	AT2G43570	chitinase, putative	5.2857018	
260556_at	AT2G43620	chitinase, putative	29.559217	
246821_at	AT5G26920	CBP60G	2.2415211	
267545_at	AT2G32690	GRP23	1.9725178	
265560_at	AT2G05520	GRP-3	2.021071	
257679_at	AT3G20470	GRP5	6.275385	
247575_at	AT5G61030	GR-RBP3	1.6348057	
252058_at	AT3G52470	harpin-induced family protein	1.8302335	
249915_at	AT5G22870	harpin-induced protein-related	1.5691336	
266118_at	AT2G02130	LCR68	2.6165984	
266119_at	AT2G02100	LCR69	2.9240267	
248932_at	AT5G46050	PTR3	3.3541954	
250493_at	AT5G09800	U-box domain-containing protein	2.4560103	
254159_at	AT4G24240	WRKY7	1.5596933	
245051_at	AT2G23320	WRKY15	2.200501	
253485_at	AT4G31800	WRKY18	2.7839494	
263536_at	AT2G25000	WRKY60	2.0139513	
248611_at	AT5G49520	WRKY48	2.1066833	
246104_at	AT5G28650	WRKY74	1.7966839	
260432_at	AT1G68150	WRKY9	1.7055966	
260403_at	AT1G69810	WRKY36	2.292045	
261429_at	AT1G18860	WRKY61	1.5777873	
262381_at	AT1G72900	disease resistance protein	1.812351	
245768_at	AT1G33590	LRR protein-related	2.5433743	
259655_at	AT1G55210	disease resistance response	3.1758099	
256781_at	AT3G13650	disease resistance response	4.0735445	
254907_at	AT4G11190	dirigent family protein	4.671053	
263437_at	AT2G28670	fibroin-related	1.8179097	
246395_at	AT1G58170	dirigent protein-related	2.0880437	
247413_at	AT5G63020	disease resistance protein	2.0455496	
264910_at	AT1G61100	disease resistance protein	1.5549846	
256303_at	AT1G69550	disease resistance protein	1.8827975	
262366_at	AT1G72890	disease resistance protein	1.738103	
254553_at	AT4G19530	disease resistance protein	2.6902409	
260312_at	AT1G63880	disease resistance protein	2.6633203	
248875_at	AT5G46470	disease resistance protein	1.7612915	
252648_at	AT3G44630	disease resistance protein	1.9751819	
245450_at	AT4G16880	disease resistance protein-related	4.903388	
Senescence				
256300_at	AT1G69490	NAP (NAC-like, activated by AP3/PI)	2.3724163	
266292_at	AT2G29350	SAG13; alcohol dehydrogenase/ oxidoreductase	2.8962815	
255479_at	AT4G02380	SAG21; AtLEA05	2.9276352	
252117_at	AT3G51430	YLS2; strictosidine synthase	1.8107271	
266167_at	AT2G38860	YLS5	2.696613	

Probe Set ID	AGI	Short/Full name	Fold change	RT-qPCR
249759_at	AT5G24380	YSL2 (YELLOW STRIPE LIKE 2)	2.0327816	
248276_at	AT5G53550	YSL3 (YELLOW STRIPE LIKE 3)	1.6124862	
Cell Death				
259100_at	AT3G04870 /// AT3G04880	ZDS (ZETA-CAROTENE DESATURASE)	1.5684819	
262482_at	AT1G17020	SRG1 (SENESCENCE-RELATED GENE 1)	1.6551807	
246831_at	AT5G26340	MSS1	1.8323759	
266447_at	AT2G43290	MSS3	1.6086613	
254021_at	AT4G25650	ACD1-LIKE (ACD1-LIKE)	1.5956136	
246194_at	AT4G37000	ACD2 (ACCELERATED CELL DEATH 2)	1.567585	
246304_at	AT3G51840	ACX4 (ACYL-COA OXIDASE 4)	1.6010183	
Drought/salt/osmotic stress				
247655_at	AT5G59820	RHL41, ZAT2	1.5891399	
261564_at	AT1G01720	ATAF1	1.604277	
254085_at	AT4G24960	ATHVA22D	1.8341898	
254889_at	AT4G11650	ATOSM34 (osmotin 34)	2.966169	
257022_at	AT3G19580	AZF2	2.0028732	
249139_at	AT5G43170	AZF3	1.7434927	
251870_at	AT3G54510	ERD protein-related	1.9896985	
246594_at	AT5G14800	P5CR	1.5408386	
263918_at	AT2G36590	ProT3	2.6118112	
255795_at	AT2G33380	RD20	3.8504097	
246908_at	AT5G25610	RD22	1.6832224	
258498_at	AT3G02480	ABA-responsive protein-related	2.4454384	
248155_at	AT5G54390	AHL	1.8904647	
267069_at	AT2G41010	ATCAMP25	1.8647299	
248607_at	AT5G49480	ATCP1	2.0608647	
250351_at	AT5G12030	AT-HSP17.6A	2.3679368	
266464_at	AT2G47800	ATMRP4	1.9282628	
266225_at	AT2G28900	ATOEP16-1	2.1373036	
260551_at	AT2G43510	ATT11r	3.3028703	
252988_at	AT4G38410	dehydrin, putative	4.0390625	
247352_at	AT5G63650	SNRK2.5	1.8931242	
267254_at	AT2G23030	SNRK2.9	1.8098142	
247043_at	AT5G66880	SNRK2.3	2.0553129	
246911_at	AT5G25810	tny (TINY)	1.8862898	
253412_at	AT4G33000	CBL10	1.8076532	
267467_at	AT2G30580	DRIP2	1.5764848	
257315_at	AT3G30775	ERD5	1.9173123	
254239_at	AT4G23400	PIP1;5	2.03393	
247586_at	AT5G60660	PIP2;4	2.4168193	
245399_at	AT4G17340	TIP2;2	2.4190283	
266649_at	AT2G25810	TIP4;1	1.5940753	
255381_at	AT4G03510	RMA1	2.1095874	
267180_at	AT2G37570	SLT1	2.4638617	
Cold stress				
261196_at	AT1G12860	SCRM2 (SCREAM 2)	2.1826549	
253129_at	AT4G36020	CSDP1	1.6218647	
265480_at	AT2G15970	COR413-PM1	1.5814444	
252135_at	AT3G50830	COR413-PM2	1.5400985	
259789_at	AT1G29395	COR414-TM1	1.7639424	
252102_at	AT3G50970	LTI30	1.760735	
248337_at	AT5G52310	LTI78	1.7038006	
Heat stress				

Probe Set ID	AGI	Short/Full name	Fold change	RT-qPCR
246214_at	AT4G36990	HSF4 (HEAT SHOCK FACTOR 4)	1.6289104	
Oxidative stress				
261648_at	AT1G27730	STZ; ZAT10 (salt tolerance zinc finger)	2.751101	
255500_at	AT4G02390	APP	1.8697174	
250633_at	AT5G07460	PMSR2	2.0908616	
245253_at	AT4G15440	HPL1 (HYDROPEROXIDE LYASE 1)	1.51994	
260706_at	AT1G32350	AOX1D (alternative oxidase 1D)	2.7287993	
250412_at	AT5G11150	ATVAMP713	1.7295301	
259517_at	AT1G20630	CAT1 (CATALASE 1); catalase	1.9759789	
253174_at	AT4G35090	CAT2 (CATALASE 2); catalase	1.8638768	
259965_at	AT1G53670	MSRB1 (methionine sulfoxide reductase B 1)	1.6690862	
253237_at	AT4G34240	ALDH311	1.5484588	
259511_at	AT1G12520	ATCCS (COPPER CHAPERONE FOR SOD1)	1.7520342	
257227_at	AT3G27820	MDAR4	1.6878024	
260408_at	AT1G69880	ATH8 (thioredoxin H-type 8)	4.0228195	
251985_at	AT3G53220	thioredoxin family protein	3.582015	
255230_at	AT4G05390	ATRFNR1 (ROOT FNR 1); FAD binding	2.4147942	
253382_at	AT4G33040	glutaredoxin family protein	1.6712667	
261958_at	AT1G64500	glutaredoxin family protein	2.3616302	
253112_at	AT4G35970	APX5 (ASCORBATE PEROXIDASE 5)	1.5473253	
253223_at	AT4G35000	APX3 (ASCORBATE PEROXIDASE 3)	1.5035471	
252862_at	AT4G39830	L-ascorbate oxidase, putative	1.8905897	
246021_at	AT5G21100	L-ascorbate oxidase, putative	1.6500018	
264001_at	AT2G22420	peroxidase 17 (PER17) (P17)	3.0378993	
265471_at	AT2G37130	peroxidase 21 (PER21) (P21) (PRXR5)	2.003713	
257952_at	AT3G21770	peroxidase 30 (PER30) (P30) (PRXR9)	1.9234072	
249227_at	AT5G42180	peroxidase 64 (PER64) (P64) (PRXR4)	1.6612618	
247091_at	AT5G66390	peroxidase 72 (PER72) (P72) (PRXR8)	2.732552	
249459_at	AT5G39580	peroxidase, putative	4.622013	
246228_at	AT4G36430	peroxidase, putative	15.421506	
254914_at	AT4G11290	peroxidase, putative	1.6758393	
255110_at	AT4G08770	peroxidase, putative	2.035024	
255111_at	AT4G08780	peroxidase, putative	3.771507	
246149_at	AT5G19890	peroxidase, putative	5.769599	
261606_at	AT1G49570	peroxidase, putative	5.8492837	
253332_at	AT4G33420	peroxidase, putative	2.0883129	
259276_at	AT3G01190	peroxidase 27 (PER27) (P27) (PRXR7)	1.8958764	
250059_at	AT5G17820	peroxidase 57 (PER57) (P57) (PRXR10)	3.4667926	
246991_at	AT5G67400	peroxidase 73 (PER73) (P73) (PRXR11)	3.1703987	
247327_at	AT5G64120	peroxidase, putative	1.8913475	
253667_at	AT4G30170	peroxidase, putative	2.1206048	
266941_at	AT2G18980	peroxidase, putative	2.1883948	
261157_at	AT1G34510	peroxidase, putative	2.2025516	
247297_at	AT5G64100	peroxidase, putative	2.4834049	
266191_at	AT2G39040	peroxidase, putative	2.5197608	
247326_at	AT5G64110	peroxidase, putative	2.6830137	
253998_at	AT4G26010	peroxidase, putative	3.2920783	
249934_at	AT5G22410	peroxidase, putative	3.613305	
250157_at	AT5G15180	peroxidase, putative	1.6550885	
252238_at	AT3G49960	peroxidase, putative	3.7340977	
Mitochondrial functions				
257947_at	AT3G21720	ICL (ISOCITRATE LYASE)	7.436195	
248434_at	AT5G51440	23.5 kDa mitochondrial small heat shock protein	3.236556	

Probe Set ID	AGI	Short/Full name	Fold change	RT-qPCR
255259_at	AT4G05020	NDB2 (NAD(P)H dehydrogenase B2)	1.7576138	
265422_at	AT2G20800	NDB4 (NAD(P)H dehydrogenase B4)	2.0660262	
265188_at	AT1G23800	ALDH2B7	1.5168648	
252131_at	AT3G50930	BCS1 (CYTOCHROME BC1 SYNTHESIS)	2.09492	
264000_at	AT2G22500	UCP5 (UNCOUPLING PROTEIN 5)	1.5354886	
245716_at	AT5G08740	NDC1 (NAD(P)H dehydrogenase C1)	1.7873391	
256765_at	AT3G22200	POP2 (POLLEN-PISTIL INCOMPATIBILITY 2)	1.8130904	
Chlorophyll biosynthesis				
255941_at	AT1G20350	ATTIM17-1	3.4753091	
258321_at	AT3G22840	EARLY LIGHT-INDUCIBLE PROTEIN	7.935653	
245306_at	AT4G14690	EARLY LIGHT-INDUCIBLE PROTEIN 2	4.5258865	
249325_at	AT5G40850	UPM1 (UROPHORPHYRIN METHYLASE 1)	2.6233687	
245242_at	AT1G44446	CHI (CHLORINA 1); chlorophyllide a oxygenase	1.8794883	
248920_at	AT5G45930	CHLI2 (MAGNESIUM CHELATASE I2)	1.8307958	
256020_at	AT1G58290	HEMA1; glutamyl-tRNA reductase	1.6662487	
255826_at	AT2G40490	HEME2; uroporphyrinogen decarboxylase	1.74545	
264839_at	AT1G03630	POR C	2.0824742	
Chloroplast				
263715_at	AT2G20570	GPR11; GLK1	1.722119	
259129_at	AT3G02150	PTF1 (PLASTID TRANSCRIPTION FACTOR 1)	1.5384945	
245528_at	AT4G15530	PPDK (pyruvate orthophosphate dikinase)	1.8343517	
265742_at	AT2G01290	ribose-5-phosphate isomerase	1.9409654	
249266_at	AT5G41670	6-phosphogluconate dehydrogenase	1.8136183	
260285_at	AT1G80560	3-isopropylmalate dehydrogenase	1.6410071	
245878_at	AT1G26190	phosphoribulokinase/uridine kinase family protein	1.5347071	
260284_at	AT1G80380	phosphoribulokinase/uridine kinase-related	1.8263346	
262648_at	AT1G14030	RUBISCO	1.6315974	
259185_at	AT3G01550	PPT2 (PHOSPHOENOLPYRUVATE (PEP))	2.179108	
263491_at	AT2G42600	ATPPC2	1.5495543	
255587_at	AT4G01480	AtPPa5	1.8697146	
265382_at	AT2G16790	shikimate kinase family protein	1.7897999	
266463_at	AT2G47840	tic20 protein-related	2.1186688	
255430_at	AT4G03320	tic20-IV	1.8815329	
245193_at	AT1G67810	SUFE2 (SULFUR E 2); enzyme activator	4.479765	
248493_at	AT5G51100	FSD2 (FE SUPEROXIDE DISMUTASE 2)	1.9135171	
265722_at	AT2G40100	LHCB4.3 (light harvesting complex PSII)	2.4080374	
257093_at	AT3G20570	plastocyanin-like domain-containing protein	2.137312	
259801_at	AT1G72230	plastocyanin-like domain-containing protein	2.1558871	
261975_at	AT1G64640	plastocyanin-like domain-containing protein	2.251465	
248236_at	AT5G53870	plastocyanin-like domain-containing protein	3.8572476	
257948_at	AT3G21740	APO4	2.2425325	
262202_at	AT2G01110	APG2	1.7118134	
249927_at	AT5G19220	APL1	1.6962466	
263256_at	AT1G10500	ATCPISCA	1.5240275	
248459_at	AT5G51020	CRL (CRUMPLED LEAF)	1.8223033	
248402_at	AT5G52100	err1 (chlororespiration reduction 1)	2.063625	
248075_at	AT5G55740	CRR21 (chlororespiratory reduction 21)	2.9938445	
260821_at	AT1G06820	CRTISO (CAROTENOID ISOMERASE)	1.825648	
259193_at	AT3G01480	CYP38 (cyclophilin 38)	1.6426872	
267471_at	AT2G30390	FC2 (FERROCHELATASE 2); ferrocyclase	1.8871746	
248962_at	AT5G45680	FK506-binding protein 1 (FKBP13)	1.6426774	
261218_at	AT1G20020	FNR2	1.6792315	
254181_at	AT4G23940	FtsH protease, putative	1.5250738	

Probe Set ID	AGI	Short/Full name	Fold change	RT-qPCR
262473_at	AT1G50250	FTSH1 (FtsH protease 1)	1.8584148	
246226_at	AT4G37200	HCF164	1.6135795	
255764_at	AT1G16720	HCF173	1.6241134	
251814_at	AT3G54890	LHCA1; chlorophyll binding	1.5695097	
252430_at	AT3G47470	LHCA4	1.6398041	
258239_at	AT3G27690	LHCB2.3; chlorophyll binding	1.5767919	
251969_at	AT3G53130	LUT1 (LUTEIN DEFICIENT 1)	1.6673442	
247936_at	AT5G57030	LUT2 (LUTEIN DEFICIENT 2)	1.805604	
262506_at	AT1G21640	NADK2; NAD+ kinase/ calmodulin binding	2.1550481	
253479_at	AT4G32360	NADP adrenodoxin-like ferredoxin reductase	1.5828353	
261788_at	AT1G15980	NDF1	2.3510303	
264799_at	AT1G08550	NPQ1	2.814829	
245118_at	AT2G41680	NTRC	1.5442413	
255982_at	AT1G34000	OHP2 (ONE-HELIX PROTEIN 2)	1.5868531	
246508_at	AT5G16150	PGLCT (PLASTIDIC GLC TRANSLOCATOR)	1.5717859	
254298_at	AT4G22890	PGR5-LIKE A	2.2330859	
245368_at	AT4G15510	photosystem II reaction center PsbP	1.5976424	
258223_at	AT3G15840	PIFI	2.364555	
266767_at	AT2G46910	plastid-lipid associated protein PAP	1.6563066	
245744_at	AT1G51110	plastid-lipid associated protein PAP	1.9713004	
245745_at	AT1G51110	plastid-lipid associated protein PAP	2.2062986	
266979_at	AT2G39470	PPL2 (PsbP-like protein 2); calcium ion binding	1.9862783	
255720_at	AT1G32060	PRK (PHOSPHORIBULOKINASE)	1.8166684	
261746_at	AT1G08380	PSAO (photosystem I subunit O)	1.5407245	
252130_at	AT3G50820	PSBO2 (PHOTOSYSTEM II SUBUNIT O-2)	1.6019964	
255248_at	AT4G05180	PSBQ-2; calcium ion binding	1.5585603	
259038_at	AT3G09210	PTAC13	1.5069318	
254727_at	AT4G13670	PTAC5	1.5192653	
253251_at	AT4G34730	ribosome-binding factor A family protein	2.0939846	
261801_at	AT1G30520	AAE14 (Acyl-Activating Enzyme 14)	2.0332632	
264963_at	AT1G60600	ABC4	1.7971622	
265998_at	AT2G24270	ALDH11A3	1.8835961	
250133_at	AT5G16400	ATF2; enzyme activator	1.7738445	
264383_at	AT2G25080	ATGPX1 (GLUTATHIONE PEROXIDASE 1)	2.4333675	
252516_at	AT3G46100	ATHRS1 (HISTIDYL-TRNA SYNTHETASE 1)	1.5882456	
249864_at	AT5G22830	ATMGT10 (MAGNESIUM (MG))	2.0820243	
264641_at	AT1G09130	ATP-dependent Clp protease proteolytic subunit	1.5446063	
261141_at	AT1G19740	protease La (LON) domain-containing protein	1.9699486	
261118_at	AT1G75460	protease La (LON) domain-containing protein	2.3165329	
254460_at	AT4G21210	ATRP1	2.156923	
261751_at	AT1G76080	CDSP32	1.8513979	
257222_at	AT3G27925	DEGP1 (DegP protease 1)	1.8611999	
247401_at	AT5G62790	DXR	1.7201169	
247637_at	AT5G60600	HDS	1.7690102	
262612_at	AT1G14150	oxygen evolving enhancer 3 (PsbQ) family protein	2.6030343	
258956_at	AT3G01440	oxygen evolving enhancer 3 (PsbQ) family protein	1.5868988	
264781_at	AT1G08540	RNA POLYMERASE SIGMA SUBUNIT 2	1.8304433	
250255_at	AT5G13730	SIG4 (SIGMA FACTOR 4); DNA binding	1.7574803	
262879_at	AT1G64860	SIGA (SIGMA FACTOR A); DNA binding	1.7211034	
251929_at	AT3G53920	RNA POLYMERASE SIGMA-SUBUNIT C	1.9482684	
262526_at	AT1G17050	SPS2 (Solanesyl diphosphate synthase 2)	1.6165422	
260036_at	AT1G68830	STN7 (Stt7 homolog STN7)	2.2916005	
259707_at	AT1G77490	TAPX	1.5298173	

Probe Set ID	AGI	Short/Full name	Fold change	RT-qPCR
264185_at	AT1G54780	thylakoid lumen 18.3 kDa protein	1.5544248	
248224_at	AT5G53490	thylakoid luminal 17.4 kDa protein, chloroplast	1.7080461	
251701_at	AT3G56650	thylakoid luminal 20 kDa protein	1.6188306	
264959_at	AT1G77090	thylakoid luminal 29.8 kDa protein	1.5188398	
255482_at	AT4G02510	TOC159	1.5132418	
258607_at	AT3G02730	TRXF1 (THIOREDOXIN F-TYPE 1)	2.0225306	
258398_at	AT3G15360	TRX-M4	1.6238353	
267196_at	AT2G30950	VAR2 (VARIEGATED 2)	2.064759	
Peroxisome				
262629_at	AT1G06460	ALPHA-CRYSTALLIN DOMAIN 32.1	2.0360222	
267512_at	AT2G45690	SSE1 (SHRUNKEN SEED 1)	1.6312973	
Vacuole				
251649_at	AT3G57330	ACA11 (autoinhibited Ca ²⁺ -ATPase 11)	1.6595609	
250336_at	AT5G11720	alpha-glucosidase 1 (AGLU1)	1.6601692	
257719_at	AT3G18440	AtALMT9	1.9045236	
266782_at	AT2G29120	ATGLR2.7	1.9702756	
256541_at	AT1G42540	ATGLR3.3	1.8697137	
264587_at	AT1G05200	ATGLR3.4	2.4336822	
Endoplasmic reticulum				
266326_at	AT2G46650	CB5-C (CYTOCHROME B5 ISOFORM C)	2.8620958	
264655_at	AT1G09070	SRC2	1.8971463	
267318_at	AT2G34770	FAH1 (FATTY ACID HYDROXYLASE 1)	1.913421	
RNA processing				
250538_at	AT5G08620	STRS2 (STRESS RESPONSE SUPPRESSOR 2)	1.9279337	
252679_at	AT3G44260	CCR4-NOT transcription complex protein	1.5028583	
254475_at	AT4G20440	smB	1.5297631	
251956_at	AT3G53460	CP29; RNA binding / poly(U) binding	1.5359806	
266510_at	AT2G47990	SWA1 (SLOW WALKER1); nucleotide binding	1.6792594	
261603_at	AT1G49600	ATRBP47A	1.7240838	
245518_at	AT4G15850	ATRH1	1.5379623	
259347_at	AT3G03920	Gar1 RNA-binding region family protein	1.9525925	
264868_at	AT1G24090	RNase H domain-containing protein	1.9281441	
262906_at	AT1G59760	ATP-dependent RNA helicase, putative	1.5660385	
262931_at	AT1G65700	small nuclear ribonucleoprotein, putative	2.4171515	
267627_at	AT2G42270	U5 small nuclear ribonucleoprotein helicase	1.594383	
246139_at	AT5G19900	PRL1-interacting factor A, putative	2.653985	
264255_at	AT1G09140	SF2/ASF-like splicing modulator (SRP30)	1.5387652	
259666_at	AT1G55310	SR33	1.537532	
254131_at	AT4G24740	AFC2	1.6263895	
252100_at	AT3G51110	crooked neck protein, putative	1.791988	
259585_at	AT1G28090	polynucleotide adenylyltransferase family protein	1.5173122	
248106_at	AT5G55100	SWAP (Suppressor-of-White-A-Pricot)	1.9796064	
253095_at	AT4G37510	ribonuclease III family protein	1.566916	
250367_s_at	AT5G11170 /// AT5G11200		1.5078006	
260525_at	AT2G47250	RNA helicase, putative	1.857975	
254679_at	AT4G18120	AML3 (<i>ARABIDOPSIS</i> MEI2-LIKE 3)	1.6065916	
259147_at	AT3G10360	APUM4 (<i>Arabidopsis</i> Pumilio 4); RNA binding	1.5701797	
245605_at	AT4G14300	heterogeneous nuclear ribonucleoprotein, putative	1.5056263	
258643_at	AT3G08010	ATAB2; RNA binding	1.5536424	
246493_at	AT5G16180	CRS1	1.9728875	
263014_at	AT1G23400	CAF2; RNA splicing factor	2.012493	
265484_at	AT2G15820	OTP51	1.510979	
248815_at	AT5G46920	intron maturase, type II family protein	2.1412392	

Probe Set ID	AGI	Short/Full name	Fold change	RT-qPCR
261652_at	AT1G01860	PFC1 (PALEFACE 1)	1.634756	
259919_at	AT1G72560	PSD (PAUSED); nucleobase, nucleoside	1.6979415	
259825_at	AT1G66260	RNA and export factor-binding protein, putative	1.5458808	
247653_at	AT5G59950	RNA and export factor-binding protein, putative	1.9658543	
245512_at	AT4G15770	RNA binding / protein binding	1.9107213	
258634_at	AT3G08000	RNA-binding protein, putative	1.6864842	
253748_at	AT4G28990	RNA-binding protein-related	4.348943	
253686_at	AT4G29750	RNA binding	1.8572518	
255969_at	AT1G22330	RNA binding / nucleic acid binding	1.6440358	
247669_at	AT5G60170	RNA binding / nucleic acid binding	1.5959642	
255411_at	AT4G03110	RNA-binding protein, putative	1.6956824	
248905_at	AT5G46250	RNA recognition motif (RRM)-containing protein	1.5347974	
252588_at	AT3G45630	RNA recognition motif (RRM)-containing protein	1.5952182	
259209_at	AT3G09160	RNA recognition motif (RRM)-containing protein	1.6368687	
248063_at	AT5G55550	RNA recognition motif (RRM)-containing protein	1.7624593	
259984_at	AT1G76460	RNA recognition motif (RRM)-containing protein	1.7856083	
251857_at	AT3G54770	RNA recognition motif (RRM)-containing protein	1.8461534	
264698_at	AT1G70200	RNA recognition motif (RRM)-containing protein	1.9179306	
266002_at	AT2G37310	pentatricopeptide (PPR) repeat-containing protein	1.5073009	
258991_at	AT3G08820	pentatricopeptide (PPR) repeat-containing protein	1.5091655	
263143_at	AT1G03100	pentatricopeptide (PPR) repeat-containing protein	1.5244429	
260620_at	AT1G08070	pentatricopeptide (PPR) repeat-containing protein	1.5521516	
246383_at	AT1G77360	pentatricopeptide (PPR) repeat-containing protein	1.5551617	
264946_at	AT1G77010	pentatricopeptide (PPR) repeat-containing protein	1.5572852	
267445_at	AT2G33680	pentatricopeptide (PPR) repeat-containing protein	1.5589457	
249529_at	AT5G38730	pentatricopeptide (PPR) repeat-containing protein	1.5777707	
266998_at	AT2G34400	pentatricopeptide (PPR) repeat-containing protein	1.5798099	
257607_at	AT3G13880	pentatricopeptide (PPR) repeat-containing protein	1.5812722	
250115_at	AT5G16420	pentatricopeptide (PPR) repeat-containing protein	1.5847099	
248803_at	AT5G47460	pentatricopeptide (PPR) repeat-containing protein	1.5859282	
258174_at	AT3G21470	pentatricopeptide (PPR) repeat-containing protein	1.5867025	
246262_at	AT1G31790	pentatricopeptide (PPR) repeat-containing protein	1.5937449	
246249_at	AT4G36680	pentatricopeptide (PPR) repeat-containing protein	1.6020479	
260224_at	AT1G74400	pentatricopeptide (PPR) repeat-containing protein	1.604175	
252245_at	AT3G49710	pentatricopeptide (PPR) repeat-containing protein	1.6170187	
260217_at	AT1G74600	pentatricopeptide (PPR) repeat-containing protein	1.6176622	
261277_at	AT1G20230	pentatricopeptide (PPR) repeat-containing protein	1.6180508	
259003_at	AT3G02010	pentatricopeptide (PPR) repeat-containing protein	1.6270918	
250283_at	AT5G13270	pentatricopeptide (PPR) repeat-containing protein	1.6287106	
249436_at	AT5G39980	pentatricopeptide (PPR) repeat-containing protein	1.6441641	
250523_at	AT5G08510	pentatricopeptide (PPR) repeat-containing protein	1.6479119	
249222_at	AT5G42450	pentatricopeptide (PPR) repeat-containing protein	1.65056	
263719_at	AT2G13600	pentatricopeptide (PPR) repeat-containing protein	1.6519275	
264739_at	AT1G62260	pentatricopeptide (PPR) repeat-containing protein	1.6560229	
255153_at	AT4G08210	pentatricopeptide (PPR) repeat-containing protein	1.6711028	
246458_at	AT5G16860	pentatricopeptide (PPR) repeat-containing protein	1.6775078	
251583_at	AT3G58590	pentatricopeptide (PPR) repeat-containing protein	1.6878772	
257395_at	AT2G15630	pentatricopeptide (PPR) repeat-containing protein	1.7147502	
245620_at	AT4G14050	pentatricopeptide (PPR) repeat-containing protein	1.7446529	
264666_at	AT1G09680	pentatricopeptide (PPR) repeat-containing protein	1.7446606	
256919_at	AT3G18970	pentatricopeptide (PPR) repeat-containing protein	1.7737354	
249965_at	AT5G19020	pentatricopeptide (PPR) repeat-containing protein	1.8101655	
247550_at	AT5G61370	pentatricopeptide (PPR) repeat-containing protein	1.8390801	

Probe Set ID	AGI	Short/Full name	Fold change	RT-qPCR
257685_at	AT3G12770	pentatricopeptide (PPR) repeat-containing protein	1.8735757	
253170_at	AT4G35130	pentatricopeptide (PPR) repeat-containing protein	1.8928354	
259746_at	AT1G71060	pentatricopeptide (PPR) repeat-containing protein	1.896853	
252899_at	AT4G39530	pentatricopeptide (PPR) repeat-containing protein	1.9041903	
265931_at	AT2G18520	pentatricopeptide (PPR) repeat-containing protein	1.9841715	
258088_at	AT3G14580	pentatricopeptide (PPR) repeat-containing protein	2.0137677	
259945_at	AT1G71460	pentatricopeptide (PPR) repeat-containing protein	2.0865412	
252386_at	AT3G47840	pentatricopeptide (PPR) repeat-containing protein	2.105832	
248871_at	AT5G46680	pentatricopeptide (PPR) repeat-containing protein	2.1581652	
256027_at	AT1G34160	pentatricopeptide (PPR) repeat-containing protein	2.2145205	
245673_at	AT1G56690	pentatricopeptide (PPR) repeat-containing protein	2.2939808	
246052_at	AT5G08310	pentatricopeptide (PPR) repeat-containing protein	2.3351974	
259285_at	AT3G11460	pentatricopeptide (PPR) repeat-containing protein	2.3613734	
253019_at	AT4G38010	pentatricopeptide (PPR) repeat-containing protein	2.3969567	
247099_at	AT5G66500	pentatricopeptide (PPR) repeat-containing protein	2.4061205	
257193_at	AT3G13160	pentatricopeptide (PPR) repeat-containing protein	2.4998543	
249470_at	AT5G39350	pentatricopeptide (PPR) repeat-containing protein	2.8430393	
248307_at	AT5G52850	pentatricopeptide (PPR) repeat-containing protein	2.9527457	
266668_at	AT2G29760	pentatricopeptide (PPR) repeat-containing protein	3.2904086	
246019_at	AT5G10690	pentatricopeptide (PPR) repeat-containing protein	1.5256804	
253589_at	AT4G30825	pentatricopeptide (PPR) repeat-containing protein	2.052063	
250164_at	AT5G15280	pentatricopeptide (PPR) repeat-containing protein	1.5137926	
254483_at	AT4G20740	pentatricopeptide (PPR) repeat-containing protein	1.5189918	
261762_at	AT1G15510	pentatricopeptide (PPR) repeat-containing protein	1.6175226	
248640_at	AT5G48910	pentatricopeptide (PPR) repeat-containing protein	1.6217076	
264177_at	AT1G02150	pentatricopeptide (PPR) repeat-containing protein	1.7156695	
246901_at	AT5G25630	pentatricopeptide (PPR) repeat-containing protein	1.7480935	
246572_at	AT5G15010	pentatricopeptide (PPR) repeat-containing protein	1.7759691	
259295_at	AT3G05340	pentatricopeptide (PPR) repeat-containing protein	1.8706292	
263550_at	AT2G17033	pentatricopeptide (PPR) repeat-containing protein	1.8837788	
250257_at	AT5G13770	pentatricopeptide (PPR) repeat-containing protein	2.0262036	
247100_at	AT5G66520	pentatricopeptide (PPR) repeat-containing protein	2.0328872	
258804_at	AT3G04760	pentatricopeptide (PPR) repeat-containing protein	2.049196	
246313_at	AT1G31920	pentatricopeptide (PPR) repeat-containing protein	2.0515435	
258355_at	AT3G14330	pentatricopeptide (PPR) repeat-containing protein	2.2108557	
249247_at	AT5G42310	pentatricopeptide (PPR) repeat-containing protein	2.4218826	
253495_at	AT4G31850	PGR3 (PROTON GRADIENT REGULATION 3)	4.0040317	
262658_at	AT1G14220	ribonuclease T2 family protein	1.6136549	
DNA replication				
264674_at	AT1G09815	POLD4 (POLYMERASE DELTA 4)	1.5576817	
248099_at	AT5G55300	DNA TOPOISOMERASE I ALPHA	2.033682	
261471_at	AT1G14460	DNA polymerase-related	1.5371673	
248891_at	AT5G46280	DNA replication licensing factor, putative	1.7185278	
255513_at	AT4G02060	PRL (PROLIFERA) MCM7; ATP binding	1.6089385	
266959_at	AT2G07690	minichromosome maintenance family protein	1.6566215	
256374_at	AT1G66730	ATP dependent DNA ligase family protein	1.6610441	
DNA repair				
248668_at	AT5G48720	XR11 (X-RAY INDUCED TRANSCRIPT 1)	1.652782	
256237_at	AT3G12610	DRT100	1.5297197	
257701_at	AT3G12710	methyladenine glycosylase family protein	2.0576632	
249848_at	AT5G23220	NIC3 (NICOTINAMIDASE 3)	2.4771512	
248628_at	AT5G48960	5' nucleotidase family protein	2.1187263	
259928_at	AT1G34380	5'-3' exonuclease family protein	1.6525367	

Probe Set ID	AGI	Short/Full name	Fold change	RT-qPCR
256077_at	AT1G18090	exonuclease, putative	1.9185951	
265706_at	AT2G03390	uvrB/uvrC motif-containing protein	1.6005719	
265707_at	AT2G03390	uvrB/uvrC motif-containing protein	1.8039633	
266572_at	AT2G23840	HNH endonuclease domain-containing protein	5.8171067	
258621_at	AT3G02830	ZFN1 (ZINC FINGER PROTEIN 1)	1.6693206	
250128_at	AT5G16540	ZFN3 (ZINC FINGER NUCLEASE 3)	1.5502117	
Chromatin&nuclear transport				
262600_at	AT1G15340	MBD10; DNA binding / methyl-CpG binding	1.6571203	
255963_at	AT1G22310	MBD8; methyl-CpG binding	1.508632	
253337_at	AT4G33470	hda14 (histone deacetylase 14)	1.913197	
255843_at	AT2G33540	CPL3	1.6693019	
258974_at	AT3G01890	SWIB complex	1.671362	
263349_at	AT2G13370	CHR5	1.7529496	
256091_at	AT1G20693	HMGB2	1.7954547	
261782_at	AT1G76110	high mobility group (HMG1/2) family protein	2.787873	
254233_at	AT4G23800	high mobility group (HMG1/2) family protein	2.0431583	
257655_at	AT3G13350	high mobility group (HMG1/2) family protein	1.8415569	
263412_at	AT2G28720	histone H2B, putative	4.8085012	
252223_at	AT3G49850	TRB3 transcription factor	1.5142031	
255718_at	AT1G32070	ATNSI	1.7486756	
258333_at	AT3G16000	MFP1	2.1555486	
259943_at	AT1G71480	nuclear transport factor 2 (NTF2) family protein	2.4810266	
256852_at	AT3G18610	ATRANGAP1	3.187492	
246061_at	AT5G19320	RANGAP2	1.887825	
258085_at	AT3G26100	regulator of chromosome condensation (RCC1)	2.2484763	
262375_at	AT1G73100	SUVH3 (SU(VAR)3-9 HOMOLOG 3)	1.5443825	
265347_at	AT2G22740	SUVH6; methyl-CpG binding	1.8774747	
259609_at	AT1G52410	TSA1 (TSK-ASSOCIATING PROTEIN 1)	1.8927872	
253175_at	AT4G35050	MSI3 (MULTICOPY SUPPRESSOR OF IRA1 3)	2.835047	
261130_at	AT1G04870	PRMT10; methyltransferase	1.8114408	
257352_at	AT2G34900	IMB1 (IMBIBITION-INDUCIBLE 1)	1.6762367	
266189_at	AT2G39020	GCN5-related N-acetyltransferase	1.7571893	
265668_at	AT2G32020	GCN5-related N-acetyltransferase	4.2181454	
253057_at	AT4G37670	GCN5-related N-acetyltransferase	1.5850574	
266826_at	AT2G22910	GCN5-related N-acetyltransferase	1.6283807	
253823_at	AT4G28030	GCN5-related N-acetyltransferase	1.8288189	
Phospholipid/inositol signaling				
250848_at	AT5G04510	PKD1	1.5635959	
252410_at	AT3G47450	NOA1 (NO ASSOCIATED 1); GTPase	1.5326784	
251711_at	AT3G56960	PIP5K4	1.6363449	
260636_at	AT1G62430	ATCDS1; phosphatidate cytidyltransferase	1.7991081	
262003_at	AT1G64460	phosphatidylinositol 3- and 4-kinase	1.6059046	
259721_at	AT1G60890	phosphatidylinositol-4-phosphate 5-kinase	1.5502559	
260466_at	AT1G10900	phosphatidylinositol-4-phosphate 5-kinase f	2.6391344	
246180_at	AT5G20840	phosphoinositide phosphatase family protein	1.7768534	
252737_at	AT3G43220	phosphoinositide phosphatase family protein	1.8697897	
266693_at	AT2G19800	MIOX2 (MYO-INOSITOL OXYGENASE 2)	2.580798	
258613_at	AT3G02870	VTC4; 3'(2'),5'-bisphosphate nucleotidase	1.9894878	
GTPases/vesicle transport				
246524_at	AT5G15860	ATPCME	1.6216416	
259398_at	AT1G17700	PRA1.F1	2.7191083	
256785_at	AT3G13720	PRA8	1.576094	
264395_at	AT1G12070	Rho GDP-dissociation inhibitor family protein	1.8151741	

Probe Set ID	AGI	Short/Full name	Fold change	RT-qPCR
247210_at	AT5G65020	ANNAT2 (Annexin <i>Arabidopsis</i> 2)	1.569642	
253757_at	AT4G28950	ROP9	1.9956322	
251960_at	AT3G53610	ATRAB8; GTP binding	1.6453077	
259611_at	AT1G52280	AtRABG3d	1.6104625	
259836_at	AT1G52240	ROPGEF11	2.7483742	
245278_at	AT4G17730	SYP23 (SYNTAXIN OF PLANTS 23)	1.5794866	
250740_at	AT5G05760	SYP31 (SYNTAXIN OF PLANTS 31)	1.939873	
262695_at	AT1G75850	VPS35B (VPS35 HOMOLOG B)	1.6601982	
Ca2/Calmodulin				
249583_at	AT5G37770	TCH2 (TOUCH 2); calcium ion binding	1.7015792	
267083_at	AT2G41100	TCH3 (TOUCH 3); calcium ion binding	2.7471566	
266421_at	AT2G38540	LPI1; calmodulin binding	1.5800452	
256129_at	AT1G18210	calcium-binding protein, putative	2.0600157	
257024_at	AT3G19100	calcium-dependent protein kinase, putative	1.5848745	
256839_at	AT3G22930	calmodulin, putative	2.042213	
263795_at	AT2G24610	ATCNGC14; calmodulin binding	1.8381972	
Polyamines				
245947_at	AT5G19530	ACL5 (ACAULIS 5); spermine synthase	1.5266083	
246490_at	AT5G15950	adenosylmethionine decarboxylase family protein	2.4277089	
Peptide factors & transporters				
247037_at	AT5G67070	RALFL34 (ralf-like 34); signal transducer	1.711497	
247109_at	AT5G65870	ATPSK5 (PHYTOSULFOKINE 5 PRECURSOR)	3.1584706	
247704_at	AT5G59510	RTFL5 (ROTUNDIFOLIA LIKE 5)	4.6355066	
Transcription factors				
259908_at	AT1G60850	ATRPAC42	1.5529155	
245569_at	AT4G14660	NRPE7; DNA-directed RNA polymerase	1.7998123	
266135_at	AT2G45100	RNA polymerase II transcription factor	1.5569211	
261942_at	AT1G22590	AGL87 MADS-box family protein	2.1186974	
264148_at	AT1G02220	ANAC003	1.9691254	
263584_at	AT2G17040	anac036	1.6708747	
265260_at	AT2G43000	anac042	2.356499	
250208_at	AT5G14000	anac084	2.0146034	
258059_at	AT3G29035	ATNAC3	1.9707448	
266175_at	AT2G02450	ANAC035	1.5417438	
255585_at	AT4G01550	anac069	1.872525	
264481_at	AT1G77200	AP2 domain-containing transcription factor TINY	1.556843	
261327_at	AT1G44830	AP2 domain-containing transcription factor TINY	1.7447348	
245173_at	AT2G47520	AP2 domain-containing transcription factor	1.7755783	
255926_at	AT1G22190	AP2 domain-containing transcription factor	2.0249312	
252859_at	AT4G39780	AP2 domain-containing transcription factor	1.7038631	
260030_at	AT1G68880	AtbZIP	2.1044636	
253064_at	AT4G37730	AtbZIP7	1.5062675	
261114_at	AT1G75390	AtbZIP44	1.5056126	
261815_at	AT1G08320	bZIP family transcription factor	1.543994	
248208_at	AT5G53980	ATHB52	2.7404675	
264974_at	AT1G27050	ATHB54	1.7443026	
247182_at	AT5G65410	HB25 (HOMEODOMAIN PROTEIN 25)	1.5300364	
261502_at	AT1G14440	AtHB31	2.0245733	
257610_at	AT3G13810	AtIDD11	2.073872	
252175_at	AT3G50700	AtIDD2	1.7343242	
266120_at	AT2G02070	AtIDD5	1.5172065	
248460_at	AT5G50915	basic helix-loop-helix (bHLH) family protein	1.703447	
265034_at	AT1G61660	basic helix-loop-helix (bHLH) family protein	1.8108397	

Probe Set ID	AGI	Short/Full name	Fold change	RT-qPCR
263380_at	AT2G40200	basic helix-loop-helix (bHLH) family protein	1.5832576	
247151_at	AT5G65640	bHLH093 (beta HLH protein 93); DNA binding	2.2009866	
255579_at	AT4G01460	basic helix-loop-helix (bHLH) family protein	1.63526	
259010_at	AT3G07340	basic helix-loop-helix (bHLH) family protein	1.6697087	
261254_at	AT1G05805	basic helix-loop-helix (bHLH) family protein	1.7145066	
254693_at	AT4G17880	basic helix-loop-helix (bHLH) family protein	1.7788255	
248708_at	AT5G48560	basic helix-loop-helix (bHLH) family protein	2.0067875	
265342_at	AT2G18300	basic helix-loop-helix (bHLH) family protein	1.7024624	
248839_at	AT5G46690	bHLH071 (beta HLH protein 71); DNA binding	1.9244549	
260451_at	AT1G72360	ethylene-responsive element-binding protein	1.617021	
253746_at	AT4G29100	ethylene-responsive family protein	1.8105271	
245362_at	AT4G17460	HAT1; DNA binding / transcription factor	2.3220825	
251310_at	AT3G61150	HDG1 (HOMEODOMAIN GLABROUS 1)	1.5354265	
248596_at	AT5G49330	AtMYB111 (myb domain protein 111)	1.6339566	
252340_at	AT3G48920	AtMYB45 (myb domain protein 45)	1.5394807	
266469_at	AT2G31180	MYB14 (MYB DOMAIN PROTEIN 14)	1.5212485	
250099_at	AT5G17300	myb family transcription factor	2.8898904	
259432_at	AT1G01520	myb family transcription factor	1.8838267	
258724_at	AT3G09600	myb family transcription factor	2.5073445	
258723_at	AT3G09600	myb family transcription factor	3.297035	
246844_at	AT5G26660	ATMYB86 (MYB DOMAIN PROTEIN 86)	1.7160784	
259379_at	AT3G16350	myb family transcription factor	1.8814117	
248795_at	AT5G47390	myb family transcription factor	1.7743194	
257698_at	AT3G12730	myb family transcription factor	1.6269206	
247768_at	AT5G58900	myb family transcription factor	1.6375049	
257645_at	AT3G25790	myb family transcription factor	1.5123316	
255734_at	AT1G25550	myb family transcription factor	1.840429	
250810_at	AT5G05090	myb family transcription factor	1.9910599	
259365_at	AT1G13300	myb family transcription factor	4.1732154	
250031_at	AT5G18240	MYR1 (MYb-related protein 1)	1.510424	
249908_at	AT5G22760	PHD finger family protein	1.610588	
258628_at	AT3G02890	PHD finger protein-related	1.8801025	
250287_at	AT5G13330	Rap2.6L (related to AP2 6L); DNA binding	4.3569613	
245966_at	AT5G19790	RAP2.11 (related to AP2 11); DNA binding	1.6788306	
245237_at	AT4G25520	SLK1 (SEUSS-LIKE 1); transcription regulator	1.5682606	
258326_at	AT3G22760	SOL1; transcription factor	1.7401745	
267515_at	AT2G45680	TCP family transcription factor, putative	1.8550841	
246011_at	AT5G08330	TCP family transcription factor, putative	1.6977603	
256528_at	AT1G66140	ZFP4 (ZINC FINGER PROTEIN 4)	1.5335499	
252009_at	AT3G52800	zinc finger (AN1-like) family protein	1.6548063	
252924_at	AT4G39070	zinc finger (B-box type) family protein	1.9309287	
257262_at	AT3G21890	zinc finger (B-box type) family protein	1.9225402	
263739_at	AT2G21320	zinc finger (B-box type) family protein	1.657842	
260431_at	AT1G68190	zinc finger (B-box type) family protein	1.8366189	
266514_at	AT2G47890	zinc finger (B-box type) family protein	1.9897336	
250119_at	AT5G16470	zinc finger (C2H2 type) family protein	2.5470488	
258623_at	AT3G02790	zinc finger (C2H2 type) family protein	5.1235013	
262969_at	AT1G75710	zinc finger (C2H2 type) family protein	1.6278341	
Protein kinases				
261089_at	AT1G07570	APK1A; kinase/ protein serine/threonine kinase	1.7313291	
261460_at	AT1G07880	ATMPK13; MAP kinase/ kinase	1.808909	
260979_at	AT1G53510	ATMPK18; MAP kinase	1.7666793	
256075_at	AT1G18150	ATMPK8; MAP kinase	2.0078351	

Probe Set ID	AGI	Short/Full name	Fold change	RT-qPCR
257771_at	AT3G23000	CBL-INTERACTING PROTEIN KINASE 7	1.5217613	
247867_at	AT5G57630	CIPK21 (CBL-interacting protein kinase 21)	2.248663	
258300_at	AT3G23340	ckl10 (Casein Kinase I-like 10)	2.1701007	
267013_at	AT2G39180	CCR2	1.6185986	
252378_at	AT3G47570	leucine-rich repeat transmembrane protein kinase	1.6995085	
263913_at	AT2G36570	leucine-rich repeat transmembrane protein kinase	1.9117078	
266663_at	AT2G25790	leucine-rich repeat transmembrane protein kinase	2.142215	
259853_at	AT1G72300	leucine-rich repeat transmembrane protein kinase	1.8671305	
248568_at	AT5G49760	leucine-rich repeat family protein	1.553019	
256168_at	AT1G51805	leucine-rich repeat protein kinase, putative	2.4942102	
253278_at	AT4G34220	leucine-rich repeat transmembrane protein kinase	2.0262556	
261501_at	AT1G28390	protein kinase family protein	1.8577633	
254869_at	AT4G11890	protein kinase family protein	2.8670754	
258323_at	AT3G22750	protein kinase, putative	1.6658193	
251621_at	AT3G57700	protein kinase, putative	1.735013	
264284_at	AT1G61860	protein kinase, putative	1.7510844	
252511_at	AT3G46280	protein kinase-related	2.1890807	
256366_at	AT1G66880	serine/threonine protein kinase family protein	2.0800824	
260728_at	AT1G48210	serine/threonine protein kinase, putative	1.9111878	
251251_at	AT3G62220	serine/threonine protein kinase, putative	2.1767385	
255488_at	AT4G02630	protein kinase family protein	1.5342959	
251500_at	AT3G59110	protein kinase family protein	1.549877	
256121_at	AT1G18160	protein kinase family protein	1.5619036	
254251_at	AT4G23300	protein kinase family protein	1.6193614	
260759_at	AT1G49180	protein kinase family protein	1.6259619	
266080_at	AT2G37840	protein kinase family protein	1.7070556	
255266_at	AT4G05200	protein kinase family protein	1.8416061	
254242_at	AT4G23200	protein kinase family protein	2.0038257	
254250_at	AT4G23290	protein kinase family protein	2.4042754	
254931_at	AT4G11460	protein kinase family protein	2.685335	
264240_at	AT1G54820	protein kinase family protein	2.7370358	
247918_at	AT5G57610	protein kinase family protein	1.6276243	
259671_at	AT1G52290	protein kinase family protein	1.9044886	
255913_at	AT1G66980	protein kinase family protein	2.004721	
267289_at	AT2G23770	protein kinase family protein	1.5568035	
246371_at	AT1G51940	protein kinase family protein	1.7363354	
248541_at	AT5G50180	protein kinase, putative	1.5056021	
259887_at	AT1G76360	protein kinase, putative	1.5181779	
267582_at	AT2G41970	protein kinase, putative	1.9182208	
264767_at	AT1G61380	SD1-29 (S-DOMAIN-1 29); carbohydrate binding	2.0148027	
262507_at	AT1G11330	S-locus lectin protein kinase family protein	1.9403054	
265063_at	AT1G61500	S-locus protein kinase, putative	1.5024632	
264754_at	AT1G61400	S-locus protein kinase, putative	1.6865728	
259958_at	AT1G53730	SRF6 (STRUBBELIG-RECEPTOR FAMILY 6)	2.0502498	
Protein phosphatases				
254923_at	AT4G11240	TOPP7; protein serine/threonine phosphatase	1.7090288	
245194_at	AT1G67820	protein phosphatase 2C, putative	1.9210184	
253834_at	AT4G27800	protein phosphatase 2C PPH1	1.5257212	
246756_at	AT5G27930	protein phosphatase 2C, putative	1.5112001	
256441_at	AT3G10940	protein phosphatase-related	1.6026099	
Protein folding				
264947_at	AT1G77020	DNAJ heat shock family protein	1.7164258	
252828_at	AT4G39960	DNAJ heat shock family protein	1.5275946	

Probe Set ID	AGI	Short/Full name	Fold change	RT-qPCR
247274_at	AT5G64360	DNAJ heat shock family protein	1.5252781	
246817_at	AT5G27240	DNAJ heat shock family protein	1.5880448	
245182_at	AT5G12430	DNAJ heat shock family protein	1.7582313	
262194_at	AT1G77930	DNAJ heat shock family protein	1.7883136	
255088_at	AT4G09350	DNAJ heat shock family protein	2.1596444	
256221_at	AT1G56300	DNAJ heat shock family protein	4.2814126	
252935_at	AT4G39150	DNAJ heat shock family protein	1.5649503	
247733_at	AT5G59610	DNAJ heat shock family protein	1.571172	
263985_at	AT2G42750	DNAJ heat shock family protein	1.786167	
254458_at	AT4G21180	ATERDJ2B; heat shock protein binding	1.5462997	
256088_at	AT1G20810	immunophilin	1.7826933	
260542_at	AT2G43560	immunophilin	1.9552286	
245266_at	AT4G17070	peptidyl-prolyl cis-trans isomerase	2.013094	
264019_at	AT2G21130	peptidyl-prolyl cis-trans isomerase	2.0560675	
248657_at	AT5G48570	peptidyl-prolyl cis-trans isomerase, putative	3.1617744	
Proteasome & Ubiquitin				
251975_at	AT3G53230	cell division cycle protein 48, putative	1.5332229	
267524_at	AT2G30600	BTB/POZ domain-containing protein	3.4518275	
267523_at	AT2G30600	BTB/POZ domain-containing protein	3.7407467	
260058_at	AT1G78100	F-box family protein	1.5808727	
262552_at	AT1G31350	F-box family protein	1.6987662	
257574_at	AT3G20710	F-box protein-related	2.242951	
253945_at	AT4G27050	F-box family protein	1.5262641	
267116_at	AT2G32560	F-box family protein	1.5755385	
248586_at	AT5G49610	F-box family protein	1.6213635	
257530_at	AT3G03040	F-box family protein	1.6251596	
264539_at	AT1G55590	F-box family protein	1.6748185	
248016_at	AT5G56380	F-box family protein	1.6967508	
263556_at	AT2G16365	F-box family protein	1.8947537	
257447_at	AT2G04230	F-box family protein	2.8588653	
259067_at	AT3G07550	F-box family protein (FBL12)	1.5127964	
257476_at	AT1G80960	F-box protein-related	2.1671615	
254078_at	AT4G25710	kelch repeat-containing F-box family protein	1.5405915	
262986_at	AT1G23390	kelch repeat-containing F-box family protein	1.6843773	
252902_at	AT4G39560	kelch repeat-containing F-box family protein	1.7246557	
266522_at	AT2G16920	UBIQUITIN-CONJUGATING ENZYME 23	1.5000073	
256302_at	AT1G69526	UbiE/COQ5 methyltransferase family protein	1.596123	
251530_at	AT3G58520	ubiquitin thiolesterase	1.7568686	
255062_at	AT4G08940	ubiquitin thiolesterase	1.60702	
258757_at	AT3G10910	zinc finger (C3HC4-type RING finger)	1.6293161	
260770_at	AT1G49200	zinc finger (C3HC4-type RING finger)	2.4817007	
248759_at	AT5G47610	zinc finger (C3HC4-type RING finger)	3.4940007	
256093_at	AT1G20823	zinc finger (C3HC4-type RING finger)	2.062815	
251454_at	AT3G60080	zinc finger (C3HC4-type RING finger)	1.5951785	
266187_at	AT2G38970	zinc finger (C3HC4-type RING finger)	1.5343205	
254349_at	AT4G22250	zinc finger (C3HC4-type RING finger)	1.6796992	
246135_at	AT5G20885	zinc finger (C3HC4-type RING finger)	1.7410158	
252751_at	AT3G43430	zinc finger (C3HC4-type RING finger)	2.1931489	
249306_at	AT5G41400	zinc finger (C3HC4-type RING finger)	2.2985487	
247615_at	AT5G60250	zinc finger (C3HC4-type RING finger)	4.802965	
245329_at	AT4G14365	zinc finger (C3HC4-type RING finger)	4.342832	
261376_at	AT1G18660	zinc finger (C3HC4-type RING finger)	1.5307248	
259854_at	AT1G72200	zinc finger (C3HC4-type RING finger)	1.6281432	

Probe Set ID	AGI	Short/Full name	Fold change	RT-qPCR
261927_at	AT1G22500	zinc finger (C3HC4-type RING finger)	1.9429344	
251314_at	AT3G61180	zinc finger (C3HC4-type RING finger)	1.5479137	
260065_at	AT1G73760	zinc finger (C3HC4-type RING finger)	1.6711143	
253539_at	AT4G31450	zinc finger (C3HC4-type RING finger)	1.8673947	
255899_at	AT1G17970	zinc finger (C3HC4-type RING finger)	1.8794426	
250005_at	AT5G18760	zinc finger (C3HC4-type RING finger)	1.9176422	
249862_at	AT5G22920	zinc finger (C3HC4-type RING finger)	1.9700798	
Proteolysis & proteases & protease inhibitors				
250445_at	AT5G10760	aspartyl protease family protein	1.5217872	
267592_at	AT2G39710	aspartyl protease family protein	1.6254832	
261055_at	AT1G01300	aspartyl protease family protein	1.9559478	
264741_at	AT1G62290	aspartyl protease family protein	1.7775321	
248703_at	AT5G48430	aspartic-type endopeptidase	1.521327	
253331_at	AT4G33490	aspartic-type endopeptidase	1.5626373	
252241_at	AT3G50050	aspartyl protease family protein	1.7069743	
261346_at	AT1G79720	aspartyl protease family protein	2.0014377	
261224_at	AT1G20160	ATSBT5.2; identical protein binding	2.889159	
247755_at	AT5G59090	ATSBT4.12; identical protein binding	2.5497518	
246250_at	AT4G36880	CPI (CYSTEINE PROTEINASE1)	3.8489614	
265665_at	AT2G27420	cysteine proteinase, putative	2.452016	
245483_at	AT4G16190	cysteine proteinase, putative	1.5363972	
258005_at	AT3G19390	cysteine proteinase, putative	1.5550758	
257646_at	AT3G25740	MAP1B	1.6214749	
260475_at	AT1G11080	scpl31 (serine carboxypeptidase-like 31)	1.7012368	
250517_at	AT5G08260	scpl35 (serine carboxypeptidase-like 35)	3.1574316	
249216_at	AT5G42240	scpl42 (serine carboxypeptidase-like 42)	2.0076272	
258923_at	AT3G10450	SCPL7 (SERINE CARBOXYPEPTIDASE-LIKE 7)	1.7247046	
267264_at	AT2G22970	serine carboxypeptidase S10 family protein	1.5056872	
249860_at	AT5G22860	serine carboxypeptidase S28 family protein	2.0274544	
267265_at	AT2G22980	serine-type carboxypeptidase	4.6234756	
NAD/P & ATP				
259632_at	AT1G56430	NAS4	1.5032372	
264261_at	AT1G09240	NAS3	3.2997446	
250498_at	AT5G09660	PMDH2	2.1253552	
258998_at	AT3G01820	adenylate kinase family protein	2.0053797	
246651_at	AT5G35170	adenylate kinase family protein	2.4979532	
255299_at	AT4G04880	adenosine/AMP deaminase family protein	1.549504	
252507_at	AT3G46200	aTNUDT9	1.5809423	
247902_at	AT5G57350	AHA3; ATPase/ hydrogen-exporting ATPase	1.7663449	
Purine&pyrimidine				
257680_at	AT3G20330	aspartate carbamoyltransferase	1.6754414	
263239_at	AT2G16570	ATASE1	1.6666312	
265943_at	AT2G19570	CDA1 (CYTIDINE DEAMINASE 1)	1.6279646	
255529_at	AT4G02120	CTP synthase, putative	1.5005956	
255310_at	AT4G04955	ATALN (<i>Arabidopsis</i> allantoinase)	2.4221842	
263929_at	AT2G36310	URH1 (URIDINE-RIBOHYDROLASE 1)	1.6056547	
Glycolysis/Gluconeogenesis				
250868_at	AT5G03860	MLS (MALATE SYNTHASE); malate synthase	2.652906	
248138_at	AT5G54960	PDC2 (pyruvate decarboxylase-2)	1.5255806	
252300_at	AT3G49160	pyruvate kinase family protein	2.3063116	
262309_at	AT1G70820	phosphoglucomutase, putative	6.04787	
247278_at	AT5G64380	fructose-1,6-bisphosphatase family protein	1.5337827	
260837_at	AT1G43670	fructose-1,6-bisphosphatase, putative	2.143109	

Probe Set ID	AGI	Short/Full name	Fold change	RT-qPCR
251885_at	AT3G54050	fructose-1,6-bisphosphatase, putative	1.6180179	
253971_at	AT4G26530	fructose-bisphosphate aldolase, putative	4.485955	
253966_at	AT4G26520	fructose-bisphosphate aldolase, cytoplasmic	1.984834	
247534_at	AT5G61580	PFK4 (PHOSPHOFRUCTOKINASE 4)	1.5317184	
249694_at	AT5G35790	G6PD1	1.9046711	
257144_at	AT3G27300	G6PD5 (glucose-6-phosphate dehydrogenase 5)	1.5540537	
263954_at	AT2G35840	sucrose-phosphatase 1 (SPP1)	1.6511269	
255016_at	AT4G10120	ATSPS4F; sucrose-phosphate synthase	5.9214377	
256745_at	AT3G29360	UDP-glucose 6-dehydrogenase, putative	1.5009668	
249469_at	AT5G39320	UDP-glucose 6-dehydrogenase, putative	2.0031774	
252387_at	AT3G47800	aldose 1-epimerase family protein	2.0090683	
Carbohydrate transport				
258869_at	AT3G03090	AtVGT1	1.7495905	
247529_at	AT5G61520	hexose transporter, putative	1.5755159	
257805_at	AT3G18830	ATPLT5 (POLYOL TRANSPORTER 5)	1.7274072	
264400_at	AT1G61800	GPT2; antiporter	7.832648	
246831_at	AT5G26340	MSS1;STP13	1.8323759	
260143_at	AT1G71880	SUC1 (Sucrose-proton symporter 1)	2.2869253	
260170_at	AT1G71890	SUC5	2.0198724	
246783_at	AT5G27360	SFP2	1.7462044	
Carbohydrate metabolism				
246829_at	AT5G26570	ATGWD3; carbohydrate kinase	1.9452636	
254153_at	AT4G24450	PWD (PHOSPHOGLUCAN, WATER DIKINASE)	1.6267337	
245094_at	AT2G40840	DPE2 (DISPROPORTIONATING ENZYME 2)	2.207608	
247094_at	AT5G66280	GMD1	1.6792704	
266542_at	AT2G35100	ARAD1 (ARABINAN DEFICIENT 1);	1.622582	
248976_at	AT5G44930	ARAD2 (ARABINAN DEFICIENT 2); catalytic	1.9975545	
258507_at	AT3G06500	beta-fructofuranosidase, putative	1.8309476	
265118_at	AT1G62660	beta-fructosidase (BFRUCT3)	1.7112507	
256150_at	AT1G55120	ATFRUCT5	1.6028806	
266157_at	AT2G28100	ATFUC1 (alpha-L-fucosidase 1)	1.5503463	
260412_at	AT1G69830	AMY3 (ALPHA-AMYLASE-LIKE 3)	2.549348	
250007_at	AT5G18670	BMY3; beta-amylase/ catalytic/ cation binding	2.3159528	
264360_at	AT1G03310	isoamylase, putative	2.199659	
246036_at	AT5G08370	AtAGAL2	1.6113108	
245970_at	AT5G20710	BGAL7 (beta-galactosidase 7)	2.3285499	
251996_at	AT3G52840	BGAL2 (beta-galactosidase 2)	1.8747517	
247954_at	AT5G56870	BGAL4 (beta-galactosidase 4)	2.6326864	
264978_at	AT1G27120	galactosyltransferase family protein	1.680923	
252179_at	AT3G50760	GATL2 (Galacturonosyltransferase-like 2)	1.715082	
255506_at	AT4G02130	GATL6	1.64277	
251308_at	AT3G61130	GAUT1	1.6645654	
248721_at	AT5G47780	GAUT4 (Galacturonosyltransferase 4)	1.6035274	
251625_at	AT3G57260	BGL2 (BETA-1,3-GLUCANASE 2)	1.5211234	
262118_at	AT1G02850	BGLU11 (BETA GLUCOSIDASE 11)	2.7080963	
259640_at	AT1G52400	BGLU18 (BETA GLUCOSIDASE 18)	1.8079282	
259173_at	AT3G03640	BGLU25 (BETA GLUCOSIDASE 25)	2.1093333	
267645_at	AT2G32860	BGLU33 (BETA GLUCOSIDASE 33)	2.7025967	
264280_at	AT1G61820	BGLU46 (BETA GLUCOSIDASE 46)	2.9840348	
251230_at	AT3G62750	BGLU8 (BETA GLUCOSIDASE 8)	2.3539953	
253835_at	AT4G27820	BGLU9 (BETA GLUCOSIDASE 9)	1.6861207	
255517_at	AT4G02290	AtGH9B13	1.8932191	
267595_at	AT2G32990	AtGH9B8	1.5996066	

Probe Set ID	AGI	Short/Full name	Fold change	RT-qPCR
260727_at	AT1G48100	glycoside hydrolase family 28 protein	1.8607668	
258252_at	AT3G15720	glycoside hydrolase family 28 protein	2.7296567	
260024_at	AT1G30080	glycosyl hydrolase family 17 protein	1.7346468	
254536_at	AT4G19720	glycosyl hydrolase family 18 protein	1.626181	
254544_at	AT4G19820	glycosyl hydrolase family 18 protein	1.9479955	
254543_at	AT4G19810	glycosyl hydrolase family 18 protein	4.4973717	
262181_at	AT1G78060	glycosyl hydrolase family 3 protein	1.554483	
246184_at	AT5G20950	glycosyl hydrolase family 3 protein	2.085196	
254575_at	AT4G19460	glycosyl transferase family 1 protein	1.8447405	
248209_at	AT5G53990	glycosyltransferase family protein	1.5361376	
260758_at	AT1G48930	AtGH9C1	2.6073966	
249092_at	AT5G43710	glycoside hydrolase family 47 protein	1.5484738	
257651_at	AT3G16850	glycoside hydrolase family 28 protein	1.603693	
258528_at	AT3G06770	glycoside hydrolase family 28 protein	1.6771386	
245039_at	AT2G26600	glycosyl hydrolase family 17 protein	1.6142402	
264291_at	AT1G78800	glycosyl transferase family 1 protein	1.8463682	
258917_at	AT3G10630	glycosyl transferase family 1 protein	2.1696525	
265366_at	AT2G13290	glycosyl transferase family 17 protein	1.8340052	
248622_at	AT5G49360	BXL1 (BETA-XYLOSIDASE 1)	1.6894671	
257031_at	AT3G19280	FUT11 (FUCOSYLTRANSFERASE 11)	1.5223789	
263847_at	AT2G36970	UDP-glucuronosyl/UDP-glucosyl transferase	1.7329249	
245543_at	AT4G15260	UDP-glucuronosyl/UDP-glucosyl transferase	1.8843406	
256252_at	AT3G11340	UDP-glucuronosyl/UDP-glucosyl transferase	1.9577701	
248563_at	AT5G49690	UDP-glucuronosyl/UDP-glucosyl transferase	1.9946315	
257954_at	AT3G21760	UDP-glucuronosyl/UDP-glucosyl transferase	2.0197349	
267300_at	AT2G30140	UDP-glucuronosyl/UDP-glucosyl transferase	2.2144022	
266532_at	AT2G16890	UDP-glucuronosyl/UDP-glucosyl transferase	2.3206918	
261046_at	AT1G01390	UDP-glucuronosyl/UDP-glucosyl transferase	3.0298839	
263231_at	AT1G05680	UDP-glucuronosyl/UDP-glucosyl transferase	5.0169525	
245624_at	AT4G14090	UDP-glucuronosyl/UDP-glucosyl transferase	1.6590099	
260955_at	AT1G06000	UDP-glucuronosyl/UDP-glucosyl transferase	2.204128	
250751_at	AT5G05890	UDP-glucuronosyl/UDP-glucosyl transferase	1.7943444	
257949_at	AT3G21750	UGT71B1	2.4135714	
257950_at	AT3G21780	UGT71B6	1.552376	
266669_at	AT2G29750	UGT71C1	1.7044555	
256053_at	AT1G07260	UGT71C3	1.5891291	
252183_at	AT3G50740	UGT72E1	1.5287923	
264873_at	AT1G24100	UGT74B1	1.5307554	
263184_at	AT1G05560	UGT75B1	2.6724622	
250753_at	AT5G05860	UGT76C2	2.0751503	
252487_at	AT3G46660	UGT76E12	1.5816128	
247731_at	AT5G59590	UGT76E2	1.5657152	
261804_at	AT1G30530	UGT78D1	2.0900228	
246468_at	AT5G17050	UGT78D2	2.0821283	
245352_at	AT4G15490	UGT84A3; UDP-glycosyltransferase	1.5146614	
Trehalose				
260059_at	AT1G78090	ATTPPB	2.1498985	
264339_at	AT1G70290	ATTPS8	1.7521074	
252858_at	AT4G39770	trehalose-6-phosphate phosphatase, putative	1.7632717	
Fatty acid synthesis, catabolism and transport				
260869_at	AT1G43800	acyl-(acyl-carrier-protein) desaturase, putative	4.5019956	
258312_at	AT3G16170	acyl-activating enzyme 13 (AAE13)	1.6488922	
266865_at	AT2G29980	FAD3 (FATTY ACID DESATURASE 3)	1.7060461	

Probe Set ID	AGI	Short/Full name	Fold change	RT-qPCR
245612_at	AT4G14440	HCD1	1.9412233	
253285_at	AT4G34250	KCS16 (3-KETOACYL-COA SYNTHASE 16)	1.71248	
259737_at	AT1G64400	long-chain-fatty-acid--CoA ligase, putative	1.6898856	
260531_at	AT2G47240	long-chain-fatty-acid--CoA ligase family protein	2.0547917	
267606_at	AT2G26640	KCS11 (3-KETOACYL-COA SYNTHASE 11)	1.8931756	
245621_at	AT4G14070	AAE15 (acyl-activating enzyme 15)	1.5558914	
264442_at	AT1G27480	lecithin	2.0542965	
264613_at	AT1G04640	LIP2 (LIPOYLTRANSFERASE 2)	1.649436	
248625_at	AT5G48880	PKT2	2.8749459	
267496_at	AT2G30550	lipase class 3 family protein	1.6232135	
258374_at	AT3G14360	lipase class 3 family protein	1.8058681	
249999_at	AT5G18640	lipase class 3 family protein	1.5248324	
249777_at	AT5G24210	lipase class 3 family protein	1.7760361	
250008_at	AT5G18630	lipase class 3 family protein	2.195962	
260393_at	AT1G73920	lipase family protein	1.766429	
266816_at	AT2G44970	lipase-related	3.9567423	
258589_at	AT3G04290	LTL1 (LI-TOLERANT LIPASE 1)	1.8136711	
253344_at	AT4G33550	lipid binding	2.9099202	
251065_at	AT5G01870	lipid transfer protein, putative	5.909604	
267382_at	AT2G44300	lipid transfer protein-related	2.6288798	
253553_at	AT4G31050	lipoyltransferase (LIP2p)	1.5903158	
266415_at	AT2G38530	LTP2 (LIPID TRANSFER PROTEIN 2)	3.9623423	
247717_at	AT5G59320	LTP3 (LIPID TRANSFER PROTEIN 3)	21.705334	
247718_at	AT5G59310	LTP4 (LIPID TRANSFER PROTEIN 4)	1.8322208	
258675_at	AT3G08770	LTP6; lipid binding	2.612193	
266168_at	AT2G38870	protease inhibitor, putative	4.2506547	
265334_at	AT2G18370	protease inhibitor/seed storage	2.0629373	
256937_at	AT3G22620	protease inhibitor/seed storage	1.7680497	
254314_at	AT4G22470	protease inhibitor/seed storage	1.9724306	
265656_at	AT2G13820	protease inhibitor/seed storage	1.8205943	
254819_at	AT4G12500	protease inhibitor/seed storage	2.628665	
266098_at	AT2G37870	protease inhibitor/seed storage	3.3837452	
257066_at	AT3G18280	protease inhibitor/seed storage	7.4893746	
254818_at	AT4G12470	protease inhibitor/seed storage	2.7255445	
254832_at	AT4G12490	protease inhibitor/seed storage	5.130086	
265111_at	AT1G62510	protease inhibitor/seed storage	9.515188	
Cell wall				
265870_at	AT2G01660	PDLP6	1.5154395	
260666_at	AT1G19300	PARVUS (PARVUS)	1.5303742	
256825_at	AT3G22120	CWLP	2.2254286	
266070_at	AT2G18660	EXLB3 (EXPANSIN-LIKE B3 PRECURSOR)	1.8645772	
258003_at	AT3G29030	EXPA5 (EXPANSIN A5)	2.082306	
263183_at	AT1G05570	CALS1 (CALLOSE SYNTHASE 1)	1.7404894	
264146_at	AT1G02205	CER1 (ECERIFERUM 1)	1.8760643	
253309_at	AT4G33790	CER4 (ECERIFERUM 4)	1.6279298	
245228_at	AT3G29810	COBL2	1.6580914	
245463_at	AT4G17030	ATEXLB1	2.7514064	
261266_at	AT1G26770	ATEXPA10	3.696503	
261226_at	AT1G20190	ATEXPA11	3.385156	
258877_at	AT3G03220	ATEXPA13	1.6513553	
255591_at	AT4G01630	ATEXPA17	1.9336042	
253008_at	AT4G38210	ATEXPA20	2.0299609	
267590_at	AT2G39700	ATEXPA4	2.6575708	

Probe Set ID	AGI	Short/Full name	Fold change	RT-qPCR
250992_at	AT5G02260	ATEXPA9	1.5455763	
253815_at	AT4G28250	ATEXPB3	2.0838115	
259525_at	AT1G12560	ATEXPA7	1.8323361	
261099_at	AT1G62980	ATEXPA18	1.9021115	
264960_at	AT1G76930	ATEXT4 (EXTENSIN 4)	3.1801293	
245172_at	AT2G47540	pollen Ole e 1 allergen and extensin	1.9031395	
250778_at	AT5G05500	pollen Ole e 1 allergen and extensin	2.5833094	
255516_at	AT4G02270	pollen Ole e 1 allergen and extensin	4.169347	
255080_at	AT4G09030	AGP10 (ARABINO GALACTAN PROTEIN 10)	3.1623778	
253050_at	AT4G37450	AGP18 (ARABINO GALACTAN PROTEIN 18)	1.9972172	
250002_at	AT5G18690	AGP25 (ARABINO GALACTAN PROTEINS 25)	2.69579	
259550_at	AT1G35230	AGP5 (ARABINO GALACTAN-PROTEIN 5)	1.5789971	
253957_at	AT4G26320	AGP13 (arabinogalactan protein 13)	2.258545	
247965_at	AT5G56540	AGP14 (ARABINO GALACTAN PROTEIN 14)	2.5982463	
248252_at	AT5G53250	AGP22 (ARABINO GALACTAN PROTEIN 22)	3.2308464	
252833_at	AT4G40090	AGP3 (arabinogalactan-protein 3)	2.3126295	
267457_at	AT2G33790	AGP30 (ARABINO GALACTAN PROTEIN30)	3.435346	
246494_at	AT5G16190	ATCSLA11; cellulose synthase	1.6844583	
265175_at	AT1G23480	ATCSLA03	1.6370784	
265824_at	AT2G35650	ATCSLA07	2.3389857	
251771_at	AT3G56000	ATCSLA14	1.8989464	
248074_at	AT5G55730	FLA1	1.5616577	
251395_at	AT2G45470	FLA8	1.5586822	
249037_at	AT5G44130	FLA13	3.4579248	
263376_at	AT2G20520	FLA6	2.263993	
246004_at	AT5G20630	GER3 (GERMIN 3); oxalate oxidase	1.9572812	
258938_at	AT3G10080	germin-like protein, putative	1.9408653	
259478_at	AT1G18980	germin-like protein, putative	2.8674588	
249476_at	AT5G38910	germin-like protein, putative	8.380431	
259481_at	AT1G18970	GLP4 (GERMIN-LIKE PROTEIN 4)	5.06411	
245567_at	AT4G14630	GLP9 (GERMIN-LIKE PROTEIN 9)	3.448522	
254667_at	AT4G18280	glycine-rich cell wall protein-related	1.6245792	
248862_at	AT5G46730	glycine-rich protein	1.6213721	
261175_at	AT1G04800	glycine-rich protein	1.7162492	
247541_at	AT5G61660	glycine-rich protein	1.7663068	
253754_at	AT4G29020	glycine-rich protein	2.0318565	
265511_at	AT2G05540	glycine-rich protein	2.1505394	
254372_at	AT4G21620	glycine-rich protein	2.2371469	
253629_at	AT4G30450	glycine-rich protein	2.5668898	
253619_at	AT4G30460	glycine-rich protein	3.0163438	
248817_at	AT5G47020	glycine-rich protein	1.642331	
260007_at	AT1G67870	glycine-rich protein	2.4513614	
267307_at	AT2G30210	LAC3 (laccase 3); laccase	2.476108	
245706_at	AT5G04310	pectate lyase family protein	1.528304	
248681_at	AT5G48900	pectate lyase family protein	1.5509996	
245196_at	AT1G67750	pectate lyase family protein	2.0206754	
258719_at	AT3G09540	pectate lyase family protein	1.8806776	
248968_at	AT5G45280	pectinacetyl esterase, putative	1.6098166	
258888_at	AT3G05620	pectinesterase family protein	1.5248581	
250490_at	AT5G09760	pectinesterase family protein	1.5270602	
245965_at	AT5G19730	pectinesterase family protein	1.6973633	
245052_at	AT2G26440	pectinesterase family protein	1.7286155	
252740_at	AT3G43270	pectinesterase family protein	1.7565587	

Probe Set ID	AGI	Short/Full name	Fold change	RT-qPCR
250801_at	AT5G04960	pectinesterase family protein	4.809166	
254573_at	AT4G19420	pectinacylesterase family protein	1.5066277	
249807_at	AT5G23870	pectinacylesterase family protein	1.8397686	
255524_at	AT4G02330	ATPMEPCRB; pectinesterase	7.306496	
265246_at	AT2G43050	ATPMEPCRD; enzyme inhibitor/ pectinesterase	2.6203375	
245151_at	AT2G47550	pectinesterase family protein	1.6860898	
258765_at	AT3G10710	pectinesterase family protein	1.7154429	
261834_at	AT1G10640	polygalacturonase	2.8944	
262060_at	AT1G80170	polygalacturonase, putative / pectinase, putative	1.6547911	
264007_at	AT2G21140	ATPRP2 (PROLINE-RICH PROTEIN 2)	1.5851905	
252971_at	AT4G38770	PRP4 (PROLINE-RICH PROTEIN 4)	1.7655076	
256352_at	AT1G54970	ATPRP1 (PROLINE-RICH PROTEIN 1)	2.3563738	
251226_at	AT3G62680	PRP3 (PROLINE-RICH PROTEIN 3)	3.558396	
251843_x_at	AT3G54590	ATHRGP1	1.5639538	
245874_at	AT1G26250	proline-rich extensin, putative	3.6301239	
246652_at	AT5G35190	proline-rich extensin-like family protein	4.0810804	
254559_at	AT4G19200	proline-rich family protein	1.6451728	
245479_at	AT4G16140	proline-rich family protein	2.0561793	
265411_at	AT2G16630	proline-rich family protein	2.5081246	
260335_at	AT1G74000	SS3 (STRICTOSIDINE SYNTHASE 3)	1.7864653	
246682_at	AT5G33290	XGD1	1.8007371	
264157_at	AT1G65310	XTH17	1.8919324	
253608_at	AT4G30290	XTH19	4.8782287	
254042_at	AT4G25810	XTR6	2.1154673	
254044_at	AT4G25820	XTR9	5.1012073	
253763_at	AT4G28850	xyloglucan:xyloglucosyl transferase, putative	1.7921051	
247914_at	AT5G57540	xyloglucan:xyloglucosyl transferase, putative	2.228443	
247871_at	AT5G57530	xyloglucan:xyloglucosyl transferase, putative	3.308098	
Phloem proteins				
264213_at	AT1G65390	AtPP2-A5	1.8578196	
264153_at	AT1G65390	AtPP2-A5	1.8660928	
248978_at	AT5G45070	AtPP2-A8 (Phloem protein 2-A8)	1.5868131	
266235_at	AT2G02360	AtPP2-B10 (Phloem protein 2-B10)	2.2230031	
251356_at	AT3G61060	AtPP2-A13	1.7588658	
248395_at	AT5G52120	AtPP2-A14 (Phloem protein 2-A14)	1.6768422	
Amino acid metabolism & transport				
257516_at	AT1G69040	ACR4 (ACT REPEAT 4); amino acid binding	1.7266415	
264040_at	AT2G03730	ACR5; amino acid binding	1.7896264	
254300_at	AT4G22780	ACR7; amino acid binding	1.6382418	
266984_at	AT2G39570	ACT domain-containing protein	1.65027	
247218_at	AT5G65010	ASN2 (ASPARAGINE SYNTHETASE 2)	1.6831523	
263350_at	AT2G13360	AGT	1.6042578	
267035_at	AT2G38400	AGT3	2.1032617	
260309_at	AT1G70580	AOAT2	1.9173156	
264250_at	AT1G78680	ATGGH2	2.233933	
266892_at	AT2G26080	AtGLDP2	1.9592899	
265070_at	AT1G55510	BCDH BETA1	1.5983752	
258527_at	AT3G06850	BCE2	1.6640345	
253708_at	AT4G29210	GGT4	1.719259	
252570_at	AT3G45300	IVD (ISOVALERYL-COA-DEHYDROGENASE)	1.5179881	
258025_at	AT3G19480	D-3-phosphoglycerate dehydrogenase, putative	1.8886664	
265305_at	AT2G20340	tyrosine decarboxylase, putative	2.0137992	
253162_at	AT4G35630	PSAT	1.8531084	

Probe Set ID	AGI	Short/Full name	Fold change	RT-qPCR
259403_at	AT1G17745	PGDH	2.682692	
258075_at	AT3G25900	HMT-1; homocysteine S-methyltransferase	2.087862	
258160_at	AT3G17820	ATGSKB6; copper ion binding	1.5132966	
245035_at	AT2G26400	ATARD3	1.6447458	
252652_at	AT3G44720	ADT4 (arogenate dehydratase 4)	2.4678078	
261758_at	AT1G08250	ADT6 (arogenate dehydratase 6)	1.8287091	
261957_at	AT1G64660	ATMGL	4.713349	
260602_at	AT1G55920	ATSERAT2;1	1.5737426	
256022_at	AT1G58360	AAP1; NAT2 (AMINO ACID PERMEASE 1)	1.5458914	
245891_at	AT5G09220	AAP2 (AMINO ACID PERMEASE 2)	2.3070471	
246389_at	AT1G77380	AAP3; amino acid transmembrane transporter	2.1610112	
248619_at	AT5G49630	AAP6 (AMINO ACID PERMEASE 6)	1.5312438	
250161_at	AT5G15240	amino acid transporter family protein	1.5630741	
263827_at	AT2G40420	amino acid transporter family protein	1.9778428	
251024_at	AT5G02180	amino acid transporter family protein	5.069423	
Ammonium & nitrate/nitrite				
267142_at	AT2G38290	ATAMT2 (AMMONIUM TRANSPORTER 2)	2.1001482	
248551_at	AT5G50200	WR3 NTR3.1 (WOUND-RESPONSIVE 3)	1.7959006	
248790_at	AT5G47450	AtTIP2;3; ammonia transporter	2.1810217	
Sulfate				
255284_at	AT4G04610	APR1 (APS REDUCTASE 1)	3.012217	
254343_at	AT4G21990	APR3 (APS REDUCTASE 3)	2.4403985	
264901_at	AT1G23090	AST91 (SULFATE TRANSPORTER 91)	3.6730144	
255443_at	AT4G02700	SULTR3;2 (sulfate transporter 3;2)	3.0011868	
249752_at	AT5G24660	LSU2 (RESPONSE TO LOW SULFUR 2)	1.9379992	
252870_at	AT4G39940	AKN2 (APS-kinase 2)	2.0129018	
250475_at	AT5G10180	AST68; sulfate transmembrane transporter	1.9763738	
250897_at	AT5G03430	PAPS reductase family protein	1.8019344	
Phosphate				
263083_at	AT2G27190	PAP12 (PURPLE ACID PHOSPHATASE 12)	1.6239426	
248499_at	AT5G50400	PAP27 (PURPLE ACID PHOSPHATASE 27)	1.585133	
263594_at	AT2G01880	PAP7 (PURPLE ACID PHOSPHATASE 7)	2.0512636	
245698_at	AT5G04160	phosphate translocator-related	1.5208881	
253784_at	AT4G28610	PHR1	1.997733	
266672_at	AT2G29650	PHT4;1	2.2975836	
246122_at	AT5G20380	PHT4;5	1.6487892	
Iron				
245296_at	AT4G16370	ATOPT3 (OLIGOPEPTIDE TRANSPORTER)	1.5929965	
264751_at	AT1G23020	FRO3; ferric-chelate reductase	1.850476	
266162_at	AT2G28160	FRU, FIT1	1.76477	
254534_at	AT4G19680	IRT2; iron ion transmembrane transporter	2.5508492	
267029_at	AT2G38460	ATIREG1 (IRON-REGULATED PROTEIN 1)	1.7938256	
246847_at	AT5G26820	ATIREG3 (IRON-REGULATED PROTEIN 3)	1.5174626	
Potassium				
254305_at	AT4G22200	AKT2/3	1.8818417	
248888_at	AT5G46240	KAT1	2.0739248	
261536_at	AT1G01790	KEA1 (K EFFLUX ANTIporter 1)	2.001158	
255304_at	AT4G04850	KEA3; potassium ion transmembrane transporte	2.0618465	
263699_at	AT1G31120	KUP10	1.6845425	
Cu				
259008_at	AT3G09390	MT2A (METALLOTHIONEIN 2A)	2.5382004	
266353_at	AT2G01520	MLP328 (MLP-LIKE PROTEIN 328)	9.344566	
266330_at	AT2G01530	MLP329 (MLP-LIKE PROTEIN 329)	7.071243	

Probe Set ID	AGI	Short/Full name	Fold change	RT-qPCR
Zn				
257715_at	AT3G12750	ZIP1 (ZINC TRANSPORTER 1 PRECURSOR)	1.6495275	
GSTs/detoxification				
250083_at	AT5G17220	ATGSTF12	2.0011976	
267153_at	AT2G30860	ATGSTF9	2.3232887	
260406_at	AT1G69920	ATGSTU12	1.9119706	
264986_at	AT1G27130	ATGSTU13	1.9338865	
260745_at	AT1G78370	ATGSTU20	5.3771143	
262518_at	AT1G17170	ATGSTU24	2.110414	
262517_at	AT1G17180	ATGSTU25	2.422926	
252712_at	AT3G43800	ATGSTU27	1.7964178	
266267_at	AT2G29460	ATGSTU4	3.067291	
266299_at	AT2G29450	ATGSTU5	1.7587159	
266271_at	AT2G29440	ATGSTU6	2.2326825	
266296_at	AT2G29420	ATGSTU7	1.6450101	
247435_at	AT5G62480	ATGSTU9	2.4393306	
267154_at	AT2G30870	GSTF10	1.5733571	
262103_at	AT1G02940	GSTF5	2.4103403	
262516_at	AT1G17190	ATGSTU26	2.501632	
Cytochromes				
267565_at	AT2G30750	CYP71A12	7.1970477	
257623_at	AT3G26210	CYP71B23	1.7270265	
266000_at	AT2G24180	CYP71B6	1.5779507	
246620_at	AT5G36220	CYP81D1	1.6036701	
253046_at	AT4G37370	CYP81D8	6.188541	
253505_at	AT4G31970	CYP82C2	7.0742583	
252911_at	AT4G39510	CYP96A12	1.8052423	
263276_at	AT2G14100	CYP705A13	1.6298617	
261878_at	AT1G50560	CYP705A25	2.0263157	
248727_at	AT5G47990	CYP705A5	2.3638315	
266307_at	AT2G27000	CYP705A8	1.8074805	
253886_at	AT4G27710	CYP709B3	2.6583161	
263970_at	AT2G42850	CYP718	1.6765847	
257628_at	AT3G26290	CYP71B26	2.5393703	
262780_at	AT1G13090	CYP71B28	1.6996449	
256874_at	AT3G26320	CYP71B36	1.8959353	
256875_at	AT3G26330	CYP71B37	1.9189515	
257635_at	AT3G26280	CYP71B4	5.5374107	
267505_at	AT2G45560	CYP76C1	2.2589526	
256589_at	AT3G28740	CYP81D1	2.1603959	
253073_at	AT4G37410	CYP81F4	6.8489904	
255934_at	AT1G12740	CYP87A2	3.4416482	
251699_at	AT3G56630	CYP94D2	1.8480259	
Other membrane transporters				
246580_at	AT1G31770	ABC transporter family protein	1.9730309	
267008_at	AT2G39350	ABC transporter family protein	2.566301	
256969_at	AT3G21080	ABC transporter-related	2.3224075	
261969_at	AT1G65950	ABC1 family protein	1.6135421	
254133_at	AT4G24810	ABC1 family protein	2.9282484	
250824_at	AT5G05200	ABC1 family protein	1.7346252	
257184_at	AT3G13090	ATMRP8; ATPase	1.9254594	
254389_s_at	AT4G21910	MATE efflux family protein	1.7442601	
259743_at	AT1G71140	MATE efflux family protein	2.5371232	

Probe Set ID	AGI	Short/Full name	Fold change	RT-qPCR
263402_at	AT2G04050	MATE efflux family protein	13.148077	
253732_at	AT4G29140	MATE efflux protein-related	1.7562089	
262813_at	AT1G11670	MATE efflux family protein	1.7307651	
261881_at	AT1G80760	NIP6;1	1.9310266	
254606_at	AT4G19030	NLM1	3.2738025	
263904_at	AT2G36380	PDR6; ATPase	2.3716664	
251942_at	AT3G53480	PDR9 (PLEIOTROPIC DRUG RESISTANCE 9)	1.5522633	
263403_at	AT2G04040	TX1; antiporter/ multidrug efflux pump	5.8295665	
254396_at	AT4G21680	proton-dependent oligopeptide transport (POT)	1.7033848	
260410_at	AT1G69870	proton-dependent oligopeptide transport (POT)	2.2329843	
252537_at	AT3G45710	proton-dependent oligopeptide transport (POT)	1.9248589	
261937_at	AT1G22570	proton-dependent oligopeptide transport (POT)	1.6759167	
252536_at	AT3G45700	proton-dependent oligopeptide transport (POT)	1.7202774	
261924_at	AT1G22550	proton-dependent oligopeptide transport (POT)	1.8761805	
248931_at	AT5G46040	proton-dependent oligopeptide transport (POT)	1.5114332	
255877_at	AT2G40460	proton-dependent oligopeptide transport (POT)	1.5583557	
259846_at	AT1G72140	proton-dependent oligopeptide transport (POT)	2.0643044	
Vitamines				
B1				
248128_at	AT5G54770	THI1; protein homodimerization	1.6002518	
B5				
250842_at	AT5G04490	VTE5 (vitamin E pathway gene5)	1.7911696	
B6				
258336_at	AT3G16050	A37; atpdx1.2 protein heterodimerization	1.5637795	
B9/folate				
259880_at	AT1G76730	5-formyltetrahydrofolate cyclo-ligase	1.5889016	
251759_at	AT3G55630	ATDFD	2.138747	
Other unidentified functions				
264826_at	AT1G03410	2A6; oxidoreductase	1.697283	
249125_at	AT5G43450	2-oxoglutarate-dependent dioxygenase, putative	1.707935	
263668_at	AT1G04350	2-oxoglutarate-dependent dioxygenase, putative	1.9663066	
249128_at	AT5G43440	2-oxoglutarate-dependent dioxygenase, putative	2.2829196	
264843_at	AT1G03400	2-oxoglutarate-dependent dioxygenase, putative	2.3380733	
262608_at	AT1G14120	2-oxoglutarate-dependent dioxygenase, putative	2.6849072	
257587_at	AT1G56310	3'-5' exonuclease domain-containing protein	1.6546757	
247235_at	AT5G64580	AAA-type ATPase family protein	1.5090423	
256885_at	AT3G15120	AAA-type ATPase family protein	1.7330844	
250062_at	AT5G17760	AAA-type ATPase family protein	2.1659844	
263061_at	AT2G18190	AAA-type ATPase family protein	2.618111	
259507_at	AT1G43910	AAA-type ATPase family protein	8.189039	
255607_at	AT4G01130	acetylsterase, putative	1.7913544	
266403_at	AT2G38600	acid phosphatase class B family protein	1.5889264	
266395_at	AT2G43100	aconitase C-terminal domain-containing protein	2.9457977	
248394_at	AT5G52070	agenet domain-containing protein	2.2283592	
265902_at	AT2G25590	agenet domain-containing protein	2.4366229	
261930_at	AT1G22440	alcohol dehydrogenase, putative	2.6552603	
249242_at	AT5G42250	alcohol dehydrogenase, putative	3.4687004	
254572_at	AT4G19380	alcohol oxidase-related	1.7418289	
267181_at	AT2G37760	aldo/keto reductase family protein	1.6703626	
248242_at	AT5G53580	aldo/keto reductase family protein	1.5080645	
267168_at	AT2G37770	aldo/keto reductase family protein	2.6112473	
254025_at	AT4G25790	allergen V5/Tpx-1-related family protein	1.6914619	
264637_at	AT1G65560	allyl alcohol dehydrogenase, putative	2.3500545	

Probe Set ID	AGI	Short/Full name	Fold change	RT-qPCR
258692_at	AT3G08640	alphavirus core protein family	1.6909297	
258708_at	AT3G09580	amine oxidase family protein	1.5603275	
246786_at	AT5G27410	aminotransferase class IV family protein	2.3825724	
262698_at	AT1G75960	AMP-binding protein, putative	1.6665413	
263800_at	AT2G24600	ankyrin repeat family protein	2.1288462	
263401_at	AT2G04070	antiporter/ drug transporter/ transporter	2.2194757	
254011_at	AT4G26370	antitermination NusB domain-containing protein	2.070251	
264865_at	AT1G24120	ARL1 (ARG1-LIKE 1)	1.5243405	
250183_at	AT5G14510	armadillo/beta-catenin repeat family protein	1.5762875	
251919_at	AT3G53800	armadillo/beta-catenin repeat family protein	2.0672476	
266815_at	AT2G44900	F-box family protein	1.6214632	
262413_at	AT1G34780	ATAPRL4 (APR-like 4)	1.6149877	
266056_at	AT2G40810	AtATG18c	1.5011361	
252316_at	AT3G48700	ATCXE13	3.2641869	
261607_at	AT1G49660	AtCXE5 (<i>Arabidopsis thaliana</i> carboxyesterase 5)	2.239359	
253531_at	AT4G31540	ATEXO70G1	1.6114188	
263318_at	AT2G24762	AtGDU4	3.7392206	
259982_at	AT1G76410	ATL8; protein binding / zinc ion binding	2.0063088	
267397_at	AT1G76170	ATP binding	1.536125	
261689_at	AT1G50140	ATP binding / ATPase/ nucleoside-triphosphatase	2.0070138	
263435_at	AT2G28600	ATP binding / ATP-dependent helicase/	1.628543	
260089_at	AT1G73170	ATP-dependent peptidase	2.063452	
245898_at	AT5G11020	ATP binding / kinase/ protein kinase	1.7218764	
246375_at	AT1G51830	kinase/ protein serine/threonine kinase	1.9952594	
262491_at	AT1G21650	ATP binding / protein binding	2.5439658	
246449_at	AT5G16810	ATP binding / protein kinase	1.7264867	
267152_at	AT2G31040	ATP synthase protein I -related	1.7423064	
265660_at	AT2G25470	AtRLP21 (Receptor Like Protein 21)	3.117673	
261469_at	AT1G28340	AtRLP4 (Receptor Like Protein 4)	1.9119524	
261117_at	AT1G75310	AUL1; heat shock protein binding	1.5842115	
258000_at	AT3G28940	avirulence-responsive protein, putative	1.795438	
255980_at	AT1G33970	avirulence-responsive protein, putative	2.2248392	
253545_at	AT4G31310	avirulence-responsive protein-related	1.8188723	
249958_at	AT5G18970	AWPM-19-like membrane family protein	1.5881103	
248410_at	AT5G51570	band 7 family protein	1.5901918	
264899_at	AT1G23130	Bet v I allergen family protein	2.4588633	
263836_at	AT2G40330	Bet v I allergen family protein	1.5400413	
257908_at	AT3G25410	bile acid:sodium symporter family protein	1.9376678	
260082_at	AT1G78180	binding	1.758285	
262050_at	AT1G80130	binding	7.73804	
264609_at	AT1G04530	binding	1.5126605	
266617_at	AT2G29670	binding	1.580042	
261075_at	AT1G07280	binding	1.9651169	
253849_at	AT4G28080	binding	2.1706831	
248584_at	AT5G49960	binding / catalytic	1.5358564	
245793_at	AT1G32220	binding / catalytic/ coenzyme binding	1.5929406	
256655_at	AT3G18890	binding / catalytic/ coenzyme binding	1.674412	
248838_at	AT5G46800	BOU (A BOUT DE SOUFFLE); binding	1.5002275	
247114_at	AT5G65910	BSD domain-containing protein	1.6462499	
251563_at	AT3G57880	C2 domain-containing protein	1.552272	
248058_at	AT5G55530	C2 domain-containing protein	1.947283	
265394_at	AT2G20725	CAAX amino terminal protease family protein	1.985684	
264260_at	AT1G09210	calreticulin 2 (CRT2)	1.535019	

Probe Set ID	AGI	Short/Full name	Fold change	RT-qPCR
259658_at	AT1G55370	carbohydrate binding / catalytic	4.284847	
246396_at	AT1G58180	carbonic anhydrase	1.8043814	
246462_at	AT5G16940	carbon-sulfur lyase	2.549666	
258254_at	AT3G26780	catalytic	1.8266963	
262215_at	AT1G74790	catalytic	1.6430267	
261550_at	AT1G63450	catalytic	1.584108	
245292_at	AT4G15093	catalytic LigB subunit	1.6446886	
245533_at	AT4G15130	catalytic/ choline-phosphate cytidyltransferase	1.6558526	
251298_at	AT3G62040	catalytic/ hydrolase	1.5185996	
246868_at	AT5G26010	catalytic/ protein serine/threonine phosphatase	1.9128003	
259441_at	AT1G02300	cathepsin B-like cysteine protease, putative	2.286734	
260489_at	AT1G51610	cation efflux family protein	1.611809	
265102_at	AT1G30870	cationic peroxidase, putative	3.171014	
245600_at	AT4G14230	CBS domain-containing protein-related	2.480163	
261608_at	AT1G49650	cell death associated protein-related	1.6614068	
255939_at	AT1G12730	cell division cycle protein-related	1.7342563	
258494_at	AT3G02450	cell division protein ftsH, putative	2.0969067	
253425_at	AT4G32190	centromeric protein-related	2.5101156	
247742_at	AT5G58980	ceramidase family protein	1.9044195	
245876_at	AT1G26230	chaperonin, putative	1.8477997	
250446_at	AT5G10770	chloroplast nucleoid DNA-binding protein	1.7385312	
260244_at	AT1G74320	choline kinase, putative	1.6263523	
254998_at	AT4G09760	choline kinase, putative	2.2607226	
256411_at	AT1G66670	CLPP3; serine-type endopeptidase	1.5280855	
261259_at	AT1G26660	c-myc binding protein, putative	1.8102262	
245197_at	AT1G67800	copine-related	1.5191605	
262919_at	AT1G79380	copine-related	1.7354932	
252698_at	AT3G43670	copper amine oxidase, putative	1.7230642	
263438_at	AT2G28660	copper-binding family protein	2.1850762	
252296_at	AT3G48970	copper-binding family protein	4.0350776	
253880_at	AT4G27590	copper-binding protein-related	3.5556974	
247367_at	AT5G63290	coproporphyrinogen oxidase-related	1.6131994	
249983_at	AT5G18470	curculin-like (mannose-binding)	1.932379	
245323_at	AT4G16500	cysteine protease inhibitor family protein	2.0454054	
265672_at	AT2G31980	cysteine proteinase inhibitor-related	4.252468	
262397_at	AT1G49380	cytochrome c biogenesis protein family	1.8886644	
246840_at	AT5G26610	D111/G-patch domain-containing protein	1.6291854	
250064_at	AT5G17890	DAR4 (DA1-RELATED PROTEIN 4)	4.1392665	
256646_at	AT3G13590	DC1 domain-containing protein	1.6206086	
266688_at	AT2G19660	DC1 domain-containing protein	2.5089402	
254749_at	AT4G13130	DC1 domain-containing protein	1.5044366	
252240_at	AT3G50010	DC1 domain-containing protein	1.528202	
256774_at	AT3G13760	DC1 domain-containing protein	1.5286545	
267384_at	AT2G44370	DC1 domain-containing protein	1.637269	
249097_at	AT5G43520	DC1 domain-containing protein	2.0458655	
249364_at	AT5G40590	DC1 domain-containing protein	2.283682	
264616_at	AT2G17740	DC1 domain-containing protein	2.752927	
258554_at	AT3G06980	DEAD/DEAH box helicase, putative	1.7550753	
266920_at	AT2G45750	dehydration-responsive family protein	1.6308354	
266439_s_at	AT2G43200	dehydration-responsive family protein	1.7179196	
251713_at	AT3G56080	dehydration-responsive protein-related	2.259453	
247780_at	AT5G58770	dehydrodolichyl diphosphate synthase, putative	2.0186942	
258108_at	AT3G23570	dienelactone hydrolase family protein	2.6046112	

Probe Set ID	AGI	Short/Full name	Fold change	RT-qPCR
258782_at	AT3G11750	dihydroneopterin aldolase, putative	2.2450833	
245122_at	AT2G47420	dimethyladenosine transferase, putative	1.997435	
258622_at	AT3G02720	DJ-1 family protein / protease-related	2.1540198	
261383_at	AT1G05380	DNA binding	1.5680636	
257373_at	AT2G43140	DNA binding / transcription factor	1.7488604	
267089_at	AT2G38300	DNA binding / transcription factor	2.1650832	
251365_at	AT3G61310	DNA-binding family protein	1.5192395	
263963_at	AT2G36080	DNA-binding protein, putative	1.8686289	
249677_at	AT5G35970	DNA-binding protein, putative	1.9056187	
245382_at	AT4G17800	DNA-binding protein-related	1.6101971	
248564_at	AT5G49700	DNA-binding protein-related	1.906567	
254492_at	AT4G20260	DREPP	1.8598949	
249481_at	AT5G38900	DSBA oxidoreductase family protein	2.9053075	
258460_at	AT3G17330	ECT6	1.5817245	
266471_at	AT2G31060	elongation factor family protein	1.5306209	
251360_at	AT3G61210	embryo-abundant protein-related	1.9587549	
254318_at	AT4G22530	embryo-abundant protein-related	2.052431	
266368_at	AT2G41380	embryo-abundant protein-related	1.7430819	
266011_at	AT2G37440	endonuclease/exonuclease/phosphatase	1.9019017	
252095_at	AT3G51000	epoxide hydrolase, putative	1.8181264	
252478_at	AT3G46540	clathrin assembly protein-related	2.1382337	
257104_at	AT3G25040	ER lumen protein retaining receptor, putative	1.5125822	
246041_at	AT5G19290	esterase/lipase/thioesterase family protein	1.5792025	
266977_at	AT2G39420	esterase/lipase/thioesterase family protein	1.7146975	
266485_at	AT2G47630	esterase/lipase/thioesterase family protein	1.7462125	
262561_at	AT1G34340	esterase/lipase/thioesterase family protein	2.2193213	
245885_at	AT5G09440	EXL4 (EXORDIUM LIKE 4)	1.8769915	
255526_at	AT4G02350	exocyst complex subunit Sec15-like	1.5144876	
256858_at	AT3G15140	exonuclease family protein	2.767486	
245961_at	AT5G19670	exostosin family protein	1.7724173	
246162_at	AT4G36400	FAD linked oxidase family protein	1.557801	
249045_at	AT5G44380	FAD-binding domain-containing protein	1.7813766	
254432_at	AT4G20830	FAD-binding domain-containing protein	2.9996667	
249051_at	AT5G44390	FAD-binding domain-containing protein	1.6177428	
264527_at	AT1G30760	FAD-binding domain-containing protein	1.9794489	
249046_at	AT5G44400	FAD-binding domain-containing protein	2.0715802	
249047_at	AT5G44410	FAD-binding domain-containing protein	2.2322073	
266711_at	AT2G46740	FAD-binding domain-containing protein	2.2646441	
263228_at	AT1G30700	FAD-binding domain-containing protein	2.316206	
261005_at	AT1G26420	FAD-binding domain-containing protein	2.9316661	
261006_at	AT1G26410	FAD-binding domain-containing protein	4.5728617	
261021_at	AT1G26380	FAD-binding domain-containing protein	5.1133084	
261020_at	AT1G26390	FAD-binding domain-containing protein	7.406141	
267005_at	AT2G34460	flavin reductase-related	1.6524025	
248771_at	AT5G47790	forkhead-associated domain-containing protein	1.7288586	
259021_at	AT3G07540	formin homology 2 domain-containing protein	1.5233238	
245417_at	AT4G17360	formyltetrahydrofolate deformylase	2.068856	
245954_at	AT5G28530	FRS10 (FAR1-related sequence 10)	1.5495956	
262736_at	AT1G28570	GDSL-motif lipase, putative	1.6749247	
262749_at	AT1G28580	GDSL-motif lipase, putative	2.0619638	
252363_at	AT3G48460	GDSL-motif lipase/hydrolase family protein	1.5116636	
259308_at	AT3G05180	GDSL-motif lipase/hydrolase family protein	1.5186511	
248118_at	AT5G55050	GDSL-motif lipase/hydrolase family protein	1.5395868	

Probe Set ID	AGI	Short/Full name	Fold change	RT-qPCR
265261_at	AT2G42990	GDSL-motif lipase/hydrolase family protein	1.6653017	
250918_at	AT5G03610	GDSL-motif lipase/hydrolase family protein	1.7832047	
267121_at	AT2G23540	GDSL-motif lipase/hydrolase family protein	1.7960296	
251968_at	AT3G53100	GDSL-motif lipase/hydrolase family protein	1.8124875	
259786_at	AT1G29660	GDSL-motif lipase/hydrolase family protein	1.8520976	
261981_at	AT1G33811	GDSL-motif lipase/hydrolase family protein	1.963692	
253660_at	AT4G30140	GDSL-motif lipase/hydrolase family protein	7.4966903	
264551_at	AT1G09460	glucan endo-1,3-beta-glucosidase-related	1.6683868	
256746_at	AT3G29320	glucan phosphorylase, putative	1.7916292	
249729_at	AT5G24410	glucosamine	1.9019375	
251746_at	AT3G56060	glucose-methanol-choline (GMC) oxidoreductase	1.5432793	
249337_at	AT5G41080	glycerophosphoryl diester phosphodiesterase	2.770665	
258038_at	AT3G21260	glycolipid transfer protein-related	1.9155457	
255814_at	AT1G19900	glyoxal oxidase-related	3.178043	
251669_at	AT3G57180	GTP binding	1.7122525	
258545_at	AT3G07050	GTP-binding family protein	1.632295	
265330_at	AT2G18440	GUT15	2.6652622	
252366_at	AT3G48420	haloacid dehalogenase-like hydrolase	1.6154468	
251028_at	AT5G02230	haloacid dehalogenase-like hydrolase	1.6959851	
256440_at	AT3G10970	haloacid dehalogenase-like hydrolase	1.7318385	
266363_at	AT2G41250	haloacid dehalogenase-like hydrolase	1.7418654	
265680_at	AT2G32150	haloacid dehalogenase-like hydrolase	1.7935843	
254874_at	AT4G11570	haloacid dehalogenase-like hydrolase	2.1254437	
259633_at	AT1G56500	haloacid dehalogenase-like hydrolase	1.7464687	
257848_at	AT3G13030	hAT dimerisation domain-containing protein	1.5180459	
248752_at	AT5G47600	heat shock protein-related	1.9600347	
246095_at	AT5G19310	homeotic gene regulator, putative	1.583775	
260014_at	AT1G68010	HPR; glycerate dehydrogenase/ poly(U) binding	1.5117365	
265699_at	AT2G03550	hydrolase	1.8759567	
262229_at	AT1G68620	hydrolase	2.543345	
265341_at	AT2G18360	hydrolase, alpha/beta fold family protein	1.5037339	
261661_at	AT1G18360	hydrolase, alpha/beta fold family protein	1.5300606	
246199_at	AT4G36530	hydrolase, alpha/beta fold family protein	1.5767158	
262151_at	AT1G52510	hydrolase, alpha/beta fold family protein	1.6928821	
254783_at	AT4G12830	hydrolase, alpha/beta fold family protein	2.082774	
257533_at	AT3G10840	hydrolase, alpha/beta fold family protein	2.2293935	
253627_at	AT4G30650	hydrophobic protein, putative	2.5433044	
250500_at	AT5G09530	hydroxyproline-rich glycoprotein family protein	1.5303197	
254262_at	AT4G23470	hydroxyproline-rich glycoprotein family protein	1.5904908	
245889_at	AT5G09480	hydroxyproline-rich glycoprotein family protein	1.6455847	
248592_at	AT5G49280	hydroxyproline-rich glycoprotein family protein	2.20266	
259318_at	AT3G01100	HYP1 (HYPOTHETICAL PROTEIN 1)	1.7018777	
250967_at	AT5G02790	In2-1 protein, putative	1.7648133	
250983_at	AT5G02780	In2-1 protein, putative	1.6874177	
258905_at	AT3G06390	integral membrane family protein	1.5671592	
260676_at	AT1G19450	sugar transporter family protein	2.9154387	
265669_at	AT2G32040	integral membrane transporter family protein	1.7816577	
254110_at	AT4G25260	invertase/pectin methylesterase inhibitor	2.7632477	
266352_at	AT2G01610	invertase/pectin methylesterase inhibitor	1.6530597	
257876_at	AT3G17130	invertase/pectin methylesterase inhibitor	1.7989237	
252437_at	AT3G47380	invertase/pectin methylesterase inhibitor	2.8411496	
247477_at	AT5G62340	invertase/pectin methylesterase inhibitor	3.2749047	
250233_at	AT5G13460	IQD11 (IQ-domain 11); calmodulin binding	1.6242057	

Probe Set ID	AGI	Short/Full name	Fold change	RT-qPCR
250872_at	AT5G03960	IQD12 (IQ-domain 12); calmodulin binding	2.7962704	
254293_at	AT4G23060	IQD22 (IQ-domain 22); calmodulin binding	1.9595461	
247464_at	AT5G62070	IQD23 (IQ-domain 23); calmodulin binding	1.6502906	
265051_at	AT1G52100	jacalin lectin family protein	1.8570902	
266838_at	AT2G25980	jacalin lectin family protein	1.9203633	
261133_at	AT1G19715	jacalin lectin family protein	2.1856048	
249675_at	AT5G35940	jacalin lectin family protein	2.71248	
265048_at	AT1G52050	jacalin lectin family protein	3.2220354	
265050_at	AT1G52070	jacalin lectin family protein	6.4247847	
266988_at	AT2G39310	JAL22 (JACALIN-RELATED LECTIN 22)	2.0212276	
261674_at	AT1G18270	ketose-bisphosphate aldolase class-II	1.7519495	
253964_at	AT4G26480	KH domain-containing protein	2.2558699	
247994_at	AT5G56140	KH domain-containing protein	2.646001	
254255_at	AT4G23220	kinase	2.0102212	
267518_at	AT2G30500	kinase interacting family protein	1.553191	
265673_at	AT2G32090	lactoylglutathione lyase family protein	2.1757057	
262338_at	AT1G64185	lactoylglutathione lyase family protein	2.6920807	
249258_at	AT5G41650	lactoylglutathione lyase family protein	3.1532664	
247645_at	AT5G60530	LEA protein-related	1.6222231	
247634_at	AT5G60520	LEA protein-related	1.6878922	
248178_at	AT5G54370	LEA protein-related	2.5462782	
252568_at	AT3G45410	lectin protein kinase family protein	1.5151386	
257206_at	AT3G16530	legume lectin family protein	5.8071656	
250942_at	AT5G03350	legume lectin family protein	2.2060585	
261368_at	AT1G53070	legume lectin family protein	2.9934235	
261367_at	AT1G53080	legume lectin family protein	4.052662	
257924_at	AT3G23190	lesion inducing protein-related	1.5400879	
248945_at	AT5G45510	leucine-rich repeat family protein	1.7632282	
260041_at	AT1G68780	leucine-rich repeat family protein	1.6515455	
245765_at	AT1G33600	leucine-rich repeat family protein	1.8178284	
250277_at	AT5G12940	leucine-rich repeat family protein	1.9258535	
261559_at	AT1G01780	LIM domain-containing protein	2.2887518	
257666_at	AT3G20270	lipid-binding serum glycoprotein family protein	1.5915501	
256652_at	AT3G18850	LPAT5; acyltransferase	1.5570333	
256062_at	AT1G07090	LSH6 (LIGHT SENSITIVE HYPOCOTYLS 6)	3.7674172	
254234_at	AT4G23680	major latex protein-related / MLP-related	3.198264	
254225_at	AT4G23670	major latex protein-related / MLP-related	2.6653914	
261177_at	AT1G04770	male sterility MS5 family protein	1.7848606	
247621_at	AT5G60340	maoC-like dehydratase domain-containing protein	1.6040436	
249817_at	AT5G23820	ML domain-containing protein	2.8677351	
258831_at	AT3G07080	membrane protein	1.5964475	
264584_at	AT1G05140	membrane-associated zinc metalloprotease	1.5059772	
267061_at	AT2G32480	membrane-associated zinc metalloprotease	1.6883101	
255626_at	AT4G00780	MATH domain-containing protein	1.5964066	
256577_at	AT3G28220	MATH domain-containing protein	1.703505	
264166_at	AT1G65370	MATH domain-containing protein	1.8284982	
255025_at	AT4G09900	MES12 (METHYL ESTERASE 12); hydrolase	2.2009983	
255026_at	AT4G09900	MES12 (METHYL ESTERASE 12); hydrolase	2.588208	
245349_at	AT4G16690	MES16 (METHYL ESTERASE 16)	1.9233598	
254385_s_at	AT4G21830 /// AT4G21840	SeIR domain-containing protein	3.6570303	
255298_at	AT4G04840	SeIR domain-containing protein	1.8297799	
259179_at	AT3G01660	methyltransferase	1.6056182	
253688_at	AT4G29590	methyltransferase	2.022881	

Probe Set ID	AGI	Short/Full name	Fold change	RT-qPCR
259842_at	AT1G73600	phosphoethanolamine N-methyltransferase	1.8260796	
252944_at	AT4G39320	microtubule-associated protein-related	1.7480888	
251029_at	AT5G02050	mitochondrial glycoprotein family protein	1.5976824	
251106_at	AT5G01500	mitochondrial substrate carrier family protein	1.6384698	
263943_at	AT2G35800	mitochondrial substrate carrier family protein	1.6392478	
247498_at	AT5G61810	mitochondrial substrate carrier family protein	1.7257828	
254120_at	AT4G24570	mitochondrial substrate carrier family protein	1.5403104	
251090_at	AT5G01340	mitochondrial substrate carrier family protein	1.9516838	
255465_at	AT4G02990	mTERF family protein	1.5578307	
266899_at	AT2G34620	mTERF-related	1.7264514	
259378_at	AT3G16310	mitotic phosphoprotein N' end (MPPN)	2.125258	
262312_at	AT1G70830	MLP28 (MLP-LIKE PROTEIN 28)	2.1161938	
262260_at	AT1G70850	MLP34 (MLP-LIKE PROTEIN 34)	6.8695917	
263034_at	AT1G24020	MLP423 (MLP-LIKE PROTEIN 423)	1.9996699	
262304_at	AT1G70890	MLP43 (MLP-LIKE PROTEIN 43)	2.438423	
252993_at	AT4G38540	monooxygenase, putative (MO2)	2.3280883	
247356_at	AT5G63800	MUM2 (MUCILAGE-MODIFIED 2)	1.6005565	
260292_at	AT1G63680	MURE	1.9144739	
263161_at	AT1G54020	myrosinase-associated protein, putative	1.5144175	
251730_at	AT3G56330	N2-dimethylguanosine tRNA methyltransferase	1.7325195	
251656_at	AT3G57170	Gpi1 family protein	1.5587091	
254468_at	AT4G20460	NAD-dependent epimerase/dehydratase	1.7526261	
250337_at	AT5G11790	Ndr family protein	1.5089518	
258736_at	AT3G05900	neurofilament protein-related	1.9242885	
251773_at	AT3G55960	NLI interacting factor (NIF) family protein	1.817612	
257285_at	AT3G29760	NLI interacting factor (NIF) family protein	2.0070488	
250217_at	AT5G14120	nodulin family protein	1.5365392	
253215_at	AT4G34950	nodulin family protein	1.8792892	
266993_at	AT2G39210	nodulin family protein	1.9482728	
265414_at	AT2G16660	nodulin family protein	2.3232033	
257272_at	AT3G28130	nodulin MtN21 family protein	1.5701296	
265967_at	AT2G37450	nodulin MtN21 family protein	1.5870719	
255129_at	AT4G08290	nodulin MtN21 family protein	1.6862296	
255127_at	AT4G08300	nodulin MtN21 family protein	1.822522	
255576_at	AT4G01440	nodulin MtN21 family protein	1.954046	
257300_at	AT3G28080	nodulin MtN21 family protein	1.9754423	
261335_at	AT1G44800	nodulin MtN21 family protein	4.5414596	
258421_at	AT3G16690	nodulin MtN3 family protein	1.8871633	
257823_at	AT3G25190	nodulin, putative	1.8720144	
267268_at	AT2G02570	nucleic acid binding	1.5000335	
267078_at	AT2G40960	nucleic acid binding	3.128771	
257519_at	AT3G01210	nucleic acid binding / oxidoreductase	1.5545285	
265249_at	AT2G01940	nucleic acid binding	1.6878722	
266659_at	AT2G25850	nucleotidyltransferase family protein	1.6012844	
257002_at	AT3G14100	oligoridylate-binding protein, putative	1.5450536	
261216_at	AT1G33030	O-methyltransferase family 2 protein	1.6022544	
251295_at	AT3G62000	O-methyltransferase family 3 protein	1.9487283	
248330_at	AT5G52810	ornithine cyclodeaminase	1.8949392	
247951_at	AT5G57240	ORP4C	1.6136652	
251558_at	AT3G57810	OTU-like cysteine protease family protein	1.9371134	
257009_at	AT3G14160	oxidoreductase	1.5647548	
251057_at	AT5G01780	oxidoreductase	1.5830094	
245418_at	AT4G17370	oxidoreductase family protein	1.9951875	

Probe Set ID	AGI	Short/Full name	Fold change	RT-qPCR
256647_at	AT3G13610	oxidoreductase	1.9229063	
254975_at	AT4G10500	oxidoreductase	3.6898186	
256892_at	AT3G19000	oxidoreductase	1.5738422	
263135_at	AT1G78550	oxidoreductase	1.6716243	
247774_at	AT5G58660	oxidoreductase	1.8222377	
250793_at	AT5G05600	oxidoreductase	1.8765954	
260072_at	AT1G73650	oxidoreductase	3.4735532	
265182_at	AT1G23740	oxidoreductase	1.5205878	
251402_at	AT3G60290	oxidoreductase	1.6307861	
251408_at	AT3G60340	palmitoyl protein thioesterase family protein	1.5001253	
248812_at	AT5G47330	palmitoyl protein thioesterase family protein	1.8309441	
264850_at	AT2G17340	pantothenate kinase-related	2.2918231	
262264_at	AT1G42470	patched family protein	1.559238	
255160_at	AT4G07820	pathogenesis-related protein, putative	2.283638	
261691_at	AT1G50060	pathogenesis-related protein, putative	2.3849297	
253301_at	AT4G33720	pathogenesis-related protein, putative	2.4503496	
253104_at	AT4G36010	pathogenesis-related thaumatin family protein	1.8301865	
262727_at	AT1G75800	pathogenesis-related thaumatin family protein	2.0470042	
261882_at	AT1G80770	PDE318 (pigment defective 318)	1.7524595	
254805_at	AT4G12480	pEARL1; lipid binding	1.9206252	
248899_at	AT5G46390	peptidase S41 family protein	1.6332184	
250926_at	AT5G03555	permease	1.5929358	
255429_at	AT4G03410	peroxisomal membrane protein-related	1.543027	
260155_at	AT1G52870	peroxisomal membrane protein-related	1.9809084	
253858_at	AT4G27600	pfkB-type carbohydrate kinase family protein	1.6282749	
248381_at	AT5G51830	pfkB-type carbohydrate kinase family protein	1.5446119	
261136_at	AT1G19600	pfkB-type carbohydrate kinase family protein	1.5079275	
255450_at	AT4G02850	phenazine biosynthesis PhzC	1.6423967	
264645_at	AT1G08940	phosphoglycerate	1.5738606	
254150_at	AT4G24350	phosphorylase family protein	1.6932391	
248333_at	AT5G52390	photoassimilate-responsive protein, putative	1.5820667	
264807_at	AT1G08700	presenilin family protein	1.7860678	
261070_at	AT1G07390	protein binding	1.6383039	
247948_at	AT5G57130	protein binding	2.2082217	
258899_at	AT3G05675	protein binding	1.6586106	
252834_at	AT4G40070	protein binding / zinc ion binding	1.7728797	
253071_at	AT4G37880	protein binding / zinc ion binding	1.5191481	
258635_at	AT3G08020	protein binding / zinc ion binding	1.5307742	
262512_at	AT1G17145	protein binding / zinc ion binding	1.6337717	
252464_at	AT3G47160	protein binding / zinc ion binding	2.6069381	
248344_at	AT5G52280	protein transport protein-related	1.9159651	
250181_at	AT5G14460	pseudouridine synthase/ transporter	1.6906081	
257534_at	AT3G09670	PWWP domain-containing protein	1.6334084	
249409_at	AT5G40340	PWWP domain-containing protein	2.5785995	
252671_at	AT3G44190	pyridine nucleotide-disulphide oxidoreductase	1.808702	
253951_at	AT4G26860	pyridoxal phosphate binding	1.6162548	
245626_at	AT1G56700	pyrrolidone-carboxylate peptidase	1.5489781	
249797_at	AT5G23750	remorin family protein	1.5486017	
246205_at	AT4G36970	remorin family protein	1.7949919	
266553_at	AT2G46170	reticulon family protein (RTNLB5)	1.5291336	
253860_at	AT4G27700	rhodanese-like domain-containing protein	2.2411075	
258989_at	AT3G08920	rhodanese-like domain-containing protein	1.670148	
249510_at	AT5G38510	rhomboid family protein	2.0961738	

Probe Set ID	AGI	Short/Full name	Fold change	RT-qPCR
258316_at	AT3G22660	rRNA processing protein-related	1.5723357	
266503_at	AT2G47780	rubber elongation factor (REF) protein-related	7.698143	
261945_at	AT1G64530	RWP-RK domain-containing protein	1.7917091	
255104_at	AT4G08685	SAH7	1.6410863	
248808_at	AT5G47510	SEC14 cytosolic factor family protein	1.6942964	
259804_at	AT1G72160	SEC14 cytosolic factor family protein	1.978014	
255923_at	AT1G22180	SEC14 cytosolic factor family protein	2.0330088	
261116_at	AT1G75370	SEC14 cytosolic factor, putative	1.7741582	
261151_at	AT1G19650	SEC14 cytosolic factor, putative	1.811822	
252099_at	AT3G51250	dehydration-associated protein-related	1.5681344	
260137_at	AT1G66330	senescence-associated family protein	1.55733	
248820_at	AT5G47060	senescence-associated protein-related	1.820954	
262162_at	AT1G78020	senescence-associated protein-related	2.0303762	
247212_at	AT5G65040	senescence-associated protein-related	2.5471683	
250170_at	AT5G14260	SET domain-containing protein	1.6800432	
251309_at	AT3G61220	short-chain dehydrogenase/reductase (SDR)	2.5179195	
254764_at	AT4G13250	short-chain dehydrogenase/reductase (SDR)	1.5619106	
266265_at	AT2G29340	short-chain dehydrogenase/reductase (SDR)	1.6101948	
254928_at	AT4G11410	short-chain dehydrogenase/reductase (SDR)	1.7907891	
247178_at	AT5G65205	short-chain dehydrogenase/reductase (SDR)	1.8288189	
267169_at	AT2G37540	short-chain dehydrogenase/reductase (SDR)	2.6533062	
251013_at	AT5G02540	short-chain dehydrogenase/reductase (SDR)	2.704926	
261956_at	AT1G64590	short-chain dehydrogenase/reductase (SDR)	2.7543864	
254759_at	AT4G13180	short-chain dehydrogenase/reductase (SDR)	1.8147951	
266015_at	AT2G24190	short-chain dehydrogenase/reductase (SDR)	1.7103451	
246229_at	AT4G37160	sks15 (SKU5 Similar 15); copper ion binding	2.4519784	
267287_at	AT2G23630	sks16 (SKU5 Similar 16); copper ion binding	1.6582518	
252989_at	AT4G38420	sks9 (SKU5 Similar 9); copper ion binding	2.2872217	
262536_at	AT1G17100	SOUL heme-binding family protein	1.7806203	
266097_at	AT2G37970	SOUL-1; binding	1.6485145	
252092_at	AT3G51420	SSL4 (STRICTOSIDINE SYNTHASE-LIKE 4)	1.5502859	
254839_at	AT4G12400	stress-inducible protein, putative	1.7276042	
246251_at	AT4G37220	stress-responsive protein, putative	1.9983677	
260386_at	AT1G74010	strictosidine synthase family protein	2.939677	
252068_at	AT3G51440	strictosidine synthase family protein	1.7098526	
251658_at	AT3G57020	strictosidine synthase family protein	1.9380662	
265768_at	AT2G48020	sugar transporter, putative	1.7415645	
245702_at	AT5G04220	SYTC	2.361894	
252043_at	AT3G52390	tatD-related deoxyribonuclease family protein	1.9384363	
261985_at	AT1G33750	terpene synthase/cyclase family protein	1.6383803	
255751_at	AT1G31950	terpene synthase/cyclase family protein	2.1682253	
248736_at	AT5G48110	terpene synthase/cyclase family protein	3.4629803	
260109_at	AT1G63260	TET10 (TETRASPANIN10)	1.723309	
265935_at	AT2G19580	TET2 (TETRASPANIN2)	1.7626134	
266526_at	AT2G16980	tetracycline transporter	1.5247074	
257730_at	AT3G18420	tetratricopeptide repeat (TPR)	1.8021008	
259549_at	AT1G35290	thioesterase family protein	1.5565565	
248391_at	AT5G52030	TraB protein-related	1.5164511	
250234_at	AT5G13420	transaldolase, putative	1.5964099	
264264_at	AT1G09250	transcription factor	1.8328258	
258511_at	AT3G06590	transcription factor	1.9428674	
246230_at	AT4G36710	transcription factor	1.7155933	
258742_at	AT3G05800	transcription factor	3.6698554	

Probe Set ID	AGI	Short/Full name	Fold change	RT-qPCR
265160_at	AT1G31050	transcription factor	1.62774	
259562_at	AT1G21200	transcription factor	1.7091235	
247419_at	AT5G63080	transcription factor jumonji (jnjC)	1.6650364	
257985_at	AT3G20810	transcription factor jumonji (jnjC)	2.4340158	
248559_at	AT5G50010	transcription factor/ transcription regulator	1.887329	
260527_at	AT2G47270	transcription factor/ transcription regulator	2.460366	
255666_at	AT4G00390	transcription regulator	1.5307301	
253144_at	AT4G35540	transcription regulator/ zinc ion binding	1.6888245	
254638_at	AT4G18740	transcription termination factor	1.6777387	
245930_at	AT5G09240	transcriptional coactivator p15	2.150679	
248347_at	AT5G52250	transducin family protein	1.823144	
262641_at	AT1G62730	transferase	2.447916	
248723_at	AT5G47950	transferase family protein	1.523871	
257428_at	AT1G78990	transferase family protein	1.5384805	
250550_at	AT5G07870	transferase family protein	1.576951	
252199_at	AT3G50270	transferase family protein	1.8419832	
250968_at	AT5G02890	transferase family protein	2.122074	
249493_at	AT5G39080	transferase family protein	2.1750736	
245556_at	AT4G15400	transferase family protein	2.2525573	
251144_at	AT5G01210	transferase family protein	2.4163227	
267337_at	AT2G39980	transferase family protein	2.6798098	
249188_at	AT5G42830	transferase family protein	3.505421	
249494_at	AT5G39050	transferring acyl groups	2.3274262	
254910_at	AT4G11175	translation initiation factor IF-1,	2.2514596	
264170_at	AT1G02260	transmembrane protein, putative	1.6604066	
247415_at	AT5G63060	transporter	2.0666943	
255181_at	AT4G08110	transposable element gene	1.5947112	
248510_at	AT5G50315	transposable element gene	1.7978995	
264824_at	AT1G03420	transposable element gene	1.8487127	
256976_at	AT3G21020	transposable element gene	1.9937522	
245449_at	AT4G16870	transposable element gene	2.2619362	
259573_at	AT1G20390	transposable element gene	2.7320194	
257057_at	AT3G15310	transposable element gene	7.181499	
246852_at	AT5G26880	tRNA/rRNA methyltransferase	1.6996483	
250763_at	AT5G06060	troponin reductase, putative	1.5482316	
266280_at	AT2G29260	troponin reductase, putative	1.8557602	
266275_at	AT2G29370	troponin reductase, putative	1.8900877	
266277_at	AT2G29310	troponin reductase, putative	2.086177	
266278_at	AT2G29300	troponin reductase, putative	2.3896403	
266293_at	AT2G29360	troponin reductase, putative	3.4145024	
245943_at	AT5G19500	tryptophan/tyrosine permease family protein	1.5319026	
251584_at	AT3G58620	TTL4	1.6946188	
253697_at	AT4G29700	type I phosphodiesterase	2.2465868	
259371_at	AT1G69080	universal stress protein (USP) family protein	1.6458726	
257672_at	AT3G20300	unknown protein	1.6840833	
246125_at	AT5G19875	unknown protein	1.8390685	
247754_at	AT5G59080	unknown protein	2.2059689	
258419_at	AT3G16670	unknown protein	2.667822	
262373_at	AT1G73120	unknown protein	2.6890152	
259479_at	AT1G19020	unknown protein	2.724898	
246547_at	AT5G14970	unknown protein	1.5985608	
256114_at	AT1G16850	unknown protein	1.7032913	
262045_at	AT1G80240	unknown protein	1.7805847	

Probe Set ID	AGI	Short/Full name	Fold change	RT-qPCR
262871_at	AT1G65010	unknown protein	1.6278375	
245952_at	AT5G28500	unknown protein	1.5000198	
260268_at	AT1G68490	unknown protein	1.5012022	
255385_at	AT4G03610	unknown protein	1.5026034	
255252_at	AT4G04990	unknown protein	1.5032289	
254921_at	AT4G11300	unknown protein	1.5046312	
262664_at	AT1G13970	unknown protein	1.5066125	
253557_at	AT4G31115	unknown protein	1.509913	
265734_at	AT2G01260	unknown protein	1.5099281	
266618_at	AT2G35480	unknown protein	1.510736	
259103_at	AT3G11690	unknown protein	1.5139099	
257745_at	AT3G29240	unknown protein	1.5149574	
256883_at	AT3G26440	unknown protein	1.5157923	
249329_at	AT5G40960	unknown protein	1.5159612	
265269_at	AT2G42950	unknown protein	1.5164906	
259586_at	AT1G28100	unknown protein	1.5168614	
254965_at	AT4G11090	unknown protein	1.517856	
257477_at	AT1G10660	unknown protein	1.5197606	
255331_at	AT4G04330	unknown protein	1.5212206	
245864_at	AT1G58070	unknown protein	1.525915	
245486_x_at	AT4G16240	unknown protein	1.5275494	
262262_at	AT1G70780	unknown protein	1.5297294	
257209_at	AT3G14920	unknown protein	1.5316902	
246343_at	AT3G56720	unknown protein	1.5326648	
255602_at	AT4G01026	unknown protein	1.5376071	
245082_at	AT2G23270	unknown protein	1.5383626	
246315_at	AT3G56870	unknown protein	1.5436759	
250937_at	AT5G03230	unknown protein	1.5440329	
251009_at	AT5G02640	unknown protein	1.5444063	
266795_at	AT2G03070	unknown protein	1.5446348	
249622_at	AT5G37550	unknown protein	1.5458431	
266874_at	AT2G44760	unknown protein	1.5484385	
265457_at	AT2G46550	unknown protein	1.5490798	
253044_at	AT4G37290	unknown protein	1.5491447	
259903_at	AT1G74160	unknown protein	1.5493364	
253475_at	AT4G32290	unknown protein	1.550332	
245502_at	AT4G15640	unknown protein	1.5505278	
250009_at	AT5G18440	unknown protein	1.553221	
254356_at	AT4G22190	unknown protein	1.5538553	
247407_at	AT5G62900	unknown protein	1.5563302	
250920_at	AT5G03390	unknown protein	1.556647	
247734_at	AT5G59400	unknown protein	1.5578818	
261170_at	AT1G04910	unknown protein	1.5585661	
248286_at	AT5G52870	unknown protein	1.5624181	
262544_at	AT1G15420	unknown protein	1.5683378	
246736_at	AT5G27560	unknown protein	1.568987	
257773_at	AT3G29185	unknown protein	1.5709854	
251650_at	AT3G57360	unknown protein	1.5710164	
248621_at	AT5G49350	unknown protein	1.5808792	
247885_at	AT5G57830	unknown protein	1.5823503	
245097_at	AT2G40935	unknown protein	1.5850526	
259017_at	AT3G07310	unknown protein	1.587893	
248167_at	AT5G54530	unknown protein	1.5894237	

Probe Set ID	AGI	Short/Full name	Fold change	RT-qPCR
254752_at	AT4G13160	unknown protein	1.5916077	
247903_at	AT5G57340	unknown protein	1.5927556	
253182_at	AT4G35190	unknown protein	1.5945193	
251292_at	AT3G61920	unknown protein	1.597092	
253283_at	AT4G34090	unknown protein	1.5982443	
251142_at	AT5G01015	unknown protein	1.5984621	
252204_at	AT3G50340	unknown protein	1.5998857	
257248_at	AT3G24150	unknown protein	1.6019279	
248291_at	AT5G53020	unknown protein	1.6040497	
248218_at	AT5G53710	unknown protein	1.6110489	
249747_at	AT5G24600	unknown protein	1.611057	
246158_at	AT5G19855	unknown protein	1.6135173	
260995_at	AT1G12120	unknown protein	1.6142612	
262396_at	AT1G49470	unknown protein	1.6157355	
257567_at	AT3G23930	unknown protein	1.6191151	
258608_at	AT3G03020	unknown protein	1.6211892	
265312_at	AT2G20240	unknown protein	1.6216489	
252533_at	AT3G46110	unknown protein	1.6287366	
248694_at	AT5G48340	unknown protein	1.629458	
250265_at	AT5G12900	unknown protein	1.6358489	
248282_at	AT5G52900	unknown protein	1.6398712	
266738_at	AT2G47010	unknown protein	1.6409137	
261509_at	AT1G71740	unknown protein	1.6414264	
252552_at	AT3G45900	unknown protein	1.641753	
262313_at	AT1G70900	unknown protein	1.6436312	
262533_at	AT1G17090	unknown protein	1.6489546	
260442_at	AT1G68220	unknown protein	1.649894	
250850_at	AT5G04550	unknown protein	1.6500795	
250689_at	AT5G06610	unknown protein	1.6514302	
266898_at	AT2G45990	unknown protein	1.6520272	
267037_at	AT2G38320	unknown protein	1.653777	
256599_at	AT3G14760	unknown protein	1.6573522	
255900_at	AT1G17830	unknown protein	1.663229	
252659_at	AT3G44430	unknown protein	1.6635442	
257412_at	AT1G22980	unknown protein	1.6635509	
256262_at	AT3G12150	unknown protein	1.6643635	
248663_at	AT5G48590	unknown protein	1.6659697	
246748_at	AT5G27730	unknown protein	1.669295	
251725_at	AT3G56260	unknown protein	1.6719729	
247899_at	AT5G57345	unknown protein	1.6781341	
253654_at	AT4G30060	unknown protein	1.680983	
247556_at	AT5G61040	unknown protein	1.6873323	
262945_at	AT1G79510	unknown protein	1.6969974	
253782_at	AT4G28590	unknown protein	1.7089949	
251684_at	AT3G56410	unknown protein	1.7144289	
263709_at	AT1G09310	unknown protein	1.7152784	
255456_at	AT4G02920	unknown protein	1.722859	
261641_at	AT1G27670	unknown protein	1.7229744	
245181_at	AT5G12420	unknown protein	1.7254591	
248709_at	AT5G48470	unknown protein	1.7257975	
256076_at	AT1G18060	unknown protein	1.73328	
253893_at	AT4G27390	unknown protein	1.7362646	
255318_at	AT4G04190	unknown protein	1.7373198	

Probe Set ID	AGI	Short/Full name	Fold change	RT-qPCR
263115_at	AT1G03055	unknown protein	1.7376374	
245730_at	AT1G73470	unknown protein	1.7434653	
267602_at	AT2G32970	unknown protein	1.7466255	
259180_at	AT3G01680	unknown protein	1.7475153	
249136_at	AT5G43180	unknown protein	1.747964	
246487_at	AT5G16030	unknown protein	1.7525514	
259460_at	AT1G44000	unknown protein	1.7544745	
264909_at	AT2G17300	unknown protein	1.7546452	
261558_at	AT1G01770	unknown protein	1.7575872	
250122_at	AT5G16520	unknown protein	1.7576779	
252353_at	AT3G48200	unknown protein	1.7578527	
258211_at	AT3G17890	unknown protein	1.7598815	
245421_at	AT4G17430	unknown protein	1.7651693	
249340_at	AT5G41140	unknown protein	1.7671824	
247486_at	AT5G62140	unknown protein	1.7752998	
245432_at	AT4G17100	unknown protein	1.775504	
249988_at	AT5G18310	unknown protein	1.7760909	
262574_at	AT1G15230	unknown protein	1.7767262	
245906_at	AT5G11070	unknown protein	1.7770673	
264024_at	AT2G21180	unknown protein	1.7789516	
256066_at	AT1G06980	unknown protein	1.7802259	
245028_at	AT2G26570	unknown protein	1.7841861	
249230_at	AT5G42070	unknown protein	1.7843037	
265999_at	AT2G24100	unknown protein	1.7870593	
251445_at	AT3G59870	unknown protein	1.7870636	
247194_at	AT5G65480	unknown protein	1.7904397	
264207_at	AT1G22750	unknown protein	1.790994	
251039_at	AT5G02020	unknown protein	1.7924706	
256090_at	AT1G20816	unknown protein	1.7978451	
246446_at	AT5G17640	unknown protein	1.8019776	
253796_at	AT4G28460	unknown protein	1.8054652	
254200_at	AT4G24110	unknown protein	1.808258	
258124_at	AT3G18215	unknown protein	1.8087167	
264096_at	AT1G78995	unknown protein	1.817065	
256266_at	AT3G12320	unknown protein	1.8270901	
257540_at	AT3G21520	unknown protein	1.8342046	
249701_at	AT5G35460	unknown protein	1.8390228	
245795_at	AT1G32160	unknown protein	1.8499662	
252866_at	AT4G39840	unknown protein	1.8538244	
249167_at	AT5G42860	unknown protein	1.8565569	
260359_at	AT1G69210	unknown protein	1.8598208	
246231_at	AT4G37080	unknown protein	1.8625839	
254208_at	AT4G24175	unknown protein	1.8681204	
254561_at	AT4G19160	unknown protein	1.8708191	
254797_at	AT4G13030	unknown protein	1.8737469	
254697_at	AT4G17970	unknown protein	1.8744797	
246057_at	AT5G08400	unknown protein	1.8783635	
267199_at	AT2G30990	unknown protein	1.8874519	
248624_at	AT5G48790	unknown protein	1.8998588	
264343_at	AT1G11850	unknown protein	1.9027596	
246919_at	AT5G25460	unknown protein	1.9028807	
265628_at	AT2G27290	unknown protein	1.903366	
255528_at	AT4G02090	unknown protein	1.9117486	

Probe Set ID	AGI	Short/Full name	Fold change	RT-qPCR
265387_at	AT2G20670	unknown protein	1.9146509	
261292_at	AT1G36940	unknown protein	1.9194002	
250438_at	AT5G10580	unknown protein	1.9340395	
249384_at	AT5G39890	unknown protein	1.9544474	
259624_at	AT1G43020	unknown protein	1.9561497	
251117_at	AT3G63390	unknown protein	1.9565588	
261456_at	AT1G21050	unknown protein	1.9599565	
261638_at	AT1G49975	unknown protein	1.9657371	
265192_at	AT1G05060	unknown protein	1.9678109	
263227_at	AT1G30750	unknown protein	1.9723508	
254317_at	AT4G22510	unknown protein	1.9813095	
263640_at	AT2G25270	unknown protein	1.9879594	
249610_at	AT5G37360	unknown protein	1.996698	
255648_at	AT4G00910	unknown protein	2.004879	
262873_at	AT1G64700	unknown protein	2.0073297	
258424_at	AT3G16750	unknown protein	2.0093713	
258988_at	AT3G08890	unknown protein	2.014225	
267409_at	AT2G34910	unknown protein	2.0210664	
255774_at	AT1G18620	unknown protein	2.030881	
247977_at	AT5G56850	unknown protein	2.0383523	
246989_at	AT5G67350	unknown protein	2.0404007	
247177_at	AT5G65300	unknown protein	2.0455291	
250098_at	AT5G17350	unknown protein	2.0545843	
254982_at	AT4G10470	unknown protein	2.073476	
267549_at	AT2G32640	unknown protein	2.0780742	
251219_at	AT3G62390	unknown protein	2.083068	
251788_at	AT3G55420	unknown protein	2.0961692	
260656_at	AT1G19380	unknown protein	2.0992165	
250728_at	AT5G06440	unknown protein	2.1041198	
248685_at	AT5G48500	unknown protein	2.1041849	
247049_at	AT5G66440	unknown protein	2.1049533	
260332_at	AT1G70470	unknown protein	2.1067495	
245336_at	AT4G16515	unknown protein	2.1079345	
253548_at	AT4G30993	unknown protein	2.112447	
267003_at	AT2G34340	unknown protein	2.1374886	
246998_at	AT5G67370	unknown protein	2.16518	
245629_at	AT1G56580	unknown protein	2.180044	
245893_at	AT5G09270	unknown protein	2.2169614	
245948_at	AT5G19540	unknown protein	2.2199244	
260004_at	AT1G67860	unknown protein	2.2330606	
257502_at	AT1G78110	unknown protein	2.2464082	
259856_at	AT1G68440	unknown protein	2.2539241	
263002_at	AT1G54200	unknown protein	2.2869596	
257061_at	AT3G18250	unknown protein	2.3201556	
249918_at	AT5G19240	unknown protein	2.3213508	
251372_at	AT3G60520	unknown protein	2.3425806	
255825_at	AT2G40475	unknown protein	2.3524852	
253298_at	AT4G33560	unknown protein	2.357098	
248257_at	AT5G53410	unknown protein	2.3813617	
257026_at	AT3G19200	unknown protein	2.386547	
266364_at	AT2G41230	unknown protein	2.3882363	
246892_at	AT5G25500	unknown protein	2.404707	
259166_at	AT3G01670	unknown protein	2.4329562	

Probe Set ID	AGI	Short/Full name	Fold change	RT-qPCR
251113_at	AT5G01370	unknown protein	2.438628	
246997_at	AT5G67390	unknown protein	2.461085	
260682_at	AT1G17510	unknown protein	2.4637716	
264342_at	AT1G12080	unknown protein	2.478165	
250211_at	AT5G13880	unknown protein	2.4787962	
246792_at	AT5G27290	unknown protein	2.5191965	
265276_at	AT2G28400	unknown protein	2.5473936	
261247_at	AT1G20070	unknown protein	2.559162	
263287_at	AT2G36145	unknown protein	2.56717	
259207_at	AT3G09050	unknown protein	2.5780766	
261500_at	AT1G28400	unknown protein	2.5951643	
256725_at	AT2G34070	unknown protein	2.6062582	
265083_at	AT1G03820	unknown protein	2.6358678	
260232_at	AT1G74640	unknown protein	2.636958	
247882_at	AT5G57785	unknown protein	2.6791136	
248509_at	AT5G50335	unknown protein	2.681272	
266707_at	AT2G03310	unknown protein	2.6897855	
249355_at	AT5G40500	unknown protein	2.762228	
245341_at	AT4G16447	unknown protein	2.778537	
249211_at	AT5G42680	unknown protein	2.7822497	
259791_at	AT1G29700	unknown protein	2.7959661	
266222_at	AT2G28780	unknown protein	2.806333	
267063_at	AT2G41120	unknown protein	2.827714	
259325_at	AT3G05320	unknown protein	2.8446975	
247252_at	AT5G64770	unknown protein	2.8525653	
266017_at	AT2G18690	unknown protein	2.9324787	
246001_at	AT5G20790	unknown protein	3.1062589	
251050_at	AT5G02440	unknown protein	3.110206	
261951_at	AT1G64490	unknown protein	3.1261227	
264738_at	AT1G62250	unknown protein	3.202438	
264725_at	AT1G22885	unknown protein	3.3233588	
260841_at	AT1G29195	unknown protein	3.3327844	
252539_at	AT3G45730	unknown protein	3.419017	
247959_at	AT5G57080	unknown protein	3.4983752	
258397_at	AT3G15357	unknown protein	3.5400052	
259520_at	AT1G12320	unknown protein	3.6129613	
257517_at	AT3G16330	unknown protein	3.7596514	
257724_at	AT3G18510	unknown protein	3.7643797	
265611_at	AT2G25510	unknown protein	3.9686885	
245642_at	AT1G25275	unknown protein	4.015522	
256442_at	AT3G10930	unknown protein	4.2193384	
260522_x_at	AT2G41730	unknown protein	4.3004494	
251155_at	AT3G63160	unknown protein	4.939906	
253155_at	AT4G35720	unknown protein	7.702714	
264635_at	AT1G65500	unknown protein	11.868725	
253197_at	AT4G35250	vestitone reductase-related	1.5650331	
260261_at	AT1G68450	VQ motif-containing protein	1.9467709	
256793_at	AT3G22160	VQ motif-containing protein	2.0984254	
246289_at	AT3G56880	VQ motif-containing protein	2.653596	
256741_at	AT3G29375	XH domain-containing protein	1.8893478	
263773_at	AT2G21370	xylulose kinase, putative	1.5614374	
263106_at	AT2G05160	zinc finger (CCCH-type) family protein	2.01636	
255508_at	AT4G02220	zinc finger (MYND type) family protein	1.5025324	

Probe Set ID	AGI	Short/Full name	Fold change	RT-qPCR
246891_at	AT5G25490	zinc finger (Ran-binding) family protein	1.9844438	
258689_at	AT3G07940	zinc finger and C2 domain protein, putative	1.5401341	
260484_at	AT1G68360	zinc finger protein-related	1.5231078	
252770_at	AT3G42860	zinc knuckle (CCHC-type) family protein	1.771376	
261711_at	AT1G32700	zinc-binding family protein	1.5265605	
252592_at	AT3G45640 /// AT3G45650		1.6365851	
260130_s_at	AT1G66270 /// AT1G66280		2.5901647	
262427_s_at	AT1G47600 /// AT1G51470		2.4435294	
265174_s_at	AT1G23460 /// AT1G23470		1.5196569	
267162_s_at	AT2G05140 /// AT2G37690		1.5840219	
257723_at	AT3G18500		2.9387205	
246987_at	AT5G67300 /// AT5G67310		1.5580493	
258975_at	AT3G01970 /// AT3G01980		3.8601267	
245414_at	AT4G17300 /// AT4G17310		1.5349134	
258861_at	AT3G02050 /// AT3G02060		1.5138731	
246654_s_at	AT5G35210 /// AT5G35220		1.5972536	
252291_s_at	AT3G49110 /// AT3G49120		1.9528763	
267621_at	AT2G39680		1.8358631	
251741_at	AT3G56020 /// AT3G56040		2.2387109	
256145_at	AT1G48750 /// AT1G48760		3.4479098	
248523_s_at	AT5G50580 /// AT5G50680		1.5305419	
253764_s_at	AT4G28860 /// AT4G28880		1.5962869	
259362_s_at	AT1G13350 /// AT3G53640		1.6043737	
254265_s_at	AT4G23140 /// AT4G23160		2.029639	
260774_at	AT1G78290		1.6049348	
258632_s_at	AT3G07980 /// AT3G13530		1.6109595	
263111_s_at	AT1G65190 /// AT1G65250		1.710509	
265886_at	AT2G25610 /// AT2G25620		1.577344	
266772_s_at	AT2G03020 /// AT4G16540		1.8624344	
262503_at	AT1G21670		1.9367385	
264365_s_at	AT1G03220 /// AT1G03230		1.5526906	
257500_s_at	AT1G73300 /// AT5G36180		2.9779527	
254915_s_at	AT4G11310 /// AT4G11320		9.502294	
261457_at	AT1G21060 /// AT1G21065		1.5512079	
265899_s_at	AT1G20140 /// AT2G25700		2.1909149	
260950_s_at	AT1G06090 /// AT1G06120		1.9207387	
246252_s_at	AT4G37060 /// AT4G37070		1.7759867	
251146_at	AT3G63510 /// AT3G63520		1.6183947	
262649_at	AT1G14040		2.2172267	
249152_s_at	AT5G43350 /// AT5G43370		3.2685668	
266184_s_at	AT2G38940 /// AT3G54700		2.5263484	
265435_s_at	AT1G31885 /// AT2G21020		1.7832983	
257162_s_at	AT3G24290 /// AT3G24300		1.5634049	
254820_s_at	AT4G12510 /// AT4G12520		1.9467537	
248844_s_at	AT5G46890 /// AT5G46900		13.179846	
267238_at	AT2G44130 /// AT2G44140		1.8292723	
264885_s_at	AT1G61180 /// AT1G61190 /// AT1G61300 /// AT1G61310		2.0084157	
266743_at	AT2G02990 /// AT2G16300		1.7609993	
262119_s_at	AT1G02920 /// AT1G02930		3.4493015	
249195_s_at	AT5G42500 /// AT5G42510		1.9160825	
265920_s_at	AT2G15120 /// AT2G15220		3.4168923	
267596_s_at	AT2G33050 /// AT2G33060		1.6867723	
262374_s_at	AT1G72910 /// AT1G72930		1.8660525	

Probe Set ID	AGI	Short/Full name	Fold change	RT-qPCR
263063_s_at	AT2G18140 /// AT2G18150		5.9758935	
267053_s_at	AT2G38380 /// AT2G38390		1.8735954	
264567_s_at	AT1G05240 /// AT1G05250		4.2234864	
254431_at	AT4G20830 /// AT4G20840		2.0844178	
254283_s_at	AT4G22870 /// AT4G22880		2.2960758	
253340_s_at	AT4G33260 /// AT4G33270		1.7477918	
265439_at	AT2G21045		1.6798288	
252208_at	AT3G50380		1.5150273	
266643_s_at	AT2G29710 /// AT2G29730		1.5902697	
266279_at	AT2G29280 /// AT2G29290		1.9058206	
255436_at	AT4G03140 /// AT4G03150		2.1078105	
256304_at	AT1G69523 /// AT1G69526		2.1525755	
258977_s_at	AT3G02020 /// AT5G14060		1.9851284	
255895_at	AT1G17990 /// AT1G18020		2.2360113	
257638_at	AT3G25820 /// AT3G25830		2.971062	
256994_s_at	AT3G25820 /// AT3G25830		10.150962	
265200_s_at	AT2G36790 /// AT2G36800		3.5977175	
253268_s_at	AT4G34131 /// AT4G34135		1.7849458	
263706_s_at	AT1G31180 /// AT5G14200		1.7178859	
257175_s_at	AT3G23470 /// AT3G23480		1.6862503	
254163_s_at	AT4G24340 /// AT4G24350		1.7582254	
266746_s_at	AT2G02930 /// AT4G02520		2.1706898	
248566_s_at	AT5G49730 /// AT5G49740		4.227658	
261144_s_at	AT1G19660 /// AT1G75380		2.5843263	
261663_at	AT1G18330 /// AT3G10113		1.9896438	
247544_at	AT5G61670		1.514426	
248636_at			2.0504756	
267126_s_at	AT2G23590 /// AT2G23600		1.7098467	
261149_s_at	AT1G19550 /// AT1G19570		1.5242447	
249417_at	AT5G39670 /// AT5G39680		1.7274963	
254053_s_at	AT4G25300 /// AT4G25310		1.5300661	
267290_at	AT2G23740 /// AT2G23750		1.760763	
259381_s_at	AT3G16390 /// AT3G16400 /// AT3G16410		2.9245532	
262377_at	AT1G73100 /// AT1G73110		1.5196246	
253160_at	AT4G35760		1.725482	
251124_s_at	AT5G01040 /// AT5G01050		2.1428976	
247321_s_at	AT5G09350 /// AT5G64070		1.680062	
251279_at	AT3G61800		1.5074337	
252481_at	AT3G46630		1.5080398	
266660_at	AT2G25920		1.5143076	
250773_at	AT5G05430		1.5150957	
263268_at			1.5171072	
248226_at	AT5G53750		1.5205069	
253424_at	AT4G32330		1.5216349	
253687_at	AT4G29520		1.5226287	
259300_at	AT3G05100		1.5262424	
266596_at	AT2G46150		1.5333906	
261868_s_at	AT1G11450 /// AT1G11460		1.5360944	
251400_at	AT3G60420		1.5364997	
245601_at	AT4G14240		1.5381271	
254750_at	AT4G13140		1.5396694	
248191_at	AT5G54120 /// AT5G54130		1.5436493	
249237_at	AT5G42050		1.550877	

Probe Set ID	AGI	Short/Full name	Fold change	RT-qPCR
249358_at	AT5G40510		1.5547956	
253437_at	AT4G32460		1.556685	
262700_at	AT1G76020		1.5646147	
266355_at	AT2G01400 /// AT2G01410		1.5704137	
267520_at	AT2G30460		1.570654	
256332_at	AT1G76890		1.5720258	
253752_at	AT4G28910		1.5731462	
256215_at	AT1G50900		1.5828607	
262205_at	AT2G01080		1.585504	
254364_at	AT4G22020		1.5874676	
244951_s_at	AT2G07723		1.590135	
252039_at	AT3G52155		1.5912727	
251879_at	AT3G54200		1.5948136	
260553_at	AT2G41800		1.5973891	
251461_at	AT3G59780		1.6075972	
261205_at	AT1G12790		1.6090313	
250887_at			1.6168001	
247488_at	AT5G61820		1.6213262	
251516_s_at	AT3G59310 /// AT3G59320		1.6219981	
253025_at	AT4G38110 /// AT4G38120		1.6300201	
244934_at			1.6346385	
251951_s_at	AT1G55710 /// AT3G53630 /// AT4G18690		1.6388726	
265217_s_at	AT1G05090 /// AT4G20720		1.6440159	
257334_at			1.6455638	
257611_at	AT3G26580		1.6569904	
246898_at	AT5G25580		1.6595087	
246982_s_at	AT2G10560 /// AT5G04860		1.6623924	
251211_s_at	AT3G62470 /// AT3G62540 /// AT5G14820		1.6670395	
264299_s_at	AT1G78850 /// AT1G78860		1.6725248	
260586_at	AT2G43630		1.6816547	
256824_at			1.6821725	
267130_at	AT2G23390		1.6932073	
264288_at	AT1G62045		1.7114049	
256356_s_at	AT1G66500 /// AT5G43620		1.7210673	
261221_at	AT1G19960		1.7287238	
264086_at	AT2G31190		1.7294381	
255962_at	AT1G22330 /// AT1G22335		1.7399623	
267161_at	AT2G37680		1.7463719	
251349_s_at	AT3G11030 /// AT3G61020		1.7615092	
255600_s_at	AT4G01020 /// AT5G10370		1.7961302	
252473_s_at	AT3G46610 /// AT5G14350		1.7991248	
250307_at	AT5G12160 /// AT5G12170		1.8001164	
249628_at	AT5G37580		1.8008771	
264475_s_at	AT1G77150 /// AT1G77170		1.8074992	
267057_at	AT2G32500		1.814274	
255621_at	AT4G01390		1.8187162	
253804_at	AT4G28220 /// AT4G28230		1.8198683	
246173_s_at	AT3G61520 /// AT5G28370 /// AT5G28460		1.8267562	
253294_at	AT4G33750		1.839282	
253421_at	AT4G32340		1.865585	
249894_at	AT5G22580		1.8683914	
266426_x_at	AT2G07140		1.8940682	
260277_at	AT1G80520		1.9186556	

Probe Set ID	AGI	Short/Full name	Fold change	RT-qPCR
250306_at	AT5G12160 /// AT5G12170		1.9239167	
247166_at	AT5G65840		1.9297134	
251095_at	AT5G01510		1.9431716	
251072_at	AT5G01740		1.9452783	
245638_s_at	AT1G24822 /// AT1G24996 /// AT1G25097 /// AT1G25170		1.9646324	
266956_at	AT2G34510		1.9758885	
245565_at	AT4G14605		1.987652	
246476_at	AT5G16730		2.0241868	
267644_s_at	AT2G32870 /// AT2G32880		2.0249925	
263941_at	AT2G35870		2.067356	
260446_at	AT1G72420		2.0680113	
260919_at	AT1G21525		2.1609073	
259546_at	AT1G35350		2.1652515	
250268_s_at	AT5G12950 /// AT5G12960		2.2346313	
254580_at	AT4G19390		2.3098097	
257761_at	AT3G23090		2.3494432	
260028_at	AT1G29980		2.353944	
266071_at	AT2G18670 /// AT2G18680		2.4063714	
256906_at	AT3G24000		2.41309	
257860_at	AT3G13062		2.4297645	
264251_at	AT1G09190		2.4338202	
257772_at	AT3G23080		2.5390007	
256603_at	AT3G28270		2.602393	
258609_at	AT3G02910		2.6031966	
260112_at	AT1G63310		2.6101959	
247950_at	AT5G57230		2.6282492	
261785_at	AT1G08230		2.6394556	
261542_at	AT1G63560		2.7287333	
249784_at	AT5G24280		2.7441578	
260048_at	AT1G73750		2.8286943	
252246_at	AT3G49730		2.926025	
256376_s_at	AT1G66690 /// AT1G66700		2.9702606	
253004_at	AT4G38280 /// AT4G38290 /// AT4G38330		3.0117996	
259411_at	AT1G13410		3.2663643	
251438_s_at	AT3G59930 /// AT5G33355		3.436262	
249191_at	AT5G42760		3.4524345	
247339_at	AT5G63690		3.5374858	
266806_at	AT2G30000		3.5416448	
256096_at	AT1G13650		5.255266	
265049_at	AT1G52060		5.303386	
266680_s_at	AT2G19850 /// AT3G54730		8.906418	

6. ACKNOWLEDGEMENTS

I would like to thank Prof. Csaba Koncz for his great supervision. The three past years was a turning point in my scientific life that was not possible without his support.

I am thankful to Prof. Dr. George Coupland for his helpful support.

I am grateful to my co-supervisor Dr. Seth Davis, who was very resourceful in giving great advices on my presentations.

I thank Prof. Dr. Martin Hülskamp and Prof. Dr. Ulf-Ingo Flügge, the committee members of thesis defence.

I kindly acknowledge Dr. Mihály Horváth, Dr. Zsuzsa Koncz, and Dr. Kishore Panigrahi for fruitful discussions and assistance in protein purification.

I thank Dr. Thomas Colby, Dr. Jürgen Schmidt, and Anne Harzen for 2D and mass spectrometry analysis.

I am grateful to Dr. Farshad Roodbar Kelari for preparing DNA profiling.

I gratefully thank International Max Planck Research School for funding and Dr. Olof P. Persson, IMPRS coordinator.

Many thanks to the present (Marta, Nico, Femke, Hasnain, Farshad, Sabine, Tomasz, and Zsuzsa) and previous members (Gergely, Mihály, and Dóra) of the Koncz group for nice working atmosphere in every aspect. I keep them in my mind forever.

Thanks to Dr. Elmon Schmelzer for teaching Confocal Laser Microscope and to Dr. Farnusch Kaschani and Martin Martens for German translation of the abstract German and correction of the C.V.

Finally, I would like to thank deeply my wife, Mahdieh Alipour Kermani, for unconditional love and support.

Erklärung

Ich versichere, daß ich die von mir vorgelegte Dissertation selbständig angefertigt, die benutzten Quellen und Hilfsmittel vollständig angegeben und die Stellen der Arbeit - einschließlich Tabellen, Karten und Abbildungen -, die anderen Werken im Wortlaut oder dem Sinn nach entnommen sind, in jedem Einzelfall als Entlehnung kenntlich gemacht habe; daß diese Dissertation noch keiner anderen Fakultät oder Universität zur Prüfung vorgelegen hat; daß sie - abgesehen von unten angegebenen Teilpublikationen - noch nicht veröffentlicht worden ist sowie, daß ich eine solche Veröffentlichung vor Abschluß des Promotionsverfahrens nicht vornehmen werde.

Die Bestimmungen der Promotionsordnung sind mir bekannt. Die von mir vorgelegte Dissertation ist von Prof. Dr. George Coupland betreut worden.

Köln den 12 Oktober 2009

Lebenslauf

Name Hajheidari
Vorname Mohsen
Geburtsort Karaj, Iran
Geburtstag 27. August 1975
Nationalität Iran
Familienstand verheirat

Studium

Seit Oct. 2006 Universität zu Köln:
 Doktorand am Max-Planck-Institute für Züchtungsforschung in Köln unter der Leitung von Prof. Dr. George Coupland, Besuch der “International Max Planck Research School (IMPRS)”, Schwerpunkt: Genetik, Molekularbiologie
 Betreuer: Dr. Csaba Koncz

Dec. 2001- Aug. 2006 Wissenschaftlicher Mitarbeiter im Landwirtschaftlich Biotechnologie Forschungsinstitut des Iran

Sep.1999 - Dec. 2001 RAZI Universität:
 M. Sc. Abschluß in Pflanzenzüchtung
 Diplomarbeit im Fachgebiet Biotechnologie. Thema: “Molecular Analysis of Transgenic Rice”

Sep. 1994 - Dec. 1998 Guilan Universität:
 B. Sc. in Pflanzenbau und Pflanzenzüchtung

Schulbildung

1989-1993 Gymnasium Shohadaie Enghelab Eslami, Karaj
 1986-1989 Mittelschule Kherad, Karaj
 1981-1986 Grundschule Shahid Maleki, Karaj

Publikationen

- **Hajheidari, M.**, Eivazi, A. R., Buchanan, B. B., Wong, J. H., Majidi, I. and Hosseini Salekdeh, Gh. (2007). A proteomic approach to discovering drought related responsive proteins in wheat grain. Journal of Proteome Research, 6, 1451-1460.

-
- Gazanchian, A ., **Hajheidari, M***, Khosh Kholgh sima, N. A. and Hosseini Salekdeh, Gh. (2007). Proteome response of *Elymus elongatum* (Host). to severe water stress and recovery. Journal of Experimental Botany, 58, 291-300.

*equal contribution

- Baharvand, H., **Hajheidari, M.**, Zonouzi, R., Kazemi Ashtiani, S., Hosseinkhani, S. and Hosseini Salekdeh, Gh. 2006. Comparative proteomic analysis of mouse embryonic stem cells and neonatal-derived cardiomyocytes. Biochemical and Biophysical Research Communications, 349, 1041-1049.
- Baharvand, H., **Hajheidari, M.**, Kazemi Ashtiani, S. and Hosseini Salekdeh, Gh. (2006). Proteomic signature of human embryonic stem cells. Proteomics, 6, 3544-3549.
- Askari, H., Edquist, J., **Hajheidari, M.**, Kafi, M. and Hosseini Salekdeh, Gh. (2006). Effects of salinity levels on proteome of *Suaeda aegyptiaca* leaves. Proteomics, 6, 2542-2554.
- **Hajheidari, M.**, Abdollahian-Noghabi, M., Askari, H., Heidari, M., Sadeghian, S. Y., Ober, E. S. and Hosseini Salekdeh, Gh. (2005). Proteome analysis of sugar beet leaves under drought stress. Proteomics, 5, 950-960.